OXIDATIVE DEHYDROGENATION OF ETHYLBENZENE

TOMOHIKO TAGAWA

DEPARTMENT OF SYNTHETIC CHEMISTRY
FACULTY OF ENGINEERING
NAGOYA UNIVERSITY

1981

A Dissertation

for

The Degree of Doctor of Engineering

handed in

Department of Synthetic Chemistry

Faculty of Engineering

Nagoya University

December, 1981

Chief-Referee: Professor Y. Murakami

Co-Referees: Professor Y. Yamashita

Professor K. Sugiyama

Professor Y. Izumi

Assistant Professor T. Hattori

Preface

This dissertation has been carried out during 1978 - 1981 as a doctorate thesis under the direction of

Professor Yuichi Murakami

at the Institute of Synthetic Chemistry, Faculty of Engineering, Nagoya University.

This thesis presents the studies on OXIDATIVE DEHYDROGENATION OF ETHYLBENZENE which deals mainly with the elucidation of the reaction mechanism and its application for the catalyst design for the present reaction.

The author wishes to express his sincere gratitude to Professor Yuichi Murakami for his kind and fruitful suggestions and encouragement throughout the course of this work.

He would like to make a grateful acknowledgment to Dr. Tadashi Hattori for his profound interest and helpful discussions. He thanks also Dr. Miki Niwa and Dr. Akira Miyamoto for their valuable discussions, and Mr. Kazuyoshi Iwayama, Mr. Yuzuru Ishida, Mr. Shigemi Kataoka and Mr. Satoshi Itoh for their colaboration. He extends his gratefulness to Mr. Yukio Kosaki and Mr. Hirofumi Itoh, and the rest of the members in the Laboratory of Professor Murakami for their valuable discussions and hearty cooperation with him.

The English text was duly emended by Miss Carmela V. Hidalgo and partly typed by Miss Akemi Hiramatsu, whose assistances I acknowledge with thanks.

Finally, an acknowledgment must be made to my parents for thier patience and understanding, without which this work would not have been possible.

Tomohiko Tagawa

Department of synthetic Chemistry
Faculty of Engineering
Nagoya University
December, 1981

CONTENTS

Chapter 1

INTRODUCTION

INTRODUCTION

Since the "Oil Crisis" in 1973, how to save energy becomes the most important subject in the chemical industries, and catalysts attract interests as would have the keys to solve the problems. Thus, new catalytic systems to save energy have been desired to be developed and the subject treated in this thesis is one part of these studies on the development of the energy saving processes. The methodology of the development of catalysts has sometimes depended on the chance meeting with catalysts, therefore, a new methodology to design catalysts with high efficiency is now desired. Another interest of this study is how to use the program of the catalyst design in an actual development of new catalysts.

Oxidative Dehydrogenation of Ethylbenzene

Styrene production

Impetus for the commercial production of styrene in the United States was stimulated by the critical need for a substitute for natural rubber which developed suddenly during World war II after crude rubber sources from Southeast Asia were cut off. From many proposals to solve this problem, a decision was made to launch a major effor to develop and produce a copolymer of styrene and butadiene, a rubber-like substance which could replace the natural material. In Japan, styrene monomer had been first produced in 1960. As shown in Fig. 1, the production of styrene monomer in Japan increases steeply at about 100 times during these two decades, and styrene is now one of the basic products in the petrochemical industry as a raw material for polystyrene, synthetic rubber, unsaturated polyester, ABS resin and so on. Catalyst research for styrene synthesis has been of interest to many chemical manufacturers because, as mentioned above, styrene monomer is such a large-volume chemical and a steady growth of styrene

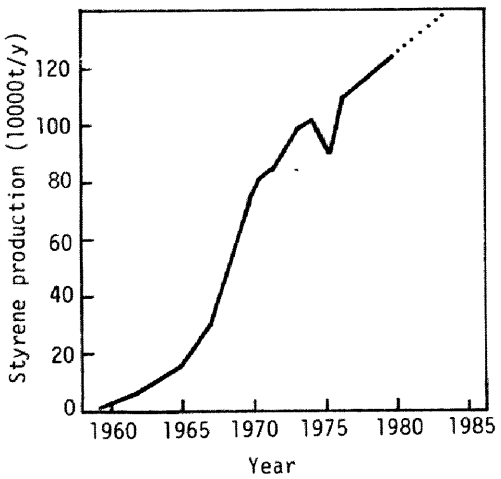

FIGURE 1 Production of Styerne monomer in Japan.

market is predicted [1,2,3]. Styrene monomeris now produced *via* ethylbenzene. For the production of ethylbenzene in a industrial scale, details are summarized elsewhere [2].

Dehydrogenation of ethylbenzene

The industrial production of styrene depends on the dehydrogenation reaction of ethylbenzene [1,2,3]. The dehydrogenation reaction on a commercial scale is generally conducted in the vapor phase at 850 - 950 K with a large amount of superheated steam, just below the temperature region where thermal cracking becomes significant. The by-products are benzeneand toluene in the liquid effluents, and small amounts of CO, CO_2, CH_4, C_2H_4, and C_2H_6 are formed as gaseous products.

As the catalysts for the dehydrogenation process, 50ZnO-40Al_2O_3-10CaO, 74.4ZnO-7.6 Al_2O_3-7.4CaO-4.7MgO-2.8K_2CrO_4-2.8K_2SO_4 (Lul44), and 85Fe_2O_3-7.7ZnO-0.5KOH-0.3K_2CrO_4-0.7Al_2O_3-0.5CaO-0.5MgO-0.3KSO_4 were developed by I.G. Farben Co., and also 72.4MgO-18.4 Fe_2O_3-4.6CuO-4.6K_2O (Standard 1707) and 89Fe_2O_3-2Cr_2O_3-9K_2CO_3 (Shell 105) were developed and are now widely used. The improvement of catalysts has also been devoted and Fe_2O_3-Cr_2O_3-V_2O_5-Co_2O_3-K_2O (Shell), Fe_2O_3-Mo_2O_3-CeO-K_2O-cement (Girdler), Fe_2O_3-K_2CO_3-$K_2Cr_2O_7$ -V_2O_5-cement (Dow) and so on have been reported [2]. In them, Shell 105 catalyst is widely used and its catalytic performances are as follows; conversion = 60 % and selectivity = 84 %, under reaction temperature = 893 K, LHSV = 1 h^{-1}, H_2O/ethylbenzene = 12 in molar ratio [2,4] or conversion = 40 % and selectivity = 90 % under reaction temperature = 933 K, H_2O/ethylbenzene = 13, reaction pressure = 0.4 kg/cm^2·g [5].

In spite of such improved conversion and selectivity, the distribution of products is limited by equilibrium. The equilibrium constants of this reaction areshown in Table 1 and the equilibrium conversion curve is shown in Fig. 2 [5]. As these datas

TABLE 1

Equilibrium Constants for the dehydrogenation of ethylbenzene

Temperature [K]	ΔH°kcal/mol	ΔF°kcal/mol	$\log_{10}K$	K_p atm
298.16	28.100	19.892	-14.5386	2.61×10^{-15}
300	28.107	19.843	-14.4522	3.53×10^{-15}
400	28.612	16.999	- 9.2891	5.14×10^{-10}
500	29.021	14.066	- 6.1477	7.21×10^{-7}
600	29.322	11.024	- 4.0160	9.65×10^{-5}
700	29.511	7.949	- 2.4817	3.30×10^{-3}
800	29.712	4.858	- 1.3269	4.71×10^{-2}
900	29.824	1.751	- 0.4252	3.75×10^{-1}
1000	29.891	- 1.383	0.3022	2.00
1100	29.920	- 4.510	0.8961	7.87
1200	29.910	- 7.620	1.3877	2.44×10^{1}
1300	29.870	-10.760	1.8090	6.44×10^{1}
1400	29.810	-13.880	2.1667	1.44×10^{2}
1500	29.73	-16.990	.2.4752	2.99×10^{2}

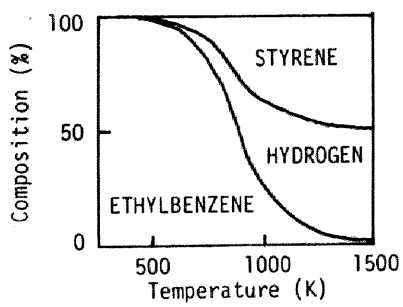

FIGURE 2 Equilibrium conversion curve of dehydrogenation of ethylbenzene

show, this is an endothermic reaction effected by an equlibrium which favors the products as the temperature is increased and the pressure reduced. A large amount of super-heated steam is used as the additive to provide heat needed for the reaction, to reduce the partial pressures of ethylbenzene and hydrogen, and to keep the catalyst clean and active. These requirements for high temperature and superheated steam do not meet the saving energy, and the oxidative dehydrogenation process is thusly increasing in importance. Performances of them in the practical scale are listed later in the case of butene to butadiene.

Oxidative dehydrogenation reaction

Oxidative dehydrogenation reaction represented by equation (1) is an exothermic

$$\Phi\text{-}C_2H_5 + \frac{1}{2}O_2 \longrightarrow \Phi\text{-}C_2H_3 + H_2O\ ; \quad \Delta H = -30\ \text{kcal/mol}. \qquad (1)$$

reaction and there is no limitation by the equilibrium. This can lower the reaction temperature and feed of super-heated steam is, theoretically, not required. Through put of an existing or new plant could be substantially increased with a corresponding reaction in capital and operating costs. Operation more nearly under isothermal conditions could aid the yield and conversion [1]. Thus, the oxidative dehydrogenation reaction can well meet the currently desired requirement of process development and is attracting considerable attetntion [4 - 11]. The use of halogen, SO_2 and S as oxidants is also possible and good results have been reported and summarized elsewhere [6,7,12], however, the high costs of hydrogen acceptors such as halogen and SO_2, the corrosion of apparatus, and incorporation of hydrogen acceptors into the products such as sulfides and halides make it difficult to use them in the large scale production such as styrene and butadiene. The direct oxidation of hydrocarbons to oxygen containing products has been developed as have oxidation process such as ammoxidation and oxichlorination. These situations suggest the possibility to realize the oxidative dehydrogenation process by air or oxygen. Actually, Some oxidative dehydrogenation process of butene to butadiene have been developed on a commercial scale by Phillips Petroleum Co. and Petro tex Co. [13,14], but that of ethylbenzene to styrene has not.

In Table 2, catalysts for oxidative dehydrogenation of ethylbenzene recently reported are summarized together with their catalytic performances. The selectivity is not sufficient on the bismuth-molybdenum catalyst [15] which is one of the typical mild oxidation catalysts for the production of the commercial base. In the recent studies, Mn, Co, Ni, and Ni-W oxides supported on Al_2O_3 [16,17] and Mg-Mo and MgMo-Mo oxide catalysts [18,19]have been examined but only insufficient conversion and selectivity such as 5 - 6 % and 70 % at 733 K [17], and 30 % and 70 % at 773 K [18], respectively, are obtained. Better results are reported in the recent patents [4]. In the most attractive catalytic systems which appeared in the recent review [4], Fe-Cr-K [20], Ce-P [21], abd Bi-U-Al [22] systems required high reaction temperature above 773 K. Zn-P-Si [23], and Zn-Si-Al [24] systems show selectivities lower than 80 %.

LIST Performances of practically used catalysts for butene dehydrogenation and oxidative dehydrogenation in an industrial scale

Catalysts	Reaction Temperature (K)	Conversion (%)	Selectivity (%)	Steam/Butene (molar ratio)	Butene SV (h^{-1})
DEHYDROGENATION CATALYSTS					
Philips 1490	894 - 950	27 - 33	69 - 76	9 - 12	300 - 400
Standard - 1707	922	18 - 36	65 - 80	15 - 20	200 - 800
Shell - 105	894 - 950	20 - 30	70 - 80	10 - 18	500
Shell - 205	894 - 950	26 - 28	73 - 75	8	500
Dow Type - 5	866 - 950	- 40	90	18 - 20	125 - 175
OXIDATIVE DEHYDROGENATION CATALYSTS					
Philips	866	77.1	90.2	35	351
BP Chemicals	673 - 723	55 - 70	80	2	94 - 156

CATALYSTS

Philips - 1490 ; $73Fe_2O_3 - 5Cr_2O_3 - 2K_2O$

Standard - 1707 ; $72.4MgO - 18.4Fe_2O_3 - 4.6CuO - 4.6K_2O$

Shell - 105 ; $93Fe_2O_3 - 5Cr_2O_3 - 2KOH$

Shell - 205 ; Shell - 105 + K_2CO_3

Dow Type B ; $96Ca_8Ni(PO_4)_6 - 2Cr_2O_3$ - 2Graphite

Philips Petroleum; P-Sn-O or P-Sn-Li-O or Al or Ga promoted P-Fe-O or P-Fe-O see ref. 4 Table 3. Scale; 50,000 t/yr or 100,000 t/yr.

BP Chemicals ; Sn-Sb ? see ref. 4. Scale ; 730 t/yr.

These values are summarized from data shown in references 4 and 5.

Table 2

Catalysts for Oxidative Dehydrogenation of Ethylbenzene

Catalyst	Reaction Temperature (K)	Relative partial pressures			Results (%)		References
		Oxygen	Nitrogen	Steam	EB-conv.	ST-select.	
Fe_2O_3-Cr_2O_3-K_2O	883	0.11	--	12.4	72	88(B/T=3/6)	1
Ce-P	824	1.16	--	13.7	77.5	91	2
Fe-Activ. Carbon	644	--	--	--	54.7	96.3	3
Zn-P-O-SiO_2	733	1.5	--	--	50	77	4
Cr_2O_3-NiO-Al_2O_3	723	0.42	--	0.6	40	95	5
ZnO-SiO_2·Al_2O_3	723	1.6	14.4	--	64	77	6
Bi-U-O-Al_2O_3	923	2.0	3.1	--	52.1	90.4	7
Pd-γ-Al_2O_3	563	1.0	3.5	10.0	46.0	98.5	8
Pd-KBr-α-Al_2O_3	558	0.43	1.7	2.8	42.9	97.6	9
Pd-KBr-γ-Al_2O_3	553	1.0	4.0	1.9 (with continuous flow of HBr)	29.0	98.0	10
Co-Cr-Al-Mg-Si	--	--	--	--	56.0	83.0	11

(CONTINUED)

Mn/Al	673	1.0	--	--	6.0	69.0	12
Co/Al	673	1.0	--	--	4.8	73.0	12
Ni/Al	673	1.0	--	--	4.6	71.0	12
Ni-W/Al(W/Ni=1/1.6)	733	1.0	--	0.0	30.0	70.0	13
$MgMoO_4$-MoO_3	773	2.0	--	--	26.0	60.0	14
MgO-MoO_3	773	2.0	--	--	48.0	82.0	14
Be-Si	--	--	--	--	41.6	90.0	15

[a]Calculated assuming $P_{ethylbenzene} = 1.00$.

[b]References; (1) J.R. Ghublikian, British Patent, 1,176,916 (1970). (2) Dow Chemical Co., Japan Kokai, 74-12,790 (1974). (3) R.M. Benslay and A.L. Jones, U.S. Patent, 3,652,698 (1970). (4) Nitto Chemical Industries Ltd., Japan Kokai, 74-41,182 (1974). (5) Mistubishi Chemical Industries Ltd., Japanese Patent, 75-30,061 (1975). (6) Nippon Kayaku Co. Ltd., Japanese Patent, 74-42,017 (1974). (7) Nippon Shokubai Kagaku Kogyo Co. Ltd., Japanese Patent, 77-28,782 (1977). (8) K. Fujimoto, J. Yamada, and T. Kunugi, Japan Kokai, 77-23,027 (1977). (9) Mitsubishi Petrochemical Co. Ltd., Japan Kokai, 78-44,525 (1978). (10) K. Fujimoto, and T. Kunugi, Ind. Eng. Chem. Prod. Res. Dev., 20 (1981) 319. (11) T. Imai, U.S. Patent, 4,180,690 (1979). (12) C. Bagnasco, P. Ciambelli, S. Crescitelli, and G. Russo, React. Kinet. Catal. Lett., 8 (1978) 293. (13) J.C. Conesa, B. Jezowska-Trzebiatowska, and W. Oganowski, J. Mol. Catal., 4 (1978) 271. (14) W. Oganowski, J. Hanuza, J. Wrzyszcz, and B. Jezowska-Trzebiatowska, Tezisy. Dokl. Resp. Konf. Okislitel'nomu Geterogennomu Katal., 3rd, 9 (1976) 4, Chem Abst., 89-147246. (15) D.B. Tagiev, A.B. Mamedov, Z.G. Zul'fganov and Kh. H. Minachev, Kinet Katal., 20 (1979) 541, Chem Abst. 91-039022.

On Cr-Ni-Al [25] and Pd-KBr-Al [26] catalysts, the partial pressure of oxygen should be limitted to lower values than the stoichiometric pressure, in other words, high yield of styrene cannot be expected. Thus, it is difficult to obtain styrene selectively with high conversion at lower temperature on the above catalysts. The catalysts which satisfy these requirements are only Fe-activated carbon [27] and Pd-Al [28,29], but Pd-Al system is not so stable and for the continuous stabillity, a continuous flow of HBr is required.

Considering the difficulty of the investigation of catalysts for the oxidative dehydrogenation of ethylbenzene as stated above, the first target should be settled down at the conversion as high as 40 % with the selectivity as high as 90 % under the reduced pressure of steam and at a lower temperature below 723 K, such performances can be obtained in the dehydrogenation process at higher temperature with a large amount of steam. If such target could be realized, then the further investigations to improve the catalytic performances should be devoted and this sholud be the second target of this investigation.

Catalyst Design in the Development of Catalyst

Although catalysis is a subject of tremendous industrial importance, it has long been regarded by the general scientific population as being the last stronghold of alchemy. The reasons for this seem to originate with the complexity of the subject. Most catalysts are inorganic materials that catalyze organic reactants by accelerating the rate of a thermodynamically favourable process. As a result, knowledges of inorganic and physical chemistry is requred as well as organic chemistry. In addition, since many catalysts are porous solids, familiarity with solid state chemistry and with chemical engineering pronciples of mass and heat transfer are also desirable [30].

These attitudes are intensified in the context of catalyst design. In dealing even with other catalytic scientists, comments range from the polite statement that it is very interesting - but will never be of any use, though the recommendation as to where to buy a crysal ball, to the extreme statement relating monkeys, typewriters and Shakespear. Nonetheless, it is clear that the basis of a method of design does exist, and that - alothough the design methods are far from perfect - they can lead to the development of improved catalysts in shorter times.

Program of catalyst design

As mentioned above, the complexity in the catalyst developement still exisits and this easily combines to the recognition that "experimental efforts is essential in the chemical research. Over estimation of this leads to regard it impposible to design catalysts. Thus, the catalyst development today still depends on the chance meeting with catalysts during the numerous number of experimental works. Under these situations, the new method, to choose a catalyst for a given reaction by applying estab-

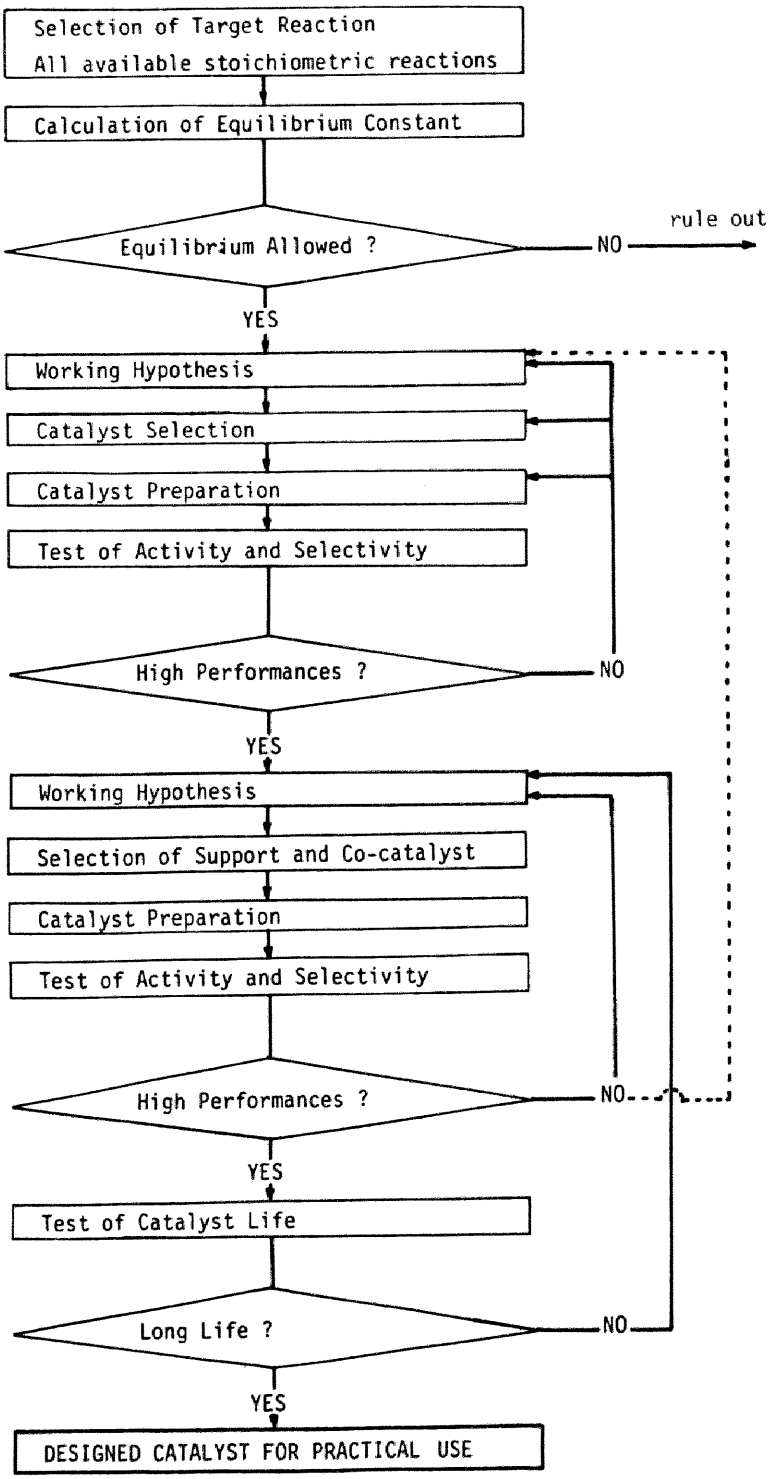

FIGURE 3 Program of catalyst design

lished conepts with high efficiency, has been required along with the recent advances in catalytic chemistry and surface chemistry. Some proposal has been done on the methodology of catalyst design [30 - 38].

In Fig. 3, one of them, which is expected to be widely used, is summarized [32 - 33]. The purpose of this program is to describe the methods that form the basis of the scientific design of catalysts on the view point of engineering. It must be emphasized that this subject is in the course of development and that this program must be regarded as a signpost rather than a final position. Catalyst design can be regarded, in many ways, as a logical application of available informations to the selection of catalyst for a target reaction. Over the years it has been possible to formalrise a procedure for doing this and this is what Fig. 3 shows.

The first step is the determination of the target reaction, considering all available stoichiometric reactions together with their equilibrium constant. The second step is to make up the working hypothesis which is constructed by all available informations related to the target reaction. The selction and preparation of catalyst based on the above hypothesis are followed. The test of the catalytic performance is conducted and the feed back of the results, as a new information, to the step of making the working hypothesis can serve further improvement of catalysts. On the catalysts which meets the desiered performances by repeating the feed back cycles, the design of co-catalyst and support is conducted by the same feed back cycles used in the design of the primary components. After satisfied all steps, the test, as the final step, of the catalyst life is conducted to judge the practical use.

Role of chemistry of catalysis in the catalyst design

In the construction step of working hypothesis, the chemistry of catalysis plays an important roles. Especially, the reaction mechanism elucidated for the target reaction directly gives the plan of catalyst design. Of course, the use of the feed back cycle *via* the working hypothesis is the strongest arms for the elucidation of the reaction mechanisms. In order to clarify the reaction mechanism and to predict the activity and selectivity, the following terms should be usefull;

(1) informations from the reaction which resembles to the target reaction,
(2) selection of resemble atoms in the periodic table,
(3) heat of formation of oxides,
(4) %d characters,
(5) lattice constants,
(6) acid and base properties.

Including above six properties, the determination of the surface characters also plays important roles in the program shown in Fig. 3. The roles of characterization of catalysts in the design and improvement of catalysts are summarized in Fig. 4 [39]. The correlation between physical characters of known catalyst and the catalytic performances, together with the supposed reaction mechanisms, gives the working hypothesis

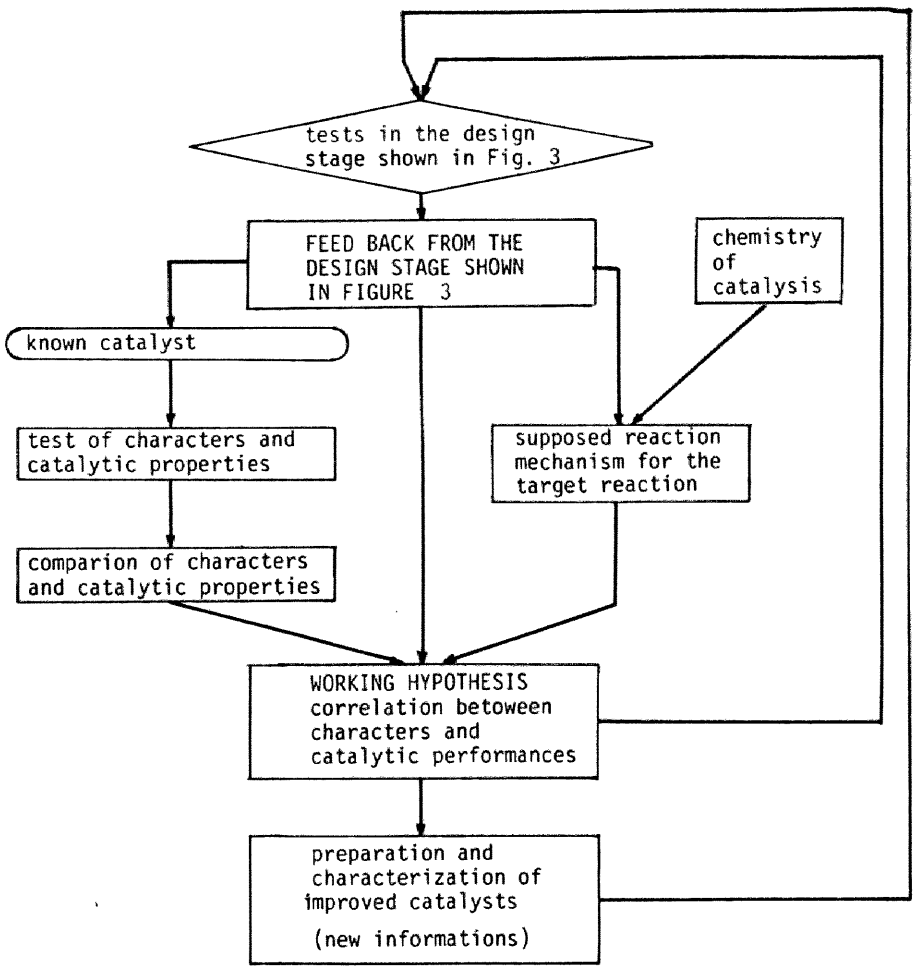

FIGURE 4 The roles of characterization of catalysts in the catalyst design.

to predict the factors which controll the activity and selectivity. The improved catalysts are prepared and characterized on the basis of the hypothesis which plays an important roles in the design stage. The feed back informations from the design stage can give a new plan for characterization,working hyothesis, and mechanism estimation. Thus, the characterization of catalysts incorporated in the feed back loop.

Reaction Mechanism of Oxidative Dehydrogenation Reaction

As stated in the previous section, the elucidation of reaction mechanism plays an important role in the design of catalysts. This also may apply in the design of the catalysts for the oxidative dehydrogenation of ethylbenzene.

A lot of studies have been done and reviewed about the reaction mechanism of the oxidation reactions, as the oxidation reaction occupies an important position both in the scientific field and the practical field. This section summarizes the available informations about the reaction mechanism of oxidaitve dehydrogenaiton reaction.

The reaction mechanisms including allylic intermediates have been determined in detail in the oxidation of olefinic compounds [40]. Studies of ^{13}C labeled propylene on Bi·Mo [41], Bi·Mo-P [42] and Cu_2O [43] suggested the symmetric allyl intermediates. The product distribution obtained in the reaction of deuterio propylene [44,45,46] on Cu_2O, Bi·Mo, and U·Sb also indicated the same intermediate of propylene, the α-hydrogen of which had been abstracted. The same intermediate was assumed by the oxidative dehydrogenation of deuterio-butene on Bi·Mo [47] and the allylic intermediates was also detected on ZnO [48] with spectroscopic methods. Moreover, the rate determining step was proved to be in the abstraction step of the α-hydrogen [45,49,50]. In spite of this, few studies have been done on the mechanism of the oxidative dehydrogenation of alkylaromatic compounds [51]

The active oxygen species for the oxidative dehydrogenation of butenes is said to be the lattice oxygen of Mo-containing oxides [52], the oxygen double-bonded to the metal ion (M=O) [53,54,55] and the adsorbed oxygen species (i.e. O^-) [53,54,56] on the ferrite spinel catalysts. Many studies have been done on the adsorbed oxygen species with the aid of ESR [57] and the activity of the adsorbed oxygen species (i.e. O_2^-, O^-, O_3^-) was also studied in the oxidation of hydrocarbons [58,59,60]. Only in the case that uv- or γ-irradiation was performed on the sample, was the adsorbed oxygen species (i.e. O_2^-) observed on the insulators, such as $SiO_2 \cdot Al_2O_3$ [57], Al_2O_3 [57], and zeolites [57,61]. On the other hand, the base catalyst such as MgO was observed to activate oxygen to form O_2^- ion without prior irradiation but only with heat treatment [62].

Role of Acid and Base Sites on the Oxidation Reaction

The overall scheme of the oxidation of a hydrocarbon can often be modeled upon that suggested by Mars and van Krevelen [63], so called as the reduction-oxidation, or redox. mechanism. This redox cycle depends upon the ability of catalyst surface sites to accept and/or donate electrons. In the formalism of molecular orbital theory, a redox reaction involves transfer of an electron to fill a bonding orbital of one reactant (to be reduced) from a partly filled antibonding orbital of the reactant to be oxidized. This is similar, but not equivalent, to an acid-base reaction in the Lewis sense, since a Lewis acid accepts electron pairs from a nonbonding orbital of a Lewis base. It is convenient, therefore, to treat the acidity and basicity of a catalyst together with

the reaction mechanism of partial oxidation reactions [64]. The investigation of the detailed role of acid and base sites in the oxidative dehydrogenation of ethylbenzene will then show not only the reaction mechaism of the present reaction but also the general role of acid and base sites in other partial oxidation reactions. Some results in the studies of the oxidation reactions suggest the participation of acid sites [65, 66] and of base sites [67] in the partial oxidation reactions such as oxidation of 1-butene on Mo-Alkai earth-As catalysts [65], oxidation of isobutene on Bi containing catalysts [66], and oxidation of propylene on Na- and P-SnO_2 catalysts [67]. The selectivity of the oxidation reactions is also said to be effected by the acid and base properties of the catalysts [68 - 72]. For example, oxidation of propylene [69] shows a dependence of selectivity on the acidity, the selectivity of oxygen incorporation and of oxidative dimerization depends on the acidic nature of the co-catalyst in the oxidation of propylene [70], and oxidation of butene to butadiene, of phenol to CO_2 and of n-hexane to CO_2 [71]. Correlations between the oxidation activity and the amount of acid and/or base sites has been reported in many reactions by Ai, and this is reviewed in references [71,73]. However, the details of the role of the acid and base sites in a molecular aspect is still not clear [74,75].

The Aim and Scope of the Present Study

The catalytic systems to get styrene selectively with saving energy from ethylbenzene by oxidative dehydrogenation is now required with great urgency. The difficulties in the separation of products from ethylbenzene requires the catalytic process of 100 % conversion with high selectivity. However, the present processes shown in Table 2 could not realize this because the selectivity of them will decrease steeply with increased conversion. Thus, the design of catalysts to realize the 100 % conversion with high selectivity is desired from another view point such as the process design.

As mentioned in the previous section, the detailed mechanism for the oxidation of aromatic compounds is required to understand the activity and selectivity of the given catalysts. How to utilize the mechanism to the catalsyst design is now under development. Thus, the application of these informations to the development of the catalysts for the oxidative dehydrogenation of ethylbenzene attracts interest both form the industrial stand point and from the scientific stand point, as stated in the previous sections.

The main aim of the present study is a systematic investigation of the reaction mechanism of the present reaction on the basis of quantitative roles of acid and base sites in a molecular aspects, and its application of the catalyst design with respect to the oxidative dehydrogenation of ethylbenzene.

In Chapter 2, a systematic screening of the catalysts are described. The details of the resulted SnO_2-P_2O_5 catalysts are investigated and reported in Chapter 3. Chapter

4 and Chapter 5 are concerned with the determination of the reaction mechanism of the present reaction using Na treated SiO_2·Al_2O_3 on the basis of the quantitative roles of acid and base site in a molecular aspect. The extension of the reaction mechanism to various catalysts are conducted and it is applied to the catalyst design in Chapter 6. The design of supports are described in Chapter 7, and the details of the resulted SnO_2/SiO_2 catalyst are described in Chapter 8. In Chapter 9, A new method to support metal oxides on the solid support from gas phse is developed and applied to the preparation of Vapor Phase Supported SnO_2/SiO_2 catalyst. The appoication of the VPS catalysts to the oxidative dehydrogenation are studied comparing with impregnated catalysts on the basis of the reaction mechanism and the supported models is described in Chapter 10. Chapter 11 summarizes the above results and discussions.

REFERENCES

1 W.W. Kaeding, Catal. Rev., 8 (1974) 307.
2 M. Imanari and Y. Watanabe, Yuki Gosei Kagaku Kai Shi, 36 (1978) 768.
3 E.H. Lee, Catal. Rev., 8 (1973) 285.
4 M. Imanari and Y. Watanabe, Petrotech, 2 (1979)339.
5 K. Hoshiai, "Shokubai Kogaku Koza Vol. 7," Chapter 2, P. 170 (1964).
6 M. Chono, Sekiyu Gakkai Shi, 16 (1973) 337 and 726.
7 Y. Morita, Sekiyu to Sekiyu kagaku, 13 (1969) 86.
8 Y. Morita and E Nishizawa, Sekiyu Gakkai Shi, 8 (1965) 935.
9 E. Echigoya and T. Watanabe, Yuki Gosei Kagaku Kai Shi, 37 (1969) 211.
10 M. Akimoto, Petrotech, 2 (1979) 57.
11 V.K. Skarchenko, Int. Chem. Eng., 9 (1969) 1.
12 Y. Morita and E. Nishizawa, Sekiyu Gakkai Shi. 11 (1968) 424.
13 P.C. Husen, K.R. Deel, and W.D. Peters, Oil Gas J., 69 (1971) 60.
14 Petro Tex Co., Chem. Eng., 78 (1971) 115,(April, 5).
15 Y. Murakami, M. Niwa, and H. Uchida, Kogyo Kagaku Zasshi, 72 (1969) 2183.
16 J.C. Conesa, A. Cortes, J. Marti, J.C. Seoane, and J. Soria, J. Catal., 58 (1979) 34.
17 C. Bagnasco, P. Ciambelli, S. Crescitelli, and G. Russo, React. Kinet. Catal. Lett. 8 (1978) 293.
18 J. Hanuza, B. Jezowska-Trzebiatowska, and W. Oganowski, J. Mol. Catal., 4 (1981) 271.
19 W. Oganowski, J. Hanuza, B. Jezowska-Trzebiatowska. and J. Wrzyszcz, J. Catal., 39 (1975) 161.
20 J.R. Ghublikian, British Patent, 1,176,916 (1970).
21 Dow Chemical Co., Japan Kokai 74-12,790 (1974).
22 Nippon Shokubai Kagaku Kogyo Co. Ltd., Japanese Patent, 77-28,782 (1977).
23 Nitto Chemical Industry Co Ltd., Japan Kokai, 74-41,182 (1974).
24 Nippon Kayaku Co. Ltd., Japanese Patent, 74-42,017 (1974).
25 Mitsubishi Chemical Industries Ltd., Japanese Patent, 75-30,061 (1975).
26 Mitsubishi Petrochemical Co. Ltd., Japan Kokai, 78-44,525 (1978).

27 R.M. Benslay and A.L. Jones, U.S. Patent 3,652,698 (1970).
28 K. Fujimoto, J. Yamada, and T. Kunugi, Japan Kokai, 77-23,027 (1977).
29 K. Fujimoto and T. Kunugi, Ind. Eng. Chem. Prod. Res., Dev., 20 (1981) 319.
30 D.L. Trimm, "Design of Industrial Catalysis," Elsevier, Amsterdam, 1980.
31 D.L. Trimm, "Preparation of Catalysts" II, p. 1, Elsevier, Amsterdam, 1979.
32 Y. Murakami, Shokubai, 21 (1979) 349.
33 Y. Murakami, 46th Annual Meeting of Japan Chemical Enginnering Soc., p.564 (1981).
34 Y. Murakami, "Shokubai Sekkei" p.1 Maki Publ., (1981).
35 Y. Yoneda, Kagaku Kogyo (1968) 989.
36 A. Ozaki, Yuki Gosei Kagaku Kai Shi, 32 (1974) 800.
37 M. Misono, Kagaku, 36 (1981) 15.
38 D.A. Dowden, Proc. 4th Int. Congr. Catal. (II), Moscow (1968), Akademiai Kaido, Budapest (1971).
39 T. Hattori, M. Niwa, and A. Miyamoto, "Shokubai Sekkei" p.87, Maki Publ., (1981).
40 G.C.A. Schuit, "Chemistry of Catalytic Process." p. 325, McGraw Hill, New York, 1979.
41 W.H.M. Sachtler, and N.H. De Boer, Proc. 3rd. Int Congr. Catal., Amsterdam, p.252 (1965).
42 T. Dozono, D.W. Thomas, and H. Wise, JCS Faraday Trans. I, 69 (1973) 620.
43 H.H. Voge, C.D. Wagner, and D.P. Stevenson, J. Catal., 2 (1963) 58.
44 C.P. Adams and T.J. Jennings, J. Catal., 2 (1963) 63.
45 C.P. Adams and T.J. Jennings, J. Catal., 3 (1964) 549.
46 R.K. Grasselli, and D.D. Suresh, J. Catal., 25 (1972) 273.
47 C.R. Adams, Proc. 3rd. Int Congr. Catal. Amsterdam p.240 (1965).
48 A.L. Dent and P.J. Kokes, J. Am. Chem. Soc., 92 (1970) 6709 and 6718, and Z. Dolejsek and J. Novakova, J. Catal., 37 (1975) 540.
49 W.R. Cares and J.W. Hightower, J. Catal., 23 (1971) 193.
50 M.A. Gibson and J.W. Hightower, J. Catal., 41 (1976) 420.
51 J. Hanuza, B. Jezowska-Trzebiatowska, and W. Oganowski, J. Mol. Catal., 4 (1978) 271.
52 J. Haber and B. Grzybowska, J. Catal. 28 (1973) 489.
53 R.J. Rennard and W.L. Kehl, J. Catal., 21 (1971) 282.
54 W.P. Caves and J.W. Hightower, J. Catal., 23 (1971) 193.
55 R.J. Rennard, R.A. Innes, Jr., and H.E. Swift, J. Catal., 30 (1973) 128.
56 K.M. Sancier, P.R. Wentrcek, and H. Wise, J. Catal., 39 (1975) 141.
57 J.H. Lunsford, Catal. Rev., 8 (1973) 135.
58 W. Keulkes, L.D. Krenzke, and T.M. Nothermann, Adv. Catal., 27 (1978) 183.
59 W.N. Delgas, G.L. Haller, R. Kellerman, and J.S. Lunsford, "Spectroscopy in Heterogeneous Catalysus." p.212, Academic Press, New York, 1979.
60 W.H.M. Sachtler, Catal.Rev., 4 (1969) 27.
61 N. Kanzaki and I. Yasumori, Bull. Chem. Soc. Japan, 52 (1979) 1923, and the references therein.

62 E.G. Derouane and V. Indovina, Chem. Phys. Lett., 14 (1972) 455.
63 P. Mars and D.W. van Krevelen, Chem. Eng. Sci. Suppl., 3 (1954) 41.
64 D.B. Dadyburjor, S.S. Jewur and E.L.I. Ruckenstein, Catal. Rev., 19 (1979) 293.
65 I. Ishikawa and T. Hayakawa, Bull. Jap. Pet. Inst., 18 (1976) 55.
66 M. Akimoto and E. Echigoya, JCS Faraday trans. I, 75 (1979) 1757; the references therein.
67 M. Egashira, I. Aso, and T. Seiyama, Kyushyu Daigaku Ko-gaku Shu-ho, 45 (1972) 704.
68 Ph.A. Batist, P.C.M. Heijden, and G.C.A. Schuit, J. Catal., 22 (1971) 411.
69 Y. Takita, A. Ozaki, and Y. Morooka, J. Catal., 27 (1974) 185.
70 T. Seiyama, M. Egashira, T. Sakamoto, and I. Aso, J. Catal., 24 (1972) 76.
71 M. Ai, Proc. 7th Int. Congr. Catal. Tokyo, Part B, p.1060, Elsevier, Amsterdam (1981).
72 K. Maruyama, H. Hattori, K. Tanabe, Bull. Chem Soc. Japan, 50 (1977) 86.
73 M. Ai, Shokubai, 18 (1976) 17, references therein.
74 T. Tagawa, Proc. 7th Int. Congr. Catal. Tokyo, Part B, p.1070, Elsevier, Amsterdam (1981), discussions for ref. 71.
75 T. Tagawa, Proc. 7th Int. Congr. Catal. Tokyo, Part B. p.1122, Elsevier, Amsterdam (1981), discussions for M.V.C. Sastri, B. Viswanathan, and C.V. Bhuvana, ibid., p.1113.

Chapter 2

SCREENING OF CATALYSTS FOR THE OXIDATIVE DEHYDROGENATION OF ETHYLBENZENE

SYNOPSIS

The oxidative dehydrogenation of ethylbenzene to styrene on various oxide catalysts has been investigated. The catalysts examined are classified into six types, considering their catalytic behaviors. In general, acidic catalysts show high selectivity. The most effective catalyst has been found to be the SnO_2-P_2O_5 catalyst prepared from $Sn(OH)_2$ and phosphoric acid. The effects of partial pressures and reaction temperature have been studied and suitable reaction conditions for the SnO_2-P_2O_5 catalyst have been determined.

INTRODUCTION

In Chapter 1, the present state of styrene production was reviewed and this can be summarized as follows: Styrene is produced on a commercial scale from ethylbenzene by a dehydrogenation reaction in the vapor phase at 850 - 950 K, just below the region where thermalcracking becomes significant. This is an endothermic reaction effected by an equilibrium which favors the products as the temperature is increased and the pressure reduced [1]. Superheated steam is used as the additive to provide the heat needed for the reaction, to reduce the partial pressures of ethylbenzene and hydrogen, and to keep the catalyst clean and active. To solve these problems in the dehydrogenation process, the oxidative dehydrogenation of paraffins, mono-olefins and alkylbenzenes has attracted considerable attention and is currently increasing in importance [2-22]. The direct oxidation of hydrocarbons to oxygen containing products has been developed, as have oxidation processes such as ammoxidation and oxychlorination. Some oxidative dehydrogenation processes of butene to butadiene have also been developed on a commercial scale [7,8], but that of ethylbenzene to styrene has not. Moreover, the selectivity is not sufficient in the oxidative dehydrogenation of ethylbenzene on the bismuth-molybdenum catalyst [9] which is one

of the typical mild oxidation catalysts for production on a commercial basis. In the recent studies, Mn, Co, Ni, and Ni-W oxides supported on Al_2O_3 [5,10] and Mg-Mo, and MgMo-Mo oxide catalysts [6,11] have been examined but only insufficient conversion and selectivity, such as 5 - 6 % and 70 % at 733 K [10], and ∿ 30 % and ∿ 70 % at 773 K [6], respectively, are obtained. The selection of suitable catalysts and appropriate reaction conditions for improved styrene yield and selectivity is then required, however, the systematic screening studies have not yet been reported.

In this study, the screening of the catalysts was carried out with a continuous flow technique and suitable reaction conditions for the SnO_2-P_2O_5 catalyst are also discussed.

EXPERIMENTAL

Materials and Catalysts

A guaranteed reagent of ethylbenzene was used after purification by a silica gel column. Guaranteed reagents of bromobenzene and the raw materials for catalysts were used without further purification.

General procedure for the preparation of catalysts was as follows: the starting materials and a small amount of water were mixed in a mortar, dried at 380 K and pressed into tablets which were crushed, sieved (20 - 48 mesh) and calcined at 773 K for 7.2 ks in a flow of air. Nitrates of bismuth and lead, antimony oxide, potassium carbonate, lithium hydroxide, and phosphoric acid were added to the tin(II) hydroxide gel for SnO_2-Bi_2O_3 (Sn-Bi), SnO_2-PbO (Sn-Pb), SnO_2-Sb_2O_5 (Sn-Sb), SnO_2-K_2O (Sn-K), SnO_2-Li_2O (Sn-Li), and SnO_2-P_2O_5 (Sn-P), respectively. Tin(II) hydroxide gel was prepared by adding more than an equivalent amount of ammonium hydroxide to a tin (II) chloride solution in order to precipitate it and then by washing with water until pH7 was obtained. Phosphoric acid was added to the hydroxide gel prepared from nitrates of lead, chromium, iron, and cadmium, a chloride of manganese, an ammonium salt of molybdenum, and tungstic acid for PbO-P_2O_5 (Pb-P), Cr_2O_3-P_2O_5(Cr-P), Fe_2O_3-P_2O_5 (Fe-P), CdO-P_2O_5(Cd-P), MnO_2-P_2O_5 (Mn-P), MoO_3-P_2O_5 (Mo-P), and WO_3-P_2O_5 (W-P), respectively. Cadmium oxide (CdO) and tin oxide (SnO_2) were prepared from the hydroxide gel of cadmium and tin, respectively. Solid phosphoric acid (Solid-P) (Nikki Chemicals CO. LTD., N-501) was used after the sieving and calcination. A compound of tin and phosphorus (Sn-P COMPD) was prepared by the reaction of $SnCl_2$ + $(NH_4)_2HPO_4$.

Procedure

The continuous flow reaction was carried out with a conventional fixed bed reactor at atmospheric pressure. The catalyst particles (4.5 g) were packed in the Pyrex reactor which was installed in a fluidized sand bath. A stream of ethylbenzene vapor, steam and oxygen was fed after dilution with nitrogen. A contact time (W/F) 77.8 g ks mol^{-1}, and a reaction temperature (T) of 723 K were used in these experi-

ments. Other reaction conditions, such as partial pressures of ethylbenzene (P_{EB}), oxygen (P_{O_2}), and steam (P_{H_2O}) are indicated in the respective figures. The liquid products were trapped in an ice bath and a dry ice-acetone bath. The gaseous products were sampled at the outlet of the reactor.

Conversion, yield, and selectivity are shown in the following equations:

ST-selectivity	= (ST formed/EB reacted)	X	100	(1)
EB-conversion	= (EB reacted/EB fed)	X	100	(2)
ST-yield	= (ST formed/EB fed)	X	100	(3)
$CO + CO_2$-yield	= (CO + CO_2 formed/EB fed X 8)	X	100	(4)
B-yield	= (B formed/EB fed)	X	100	(5)

where ST = styrene, EB = ethylbenzene, and B = benzene.

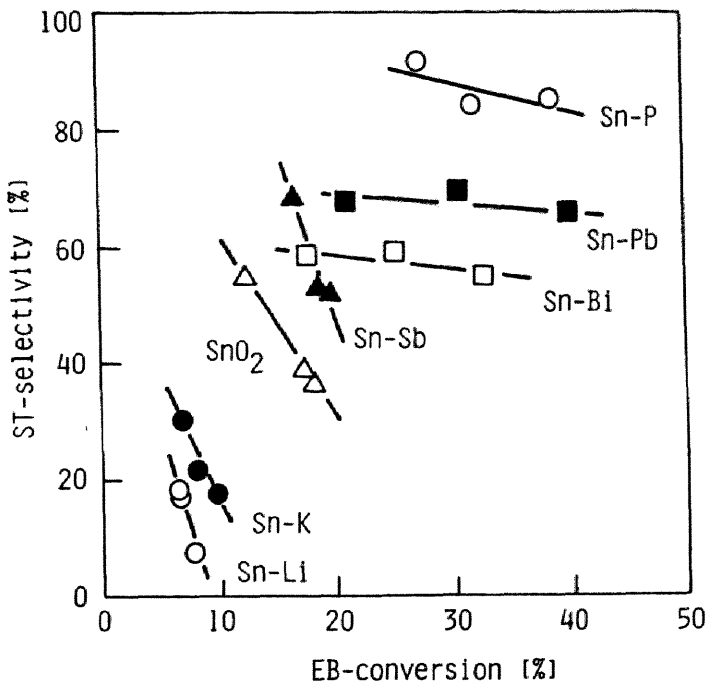

FIGURE 1 Comparison of various oxide catalysts (1) in a conventional fixed bed flow reactor. T = 723 K, W/F = 77.8 g catalyst ks mol^{-1}, P_{O_2} = 10.1 kPa, P_{H2O} = 31.7 kPa, P_{EB} = 10.1 - 20.3 kPa. Atomic ratio of the catalysts (Sn/M) = 10/1.

Analysis

The analysis of the products was carried out by gas chromatography. The analysis of gaseous products (O_2, N_2, CO and CO_2) was performed by the intermediate-cell method

[9,23] with a 25 cm silica gel + 25 cm activated carbon column at 383 K and a 2 m MS 13X column at room temperature. The liquid products were analyzed by a 2 m DOP column at 383 K with bromobenzene as an internal standard.

RESULTS AND DISCUSSION

Catalytic activity of various catalysts

The flow reaction was carried out at P_{EB} of 10.1, 13.5 and 20.3 kPa with the other conditions remaining constant. ST-selectivity was plotted against EB-conversion for comparison of the catalysts in Figures 1 and 2. The catalysts situated on the top right side of the figures can produce styrene selectively with high EB-conversion. The acidic catalysts showed higher ST-selectivity than the basic catalysts, as a general tendency.

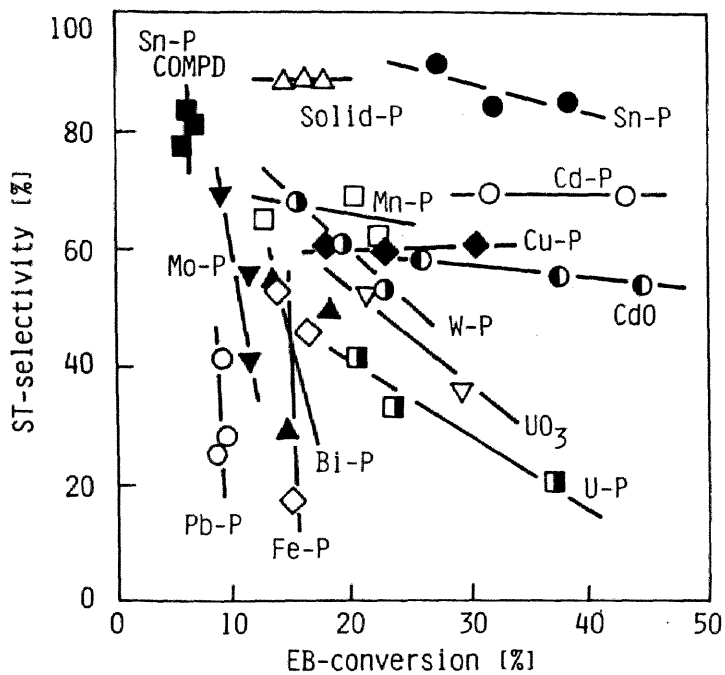

FIGURE 2 Comparison of various oxide catalysts (2) in a conventional fixed bed flow reactor. Atomic ratio of the catalysts (M/P) = 10/1 except for W-P, Mn-P, Pb-P, Cr-P, Fe-P, Bi-P (100/8.5) and Mo-P (3/2). For reaction conditions, see Figure 1.

In our previous study of this reaction, ST-selectivity was not sufficient with the BiO_2-MoO_3 catalyst [9] which is typical of mild oxidation catalysts, hence the catalytic behaviour of SnO_2, which was expected to be a milder oxidation catalyst,

with various additives was examined. As shown in Figure 1, the SnO_2 catalyst shows low EB-conversion and low ST-selectivity because of combustion which makes the conversion of oxygen 100 % and which produces a considerable amount of carbon oxides. The catalyst which displayed the highest conversion and the highest selectivity is the Sn-P catalyst. The addition of antimony and bismuth oxides improved the catalytic properties of the SnO_2 catalyst, though the effect was smaller than that of phosphorous. The Sn-Sb catalyst is known to be active for the oxidative dehydrogenation of butene and iso-pentene, but did not give good results in the case of ethylbenzene. Better results were obtained on the Sn-Pb catalyst. The addition of lithium and potassium lowered the EB-conversion while the total oxidation was greater than the oxidative dehydrogenation, which caused the low selectivity. It is significant that the addition of acidic components enhances the ST-selectivity while the basic components diminish it.

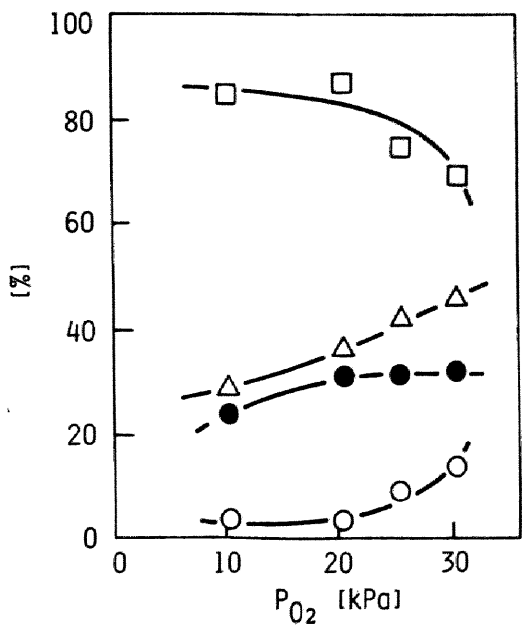

FIGURE 3 Effect of oxygen partial pressure on Sn-P (Sn/P; 10/1) catalyst calcined at 773 K for 7.2 ks. P_{EB} = 20.3 kPa. For other reaction conditions, see Figure 1. □, ST-selectivity; Δ, EB-conversion; ●, ST-yield; ○, CO + CO_2 yield.

As the addition of phosphoric acid to a SnO_2 catalyst has been shown to enhance the ST-selectivity with high EB-conversion, the catalytic behavior of various catalysts with or without phosphoric acid was studied. As shown in Figure 2, the solid phosphoric acid showed high selectivity, since only traces of carbon oxides were

produced, but the activity was low. The Pb-P catalyst (Sn and Pb are both IVa series) showed very low selectivity. The Cd-P catalyst (the electronic state of Cd^{2+} resembles that of Sn^{4+}) showed high activity and relatively high selectivity. The Sn-P COMPD catalyst, which was prepared by the reaction of tin(II) chloride and phosphoric acid, showed quite low activity. Even activity per unit surface area was lower than that of the Sn-P catalyst.

These catalysts can be classified as follows:

1) high selectivity and high conversion - Sn-P
2) high selectivity and relatively low conversion - solid phosphoric acid (Solid-P)
3) high selectivity and low conversion - Sn-P COMPD
4) relatively low selectivity and relatively high conversion - Sn-Pb, Sn-Bi, CdO, Mn-P, Cr-P, W-P, UO_3 and U-P
5) relatively low selectivity and relatively low conversion - SnO_2, Sn-Sb, Mo-P and Fe-P
6) low selectivity and low conversion - Sn-Li, Sn-K and Pb-P.

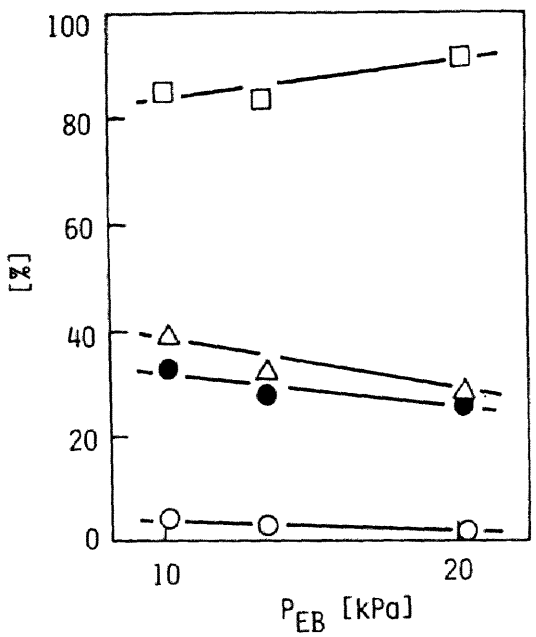

FIGURE 4 Effect of ethylbenzene partial pressure on Sn-P (Sn/P; 10/1) catalyst calcined at 773 K for 7.2 ks. For the reaction conditions and symbols, see Figures 1 and 3, respectively.

The byproducts of this reaction, which lowered the ST-selectivity, are carbon oxides, but a considerable amount of benzoic acid is also produced only on the Mo-P catalyst.

As a general tendency, shown in Figure 1, the addition of acidic components (i.e.P)

increases the selectivity, whereas the addition of basic components (K and Li) decreases it. This tendency will provide an interesting point of view that the acid-base properties of the catalyst control the catalytic behavior.

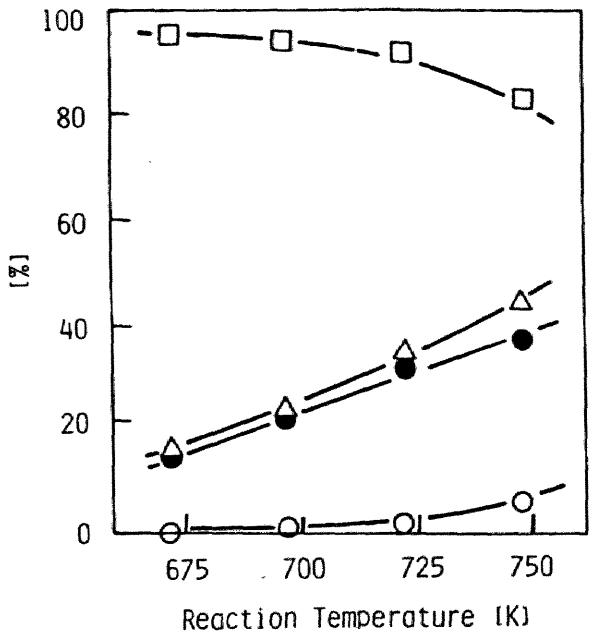

FIGURE 5 Effect of reaction temperature on Sn-P (Sn/P;10/1) calcined at 1273 K for 14.4 ks. P_{EB} = 20.3 kPa, P_{O_2} = 20.3 kPa, P_{H_2O} = 0.00 kPa. For other reaction conditions and symbols, see Figures 1 and 3, respectively.

Effects of reaction conditions on the Sn-P catalyst (the most effective catalyst) were also studied. The effect of oxygen partial pressure at 20.3 kPa of P_{EB} is shown in Figure 3. ST-selectivity decreased, despite a slight increase in the ST-yield. This tendency was apparent above 20.3 kPa of P_{O_2} because the increase in the CO + CO_2 yield surpassed that in the ST-yield. The effect of ethylbenzene partial pressure at 10.1 kPa of P_{O_2} is shown in Figure 4. Yields of carbon oxides and styrene decreased with increase in P_{EB}. ST-selectivity increased with increase in P_{EB}, because the decrement in CO + CO_2 yield surpassed that in ST-yield. The effect of reaction temperature at 20.3 kPa of P_{EB} and P_{O_2} without steam is shown in Figure 5. ST-yield increased with increase in the reaction temperature. Above 723 K, the yields of carbon oxides and benzene increased so that the ST-selectivity decreased to a great extent.

In this study, various phosphorous containing composite oxides and tin containing composite oxides have been studied and an Sn-P catalyst was found to be the most active and most selective, whereas there has been no study of the application of

Sn-containing catalysts to the oxidative dehydrogenation of ethylbenzene. Suitable reaction conditions for the Sn-P catalyst are then determined. The same results which were obtained by a typical dehydrogenation reaction at about 900 K with an H_2O/ethylbenzene ratio of 15, can be obtained at the lower reaction temperature of 723 K with a lower H_2O/ethylbenzene ratio of 1.5 by the oxidative dehydrogenation process on a Sn-P catalyst [1]. As the oxidative dehydrogenation of ethylbenzene is currently increasing in importance, many catalytic systems have been developed [2-6, 9-22] In the most attractive catalytic systems which appeared in a recent review [4], Fe-Cr-K [13], Ce-P [14] and Bi-U-Al [19] systems required high reaction temperatures, above 773 K. Zn-P-Si [15] and Zn-Si-Al [18] systems show selectivities lower than 80 %. On Cr-Ni-Al [16] and Pd-KBr-Al [21] catalysts, the partial pressure of oxygen should be limited to lower values than the stoichiometric pressure, in other words, a high yield of styrene cannot be expected. Thus, it is difficult to obtain styrene selectively with high conversion at lower temperatures on the above catalysts. The catalysts which satisfy these requirements are only Al-P [17], Fe-activated carbon [12] and Pd-Al [20]. The Sn-P system, developed in this study, is one of the catalysts which meets the above requirements. A recent patent reported that conversion and selectivity depend strongly on the catalyst composition in a complex system of Co-Cr-Al-Mg-Si oxides [22]. Therefore, the effects of changes in the catalyst composition and preparation method on the activity and selectivity are also of interest. Those on the Sn-P catalyst have been studied and are discussed in Chapt.3 of our investigation into the oxidative dehydrogenation of ethylbenzene, concerning the source of the catalytic activity [24].

REFERENCES

1 W.W. Kaeding, Catal. Rev., 8 (1974) 307.
2 V.K. Skarchenko, Int. Chem. Eng., 9 (1969) 1.
3 M. Akimoto, Petrotech, 2 (1979) 332.
4 M. Imanari and Y. Watanabe, Petrotech, 2 (1979) 339.
5 J.C. Conesa, A. Cortes, J. Marti, J.L. Seoane, and J. Soria, J. Catal., 58 (1979) 34.
6 J. Hanuza, B. Jezowska-Trzebiatowska, and W. Oganowski, J. Mol. Catal., 4 (1978) 271.
7 P.C. Husen, K.R. Deel, and W.D. Peters, Oil Gas J., 69 (1971) 60.
8 F.C. Newman, Ind. Eng. Chem., 62 (1970) 42.
9 Y. Murakami, M. Niwa, and H. Uchida, Kogyo Kagaku Zasshi, 72 (1969) 2183.
10 C. Bagnasco, P. Ciambelli, S. Crescitelli, and G. Russo, React. Kinet. Catal. Lett., 8 (1978) 293.
11 W. Oganowski, J. Hanuza, B. Jezowska-Trzebiatowska, and J. Wrzyszcz, J. Catal., 39 (1975) 161.
12 R.M. Benslay and A.L. Jones, U.S. Patent, 3,652,698 (1970).

13 J.R. Ghublikian, British Patent, 1,176,916 (1970).
14 Dow Chemical Co., Japan Kokai, 74-12,790 (1974).
15 Nitto Chemical Industry Co. Ltd., Japan Kokai, 74-41,182 (1974).
16 Mitsubishi Chemical Industries Ltd., Japanese Patent, 75-30,061 (1975).
17 Y. Murakami, Japanese Patent, 77-29,299 (1977).
18 Nippon Kayaku Co Ltd., Japanese Patent, 74-42,017 (1974).
19 Nippon Shokubai Kagaku Kogyo Co. Ltd., Japanese Patent, 77-28,782 (1977).
20 K. Fujimoto, J. Yamada, and T. Kunugi, Japan Kokai, 77-23,027 (1977).
21 Mitsubishi Petrochemical Co. Ltd., Japan Kokai, 78-44,525 (1978).
22 T. Imai, U.S. Patent, 4,180,690 (1979).
23 Y. Murakami, Bull. Chem. Soc. Japan, 32 (1959) 316.
24 Y. Murakami, K. Iwayama, H. Uchida, T. Hattori, and T. Tagawa, J. Catal., in press, Chapter 3 of this thesis.

Chapter 3

CATALYTIC BEHAVIOR OF SnO_2-P_2O_5 CATALYSTS

SYNOPSIS

The oxidative dehydrogenation of ethylbenzene "to styrene on SnO_2-P_2O_5 catalyst was investigated and the effect of catalyst composition and calcination temperature were studied. Elimination of phosphoric acid from SnO_2-P_2O_5 catalyst by nitric acid treatment and phosphoric acid treatment of the SnO_2 surface result in an increase of activity and selectivity. The catalytic behavior of SnO_2-P_2O_5 catalysts is compared with that of crystalline tin(IV) phosphate. The interdependence of catalytic activity and selectivity, catalyst crystalline structure, and BET surface area is also discussed. These indicate that a type of tin-phosphorus compound is the active component. Also an increase in activity with reaction time and by calcination is explained. A mechanism consisting of the abstraction of hydrogen from ethylbenzene by surface oxygen to form styrene and the regeneration of oxygen from gas phase to the catalyst surface is proposed, with consideration for the role of tin and phosphorus, on the basis of kinetic data in a differential flow reactor.

INTRODUCTION

As stated in the previous chapter, the oxidative dehydrogenation process is currently increasing in importance and a catalyst which shows high activity and selectivity is now desired[1]. The direct oxidation of hydrocarbons to get oxygen containing products has been developed as have some oxidation processes such as ammoxidation and oxychlorination which have been used on the industrial scale. These situations suggest the possibility of producing styrene by the oxidative dehydrogenation process, thus saving energy. However, the selectivity is not sufficient in the oxidative dehydrogenation of ethylbenzene on the bithmuth-molybdenum catalyst[2] which is one of the typical mild oxidation catalysts for the production of the commercial base.

In the screening study[3], the activity and selectivity of various oxide catalysts were examined, and SnO_2-P_2O_5 catalyst was found to show both high yield and high selectivity to styrene. In the present chapter further investigations were carried out on SnO_2-P_2O_5 catalyst. The state and the role of the phosphorus was investigated by X-ray diffraction and chemical treatment of the catalyst. The active component is discussed comparing it with crystalline tin phosphate. The mechanism of the activation of oxygen and ethylbenzene on the catalyst is also discussed on the basis of kinetic data in a differential flow reactor and by the pulse reaction technique.

EXPERIMENTAL

Catalysts

Tin oxide(SnO_2), solid phosphoric acid catalyst(Solid-P), and SnO_2-P_2O_5(Sn-P) were prepared by the method stated in the screening study[3]. A crystalline tin(IV) phosphate(c-SnP) was prepared by the method of Costantino and Gasperoni[4]. Anhydrous tin(IV) chloride was added to 1.6 l of 8M H_3PO_4 and 3M HNO_3 until the P : Sn ratio reached 30 and then the solution was refluxed for 100 h. The product was then washed with distilled water until pH 4 was obtained, dried under vacuum at room temperature for several days, pressed and sieved. The BET surface areas of c-SnP were 13.1 and 5.9 after being calcined at room temperature and 550 °C, respectively. The X-ray diffraction pattern of the c-SnP thus obtained was in good agreement with that previously reported[4].

Flow reaction

The continuous flow reaction was carried out with conventional fixed bed equipment at atmospheric pressure using a Pyrex reactor with an i.d. of 10 mm, at the center of which a Pyrex tube with an o.d. of 4 mm was installed as a cover for the thermocouple. The catalyst particles were dispersed in fused alumina particles to prevent a local increase of the temperature and packed in the reactor. The reactor was installed in an electrically heated fluidized sand bath in order to heat the catalyst bed uniformly. A stream of ethylbenzene vapor, steam, and oxygen was fed after dilution with nitrogen. A contact time (W/F) of 21.6 g·h/mol, and a reaction temperature (T) of 450 °C were used in these experiments unless otherwise stated. Other reaction conditions, such as catalyst weight (W), partial pressures of ethylbenzene (P_{EB}), oxygen (P_{O2}) and steam (P_{H2O}) are indicated in the respective figures and tables. The liquid products were trapped in an ice bath and a dry ice-acetone bath. The gaseous products were sampled at the outlet of the reactor. Peroxides in ethylbenzene were removed by a silica gel column.

Conversion, yield, and selectivity are shown in the following equations:

ST selectivity = (ST formed/EB reacted) x 100,
EB conversion = (EB reacted/EB fed) x 100,
ST yield = (ST formed/EB fed) x 100,
$CO + CO_2$ yield = ($CO + CO_2$ formed/EB fed x 8) x 100,
B yield = (B formed/EB fed) x 100,
ST = styrene, EB = ethylbenzene, B = benzene.

Analysis

The analysis of the products was carried out with gas chromatography. The analysis of gaseous products (O_2, N_2, CO, and CO_2) was performed by the intermediate-cell method [2,5] with a 25 cm silica gel + 25 cm activated-carbon column at 110 °C and a 2 m MS 13 X column at room temperature. The liquid products were analyzed by a 2 m DOP column at 110 °C with bromobenzene as an internal standard.

Pulse Reaction

Pulse equipment shown in Fig. 1 was used with oxygen-free helium as the carrier gas (Cu-Zn catalyst, Nikki Chemical Company, Ltd, N-211, reduced by H_2 was used at 300 °C to remove oxygen) [6]. The pulse size was 1 μl and the analysis of recovered ethylbenzene and the products (styrene, benzene, toluene, CO, and CO_2) was performed by the intermediate-cell method[5] with a 2 m PEG (30 % on C-22) + 0.5 m DOP (30 % on C-22) column and a 1.5 m activated-carbon column with an adequate empty tube to control the retention time. Another TCD cell was installed to determine the amount of ethylbenzene pulsed before the reactor.

RESULTS

As shown in Table 1, the Sn-P catalyst showed higher yield of styrene than the SnO_2 and Solid-P catalysts. SnO_2 showed high yield of CO and CO_2 but poor yield of styrene. Solid-P showed high selectivity but poor activity.

Effect of Composition of the Sn-P Catalyst

The effect of amounts of phosphoric acid in the Sn-P catalyst on the catalytic activity and selectivity was studied. As shown in Fig. 2, the EB conversion and ST yield increased for values of phosphoric acid below 9 %, decreased above it, and was constant for values above 15 %, while the $CO + CO_2$ yield decreased for values of phosphoric acid below 15 % and remained constant for values above it. Thus, the ST selectivity increased from 36.1 to 90 % below 9 at. % of phosphoric acid and, above 9 at. %, remained constant at 90 %. The change of surface area resembled that of ST yield.

Effect of Calcination Temperature

The effect of calcination temperature is shown in Fig. 3. The Sn-P (P, 9 at. %)

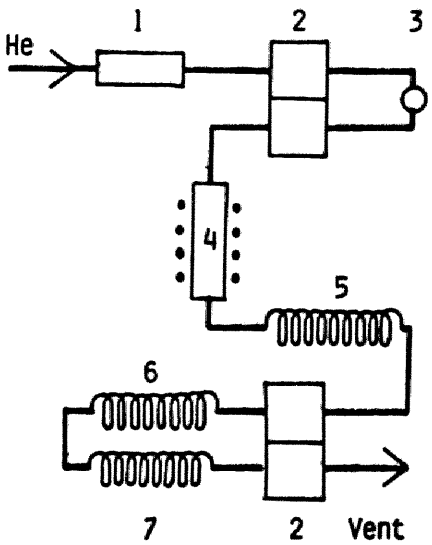

FIGURE 1 Reactor system for the pulse studies. (1) Reduced Cu-Zn catalyst for removing oxygen, (2) thermal-conductivity detector, (3) sample inlet, (4) reactor containing 250 mg of catalyst in an electrically heated Pyrex glass tube with an i.d. of 5 mm, (5) chromatographic column, PEG (2 m) + DOP (0.8 m), (6) chromatographic column, activated carbon (1.5 m), (7) empty tube.

TABLE 1
Activity and Selectivity of Sn-P Compared with SnO_2 and Solid-P[a]

Catalyst[b]	EB conversion (%)	ST selectivity (%)	Yield of $CO + CO_2$ (%)	$\frac{CO}{CO_2}$
SnO_2	17.7	39.1	4.6	0.09
Sn-P (P, 9 at. %)	32.1	83.3	2.1	0.95
Solid-P	16.5	88.5	0.7	0.86

[a] $P_{EB} : P_{O_2} : P_{H_2O} = 0.133 : 0.100 : 0.313$ atm.

[b] Catalysts are the same as those screened elsewhere [3].

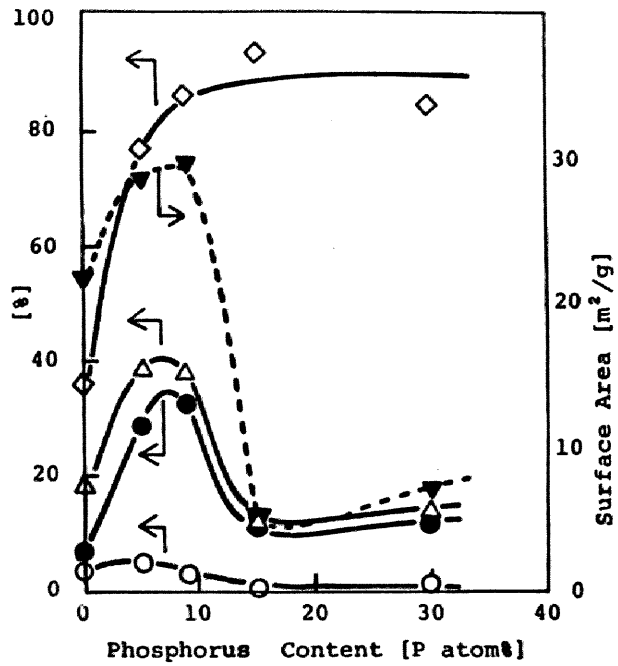

FIGURE 2 Effect of phosphoric acid contents on ST selectivity (◇), EB conversion (△), ST yield (●). CO + CO_2 yield (○), and BET surface area (▼). P_{EB} = 0.100 atm, P_{O_2} = 0.100 atm, P_{H_2O} = 0.313 atm.

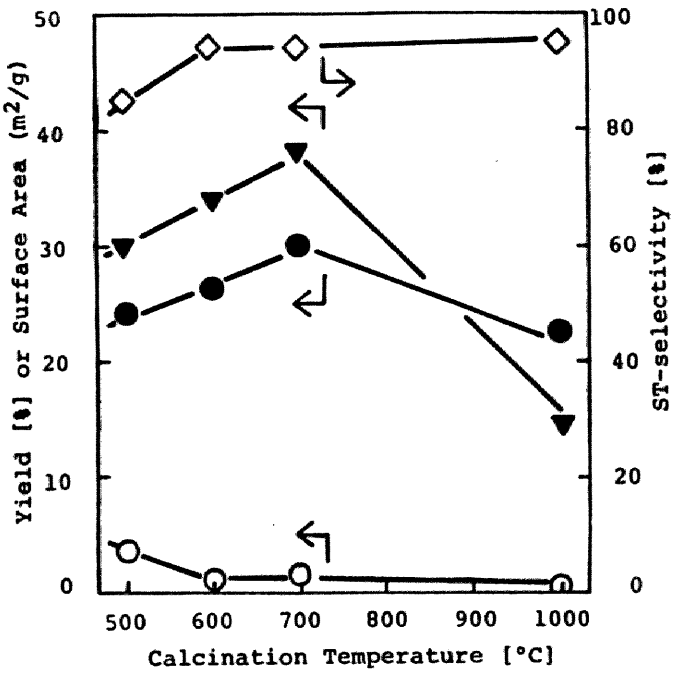

FIGURE 3 Effect of calcination temperature on Sn-P (P, 9 at. %) catalyst. P_{EB} = 0.200 atm, P_{O_2} = 0.100 atm, P_{H_2O} = 0.000 atm. For the symbols, see Figure 2.

was calcined at 500 °C for 2 h in air, and then calcined again at 600, 700, and 1000 °C for 2 h. High calcination temperatures resulted in low yields of carbon oxides and benzene. On the other hand, the ST yield and BET surface area increased until 700 °C and decreased above 700 °C. The ST selectivity also slightly increased.

Effect of Reaction Conditions

The effect of steam co-feeding in the flow reaction is shown in Table 2. The presence of steam reduced the total oxidation to one-third of that observed in the absence of steam. A corresponding amount of styrene was recovered in the presence of steam, which increased the selectivity without reducing the conversion of ethylbenzene.

The effect of the total feed rate (F) under the conditions, W = 4.5 g, P_{EB} = 0.20 atm, and P_{O_2} = 0.25 atm, is shown in Fig. 4. The decrease in W/F to zero resulted in ST selectivity as high as 100 %.

Reaction in the Differential Reactor

Oxygen partial pressure was varied with constant P_{EB} at 0.15 atm and ethylbenzene partial pressure was varied with constant P_{O_2} at 0.20 atm under the following conditions: reaction temperature = 450 °C, total feed = 290 mmol/h, and catalyst weight = 0.50 g (Sn-P, P = 9 at. % calcined at 1000 °C for 24 h). The catalyst was diluted with 8.0 g of fused alumina. The partial pressure was varied at random to avoid the influence of the change of catalytic activity with time. Under these conditions, the conversion is so low that the partial pressure in the catalyst bed can be regarded as constant. As shown in Fig. 5, the apparent reaction orders with respect to the pressure of ethylbenzene and oxygen were 0.60 and 0.47, respectively. Considering that the oxidation and oxidative dehydrogenation of olefins on the Bi-Mo catalyst have been reported to show reaction orders of 1.0 and 0.0, respectively, with respect to the pressure of olefin and oxygen, the coverage of oxygen on Sn-P can be considered to be not so high in the present reaction. This is similar to that reported on the oxidation of propylene on Sn-Sb catalyst, which too was said to depend on the oxygen partial pressure[7].

Change of Activity with Reaction Time

The activity increased gradually with time in these experiments on the Sn-P catalysts. This increment differed with P content, calcination temperature, and reaction conditions. For example, under the conditions: reaction temperature = 450 °C, W/F = 34.5 g-cat·h/mol, P_{EB} = 0.14 atm, P_{O_2} = 0.10 atm, P_{N_2} = 0.44 atm, and P_{H_2O} = 0.32 atm on Sn-P catalyst (P, 9 at. %, calcined at 600 °C for 2 h), the ST yield increased from 19.5 % at 1 h, to 23.0 % at 11 h, although the ST selectivity did not change as much.

TABLE 2

Effect of Steam on the Oxidative Dehydrogenation of Ethylbenzene[a]

P_{H_2O}[b] (atm)	Yield (%)				EB conversion (%)	ST selectivity (%)
	$CO + CO_2$	B	T	ST		
0.000	3.5	0.9	0.1	23.9	28.3	84.3
0.313	1.2	1.1	0.2	25.5	27.9	91.3

[a] Catalyst: Sn-P (P, 9 at. %) calcined at 500 °C for 2 h, 4.5 g.

[b] $P_{EB} : P_{O_2} = 0.200 : 0.100$ atm.

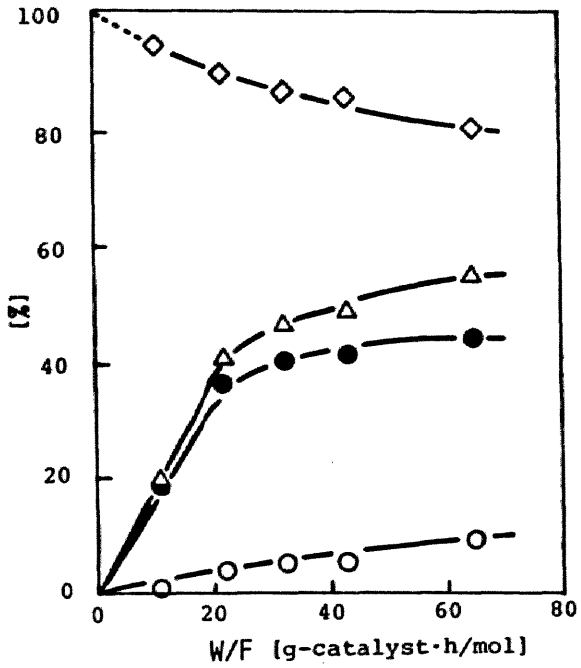

FIGURE 4 Effect of feed rate on Sn-P (P, 9 at. %) catalyst calcined at 1000 °C for 4 h. W = 4.5 g, P_{EB} = 0.200 atm, P_{O_2} = 0.25 atm, P_{H_2O} = 0.000 atm. For the symbols, see Figure 2.

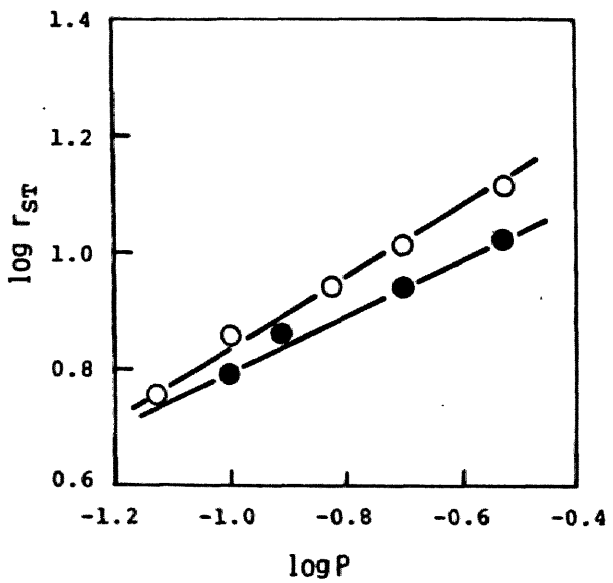

FIGURE 5 Effect of partial pressure on the rate of styrene formation in the differential reactor on Sn-P (P, 9 at. %) catalyst calcined at 1000 °C for 4 h. P_{O_2} was changed with P_{EB} = 0.15 atm (○) and P_{EB} was changed with P_{O_2} = 0.200 atm (●). W/F = 1.72 g·h/mol, P_{H_2O} = 0.000 atm.

Inhibition of Reaction

Figure 6 shows the competitive reaction of ethylbenzene with other aromatic hydrocarbons. The rate of styrene formation in the presence of hydrocarbons was compared with that in the absence of hydrocarbons as a function of the molar ratio of the hydrocarbon added to ethylbenzene. Alkylbenzenes,such as isopropylbenzene, o-xylene, toluene, and p-xylene,reduced the rate of styrene formation to one-half of that in their absence, while the presence of benzene did not change the rate. These results suggest the importance in this reaction, of alkyl groups which possess hydrogen at the α position.

Pulse Reactions

Styrene, benzene, and carbon oxides were formed when only ethylbenzene was pulsed on SnO_2 and Sn-P (P, 9 at. %) which were calcined at 500 °C. In the helium carrier which contained a slight amount of oxygen (about 20 ppm), styrene and the other products were formed by every pulse of ethylbenzene. However, as shown in Fig. 7, in the oxygen-free helium, products became undetectable after some pulses of ethylbenzene had been performed, but a pulse of oxygen (10 ml) regenerated the activity. In the cases of Bi-Mo shown in Fig. 8 and other oxide catalysts, the formation of styrene did not decrease steeply as these catalysts were reduced with pulses of ethylbenzene in the oxygen-free helium. This was similar to the case of oxygen-containing helium.

On the Solid-P catalyst, products from ethylbenzene pulse were not detected even after a pulse of oxygen (10 ml), irrespective of the presence or absence of about 20 ppm of oxygen in the carrier gas. However, the recovery of ethylbenzene was insufficient and the amount unrecovered was about 15 % for each pulse of ethylbenzene.

Effect of Treatment of SnO_2 with Phosphoric Acid

Tin dioxide was calcined at 1000 °C for 4 h and impregnated with phosphoric acid, boiled for 4 h, washed, and calcined at 500 °C for 2 h. As shown in Table 3, this catalyst showed high ST yield, high ST selectivity, and little combustion, similar to the Sn-P catalyst prepared from $Sn(OH)_2$ and phosphoric acid. As X-ray diffraction pattern and BET surface area of this catalyst showed little change, this treatment with phosphoric acid is considered to modify the surface of SnO_2.

Effect of Various Treatments of the Sn-P Catalyst

The various methods of chemical treatment of Sn-P (P, 15 at. %) calcined at 500 °C and the results of the reaction on these catalysts are shown in Table 4 along with their specific surface areas. Styrene yield and ST selectivity were not changed after being left in water for 3 days but increased a little after being left in boiling water for 11 h. Such increments in ST yield and ST selectivity were apparent after being treated in boiling 3.6 N HNO_3 for 10 h. These results are, considering the in-

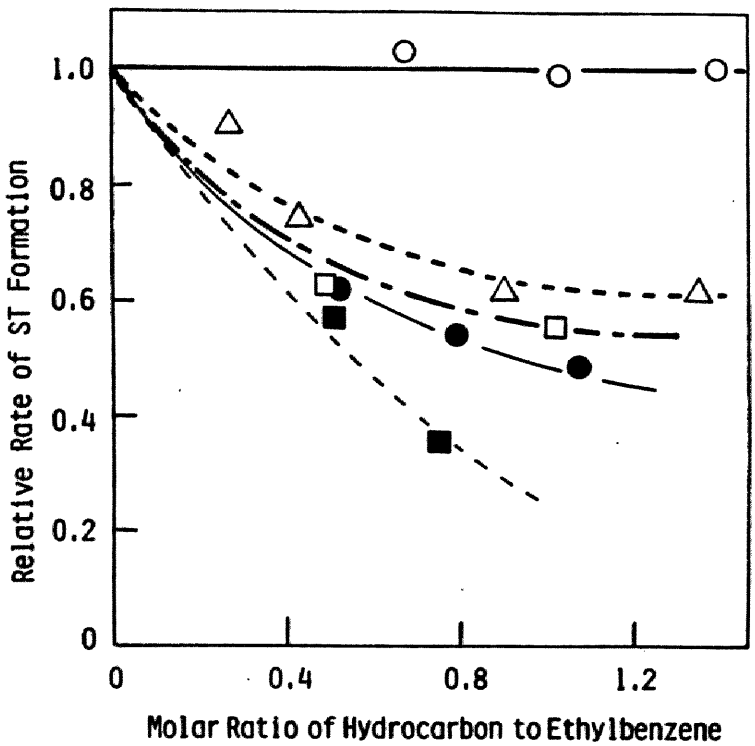

FIGURE 6 Competitive reaction on Sn-P (P, 9 at. %) catalyst calcined at 1000 °C for 4 h. Relative rate of styrene formation = r_{ST} in the presence of hydrocarbons/r_{ST} in the absence of hydrocarbons. W/F = 1.81 g·h/mol, P_{EB} = 0.100 atm, P_{O_2} = 0.100 atm, P_{H_2O} = 0.339 atm. Hydrocarbons: benzene (○), isopropylbenzene (△), *o*-xylene (□), toluene (●), *p*-xylene (■).

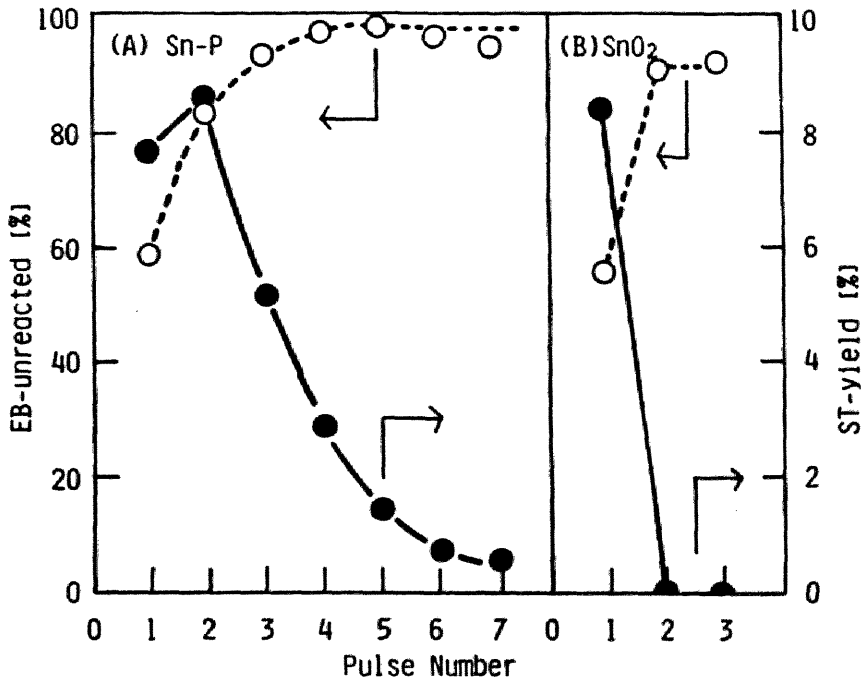

FIGURE 7 Effect of pulse number on Sn-P (P, 9 at. %) (A) and on SnO_2 (B) catalysts in the pulse reaction at 460 °C. Catalysts: calcined at 500 °C for 2 h, 250 mg. Pulse size: ethylbenzene 1 μl with 20-min interval. ST yield (●), EB unreacted (○) which was recovered after the pulse reaction.

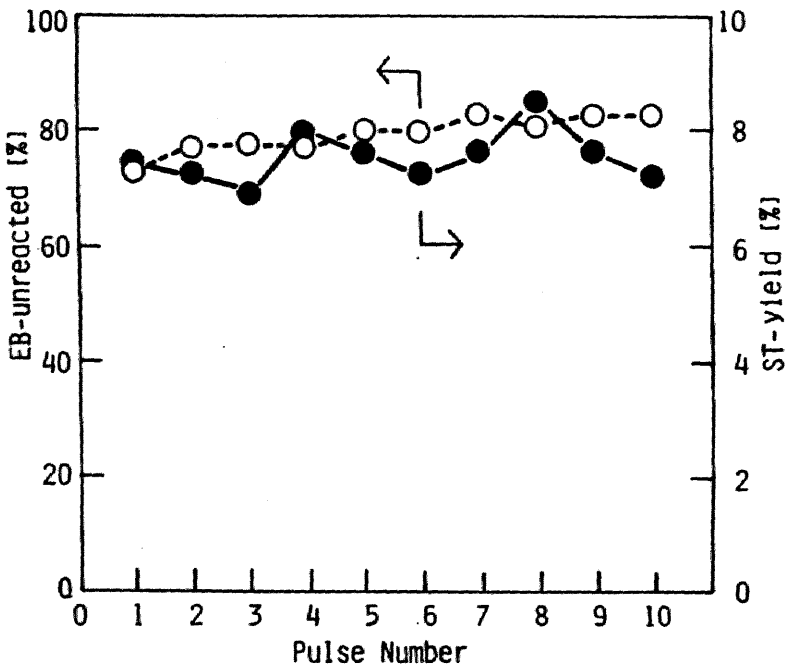

FIGURE 8 Effect of pulse number on Bi-Mo catalyst in the pulse reaction at 460 °C. For the reaction conditions and the symbols, see Fig. 7.

TABLE 3
Change of Tin Dioxide Surface Properties by Phosphoric Acid Treatment[a]

	SnO_2[b]	
	Untreated	Treated by H_3PO_4
EB conversion (%)	15.3	17.4
ST yield (%)	4.92	14.9
B yield (%)	5.09	0.64
CO + CO_2 yield (%)	5.24	1.68
ST selectivity (%)	32.2	85.6
Surface area (m^2/g)	4.1	4.0

a W/F = 15.5 g·h/mol, T = 450 °C, $P_{EB} : P_{O_2} : P_{N_2} : P_{H_2O}$ = 0.14:0.14:0.40:0.32 atm.
b Precalcined at 1000 °C for 4 h, W = 4.5 g.

TABLE 4
Effect of Elimination of Phosphoric Acid by Various Treatments[a]

Treatment	ST yield (%)	ST selectivity (%)	Surface area (m^2/g)
Untreated	13.0	87.5	4.65
In water for 3 days	13.2	87.7	5.04
In boiling water for 11 h	15.7	89.4	5.61
In boiling 3.6 N HNO_3 for 10 h	21.9	92.1	6.38

a Catalyst: Sn-P (P, 15 at.%) calcined at 500 °C, W/F = 15.5 g·h/mol, $P_{EB} : P_{O_2} : P_{N_2} : P_{H_2O}$ = 0.071:0.14:0.47:0.32 atm.

crease of BET surface area and elution of phosphoric acid from the catalyst detected by magnesia mixture, attributable to the elimination of excess phosphoric acid which covered the active surface.

The results of treatment of Sn-P (P, 9 at. %) calcined at 600 and 700 °C are shown in Table 5. The treatment in boiling 3.6 N HNO_3 increased ST yield from 13.2 and 14.2 % to 16.1 and 17.2 % on the catalysts calcined at 600 and 700 °C, respectively. Styrene-yield on the sample calcined at 700 °C was still higher after the HNO_3 treatment than that on the sample calcined at 600 °C. The effect of HNO_3 treatment before the reaction and that after the reaction for 11 h were relatively the same.

X-Ray Diffraction Experiment

In the X-ray diffraction patterns of SnO_2 and Sn-P (P, 9 at. %) catalysts calcined at various temperatures, lines other than SnO_2 could not be observed and changes in the lattice constant were not observed. The crystal size D and strain η calculated from the diffraction patterns are shown in Table 6. When the Sn-P catalyst was calcined at 700 °C, the crystal size did not change appreciably, but the strain decreased and the specific surface area increased as shown in Fig. 3. When calcined at 1000 °C, the crystal size increased and the surface area decreased. In the case of the SnO_2 catalyst, the growth of the crystal was greater and the strain was less than those of the Sn-P catalysts.

Fluorescent X-Ray Experiment

The intensity of phosphorus in the fluorescent X-ray spectra of Sn-P (P. 9 at. %) catalysts calcined at 600 °C is shown in Table 5. The amount of phosphorus decreased after the HNO_3 treatment to 80 % of the fresh state, and the same amount of the decrement was observed by the HNO_3 treatment of the sample after being used in the flow reaction.

Behavior of Crystalline Tin Phosphate

For further investigation on the cooperative effect of tin and phosphorus, oxidative dehydrogenation of ethylbenzene on the crystalline tin(Ⅳ) phosphate (C-SnP) was carried out. The activity of c-SnP was a little lower than that of the Sn-P catalyst and the selectivity was as high as that of the latter. As shown in Fig. 9, the ST yield on the uncalcined c-SnP increased with time. Reoxidation of c-SnP resulted in a further increase in the ST yield. On the other hand, the ST yield on c-SnP calcined at 550 °C for 2 h remained constant and was almost equivalent to that on the uncalcined c-SnP after the reoxidation.

DISCUSSION

Reaction Mechanism

A π-allyl mechanism is generally accepted in the oxidation of olefins. Sachtler and

TABLE 5
Change of Catalysts by Nitric Acid Treatment[a]

Calcination (°C)	Treatment	ST yield (%)	ST selectivity (%)	P amount[b] (a.u.)
600	Untreated	13.2	94.1	1801
	Boiling in 3.6 N HNO_3 for 23 h	16.1	88.6	1436
	Boiling in 3.6 N HNO_3 for 23 h after 11 h reaction	14.2	89.9	1520
700	Untreated	14.2	95.4	—
	Boiling in 3.6 N HNO_3 for 23 h	17.4	89.7	—

[a] Catalyst: Sn-P (P, 9 at. %), T = 450 °C, W/F = 15.5 g·h/mol, $P_{EB} : P_{O_2} : P_{N_2} : P_{H_2O}$ = 0.14 : 0.10 : 0.44 : 0.32 atm.

[b] Intensity of phosphorus (PKα) in the fluorescent X-ray spectrum.

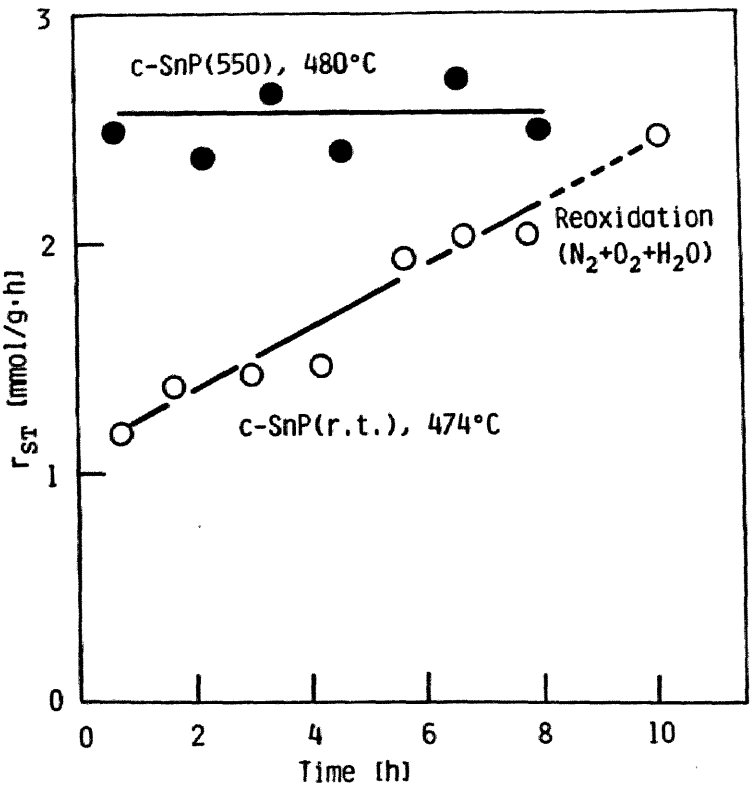

FIGURE 9 Change of activity with reaction time on c-SnP catalyst. P_{EB} = 0.158 atm, P_{O_2} = 0.196 atm, P_{H_2O} = 0.217 atm. T = 480 °C for c-SnP calcined at 550 °C for 2 h (●); T = 474 °C for c-SnP uncalcined (r.t.) (○).

TABLE 6
Size and Strain of SnO_2 Crystals in Catalysts[a]

Catalyst	Calcination Temp. (°C)	Crystal Size, D (Å)	Strain η
Sn-P	500	170	0.0045
(P, 9 at. %)	700	180	0.0019
	1000	350	0.0010
$Sn-O_2$	500	280	0.0022
	1000	2600	0.0006
	500[b]	240	0.0040

[a] X-Ray diffraction patterns were obtained by Rigaku Denki diffractometer, Model Geigerflex with CuKα radiation.
[b] Boiled in H_3PO_4.

DeBoer have reported that the rate determining step of propylene oxidation is the dissociative adsorption of propylene by the cleavage of the C-H bond in the methyl group of propylene in the ^{14}C-tracer studies[8]. Similar results have been obtained on Cu_2O catalyst[9] and phosphorus-containing Bi-Mo catalyst[10,11]. The reactions of deuterated propylene on Cu_2O, Bi-Mo, and U-Sb also suggest the existence of the π-allyl intermediate[12-14]. Such an inter mediate has also been observed on ZnO catalyst by ir studies[15]. A similar allylic intermediate has been proposed in the oxidative dehydrogenation of butenes on Bi Mo[16] and ferrite catalysts[17] and the abstraction of a hydrogen in the allyl position has been concluded to determine the rate of this reaction.

The competitive reaction also suggests the importance of the α hydrogen of ethylbenzene. As shown in Fig. 6, the relative rate of ST formation in the inhibition of the reaction decreased with some aromatic compounds but not with benzene. The relative rate decreased with the increment of the amount of the inhibitor and decreased in the order: None = benzene > isopropylbenzene > *o*-xylene > toluene > *p*-xylene. This order of inhibition is in good agreement with the enthalpies of heterolysis of hydrogen as follows (kcal/mol): phenyl(300) > benzyl(247) > *p*-methylbenzyl(240)[18]. Inhibitors, such as toluene and xylenes do not react in this reaction, showing that this inhibition

is due to the competitive adsorption of ethylbenzene and the inhibitor. These results suggest that ethylbenzene is adsorbed by the adstraction of α hydrogen on the catalyst.

In the oxidative dehydrogenation of ethylbenzene, one of the most probable mechanisms is one which consists of abstraction of hydrogen from ethylbenzene by the lattice oxygen on the surface to form styrene, and reoxidation of the catalyst by gas-phase oxygen[19].

$$EB + [O] \xrightarrow{k_1} ST + [\ ], \tag{1}$$

$$[\ ] + \frac{1}{2} O_2 \xrightarrow{k_2} [O], \tag{2}$$

where [O] represents the lattice oxygen at the surface layer of the catalyst because the bulk oxygen has been reported to be inactive[20], which is in good agreement with the results of pulse reaction shown in Fig. 7. The rates of (1) and (2) are

$$r_1 = k_1 P_{EB} \theta, \tag{3}$$

$$r_2 = k_2 P_{O_2} (1 - \theta). \tag{4}$$

As $r_1 = r_2$ in the steady state, the rate of styrene formation is given as

$$r = \frac{k_1 K_2 P_{EB} P_{O_2}}{K_1 P_{EB} + k_2 P_{O_2}}, \tag{5}$$

$$\frac{1}{r} = \frac{1}{k_1 P_{EB}} + \frac{1}{k_2 P_{O_2}}. \tag{6}$$

The reciprocal relationship between 1/r and 1/P is shown in Fig. 10. The rate constants k_1 and k_2 calculated from the slope of the plot of 1/r against $1/P_{O_2}$ in Fig. 10 were 108 and 101, and were 101 and 109 (mmol/g-cat·atm·h) from the plot of 1/r against $1/P_{EB}$. The rate constants from both plots agreed very well with one another and oxidative dehydrogenation of ethylbenzene proceeds along the proposed reduction-oxidation mechanism.

The fraction of oxidized site (θ) was about 0.5 so that the surface of the catalyst was more reduced than that of the Bi-Mo catalyst, θ of which has been reported to be about 1.

Effect of Steam

The apparent effect, shown in Table 2, of the presence of steam is to release the styrene formed to the gas phase without side reactions. Steam may inhibit the readsorption of styrene on the catalyst which results in the inhibition of further reaction of styrene to increase the selectivity.

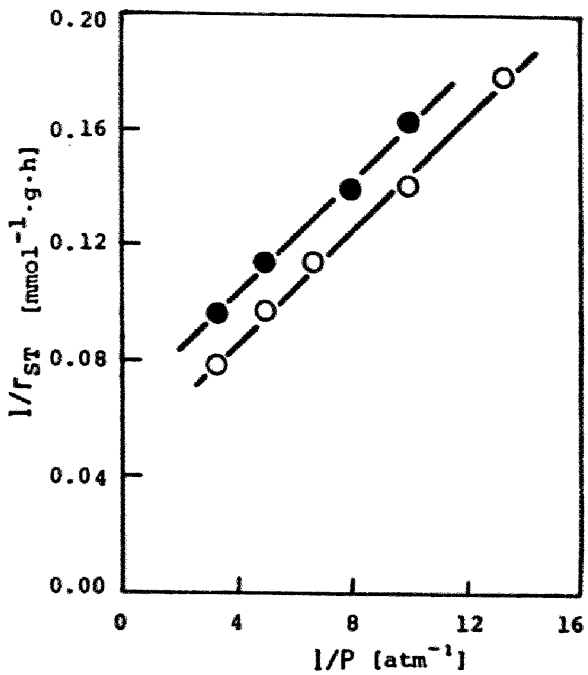

FIGURE 10 Reciprocal relations between rate and partial pressure. For the reaction conditions and the symbols, see Figure 8.

Effect of Phosphorus

One of the reasons for high activity of Sn-P is the inhibition of the growth of SnO_2 crystal by the addition of phosphorus as shown in Table 6. The crystal size of SnO_2 increased up to 280 and 2600 Å, when $Sn(OH)_2$ was calcined at 500 and 1000°C, respectively. With an addition of 9 at. % of phosphoric acid, the crystal size of SnO_2 was 170 Å when calcined at 500 °C and was only 350 Å after calcination at 1000 °C.

On the other hand, not only the catalytic activity, but also the yield of byproducts and the CO/CO_2 ratio were different between Sn-P and SnO_2 catalysts.

As is shown in Fig. 4, decreasing W/F to zero results in 100 % ST selectivity on the Sn-P catalyst, but the selectivity does not appear to reach 100 % on the SnO_2 catalyst. This shows that one of the effects of phosphorus is to inhibit the reaction to form byproducts from ethylbenzene, because the byproducts are formed from ethylbenzene and styrene in the case of the SnO_2 catalyst, but mainly from styrene in the case of the Sn-P catalyst. These results show the essential difference between the effective sites of the SnO_2 and Sn-P catalysts.

The X-ray diffraction studies showed that phosphorus does not exist in the SnO_2 crystal but rather on the surface of the SnO_2 crystal, because other diffraction peaks except for SnO_2 were not detected: Nor was any change in the lattice constant in any Sn-P catalyst detected.

The increase of activity and selectivity by water or nitric acid treatments indicates that the effective site did not dissolve into the water or the nitric acid, while an inactive substance covering the catalyst surface is removed. $Sn_2O(PO_4)_2$ prepared from tin(II) chloride treated by phosphoric acid is known not to be dissolved in nitric acid[21]. The excess methaphosphoric acid is eliminated into the liquid phase which was detected by magnesia solution and the amount of phosphorus decreased was about 20 % as shown in Table 5. The phosphoric acid treatment of SnO_2, prepared by the calcination of $Sn(OH)_2$, changed the selectivity despite the constant value of the BET surface area (Table 3) and the catalytic action resembles, but is a little lower in yield and selectivity, that of catalysts which were prepared by adding the phosphoric acid directly into $Sn(OH)_2$. The catalytic activity of Sn-P COMPD prepared from tin(II) chloride and phosphoric acid was not so high, while the selectivity was satisfactory[3]. Moreover, the increase in activity and selectivity by the removal of free phosphoric acid shows that the free phosphoric acid on the catalyst surface is not the active component. From these results, the effective active site of Sn-P catalyst can be attributed to the surface Sn-P compounds such as tin phosphate.

Origin of Change in Activity with Time and Calcination Temperature

Reasons for the increase of activity with time in the reaction or with the calcination temperature could be (1) the vaporization of free phosphoric acid on the surface to make the active site exposed and (2) the reaction of SnO_2 with phosphoric acid to

increase the amount of the active Sn-P compounds on the surface.

Styrene yield on fresh catalyst was 13.2 % and nitric acid treatment increased the value to 16.0 %. Nitric acid treatment of the catalyst which had been used for 11 h in the flow reaction gave a 16.1 % ST yield. This is in good agreement with the P content determined by fluorescent X-ray studies as shown in Table 5. These results indicate that the activity increases due to reason (1), but that the reaction of SnO_2 with phosphoric acid to form active compounds does not occur during the oxidative dehydrogenation for 11 h.

Comparing the catalysts calcined at 600 and 700 °C (Table 4), the crystal sizes were constant and the latter catalyst showed a higher ST yield even after the removal of free phosphoric acid by nitric acid treatment. This increment with the increase of calcination temperature is attributable to reason (2) and will be discussed in the following section.

Behavior of Crystalline Tin Phosphate

As the effective active site on the Sn-P catalyst is attributed to surface compounds such as tin phosphate, the details of the catalytic behavior of c-SnP were studied.

The results of the c-SnP catalysts shown in Fig. 9 indicate that the increase in the ST yield on the uncalcined c-SnP is caused by the change of the structure of the c-SnP during the reaction. This change could be assumed not to be caused by the loss of free phosphoric acid due to the following reasons: (1) c-SnP is considered not to contain excess phosphoric acid on the surface, (2) loss of phosphorus is little in the case of c-ZrP catalyst[22]. The X-ray diffraction pattern of the uncalcined c-SnP used in the reaction was different from that of the fresh c-SnP, but identical to that of the calcined c-SnP. The specific reaction rate of styrene formation on the calcined c-SnP was 0.30 and 0.38 $mmol \cdot h^{-1} \cdot m^{-2}$ at 450 and 480 °C, respectively. These values are in good agreement with those on Sn-P catalysts calcined at 600 °C: 0.27-0.32 $mmol \cdot h^{-1} \cdot m^{-2}$ at 450 °C. This result shows that the surface structure of Sn-P catalyst is similar to that of the calcined c-SnP.

At present, the crystal structure of c-SnP is not clear, but the similarities in the preparation method and the X-ray diffraction pattern suggest that the structure of c-SnP also is similar to that of c-ZrP[23]. Crystalline zirconium phosphate is dehydrated in two steps[22,24] the crystalline water is dehydrated at 130 °C and the structure water is dehydrated at 500-600 °C. DSC measurement was carried out to examine the dehydration process of c-SnP. The first mole of water was dehydrated at 130 °C similarly to c-ZrP. But the dehydration of the second mole of water appeared to start at a lower temperature than c-ZrP. The dehydration was almost complete at 550 °C. Usually, the dehydration of orthophosphate is accompanied by the condensation of phosphate to form pyrophosphate. However, the X-ray diffraction pattern of the calcined c-SnP was different from that of tin pyrophosphate, but similar to that of the unidentified

phase of c-ZrP obtained by the calcination of c-ZrP at 600 °C [22,24]. Thus, c-SnP calcined at 550 °C can be regarded as the dehydrated but noncondensed state. Such an unstable state would result in the formation of new active sites.

As described elsewhere[22] both uncalcined and calcined c-ZrP have the acid site with the acid strength of $+4.8 > H_0 > +3.3$ and $-3.0 > H_0 > -5.6$, and the acidity is attributed to the phosphate group. Thus, the calcination does not appear to modify the phosphate group. The same would be true in the case of c-SnP. The calcination of c-SnP would not modify the phosphate group which is the origin of the acidity, but would modify the state of the tin atom to form the new active site which may be active oxygen.

Role of Tin and Phosphorus Component

As mentioned above, styrene was formed from the pulse of ethylbenzene without gas-phase oxygen, and styrene was not formed after several pulses of ethylbenzene on SnO_2 and Sn-P catalysts in oxygen-free helium. These facts show that the active oxygen species are held on the catalyst even in the absence of gaseous oxygen and that the surface oxygen, once consumed by the reaction, is not supplied by the diffusion of bulk oxygen. On the other hand, the formation of styrene by every pulse of ethylbenzene in the oxygen-containing helium carrier shows that the surface oxygen once consumed by the reaction, is supplied by the adsorption of gaseous oxygen and that these catalysts can activate oxygen at very low partial pressure such as 20 ppm. This is probably related to the large values of 70.4 and 62.7 kcal/mol in the change of enthalpy and Gibbs free energy, respectively, in the change: $SnO \longrightarrow SnO_2$.

On the Solid-P catalyst, reaction did not occur but the constant amount of unrecovered ethylbenzene was observed with every pulse of ethylbenzene. This shows the relatively strong reversible adsorption of ethylbenzene and the weak adsorption of oxygen [25].

In the flow of oxygen-free helium, combustion as well as styrene formation was apparent in the first pulse of ethylbenzene on SnO_2 catalyst, but the activity disappeared by the next pulse of ethylbenzene. On the other hand, styrene was formed selectively in the several pulses of ethylbenzene on the Sn-P catalysts. These results agree with the results of the differential conditions. That is, the total oxidation occurs from styrene once formed by the oxidative dehydrogenation on Sn-P catalysts while it occurs both from styrene and ethylbenzene on SnO_2 catalyst. These results suggest that the addition of phosphorus not only produces an enhancement of the activation of ethylbenzene but is also effective in controlling the nature of the active oxygen which is related to basicity. The strongly activated oxygen on the SnO_2 catalyst, which is active enough for the total oxidation, would be weakened for suitable strength to abstract the hydrogen from ethylbenzene and not strong enough for combustion by the addition of phosphorus.

On the Sn-P catalyst, it seems that Sn, the basic component, contributes to the in-

crease of activity by the adsorption of oxygen and the supply of it to the surface reaction and that P, the acidic component, contributes to the adsorption of ethylbenzene in the active form for this reaction. Also, taking into account the results of c-SnP catalyst in addition to the above discussion, one may consider the mutual interaction of Sn and P to effect an increase in the selectivity of the oxidative dehydrogenation reaction.

This explains well the difference in the catalytic behavior of SnO_2, Solid-P, and Sn-P in the continuous flow reaction.

It is noteworthy that in this study as well as in the screening study[3] the acid-base properties of the catalyst have been shown to modify the activity and the selectivity. Hence these relationships could help to clarify the reaction mechanism and to design effective catalysts[26]. The details of the relationships between the catalytic behavior and the acid-base properties will be discussed in subsequent chapters.

CONCLUSION

The addition of phosphorus to SnO_2 catalyst increased the activity and selectivity and effected the prevention of the side reaction from ethylbenzene and the inhibition of the growth of the SnO_2 crystal. The activity and selectivity varied with the catalyst composition and the calcination temperature, and were maximized at a 10-to-1 Sn/P ratio and at a calcination temperature of 700 °C. They also increased with some chemical treatments. HNO_3 solution did not dissolve the active site but dissolved away the excess free phosphoric acid which was concentrated at the surface and convered the active site. Such an active site was also generated by the phosphoric acid treatment of the SnO_2 surface. The similarity of the catalytic behavior of Sn-P catalyst to that of crystalline tin(Ⅳ) phosphate indicates the active component to be a type of Sn-P compound. A reduction-oxidation mechanism is proposed on the basis of kinetic data in a differential flow reactor. It is suggested that tin, the basic component, activates oxygen and that phosphorus, the acidic component, activates ethylbenzene.

ACKNOWLEDGMENTS

The research was supported in part by a grant from the Asahi Glass Foundation for Contribution to Industrial Technology. The authors thank Mr. H. Hanai for some of the c-SnP studies.

REFERENCES

1 W.W. Kaeding, Catal. Rev. 8 (1974) 307.
2 Y. Murakami, M. Niwa, and H. Uchida, Kogyo Kagaku Zasshi 72 (1969) 2183.
3 Y. Murakami, K. Iwayama, H. Uchida, T. Hattori, and T. Tagawa, Appl. Catal. in press, Chapter 2.
4 U. Costantino, and A. Gasperoni, J. Chromatogr. 51 (1970) 289.
5 Y. Murakami, Bull. Chem. Soc. Japan 32 (1959) 316.

6 Y. Murakami, Shokubai 7 (1965) 120.
7 D.J. Hucknall, "Selective Oxidation of Hydrocarbons," p. 44. Academic Press, New York, 1974.
8 W.M.H. Sachtler, and N.H. Deboer, in "proceedings, 3rd International Congress on Catalysis, Amsterdam, 1964," p. 252. North-Holland, Amsterdam, 1965.
9 H.H. Voge, C.D. Wagner, and D.P. Stevenson, J. Catal. 2 (1963) 58.
10 C.C. McCain, G. Gough, and G.W. Godin, Nature 198 (1963) 989.
11 T. Dozono, D.W. Thomas, and H. Wise, J. Chem. Soc. Faraday Trans. I 69 (1973) 620.
12 C.R. Adams, and T.J. Jennings, J. Catal. 2 (1963) 63.
13 C.R. Adams, and T.J. Jennings, J. Catal.3 (1964) 549.
14 R.K. Grasselli, and D.D. Suresh, J. Catal. 25 (1972) 273.
15 A.L. Dent, and R.J. Kokes, J. Amer. Chem. Soc. 92 (1970) 6709, 6718: Z. Dolejsék, and J. Nováková, J. Catal. 37 (1975) 540.
16 Ph.A. Batist, B.C. Lippens, and G.C.A. Schuit, Catal. 5 (1966) 55.
17 W.R. Cares, and J.W. Hightower, J. Catal. 23 (1971) 193: M.A. Gibson, and J.W. Hightower, J. Catal. 41 (1976) 420.
18 J. Hine, "Structural Effects of Equilibria in Organic Chemistry," p. 219. Wiley, New York, 1975.
19 J. Hanuza, and B. Jeżowska-Trzebiatowksa, J. Mol. Catal. 4 (1978) 271.
20 I. Aso, M. Nakao, M. Egashira, N. Yamazoe, and T. Seiyama, Shokubai 18 (1976) 106.
21 J.W. Mellor, "Comprehensive Treatise in Inorganic and Theoretical Chemistry," Vol. VII, p. 482. Longmans, London, 1927.
22 T. Hattori, A. Ishiguro, and Y. Murakami, J. Inorg. Nucl. Chem 40 (1978) 1107: Nippon Kagaku Kaishi, (1977) 761.
23 A. Clearfield, and J.A. Stynes, J. Inorg. Nucl. Chem 26 (1964) 117.
24 A. Clearfield, and G.D. Smith, Inorg. Chem. 8 (1969) 431.
25 Y. Murakami, and K. Hayashi, Kogyo Kagaku Zasshi 72 (1969) 1038.
26 D.B. Dadyburjor, S.S. Jewur. and E. Ruckenstein, Catal. Rev. 19 (1979) 293.

Chapter 4

CATALYTIC ACTIVITY AND ACID AND BASE PROPERTIES OF Na-SiO_2·Al_2O_3

SYNOPSIS

The oxidative dehydrogenation of ethylbenzene on a series of SiO_2·Al_2O_3 catalysts has been carried out by continuous flow reaction. The addition of sodium has resulted in an increase of activity and a maximum yield of styrene was observed at the value of 17 μmol of Na exchanged/g-cat. The same increase in activity was observed in the pulse reaction. The pulse reaction shows that ethylbenzene is adsorbed reversibly on the catalyst and that active oxygen species is also reversibly adsorbed. Such changes in oxidation activity have been explained by the cooperative effect of the acid and base sites of the catalyst. The acid-base titration shows that the addition of one Na ion increases the number of new acid ($1.5 > Ho > -5.6$) and base ($17.2 < pKa < 26.5$) sites tremendously. The acid sites of Ho between 1.5 and -5.6 are proven to be the active sites to adsorb ethylbenzene reversibly, whose oxidation, on the other hand, occurs on the base sites of pKa between 17.2 and 26.5. The pulse and flow reactions indicate that these acid-base sites are still effective even after carbonaceous materials have deposited.

INTRODUCTION

In the previous chapters [1,2], SnO_2-P_2O_5 catalysts showed the highest activity and the highest selectivity in the oxidative dehydrogenation of ethylbenzene to styrene. In the pulse reaction of ethylbenzene on the SnO_2 catalyst, the non-selective oxidation proceeded, while on the solid-phosphoric acid catalyst, styrene was not formed but instead the unrecovery of ethylbenzene was observed. The addition of phosphorus to SnO_2 suppressed the total oxidation reaction and enhanced the formation of styrene. These results suggest the cooperative effect of the acid-base properties of the catalysts; the role of the basic component, SnO_2, is to activate oxygen and the role of the acidic component, P_2O_5, is to adsorb ethylbenzene in a suitable activated form.

Such an activation of aromatic compounds on the acid site has also been shown by quantum mechanical calculations[3].

It is important, therefore, to treat the acidity and basicity of the catalysts together with the reaction mechanism of the partial oxidation reactions. The investigation of the detailed role of acid and base sites in the oxidative dehydrogenation of ethylbenzene will then show not only the reaction mechanism of the present reaction but also the general role of acid and base sites in other partial oxidation reactions. Some results in the studies of the oxidation reactions suggest the participation of acid sites[4,5] and of base sites[6] in the partial oxidation reactions. The selectivity of the oxidation reactions is also said to be effected by the acid and base properties of the catalysts[7,8,9,10,11]. Correlations between the oxidation activity and the amount of acid and/or base sites have been reported in many reactions by Ai[10]. However, the detail of the role of the acid and base sites in a molecular aspect is still not clear.

A silica-alumina catalyst is a typical solid acid catalyst and shows an activity only in the oxidative dehydrogenation of ethylbenzene and not of olefinic compounds [12]. Therefore, this catalyst meets the purpose of this study to investigate the role of the acid and base sites on the oxidation reaction in a molecular aspect.

In the present work, the nature of the active site in the reaction of ethylbenzene on a silica-alumina catalyst is investigated. For this purpose, $SiO_2 \cdot Al_2O_3$ is treated with sodium acetate to control the acid and base properties of the catalyst. Then the effects of sodium on the catalytic activity and on the acid-base properties are studied on such sodium exchanged silica alumina catalysts. The roles of the acid and base sites in the oxidation reaction are discussed and the ranges of the acid and base strength effective for the oxidative dehydrogenation are determined.

EXPERIMENTAL

Catalysts

Sodium exchanged silica-alumina catalysts(Na-SiAl) were prepared by the ion exchange of the $SiO_2 \cdot Al_2O_3$(Nikki Chemical Co. N632(H), Al_2O_3, 25 % referred to as the original-SiAl or 0.0Na-SiAl) with sodium acetate. The original-SiAl was precalcined at 773 K for 3 h in air, and was then dipped into an aqueous solution of NaOAc for 3 days at room temperature. The content of NaOAc in the aqueous solution was varied in each case. The resultant $SiO_2 \cdot Al_2O_3$ was washed thoroughly with water, dried at 393 K for 1 day, and calcined at 773 K for 3 h in air. The Na content was determined by atomic absorption spectroscopy. The surface area was determined by the conventional BET method. The Na content written at the head of the name of the catalyst in μmol/g-cat corresponds to the increment of Na content due to the ion exchange to the amount of Na on the original-SiAl. For example, 17Na-SiAl contains 17 μmol of Na in addition to the 24 μmol of Na/g-cat on the original-SiAl. The Na content and the BET surface area of the catalysts are shown in Table 1.

Procedure

The catalytic activity was measured by using a conventional continuous flow reactor at atmospheric pressure. The catalyst particles were dispersed in fused alumina particles to prevent a local increase of the temperature and were packed in a reactor made of Pyrex glass. The reactor was installed in a fluidized sand bath which was heated electrically, in order to heat the catalyst bed uniformly. The liquid products were collected by traps cooled with ice and dry-ice, and analyzed by gas chromatography with a 1.5m PEG column and a 1m DOP column at 383 K. The gaseous products were instead analyzed by gas chromatography with a 80 cm Polapack Q column and a 1.5m MS-13X column at room temperature. Conversion of ethylbenzene was calculated on the basis of ethylbenzene fed. In each of the following figures, the reaction conditions, such as catalyst weight(W), feed rate(F), reaction temperature(T) and partial pressure of ethylbenzene(P_{EB}), oxygen(P_{O_2}), steam(P_{H_2O}), and nitrogen(P_{N_2}) are indicated.

Acid-Base properties

Acid and base distributions of the catalysts precalcined at 773 K for 2 h in air were determined by titrating with n-butyl amine [13,14] and benzoic acid[13,15] using the following indicators; Neutral red (Ho = 6.8), 4-benzeneazodiphenylamine (1.5), benzalacetophenone (-5.6), Antraquinone (-8.2), and 2,4-dinitrotoluene (-12.7) for acidities, and 4-chlorianiline (pKa = 26.5), 4-chloro-2-nitroaniline (17.2), and phenolphthalein (9.3) for basicities.

Pulse Reaction

The pulse reaction of the oxidative dehydrogenation of ethylbenzene was carried out with a conventional pulse reaction apparatus. Helium was used as a carrier gas after being purified by the passage through a silica gel trap at 77 K. The effluents were analyzed by gas chromatography with the same columns as in the case of the flow reaction. 0.2 g of catalyst was packed in a Pyrex glass tubing with an inside diameter of 4 mm, and was calcined at 768 K for 2 h in a flow of oxygen, then at 718 K for 1 h in a flow of carrier gas in the case of the fresh catalyst, immediately before the pulse reaction. In the case of the catalyst used in the flow reaction(used catalyst), which contained coke, the calcination was performed only in a flow of carrier gas at 718 K for 1 h. The pulse reaction experiments were carried out at 718 K with a helium flow rate of 0.74 cm^3/s in the following sequence. (I) 1 mm^3 of ethylbenzene only was injected (EB pulse). (II) 2 cm^3 of oxygen was injected and after 10 minutes, 1 mm^3 of ethylbenzene was injected (O_2 EB pulse). (III) 2 cm^3 of oxygen and 1 mm^3 of ethylbenzene were injected simultaneously (EB + O_2). In order to remove the coke deposited on the catalyst the catalyst was reoxidized after these pulse reactions. The reoxidation was performed in a flow of air at 718 K for 1 h and in a flow of oxygen at 768 K for 2 h in the case of the fresh catalyst, and the reoxidation in the flow of oxygen was prolonged for an additional 4 h at 768 K in the case of the used catalyst

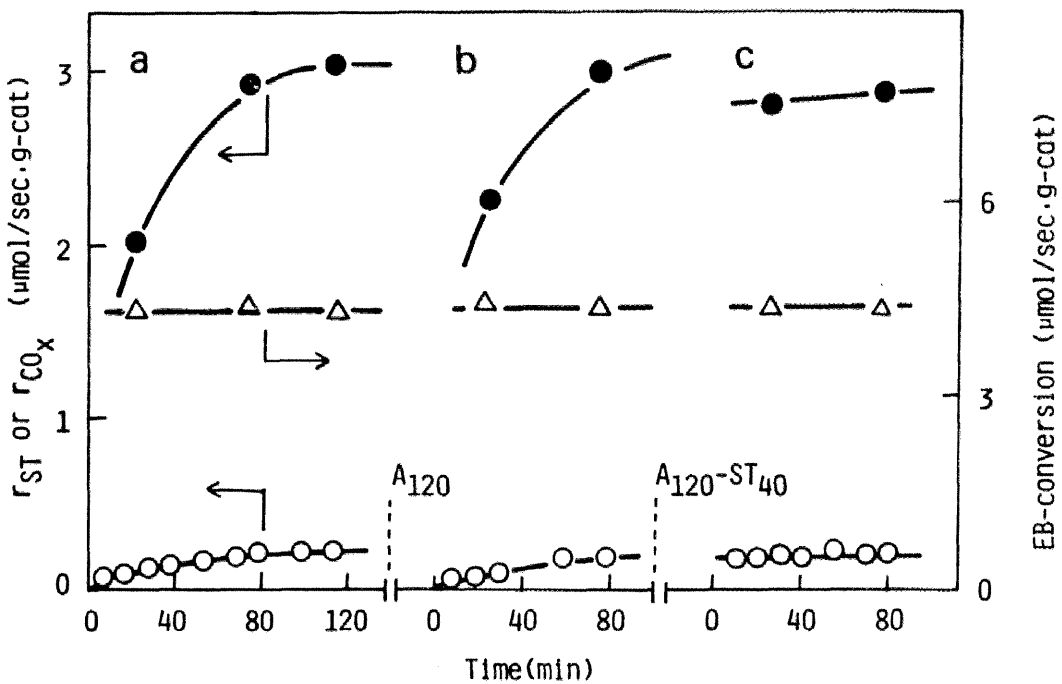

FIGURE 1 Time course of the reaction of ethylbenzene on original-SiAl catalyst. T = 723 K, W = 0.300 g, F = 290 mmol/h, P_{EB} = 0.143 atm, P_{O_2} = 0.050 atm, P_{H_2O} = 0.322 atm, and P_{N_2} = 0.485 atm. F_{EB} = 38.4 μmol/g-cat·s. △, EB conversion; ●, r_{ST}; ○, r_{CO_x}. A_{120}, reoxidation of catalyst with air at 723 K for 120 minutes; A_{120}-ST_{40}, styrene treatment of the catalyst in the absence of oxygen for 40 minutes after the reoxidation.

which had been used in the continuous flow experiment before the pulse reaction. The pulse reactions I, II, and III were carried out again on the reoxidized catalyst. Besides the standard pulse experiment mentioned above, other pulse reactions were carried out. The procedures of the experiment are described with their corresponding results.

RESULTS

Flow Reaction

Figure 1 shows the respective changes in the conversion of ethylbenzene, in the rates of formation of styrene (r_{ST}) and carbon oxides(r_{CO_x}) with time on stream. The rate of styrene formation increased gradually and reached the stationary state. A similar tendency was observed in the rate of CO and CO_2 formation. However, it is noteworthy that, in Fig. 1-a, the conversion of ethylbenzene remained constant. The formations of coke on the catalyst, a slight amount of benzene and high boiling products were also observed. High boiling products which may be the oligomer of the styrene formed may have caused about 4 % of incomplete recovery in the 38.4 μmol/g·sec of ethylbenzene fed at the stationary state. The coke formed on the catalyst was removed by the reoxidation of the used catalyst by air under the conditions shown in Fig. 1-b. The reoxidized catalyst showed the same results as were obtained in the case of the fresh catalyst. The hydrogen treatment at 723 K for 1.5 h after the reoxidation showed no effect on the time course. In fig. 1-c, the effect of the treatment of the catalyst by styrene is also shown. After the styrene treatment, r_{ST} remained constant with time.

Effect of Na on the Flow Reaction

The catalytic behavior of Na treated catalysts was studied. On each catalyst, the time course was the same as that on the original-SiAl catalyst shown in Fig. 1. The catalytic activity was varied with Na content and the order of the activity of each catalytyst did not change with the reaction time.

Figure 2 shows the effect of Na content on the rates of formation of styrene, CO + CO_2 and benzene at 90 min after the initiation of the reaction at 718 K. The rate of styrene formation which increased with Na content, achieved a maximum at 17 μmol of Na/g-cat and then decreased gradually. It is important that not only the poisoning effect but also the promoting effect of the addition of Na was observed in the oxidation reaction. The rates of the formations of benzene and Co + CO_2 respectively depended on Na-content in a similar way to that of styrene but to a lesser extent. The same tendencies were observed at 768 K.

Figure 3 shows the effect of Na-content on the apparent reaction order with respect to ethylbenzene and oxygen. The reaction order was measured under the differential reaction conditions, i.e. the degree of conversion was about 10 % . The reaction orders with respect to ethylbenzene are on the same order in magnitude as that with respect to

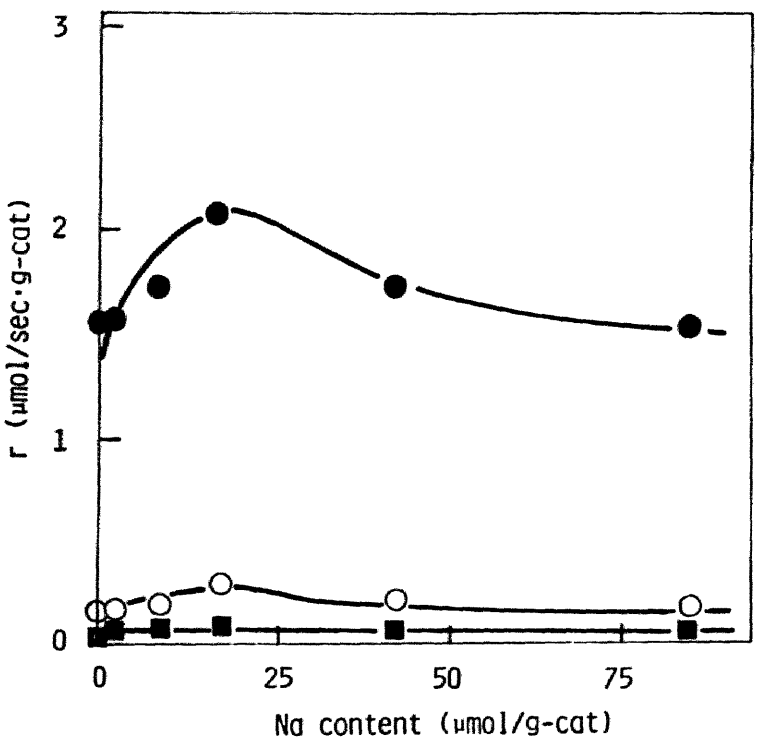

FIGURE 2 Effect of Na on the reaction rates at 723 K. ■, r_B; for the other symbols, see Figure 1. T = 723 K, W = 0.400 g, F = 255 mmol/h, P_{O_2} = 0.066 atm, P_{EB} = 0.060 atm, P_{H_2O} = 0.369 atm and P_{N_2} = 0.505 atm.

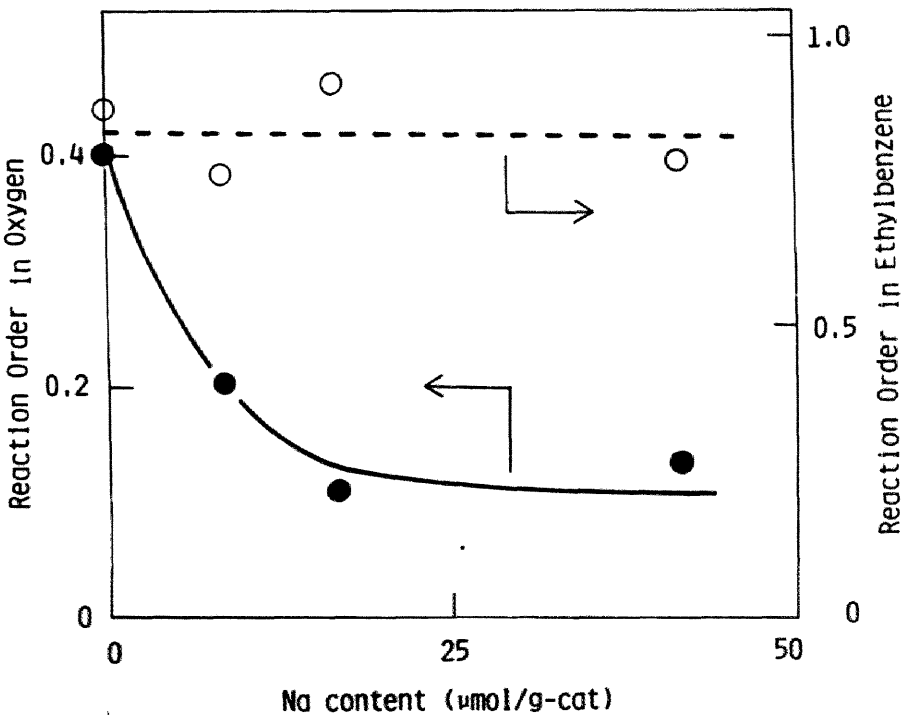

FIGURE 3 Effect of Na on the reaction order. W = 0.200 g, T = 723 K, P_{N_2} = 0.390 atm and P_{H_2O} = 0.490 atm. The reaction order with respect to O_2 (●) was measured at constant P_{EB} (= 0.061 atm), and the reaction order with respect to ethylbenzene (○) was measured at constant P_{O_2} (= 0.061 atm).

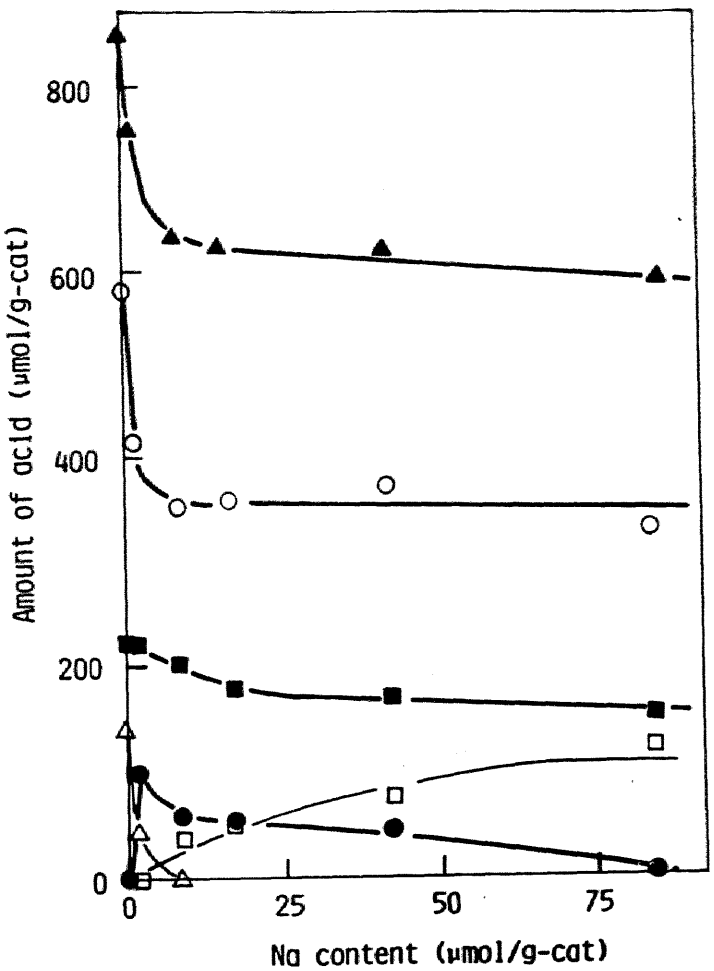

FIGURE 4 Effect of Na on the acid amount at different H_0 range: ○, 6.8∿1.5; ●, 1.5∿-5.6; □, -5.6∿-8.2; ■, -8.2∿-12.7; △, -12.7∼ ; ▲, Total amount.

oxygen. This implies that the activation of both ethylbenzene and oxygen have almost an identical rate on original-SiAl. The effect of Na-content on the reaction order with respect to ethylbenzene is not clear, but that with respect to oxygen decreased as the Na-content increased, thereby, showing that Na treatment enhances the activation of oxygen.

Acidity and Basicity of Na-$SiO_2 \cdot Al_2O_3$ Catalysts

Figure 4 shows the dependence of the amount of acid of a specified acid strength on Na content. The original-SiAl has only strong acid ($Ho < -8.2$) and weak acid ($Ho > 1.5$) sites, but no medium strength sites ($1.5 > Ho > -8.2$). The strongest acid sites ($Ho < -12.7$) decreased abruptly and then disappeared, while the strong acid sites ($-12.7 < Ho < -8.2$) decreased gradually with Na content. The weak acid sites ($Ho > 1.5$) decreased abruptly below the Na content of 8.5 μmol/g-cat and remained almost constant above it. The medium-high acid sites ($-5.6 > Ho > -8.2$) increased gradually, while the medium-low acid sites ($1.5 > Ho > -5.6$) at first increased and then decreased with the increase of Na-content. These results show that the sodium ion not only neutralizes the exchanged acid sites but also donates electrons to more than ten acid sites to reduce the acid strength. The weak acid sites may be weakened to such an extent that a portion of them cannot be detected by the present method, and this results in a decrease in the total acidity.

The basicities at various base strength of Na-SiAl catalysts are shown in Fig. 5. As the difficulty to determine the total amount of basic sites of $SiO_2 \cdot Al_2O_3$ with bromothymol blue has been reported (16), phenolphthalein ($pKa = 9.3$) was used instead. The basic sites of pKa between 9.3 and 26.5 were observed. The amount of weaker sites ($9.3 < pKa < 17.2$) did not change greatly by the Na treatment, while the more basic sites ($17.2 < pKa < 26.5$) increased from 210 μmol/g-cat to 280 μmol/g-cat as the Na-content increased to 17 μmol/g-cat. Namely, the ion exchange with Na affected not only the distribution of the acid sites but also that of the basic sites. However, the change in the base sites was not as great as that in the acid sites. The effect of one Na ion to increase the number of acid and base sites numerously indicates that the base sites are generated adjacent to the acid sites affected by the Na treatment.

Pulse Reaction

Figure 6 shows examples of the results of the pulse reaction on the fresh catalyst and the used catalyst, respectively. Figure 6-a shows the results on the fresh original-SiAl catalyst. When only ethylbenzene was injected (pulse I) and when it was injected 10 minutes later than the oxygen pulse (pulse II), benzene and ethylene were formed but not styrene. On the other hand, when ethylbenzene and oxygen were injected simultaneously (pulse III), a considerable amount of styrene and benzene were formed. No hydrogen could be detected, indicating that styrene was formed through oxidative

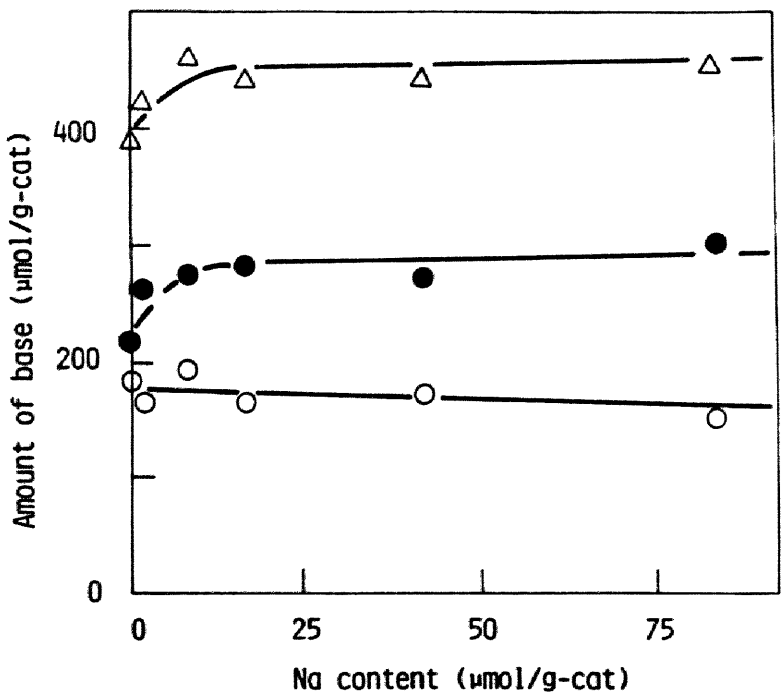

FIGURE 5 Effect of Na on the base amount at different pKa range: ○, 9.3∿17.2; ●, 17.2∿26.5; △, Total amount.

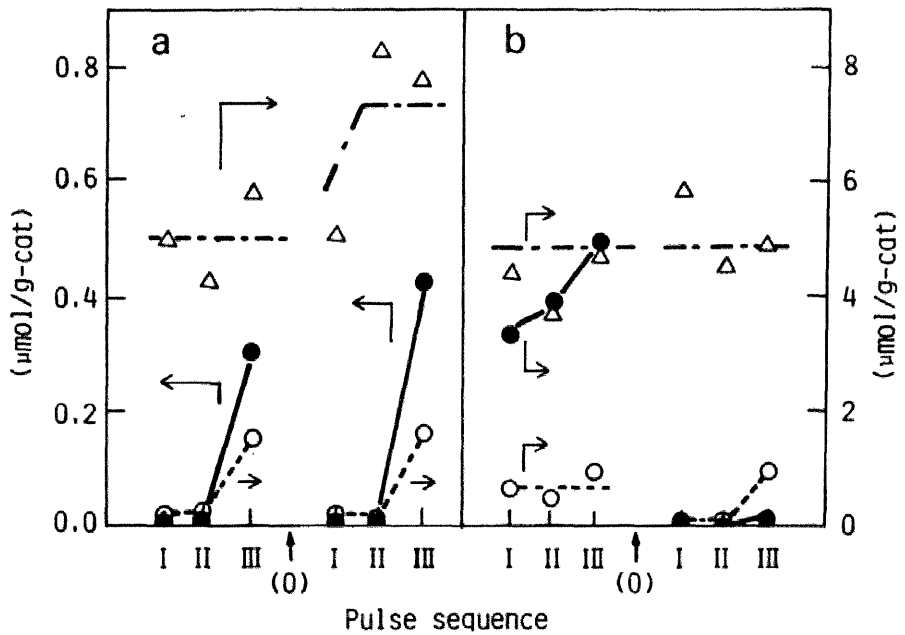

FIGURE 6 Pulse reaction on the fresh original-SiAl catalyst(a) and on the used original-SiAl catalyst(b). I, ethylbenzene pulse; II, oxygen pulse ⟶ ethylbenzene pulse; III, oxygen pulse + ethylbenzene pulse. (O), Reoxidation of the catalyst at 718 K for 1 h with air and then at 768 K for 2 h with O_2 for the fresh one and for the used one, 4 more hours with O_2 at 768 K. ●, amount of styrene formed; ○, of benzene formed; △, of ethylbenzene unrecovered.

dehydrogenation. The recovery of ethylbenzene was not complete in all pulses I, II, and III, that is, the total amount of effluents was less than the amount of ethylbenzene injected. As shown in Fig. 6-a, the amount of unrecovered ethylbenzene was essentially identical in all pulses I, II, and III.

In the case of the used catalyst, as shown in Fig. 6-b, styrene was formed not only in pulse III but also in pulses I and II, and the amount of styrene formed was larger than that on the fresh catalyst. The amount of styrene formed increased slightly as follows; pulse I II III. However, the amount of unrecovered ethylbenzene was identical to that on the fresh catalyst. The results obtained after the reoxidation of the catalyst were the same as those on the fresh catalyst shown in Fig. 6-a. This is similar to the effect of reoxidation on the continuous flow reactions.

The results on the sodium ion exchanged catalysts were similar to those on the fresh original-SiAl catalyst shown in Fig. 6-a, but the amount of the products varied with the Na-content. Figure 7 shows the effect of Na-content on the amount of styrene formed. On the fresh catalyst, styrene was formed only in the presence of oxygen (pulse III). The amount of styrene formed increased with the Na content below 8.5 μmol of Na/g-cat, reached the maximum at 8.5∿17 μmol of Na/g-cat, and then decreased gradually. Such a dependence of the activity on Na-content agrees well with that observed in the flow technique shown in Fig. 2. On the other hand, on the used catalyst, styrene was formed both in the presence and in the absence of oxygen, and the amount of styrene formed in all pulses I, II, and III increased with Na-content. But it should be noted that the difference in the amount of styrene formed between pulses III and II is almost equivalent to that formed on the fresh catalyst.

Figure 8 shows the effect of Na content on the amount of unrecovered ethylbenzene. It should be noted that, on each catalyst, the amount of unrecovered ethylbenzene remained constant throughout the pulse experiments I, II, and III, both on the fresh and used catalysts. The amount of unrecoverd ethylbenzene increased steeply with Na content below 1.7 μmol/g-cat, reached the maximum at 1.7 μmol/g-cat and then decreased gradually. It is also worth noting that the tendency of the unrecovered ethylbenzene is in good agreement with the tendency of the acidity of Ho between 1.5 and -5.6 as shown in Fig. 8. The physical meaning of unrecovered ethylbenzene will be discussed later.

DISCUSSION

In order to discuss the detailed role of the acid and base sites on the oxidation activity, catalysts with varied acidity and basicity are required. The acid and base properties of catalysts were controlled by treating the original-SiAl in NaOAc solution with various concentrations.

The results of the flow reaction shown in Fig. 2, shows that the activity is influenced by the Na-content of the catalysts. The same dependence on the Na-content was

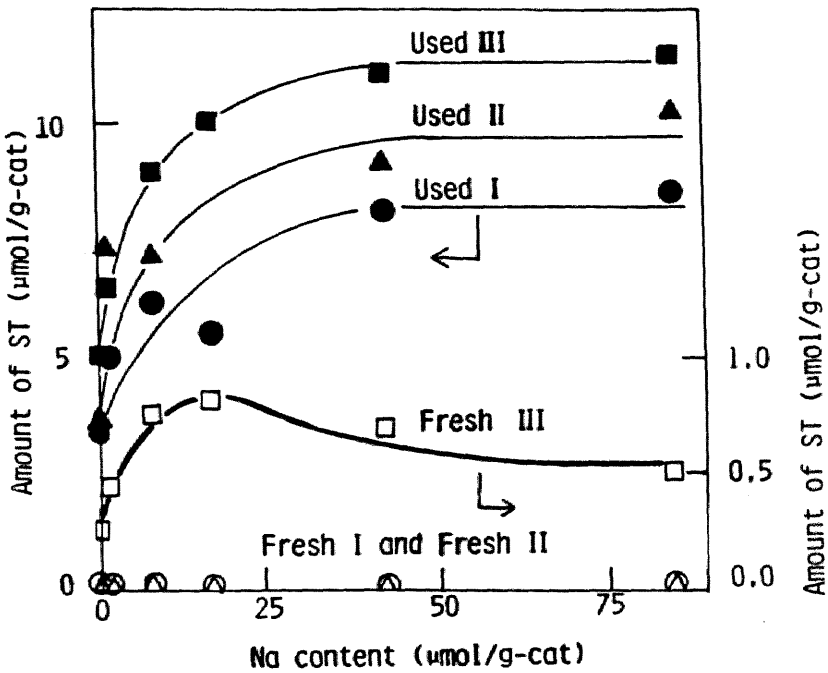

FIGURE 7 Effect of Na on the amount of styrene formed in the pulse reaction. ○, I; △, II: □, III. Open symbols for the fresh catalysts: solid symbols for the used catalysts.

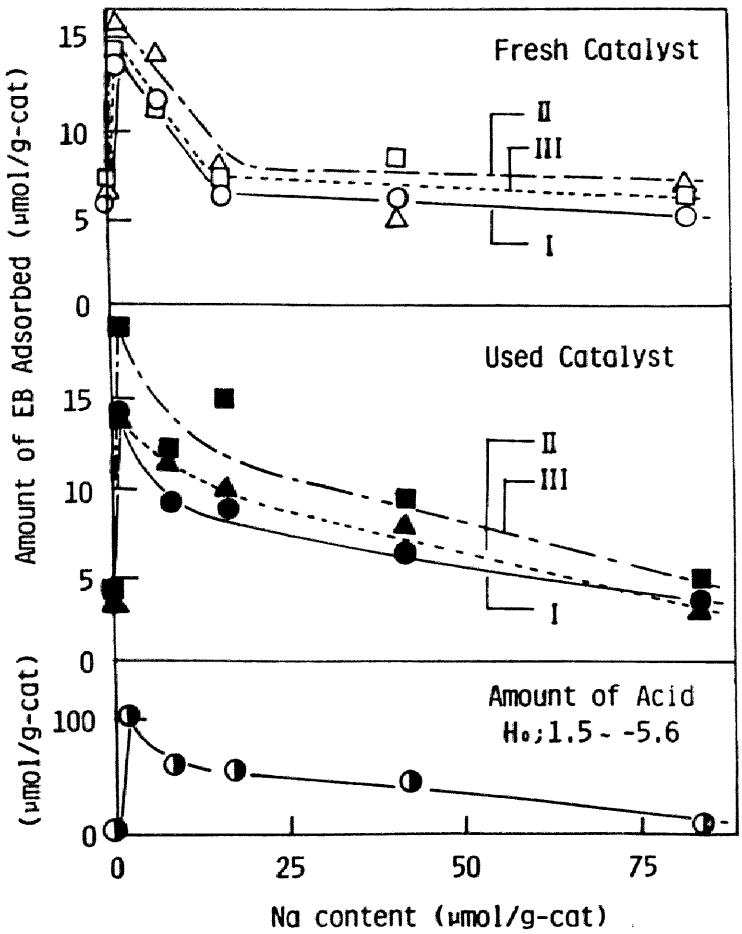

FIGURE 8 Effect of Na on the amount of ethylbenzene adsorbed and on the acid amount of $1.5 > H_0 > -5.6$ (◑). ○ , Ethylbenzene adsorbed in the pulse reaction I; △, II ; □, III. Open symbols, for the fresh catalysts; solid symbols for the used catalysts.

observed in the case of the pulse technique(Fig. 7). Such tendencies show that the addition of an adequate amount of sodium does not suppress but promotes the oxidation reaction, however, excess amount of sodium shows a poisoning effect. The tendency to have maximum activity suggests the cooperative effect of the acid and base properties of the catalysts which decrease and increase with increasing Na-content, respectively.

As shown in Figs. 4 and 5, changes in the acid and base properties with the amount of Na were observed and such changes can be interpreted as follows. The addition of one sodium ion weakens the acid strength of around ten acid sites, showing that the sodium ion effects not only the neutralization of acid sites but also the weakening of the acid strength by its inductive effect[17,18]. At the same time, the addition of sodium generated strong base sites and such effect is also understood by considering the electron donating properties of the sodium ion [18]. The result that one sodium ion weakens acid sites and enhances base sites suggests that the acid and base sites should be situated in immediate neiborhoods. Therefore, before the Na ion exchange is carried out (original-SiAl), the strong acid sites exist alone and/or with weak base sites. After the Na ion exchange, however, the strong base sites are generated and the adjacent strong acid sites are weakened. Thus the Na ion can control the acid-base properties of the catalyst without changing the BET surface area.

As shown in Fig. 1-a, the constant value of ethylbenzene conversion shows that the active site to react with ethylbenzene does not change during the flow reaction. The time course of the regenerated catalyst(shown in Fig. 1-b) in the flow reaction and the effect of the reoxidation of the catalyst in the pulse reaction(shown in Fig. 6-b) also support this. From the results of the styrene pretreatment (shown in Fig. 1-c), the apparent increase of the rate of styrene formation with time can be explained by the subsequent reaction of the styrene produced and will be discussed later.

In the pulse reaction on the used catalyst, the amount of styrene formed was largest when ethylbenzene and oxygen were pulsed at the same time, as shown in Fig. 6-b. The difference in styrene yield between pulses Ⅲ and Ⅱ, which corresponds to the amount of ethylbenzene oxidatively dehydrogenated by oxygen species from gaseous oxygen, is neary equal to the styrene yield in pulse Ⅲ on the fresh catalyst. Thus the active site on the fresh catalyst should still be effective even after the coke had deposited during the flow reaction. The agreement of the dependence of r_{ST} on Na-content in the flow reaction(Fig. 2) with that in the pulse reaction(Fig. 7) shows that the same site is active in each reaction condition. This agreement of the results of the flow reaction with pulse Ⅲ but not with I nor Ⅱ, also shows that the active oxygen is not the lattice oxygen (pulse I) nor the stable adsorbed oxygen (pulse Ⅱ) but the unstable adsorbed oxygen species (pulse Ⅲ).

As mentioned in the results section, the recovery of ethylbenzene was incomplete in all pulse reactions I, Ⅱ, and Ⅲ both on the fresh and used catalysts. Such an incomplete recovery has been observed on the solid phosphoric acid catalyst[1]. To clarify

the meaning of the incomplete recovery, repeated pulse reactions were carried out. The results are shown in Fig. 9. Two successive pulses of ethylbenzene were injected at various time intervals. The chromatogram obtained consisted of four peaks: two peaks of benzene and two peaks of ethylbenzene. No other products were formed, because no oxygen pulses were injected. The amount of benzene formed was so small that it could be neglected in the calculation of the recovery of ethylbenzene. The second ethylbenzene peak represents the degree of recovery of the second pulse. In Fig. 9, the amount of unrecovered ethylbenzene is plotted against the time interval between the two successive pulses. As the time interval decreased, the amount of unrecovered ethylbenzene decreased and the recovery became complete. These results indicate that the incomplete recovery is due to the reversible adsorption of ethylbenzene. The remaining ethylbenzene from the first pulse will increase the recovery of the second pulse. One of the present authors attributes the incomplete recovery to the strong reversible adsorption of the reactant[19]. In such a case, the recovery becomes complete by repeating the pulses of the reactant in short intervals. Thus, the results show that the incomplete recovery can be attributed to the strong reversible adsorption of ethylbenzene on the catalyst surface.

The effect of Na content on the amount of unrecovered ethylbenzene is shown in Fig. 8. It is noteworthy that the amount of adsorbed ethylbenzene on the catalyst was identical in all pulses I, II, and III both on the fresh and used catalysts. The same adsorption site is revealed to be active in every condition. The amount of adsorbed ethylbenzene increased steeply as the Na-content increased from 0.0(original) to 1.7 μmol of Na/g-cat and decreased gradually above 1.7 μmol of Na/g-cat. It is also notable that this tendency for the adsorption of ethylbenzene to vary with Na-content is similar to the tendency of the treatment of the acid sites of Ho between 1.5 and -5.6. Any other relationships between adsorption and acid sites cannot be observed in any other range of acid strength. This leads to the conclusion that the active site which adsorb ethylbenzene can be represented by acid sites in the range of acid strength 1.5 and -5.6 of Ho, which is weaker than the acid strength required for the dealkylation of alkylbenzene, i.e. $Ho < -5.6$[13,20,21]. The strong acid sites ($Ho < -5.6$) can be active for the dealkylation of alkylbenzene and the polymerization of the styrene formed, then can be covered with coke and become inactive during the stationary state of the flow reaction. However, this is not the case for acid sites weaker than $Ho = -5.6$. Such hypothesis is supported by the pulse reaction on the used catalyst which shows that an identical amount of ethylbenzene is adsorbed on it as on the fresh catalyst. From the above discussions, the time course of styrene formation (Fig. 1), in which the apparent rate of styrene formation increased with time and reached a stationary state while the conversion of ethylbenzene remained constant, can be well explained. That is; ethylbenzene is converted to styrene from the beginning of the reaction but the styrene formed is polymerized to coke which deposits gradually on the strong acid site of $Ho < -5.6$. Thus, the apparent rate of styrene formation is low at the beginnig

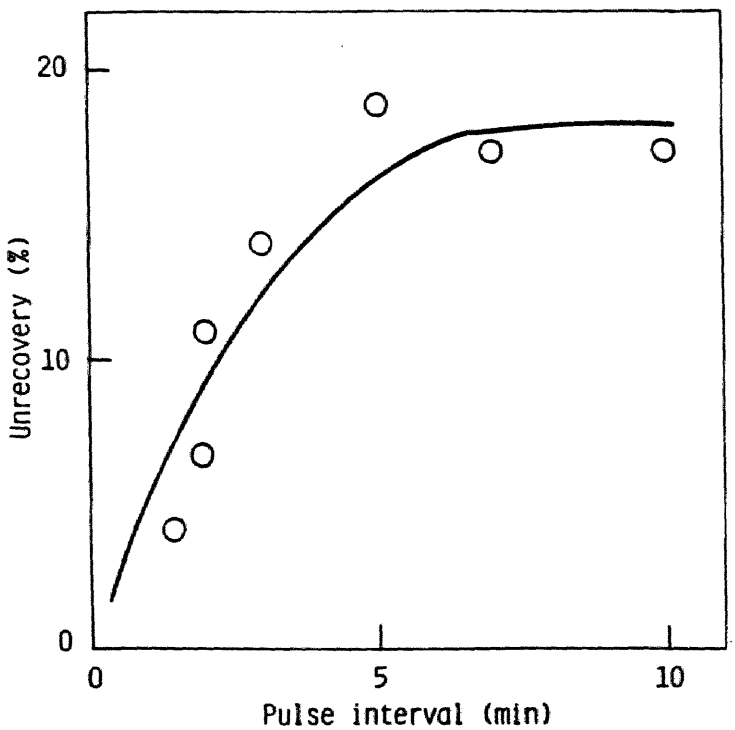

FIGURE 9 Effect of the pulse intervals in the repeated ethylbenzene pulse on the percentage unrecovery of ethylbenzene on 1.7 Na-SiAl catalyst.

of the reaction. However, since the coke formed deactivates the sites of coke formation with time, the polymerization of styrene is hindered and its formation increases to reach a stationary state. The reoxidation of the catalyst (Fig. 1-b) removes the coke away, regenerates the fresh state, and repeats the time course. The pretreatment with styrene after the reoxidation (Fig. 1-c) deactivates the coking site before the flow reaction, while the active site of the oxidative dehydrogenation of ethylbenzene is still effective, which removes the apparent increase of the rate of styrene formation with time. These interpretations of the time course are completely different from those of Alkhazov et al.[22], which has stated that the coke formed on the catalyst is an active site.

It is concluded from quantum mechanical calculations that acid sites can coordinate the benzene ring of toluene and withdraw the ring electron, resulting in the activation of α-hydrogen and its interaction with the neighboring base sites[3]. Such acid sites and neighboring base sites can exist on the Na-SiAl catalysts and the effective acid strength is revealed to be of Ho between 1.5 and -5.6.

The turnover frequency of the formation of styrene was calculated from the results obtained in the flow reaction, assuming that the active site is the acid site of Ho between 1.5 and -5.6 as discussed above;

$$\text{Turnover frequency} = \frac{r_{ST} \text{ in continuous flow reaction}}{\text{Amount of acid of } \quad 1.5 > Ho > -5.6} \quad .$$

So this turnover frequency represents the activity to produce styrene per one active site to adsorb ethylbenzene. The effect of Na-content on the turnover frequency is shown in Fig. 10. The effects at 718 K and 768 K resemble each other. It is significant that this tendencies observed in the turnover frequency is in good agreement with the tendency of the amount of base sites of pKa between 17.2 and 26.5. These results suggest that the rate determining step of this reaction is the oxidation of the reversibly adsorbed intermediate of ethylbenzene on the base sites of pKa between 17.2 and 26.5.

Such tendency for the amount of base sites to vary with Na-content is also similar to the tendency in the decrease of the reaction order with oxygen (Fig. 3) indicating that the addition of Na reduces the difficulty in activating oxygen. The formation of styrene was observed only in the pulse III, where ethylbenzene and O_2 were pulsed simultaneously on the fresh catalyst. This shows that the active oxygen species in this flow reaction is the adsorbed one with short life time on the catalyst. Thus the role of the base site of pKa 17.2 and 26.5 is concluded to adsorb oxygen into an activated form and to oxidize the adsorbed intermediate of ethylbenzene which is reversibly adsorbed on the acid sites of Ho between 1.5 and -5.6. These conclusions agree well with the role of acid and base sites assumed in the case of Sn-P catalysts[1].

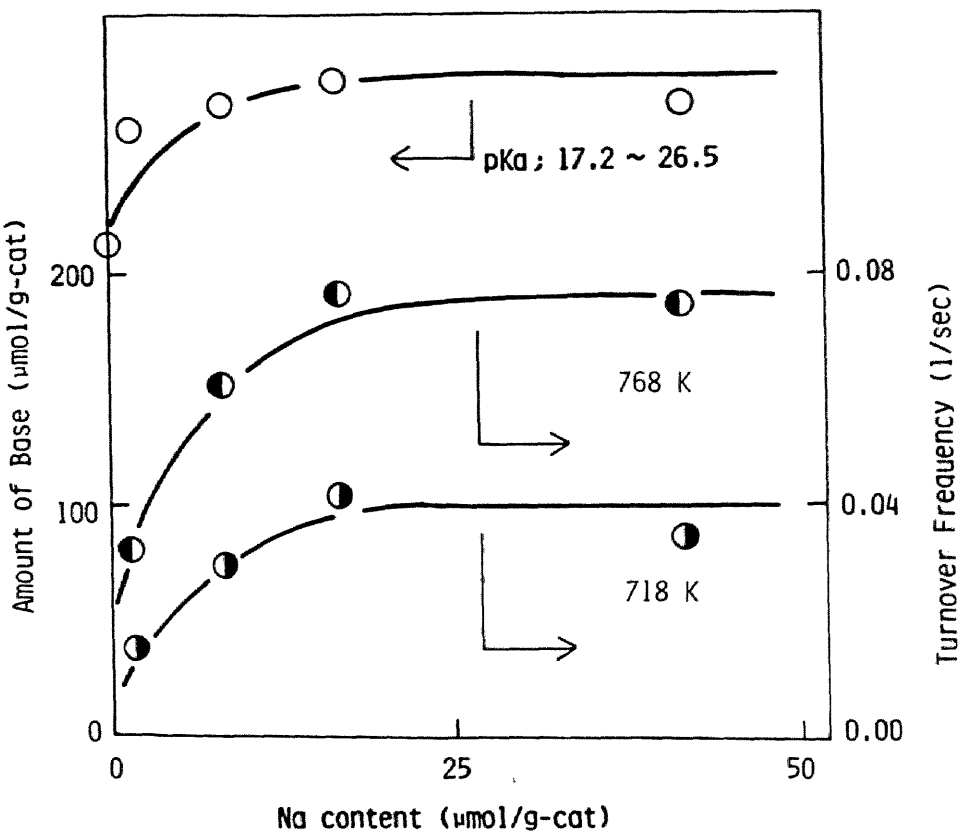

FIGURE 10 Correlation between basicity and turnover frequency.

$$\text{Turnover Frequency} = \frac{r_{ST} \text{ in continuous flow reaction}}{\text{Amount of acid of } 1.5 > H_0 > -5.6} \ ;$$

◑, at 718 K; ◐, at 768 K; ○, amount of base of $17.2 < pKa < 26.5$.

CONCLUSION

The effect of the acid and base properties on the oxidative dehydrogenation of ethylbenzene has been studied in the continuous flow reaction, pulse reaction and acid-base titrations on a series of Na-SiO_2·Al_2O_3 catalysts. As the amount of Na increases, the activity increases initially, reaches the maximum and then decreases both in the flow and pulse reactions. Such an effect of Na can be explained by the cooperative effect of the acid and base sites. The addition of Na not only eliminates a part of the acid sites but also generates moderately strong acid sites of $1.5 > H_o > -8.2$ and increases base sites of $17.2 < pKa < 26.5$. Each Na ion added increases such acid and base sites numerously. The reversible adsorption of ethylbenzene occurs on acid sites of $1.5 > H_o > -5.6$. The turnover frequency, based on the flow reaction and amount of acid sites of $1.5 > H_o > -5.6$, shows that the step to oxidize the adsorbed ethylbenzene and form styrene is effected by base sites of $17.2 < pKa < 26.5$. Such active sites required to form styrene have been shown to be still effective at the stationary state of the continuous flow reaction.

REFERENCES

1 Y. Murakami, K. Iwayama, H. Uchida, T. Hattori and T. Tagawa, J. Catal., in press; Chapter 3 of this thesis.

2 Y. Murakami, K. Iwayama, H. Uchida, T. Hattori and T. Tagawa, Appl. Catal., in press; Chapter 2 of this thesis

3 H. Itoh, A. Miyamoto and Y. Murakami, J. Catal., 64 (1980) 284.

4 I. Ishikawa and T. Hayakawa, Bull. Jap. Pet. Inst. 18 (1976) 55.

5 M. Akimoto and E. Echigoya, JCS Faraday trans. I 75 (1979) 1757; the references therein.

6 M. Egashira, I. Aso and T. Seiyama, Kyusyu Daigaku Ko-gaku Shu-ho 45 (1972) 704.

7 Ph.A. Batist, P.C.M. Heijden and G.C.A. Schuit, J. Catal., 22 (1971) 411.

8 Y. Takita, A. Ozaki and Y. Morooka, J. Catal., 27 (1974) 185.

9 T. Seiyama, M. Egashira, T. Sakamoto and I. Aso, J. Catal., 24 (1972) 76.

10 M. Ai, Proc. 7th Int. Congr. Catal., Tokyo, No B-28 (1980).

11 K. Maruyama, H. Hattori and K. Tanabe, Bull. Chem. Soc. Jap., 50 (1977) 86.

12 Y. Murakami, M. Niwa and H. Uchida, Kogyo Kagaku Zasshi 72 (1969) 2183.

13 K. Tanabe, "Solid Acid and Bases." Academic Press, New York, 1970; L. Forni, Catal. Rev., 8 (1973) 65; H.A. Benesi and B.H.C. Winquist, Adv. Catal., 27 (1978) 97.

14 H.A. Benesi, J, Am. Chem. Soc., 78 (1956) 5490.

15 H. Niiyama and E. Echigoya, Bull. Chem. Soc. Jap., 44 (1971) 1739.

16 K. Tanabe and T. Yamaguchi, J. Res. Inst. Catal. Hokkaido Univ., 11 (1964) 179.

17 B.D. Flockhart and R.C. Pink, J. Catal.,4 (1965) 90; J.D. Danforth, Proc. 2nd. Int. Congr. Catal. Paris I, (1960) 1271.

18 W. Grabowski, M. Misono and Y. Yoneda, J. Catal., 61 (1980) 103.

19 Y. Murakami and K. Hayashi, Kogyo Kagaku Zasshi, 72 (1969) 1038.
20 J.M. Parera, S.A. Hillar, J.C. Vincenzini and N. S. Figoli, J. Catal., 21 (1971) 70.
21 K. Matsuura, A. Suzuki and M. Itoh, Bull. Cem. Soc. Jap., 45 (1972) 2079.
22 T.G. Alkhazov and A.E. Lisovskii, Kinet. Catal., USSR, 17 (1976) 434.

Chapter 5

MECHANISM FOR STYRENE FORMATION

SYNOPSIS

The reaction mechanism of oxidative dehydrogenation of ethylbenzene has been investigated using the pulse technique, isotope exchange reaction, and ESR measurement. Collecting the effluents of the pulse reaction has shown the reversible adsorption of ethylbenzene. The deuterium exchange reaction has shown that the adsorbed intermediates of ethylbenzene is dissociated at the α-position. Neutrally adsorbed molecular oxygen species and O^- species are observed on the prereduced SiAl catalysts by the ESR measurement, showing the ability of the catalysts to activate gaseous oxygen. The reaction of the oxygen species with ethylbenzene has shown the active oxygen species to be O^- species. The O^- species consummed by the reaction are supplied from gaseous oxygen through O_{2ad} species. The reversible adsorption of ethylbenzene and the correlation between the turnover frequency and basicity suggest that the rate of the overall reaction at above 723 K is determined by the reaction of adsorbed ethylbenzene species and O^- in abstracting the β-hydrogen. From the above results, a reaction mechanism is proposed as follows; the acid site of Ho between 1.5 and -5.6 adsorbs ethylbenzene, reversibly abstracting the α-hydrogen at the basic OH adjacent to the acid site, and the base site of pKa between 17.2 and 26.5 activates gaseous oxygen to form O^- which abstracts the β-hydrogen.

INTRODUCTION

In the previous chapter[1], it has been concluded that the active site of the oxidative dehydrogenation of ethylbenzene exists on the native $SiO_2 \cdot Al_2O_3$ catalyst and that the acid site of Ho between 1.5 and -5.6 activates ethylbenzene and the base site of pKa between 17.2 and 26.5 activates oxygen, respectively. The reaction mechanism including allylic intermediates has been proposed in detail in the oxidation of

olefinic compounds [2]. Oxidation of ^{13}C labeled propylene on Bi·Mo[3], Bi·Mo-P[4], and Cu_2O[5] suggested the existence of the symmetric allyl intermediates. The product distribution obtained in the reaction of deuterio propyrene[6,7,8] on Cu_2O, Bi·Mo, and U·Sb also indicated the same propylene intermediate in which the α- hydrogen had been abstracted. The same intermediate was also detected on ZnO[9] using spectroscopic methods. Moreover, the rate determining step has been proven to be in the abstraction of the α-hydrogen[7, 10, 11]. In the case of ethylbenzene, a similar intermediate has been supposed, however, the details are not clear[12,13].

A number of studies have been devoted to the active oxygen species. An activity of the lattice oxygen was observed on the Mo-containing oxides[14], and activities were also found in the oxygen double bonded to the metal(M=O)[10,15,16] and in the adsorbed oxygen species(i.e. O^-) on the ferrite spinel catalysts[10,15,17]. Adsorbed oxygen species have also been proposed on other oxide catalysts[3,17,18]. In the case of Na-SiO_2·Al_2O_3 catalysts, the possibility of the participation of the lattice oxygen has been denied by the pulse reaction in the previous chapter[1]. Many studies have been done on the adsorbed oxygen species with the aid of ESR(19) and the activity of the adsorbed oxygen species (i.e. O_2^-, O^-, O_3^-) has also been studied in the oxidation of hydrocarbons[20,21,22]. The adsorbed oxygen species (i.e. O_2^-) was observed on the insulators, such as SiO_2·Al_2O_3[19], Al_2O_3[19] and zeolites[19,23], only in the case of uv- and γ-irradiated samples. On the other hand, the base catalysts such as MgO was observed to activate oxygen to form O_2^- ion without prior irradiation but only with heat treatment[24].

In this chapter, the reaction mechanism is discussed on the basis of the activation of both reactants, that is ethylbenzene and oxygen. Details of the activation of ethylbenzene are investigated using the pulse technique and deuterium exchange experiments. Those of oxygen are investigated by ESR spectroscopy. The reactivities of both adsorbed intermediates are also studied. Each step of the reaction is discussed carefully and a reaction mechanism in the molecular aspect is proposed.

EXPERIMENTAL

Catalyst

The preparation of the Na-exchanged SiO_2·Al_2O_3 catalysts(Na-SiAl) and their acid and base properties were described in the previous chapter[1]. The content of Na was written at the head of the name of the catalyst in μmol/g-cat, which means that the amount of Na increased compared to that on the original-SiO_2·Al_2O_3 due to the ion exchange. For example, 17Na-SiAl contains 17 μmol of Na in addition to the original SiAl which contained 24 mol of Na/g-cat. Pure-SiAl catalyst was prepared by the gradual hydrolysis of a mixture of aluminium alcholate and ortho ethy silicate, containing 20% Al_2O_3.

Procedure

Pulse experiments

For the collection of the effluents of the pulse reaction, a silicagel trap was installed between the reactor and the gas chromatograph. The effluents were trapped at 77 K and then heated to 423 K to be vaporized and carried to the gas chromatograph. In some cases, both gaseous and liquid effluents were simultaneously analyzed. The effluents were splitted into two; one for gas analysis and the other for liquid analysis. The chromatographic column used were the same as the one reported previously[1]. This system, which needed about twice as much carrier gas(100 ml/min) as in the ordinary pulse apparatus(44.5 ml/min), would have an effect on the amount of unrecovered reactants.

ESR measurement

The catalyst was pretreated with a conventional high vacuum apparatus in the following manner.

(1) The sample in a quartz ESR sample tube with an inside diameter of 3 mm was evacuated at 763 K for 3 h.

(2) About 11 kPa of hydrogen, purified by the silicagel trap at 77 K, was introduced onto the sample at 763 K for 0.5 h, then evacuated at 763 K for 0.5 h. This procedure was done once again, and then the sample was evacuated for an additional 2 h at 763 K.

(3) 33 kPa of vacuum distilled oxygen was introduced onto the sample at 763 K and heated for 1 h.

(4) The sample tube was cooled down to 77 K and evacuated at 77 K for 60 s. Then the sample tube was isolated from the vacuum system by a two-way glass valve.

In some cases, the sample was treated with N_2O, instead of oxygen, as follows.

(5) Nitrous oxide (N_2O) was frozen at 77 K onto the pretreated (procedure 1 and 2) sample, then evacuated at 293 K for 30 s.

(6) Nitrous oxide was frozen onto the sample again at 77 K, evacuated at 293 K untill 27 kPa, heated at 373 K for 1 h, and again evacuated at 293 K for 30 s.

(7) After the procedure (6) had been repeated, the same sample was heated at 573 K for 3 h. After N_2O was introduced as in the case of procedure (6), the sample was heated at 573 K for 3 h instead of the treatment in procedure (6) and then evacuated at 293 K for 30 s.

Following these pretreatments, ESR signal was recorded at 77 K and 293 K with a JEOL JES-ME-ESR-1X, X band spectrometer. Manganese oxide in MgO was used to calibrate the g-value. The amount of molecular oxygen species adsorbed on the catalyst was calibrated volumetrically at room temperature.

The reactivity of oxygen species was examined in the following manner. A fixed amount of ethylbenzene vapor or 1-butene was introduced onto the sample and the sample was heated at various conditions. Then the ESR signal was recorded at 77 K to measure

the change of its intensity due to the reaction with the organic substance.

RESULTS

Pulse experiments

Reaction on pure-SiAl

As shown in Table 1, a considerable amount of styrene as well as benzene and a small amount of carbon oxides were formed on pure-SiAl when ethylbenzene and oxygen were pulsed simultaneously. No hydrogen was detected. The recovery of ethylbenzene was insufficient and the unrecovery was about 1 μmol/g-cat.

To examine the physical meaning of the unrecovery of ethylbenzene, the effluents from the pulse reactor were collected for 10 min. As shown in Table 2, when effluents

TABLE 1

Product Distribution in the Pulse Reaction of Ethylbenzene in the Presence of Oxydants[a]

Catalyst Pretreatment	Pure-SiAl Fresh	Original-SiAl Prereduction[b]	Original-SiAl Prereduction[b]
Oxydant[c]	O_2	O_2	N_2O
CO	trace	0.090	trace
CO_2	0.033	0.067	-[d]
Benzene	0.161	0.262	0.211
Styrene	0.134	0.154	0.130
Unrecovered Ethylbenzene	1.103	1.404	1.263

[a] in μmol/g-cat.

[b] Pretreated in the flow of hydrogen at 723 K for 45 min.

[c] Ethylbenzene(1 μl) and oxydant; N_2O(1 ml) or O_2(0.5 ml) were pulsed onto the catalyst(0.200 g) at 723 K under the flow of He(100 ml/min) at the same time.

[d] The separation of CO_2-peak and N_2O-peak was not sufficient.

TABLE 2

The Amount of ST-formed and EB-unrecovered in the Pulse Experiment with and/or without the Trap.

Catalyst	Trap[a]	EB only[b]		EB	O_2[c]
		ST-formed[d]	EB-unrecovered[e]	ST-formed	EB-unrecovered
1.7Na-SiAl (Fresh)	none	nil	13.9	7.7×10^{-2}	12.1
	10.0	nil	4.1	7.9×10^{-2}	11.5
0.0-SiAl (Used)	none	5.3	4.4	7.9	nil
	10.0	5.1	2.3	8.7	nil

[a]Effluents were analyzed after trapped at 77 K for 10.0 minutes.

[b]Ethylbenzene (1 µl) was pulsed (Pulse I)

[c]Ethylbenzene pulsed (1 µl) was followed with O_2 pulse (2 ml). The time interval was 15 sec.

[d]Amount of styrene formed in µmol/g-cat.

eAmount of ethylbenzene unrecovered in µmol/g-cat.

were collected by the trap, the amount of unrecovery was significantly less than that obtained without the trap. On the used catalyst, the amount of unrecovered ethylbenzene decreased when the effluents were collected, although the amount of styrene formed remained essentially unchanged.

When oxygen was pulsed immediately after the ethylbenzene pulse, opposite results were obtained. On the fresh catalyst, a slight amount of styrene was observed and the recovery was not changed by the trap. However, on the used catalyst, a significant amount of styrene was detected and the recovery was complete even without the trap.

Table 3 shows the effect of the additional pulse of H_2O on the recovery of ethylbenzene. The pulse of H_2O (2 µl) was introduced after the pulse of ethylbenzene on the fresh catalyst at various time intervals. The additional H_2O pulse improved the recovery of ethylbenzene, indicating that water promotes the desorption of ethylbenzene. The same experiment using D_2O was carried out. The time intervals between the ethylbenzene and D_2O pulses were fixed at 15 s and in between this pair of pulses, 13 minutes were allotted. The effluents were collected by the trap at 77 K. The collected sample was analyzed by mass spectrometer. A small amount of benzene was formed but it could be neglected in mass analysis. With the results gathered from the mass spectrum, the deuterium distribution of the effused ethylbenzene is summarized in Table 4. The deuterium distribution in C_6 ions were calibrated with the distribution of $C_6H_5^+$, $C_6H_6^+$, and $C_6H_7^+$ peaks in the spectrum of d_0-ethylbenzene(blank test).

TABLE 3
Effect of H_2O Pulse on EB-unrecovered[a]

Pulse interval (sec)[b]		EB-unrecovered
EB(1 µl)	H_2O(2 µl)	(µmol/g-cat)
	15	5.8
	30	5.3
	∞[c]	13.9

[a]Catalyst used was 1.7Na-SiAl.

[b]Ethylbenzene pulse was followed by H_2O pulse with an indicated interval.

[c]H_2O was not pulsed.

TABLE 4
Deuterium Distribution in Recovered Ethylbenzene

Compound	Mass number[a]	Deuterium distribution (%)					
		d_0	d_1	d_2	d_3	d_4	d_5
C_8 (EB)	106	8	8	13	21	26	24
C_7	91	6	5	11	20	28	30
C_6	77	18	10	19	23	15	15

[a]Mass number of d_0-compounds.

ESR measurement

As shown in Fig. 1, the ESR spectrum changed with each of the treatments mentioned in the experimental section. The spectrum of the 17Na-SiAl after the evacuation at 763 K (procedure 1) is shown in Fig. 1-1. A symmetrical peak at g = 2.005 and a broad signal at g = @2.1 were observed. A small signal at g = 2.038 was also observed. The color of the sample was still white after this evacuation. The hydrogen treatment (procedure 2) made the color of the sample gray. The treatment almost completely removed the broad and small signals away and enhanced the symmetrical peak at g = 2.005, as shown in Fig. 1-2. The effect of the oxygen introduced (procedure 3) is shown in Fig. 1-3. The symmetrical peak at g = 2.005 decreased and the broad signal regenerated, as well as the small signal at g = 2.038. Additional new signals were observed at g = 2.119, 2.107, 2.090, 1.976, 1.888 and at lower values. These signals were not observed in the absence of the catalyst, indicating that they could be attributed to the adsorbed oxygen species. The new signals were sharpened by evacuating the sample at 77 K (procedure 4) but the amount of the signals did not change with the time of the evacuation. Such signals were obtained only when the measurement was made at 77 K, but were not observed at 293 K. However, the measurement at 77 K after the measurement at 293 K reproduced such signals reversibly. The evacuation at 293 K removed such signals irreversibly, as shown in Fig. 1-5. This treatment with oxygen (procedure 3) regenerated the white color of the sample but not completely.

The same results were obtained in all cases of the Na-SiAl and the original-SiAl, but the spin concentration was different from each other. In the case of pure-SiAl, almost the same results were obtained as in the case of Na-SiAl, except that the broad signal at g = @2.1 could not be detected.

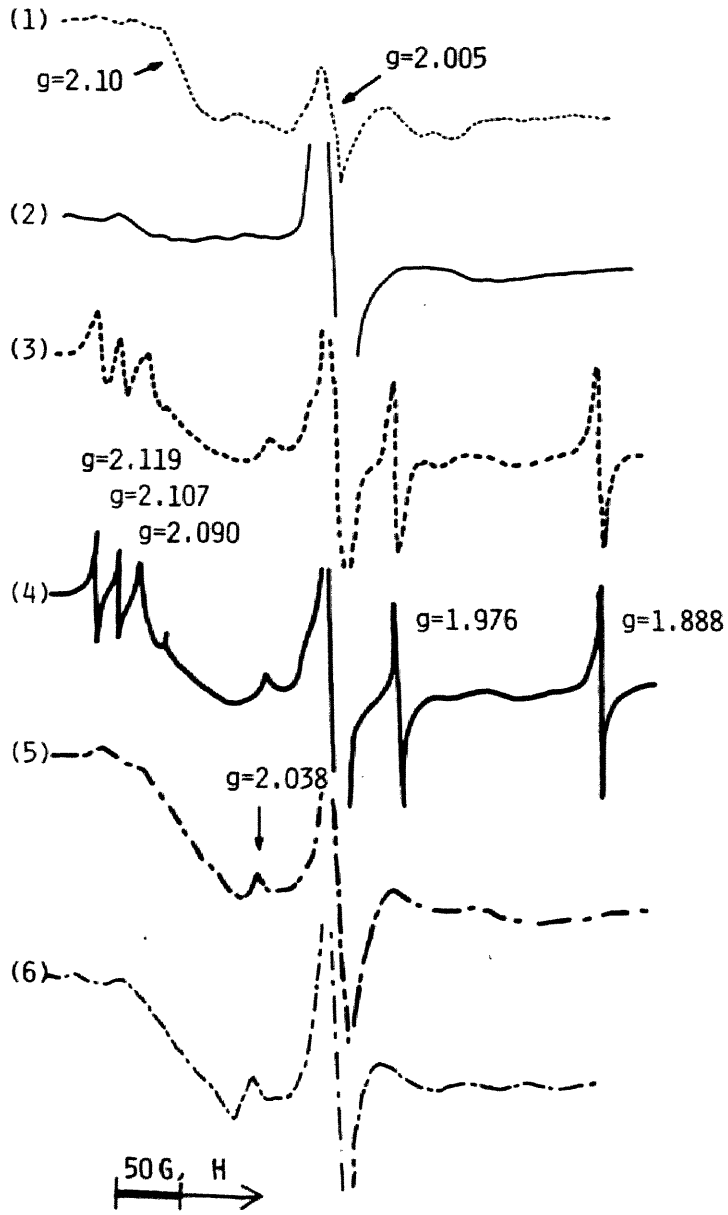

FIGURE 1 ESR spectra of 17Na-SiAl measured at 77 K: (1) after evacuation at 763 K for 3 h; (2) after repeated treatment with hydrogen(11 kPa) followed by evacuation at 763 K; (3) Sample (2) followed by exposure to 33 kPa of O_2 at 763 K for 1 h; (4) Sample (3) followed by the evacuation at 77 K for 60 s in which additional signals in the higher fields such as 4030, 4060, 4360, 4375, 4445, 4945, 4975, 5070, 5150, and 5253 Gauss (10^{-4} T) at 9.20 GHz were observed; (5) ESR spectrum of sample (4) measured at 293 K; (6) ESR spectrum of Original-SiAl measured at 77 K after the N_2O treatment.

Instead of the O_2 treatment, N_2O treatment was also examined. The evacuation and the following hydrogen treatments (procedure 1 and 2) gave the same results as was mentioned above. After N_2O was frozen onto the sample at 77 K, the evacuation was performed at 293 K for 30 s. Such treatment has been reported to give O^- species on MgO samples[25]. The signals measured at 77 K is shown in Fig. 1-6. In addition to the singlet peak at g = 2.005 which was observed before the N_2O addition, a signal at g = 2.038 and a broad signal at g = @2.1 appeared, but the size of these peaks was small. Such signals were enhanced by the further treatment of N_2O)procedure 6 and 7). The same signals were obtained when the measurement was made at 293 K, although the intensities of the signals had decreased. Signals which were observed after the treatment with O_2 (i.e. g = 2.119, 2.107, 2.090, 1.976, 1.888 and the lower) were not detected in the case of the N_2O treatment.

Assignment

The observed ESR signals could be assigned as follows. The broad signal at g = 2.1 disappeared with the H_2-treatment, appeared with the O_2-treatment and was not observed on pure-SiAl. Consequently, the signal could be attributed to the transition metal ion impurities, probably Fe^{3+}, which has been observed by Cordishi et.al. and Arakawa et.al.[26]. The singlet peak at g = 2.005 always existed on the sample in all of the treatments, indicating that this peak should be one of the defect centers as were observed on irradiated SiO_2-Al_2O_3[27] or zeolites[13,28]. Vedrine and co-workers have assigned this g-value of g = 2.005 as a V_4 center of the Si particle formed on the γ-irradiated SiAl[27]. As a doublet character signal, which at low Na content was a singlet, was observed at high Na content, this center is suggested to be influenced by the sodium ion. N_2O has been proposed to act as an electron sink[29], trapping the free electron at the surface *via* a reaction of the type;

$$N_2O + e^- \longrightarrow N_2 + O^-.$$

O^- species thus formed gave signals at $g_\perp = 2.042$ and $g_{//} = 2.002$ on MgO[25]. The small signal at g = 2.038 observed both after the oxygen and N_2O treatments could be a part of the anisotropic signal of O^-. However, another part of the anisotropic signals was difficult to detect because of the large signal originating from the V=type center discussed above. The residual signals (g = 2.119, 2.107, 2.090, 1.976, 1.888 and at lower values) were observed after oxygen treatment, but not after N_2O treatment. Consequently, these signals could be assigned as adsorbed molecular oxygen species such as O_{2ad} and O^-_{2ad} [19,30]. Signals at higher fields (with low g-values) were the characteristics of triplet radicals showing the presence of neutrally adsorbed molecular oxygen species(O_{2ad}). The signals, however, were different from those reported with gaseous molecular oxygen in the g-value, strength, and number of the signals[30]. This suggests that this oxygen species does not exist in the gas phase but is fixed on the surface. The results that the amount of the signals had not changed after the evacuation for 30 s and for 60 s at 77 K and that these signals were not observed in

the absence of the catalyst also support this. After the introduction of 1-butene at 77 K, these signals of molecular oxygen species at higher g-values decreased gradually. Such reactivity has been reported for the reaction of butene with molecular oxygen anion species(O_2^-) on zeolites[23,31].

Some additional experiments will be necessary for the precise assignment of these signals, however, it is noteworthy that the SiAl catalyst is proven to adsorb and activate oxygen. The adsorption and the activation occurred only with the hydrogen pretreatment but required no irradiation treatment, indicating that such a type of oxygen activation could occur in the oxidative dehydrogenation of ethylbenzene.

Amount of adsorbed oxygen species

The amount of adsorbed oxygen species was varied with the sodium content of the catalyst. The amounts of O^- and O_{2ad} increased until 17 μmol of Na/g-cat and remained at a stationary level above 17 mol of Na/g-cat. This relationship with Na content is similar to that of the amount of base sites of pKa between 17.2 and 26.5. Figure 2 shows the correlation of the amount of adsorbed oxygen species to the amount of base sites of pKa 17.2 ~ 26.5. The amount of O_{2ad} was calibrated volumetrically and since the large signal of V-center made it difficult to determine the amount of O^- species, the relative amount was displayed. As shown in Fig. 2, an approximate linear relationship exists between the amount of adsorbed oxygen species and the amount of effective base sites.

The amount of O^- species also changed with the treatment temperature of the catalyst with oxygen. The effect of the treatment temperature on the amount of O^- formed is shown in Fig. 3. 27 kPa of oxygen was introduced onto the sample which had been pretreated (procedure 2 and 3) and then evacuated at 77 K. The ESR signal at 77 K was obtained after the sample was heated at each condition shown in Fig. 3 and quenched immediately at 77 K.

DISCUSSION

Activation of Ethylbenzene

As shown in Table 1, a significant amount of styrene was formed only when ethylbenzene and oxygen were pulsed at the same time, while molecular hydrogen could not be observed on pure-SiAl. The same results have been obtained on commercial SiAl (origonal-SiAl) in the previous chapter[1]. This shows that styrene is formed on the SiAl surface but not on the impurities which may exist in commercial SiAl(i.e. Fe^{3+}) and that styrene is formed through an oxidative dehydrogenation process but not the simple dehydrogenation process. In this pulse reaction, a significant amount of ethylbenzene was not recovered. The same results were observed in the case of original- and Na-SiAl catalysts, and this incomplete recovery has been related to the acidity of Ho between 1.5 and -5.6 [1]. Such unrecovery has been assumed to be caused by the reversible adsorption of ethylbenzene [1,12,32]. To confirm the reversibility of

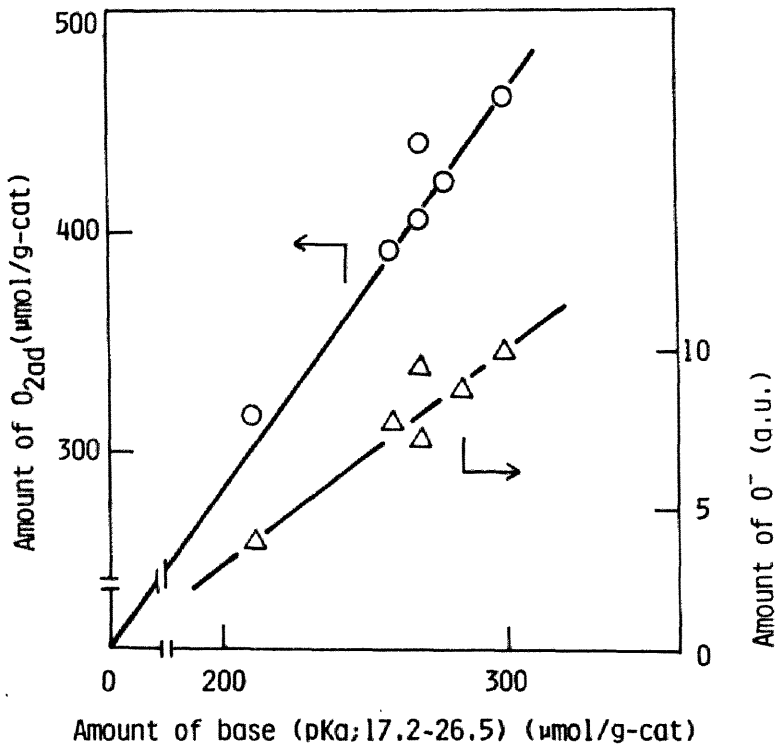

FIGURE 2 Correlations between the amount of base (pKa; 17.2 - 26.5) and the amount of O_{2ad} formed (○) and O^- formed (△) after the exposure to 33 kPa of O_2 at 763 K for 1 h.

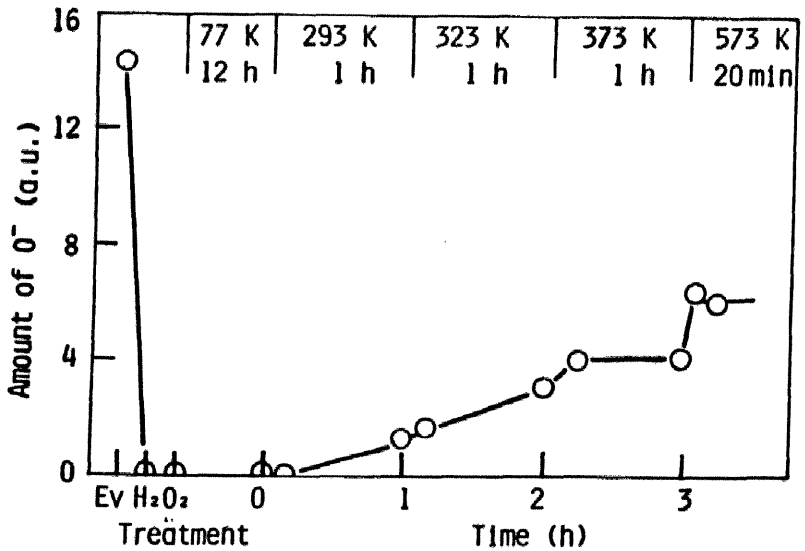

FIGURE 3 Change of the amount of O^- species on 17Na-SiAl with treated temperature in the presence of oxygen. Sample was evacuated at 763 K(Ev), treated with hydrogen at 763 K (H_2) followed by brief evacuation and the sample was quenched to 77 K immediately after the introduction of 33 pKa of O_2 at 293 K. ESR spectra were obtained at 77 K.

the adsorption of etylbenzene, the effluent was collected by a silica gel trap at 77 K. The results shown in Table 2 indicate that the incomplete recovery is due to the reversible adsorption of ethylbenzene or, in other words, due to the gradual desorption of ethylbenzene. Table 2 also shows that such site which adsorb ethylbenzene is still active even after carbonaceous compounds have deposited on the surface. Consequently, the amount of unrecovered ethylbenzene represents the ability of the catalysts to adsorb ethylbenzene. The correlation between the amount of unrecovery and that of the acid sites[1], indicates that the active sites which adsorb ethylbenzene reversibly is the acid site of Ho between 1.5 and -5.6.

The water pulse following the ethylbenzene pulse promoted the desorption of ethylbenzene, as shown in Table 3. Then the role of H_2O on the desorption of ethylbenzene was studied in the deuterium exchange experiments. The first column in Table 4 shows that about 90 % of the ethylbenzene treated with D_2O at 723 K was exchanged by deuterium. Even at maximum, the number of deuterium exchanged was five per one ethylbenzene. The deuterium distribution in molecular ions and that in C_7 ions were the same within the experimental errors. As the C_7 fragment of ethylbenzene has been reported to be produced by the cleavage of the C-C bond between the α-C and β-C of the side chain[33], the comparison of molecular ions with the C_7-ions shows the nature of the terminal methyl group. The similarity in deuterium distribution of these ions proves that the terminal methyl group is inactive for the H-D exchange from the above results. The deuteration of the aromatic ring has also been suggested. In spite of the fact that the C_6 ions are said to be formed not simply by dealkylation, the results obtained by Meyerson et.al.[33] has shown that the C_6-ions have a nature of aromatic ring preferentially. Consequently, the difference between the deuterium distribution in C_7 ions and that in C_6 ions should suggest the different nature of the hydrogen at the side chain. The deuterium distribution in the C_6 ions was lower than those in the C_7 and C_8 ions. Although the calibration performed on the C_6 ions to obtain the third column of Table 4 was not complete, a more precise correction would lower the amount of deuterium exchanged. These results show that the deuterium exchange should occur preferentially on the hydrogen at the α-carbon of the side chain (α-hydrogen). For example, the d_0-ion in C_6 ions was about 18 %, on the other hand, those in C_7 and C_8 ions were about 8 %, indicating that about 10 % of ethylbenzene is deuterated at only the α-position of the ethyl group but is not deuterated at the benzene ring. These results show that the β-hydrogen of the terminal methyl group is unexchangeable, however, the α-hydrogen and the hydrogen on the benzene ring are exchangeable. Moreover, the exchange on the α-hydrogen is predominant to that on the aromatic ring. Thus, the adsorbed species can be regarded as being dissociated reversibly at the α-position of ethylbenzene. α-Hydrogen will be abstracted by the basic site, or in other words, perhaps by the OH group adjacent to the acid site which has been identified as an adsorption site of ethylbenzene[1]. These conclusions explain the inhibiting effect of the α-hydrogen in alkylbenzenes observed in the compet-

itive reaction with ethylbenzene on Sn-P catalyst[12].

It is concluded from quantum calculations that acid sites withdraw the electron of the aromatic ring to enhance the acidic property of the α-hydrogen, and it interacts with the OH group near the acidic site[34]. This dissociative adsorption of ethylbenzene should be the case, and the mechanism of the activation of ethylbenzene is summarized in Fig. 4. It is noteworthy that ethylbenzene is reversibly adsorbed in the dissociated state at the α-position and that the active site is the acid site distributed in the range of Ho between 1.5 and - 5.6. The electron withdrawing character of such acid site is confirmed by the following two experimental results. 1) When 1.6 kPa of pyridine was adsorbed on the sample at 373 K, which had been evacuated at 743 K, the characteristic IR spectra of L-Py was observed at 1620 and 1455 cm^{-1}. This shows that Lewis acid sites are present on the surface of the catalysts. 2) The introduction of benzene solution of perylene at 293 K onto the sample which had been evacuated at 623 K results in the formation of perylene cation radicals. The amounts of which are varied with the Na-content of the catalyst and correlate with the amount of the acid sites stronger than Ho = 1.5. These results show that all or a part of the acid sites stronger than HO = 1.5 possess an electron withdrawing character. Danforth et.al. has reported that such Lewis acid sites are generated on the Aluminum ion by the Na treatment[34].

Reaction of Adsorbed Ethylbenzene with oxygen

In the formation of styrene from adsorbed ethylbenzene, the abstraction of a hydrogen at the terminal methyl group (β-hydrogen) is neccessary. As shown in Table 2, the oxygen pulse onto the adsorbed ethylbenzene produces an observable amount of styrene. This shows the ability of oxygen species to abstract β-hydrogen. The site to oxidize the adsorbed intermediate of ethylbenzene has been shown to be base sites of pKa between 17.2 and 26.5 in the previous chapter[1]. As shown in Table 2, the styrene formed from adsorbed ethylbenzene is irreversibly adsorbed on the fresh catalyst to form coke but not on the used catalyst. This shows that the coke formed in the flow reaction covers and deactivates the site to polymerize styrene and that the active site to abstract the β-hydrogen is still effective even after coke formed on the catalyst. These conclusions explain well the time course of the flow reaction[1].

Activation of Oxygen

In this chapter, the ability of SiAl catalysts to activate gaseous oxygen is confirmed. It is worth noting that such adsorption and activation of oxygen occurs only with a simple hydrogen pretreatment and requires no irradiation pretreatment. Such hydrogen treatment and the following evacuation will produce an anion vacancy by the addition of a hydrogen to the OH group and the subsequent desorption of the surface H_2O species formed. In a similar manner, the same site can be produced by the adsorption of ethylbenzene as shown in Fig. 4, followed by the desorption of the surface

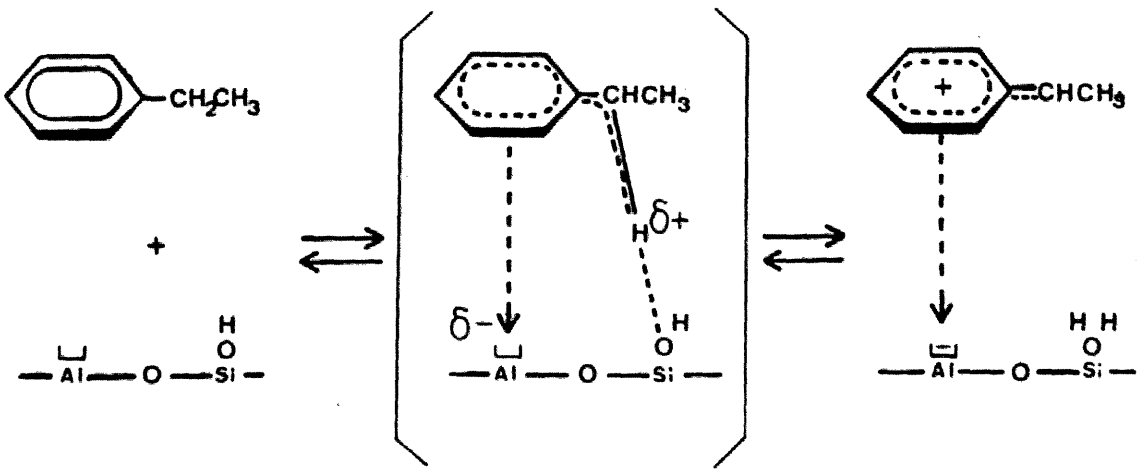

FIGURE 4 Reaction scheme for the adsorption of ethylbenzene.

water. Thus, oxygen can be adsorbed during the oxidative dehydrogenation of ethylbenzene.

Figure 2 shows the correlation of the amount of adsorbed oxygen species to the amount of base sites of pKa 17.2 ~ 26.5. The amounts of O_{2ad} and O^- are proven to be proportional to the amount of base on the sample. These results show that the amount of adsorbed oxygen species is controlled by the Na content and that the active site to form O_{2ad} and O^- is the base site of pKa between 17.2 and 26.5. Such a base site is proposed to be produced adjacent to the acid site of Ho between 1.5 and -5.6 by the inductive effect of Na-SiAl catalyst, whereas adjacent base site exists on the original-SiAl catalyst only by chance[1].

Figure 3 shows the effect of the treatment temperature on the amount of O^- formed on the catalyst with gaseous oxygen. The adsorbed molecular oxygen species (O_{2ad}) formed easily at 77 K, while the formation of O^- species was not observed at 77 K in 12 h, and the amount of O^- species gradually increased with time at 293 K and 323 K. Above 373 K, the amount of O^- increased steeply and soon reached a stationary state. These results show that at high temperatures such as reaction temperatures above 723 K, the amount of O^- will quickly reach a stationary state.

All these results suggest that O^- is formed on the base site of pKa between 17.2 and 26.5 through the well-known scheme to activate oxygen [19,36].

$$O_{2\cdot gas} \rightleftharpoons O_{2\cdot ads} \rightleftharpoons (O_{2\cdot ads}^-) \longrightarrow 2O^- \qquad \text{(Eq. 1)}$$

base site (pKa 17.2 ≈ 26.5)

As the hyperfine structure resulted from Al ion was not observed, these oxygen species may be adsorbed on the Si ion.

Reaction of Adsorbed Oxygen with Ethylbenzene

The reactivity of the adsorbed oxygen species was examined by the method described in the experimental section. About 12 μmol of ethylbenzene/g-cat was introduced onto the sample which had adsorbed O_{2ad} and O^-. The amount of O_{2ad} was unchanged at 293 K even after 120 h from the introduction of ethylbenzene, while the amount of O^- decreased gradually and reached a stationary state at 3 h. The amount of O_{2ad} decreased gradually at above 323 K. The reaction of O^- which had been produced by the N_2O treatment with ethylbenzene was also studied on original-SiAl. Even at 77 K the amount of O^- species gradually decreased with the introduction of ethylbenzene as shown in Fig. 5. At 293 K, a rapid decrease of O^- species was observed.

Styrene was formed in the pulse reaction of ethylbenzene with N_2O on the pretreated (similar to procedure 2 and 3 in the helium gas flow) SiAl catalyst. As shown in Table 1, the amount of styrene is comparable to that in the reaction with oxygen, while the combustion was suppressed. These results show that the active oxygen species of this reaction is O^- species.

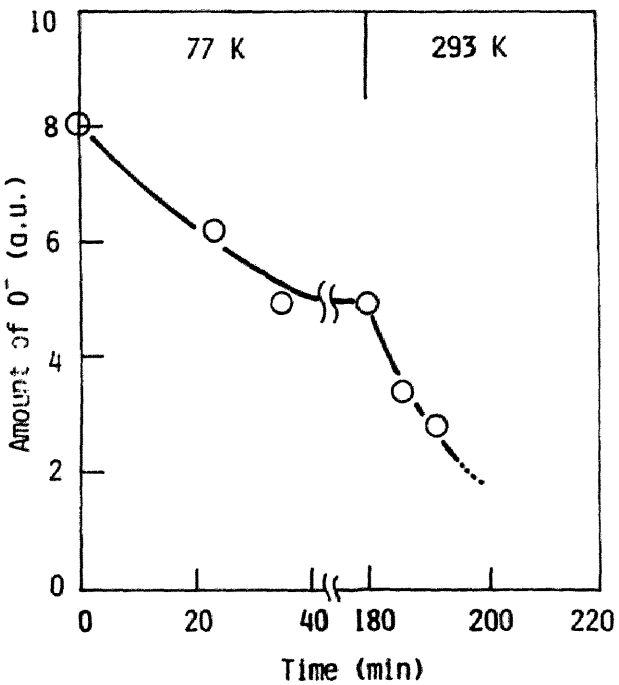

FIGURE 5 Reaction of O^- species with ethylbenzene on the Original-SiAl catalyst pretreated with N_2O along with the procedure(13).

Many studies have been devoted to the reactivity of O^-. Bohme and Young showed that the oxygen ion adds only in the case of ethylene and it abstracts a hydrogen atom or a proton from higher olefin [37]. For the simple alkanes, hydrogen atom abstraction was the only observed reaction [38]. Neta and Schuler [39] have demonstrated that the addition of O^- to double bonds and aromatic systems is relatively slow so that in most cases abstraction dominates. Kazansky et. al. [40] has also determined that the reaction of O^- with hydrocarbons is initiated by the abstraction of hydrogen by O^- to form the OH^- species. More recent work has demonstrated that O^- initiates hydrogen atom abstraction from alkanes and alkenes [41] resulting in the formation of alkenes and alkadienes, respectively. Thus, the O^- species on the catalyst surface can cause the oxidative dehydrogenation of hydrocarbons. In fact, such a mechanism has been proposed previously to explain the kinetic data on the activity of ferrite for the dehydrogenation of butenes[10,11,15,17]. A similar role of O^- species can be expected in the present reaction, that is, the O^- species abstracts the β-hydrogen of the adsorbed intermediate of ethylbenzene to form surface OH group and styrene.

Figure 6 shows the effect of Na content on the amount of O^- species and on the turnover frequency. The turnover frequency was calculated from the results obtained by the flow reaction base upon the number of acid sites of Ho between 1.5 and -5.6 which have been proven to form the adsorbed reaction intermediate of ethylbenzene. This turnover frequency represents the ability to abstract the β-hydrogen of the intermediate. The dependence of the amount of the O^- species on Na content is very similar to that of the turnover frequency on Na content, indicating that the role of the O^- species in the flow reaction is to abstract the β-hydrogen of the adsorbed reaction intermediate.

Reaction Mechanism of Oxidative Dehydrogenation of Ethylbenzene

As mentioned above, the oxidative dehydrogenation of ethylbenzene proceeds through the adsorption of ethylbenzene (Fig. 3), the activation of oxygen(Eq. 1) and the abstraction of β-hydrogen of adsorbed ethylbenzene with O^-. The reversibility of the adsorption of ethylbenzene shows that the rate determining step of this reaction is not at the adsorption of ethylbenzene but at the oxidation of the adsorbed intermediate of ethylbenzene. In this study, it is also clarified that the reaction of O^- with ethylbenzene is relatively rapid but requires an activation energy, as shown in Fig. 5. As the reaction of O^- species with hydrocarbons is said to require little activation energy, and the rate is said to be governed by the transport of hydrocarbon[40,41], the activation energy mentioned above can be attributed to the further activation of the adsorbed intermediate of ethylbenzene. The formation of O^- species also requires some activation energy, as shown in Fig. 3, but the rate of it is considered to be large at high temperature. The reaction order of this reaction was fractional in both ethylbenzene and oxygen[1], indicating that the activation of oxygen as well as that of ethylbenzene have a contribution to the rate of this reaction. However, the con-

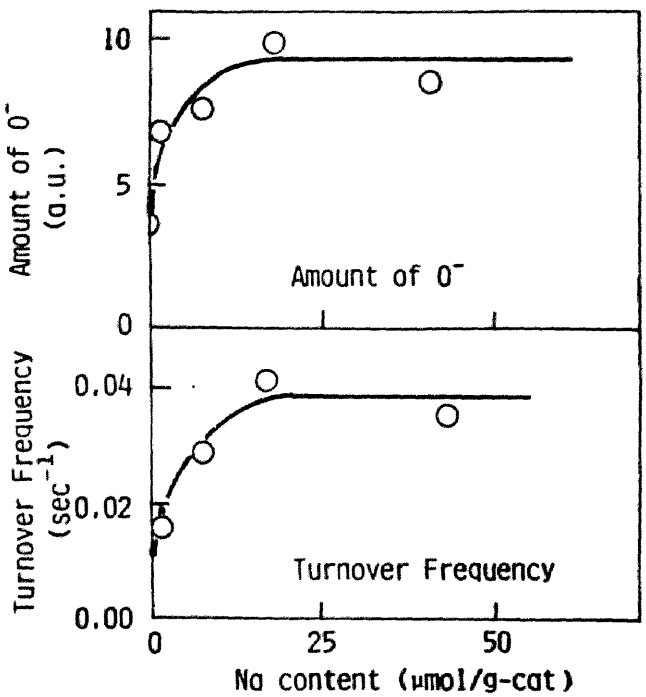

FIGURE 6 Effect of Na on the amount of O^- species and on the turnover frequency.

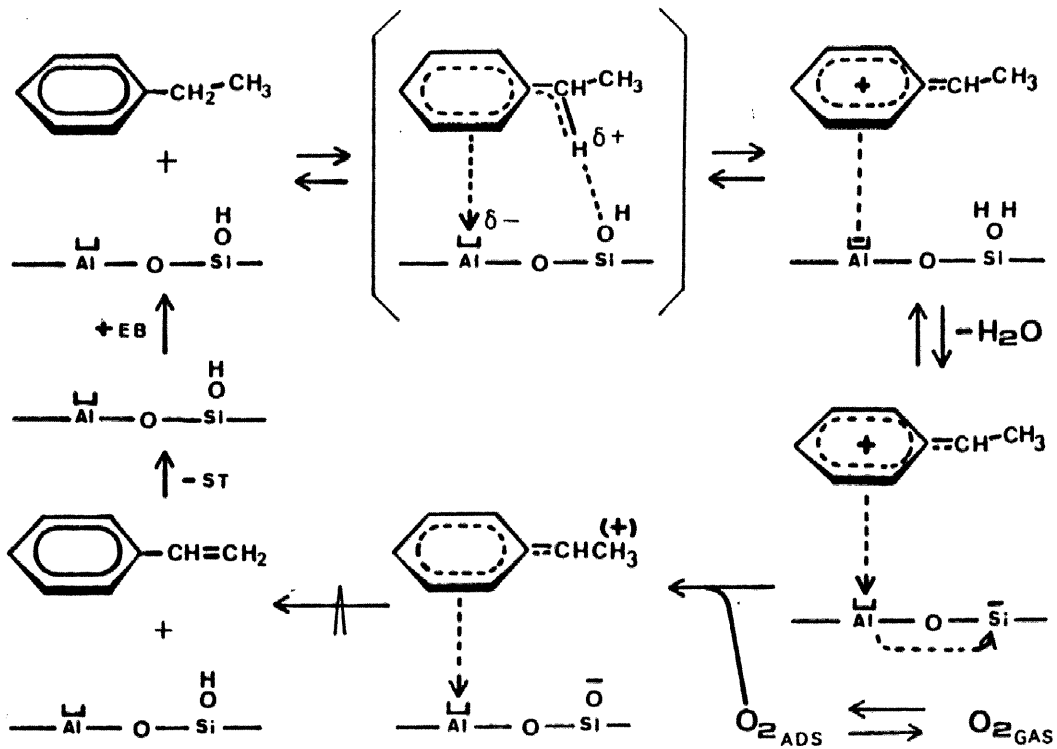

FIGURE 7 Reaction mechanism proposed for the oxidative dehydrogenation of ethylbenzene.

tribution of the activation of oxygen is considered to be small in the case of Na-SiAl catalysts, because the order in oxygen was small compared to the order in ethylbenzene. Consequently,the rate determining step of the overall reaction is proposed to be the reaction of O^- with the adsorbed intermediate of ethylbenzene to abstract the β-hydrogen.

Finally the overall reaction mechanism shown in Fig. 7 is proposed for the oxidative dehydrogenation of ethylbenzene.

1) First, ethylbenzene coordinates to the acid site of Ho between 1.5 and -5.6, and then the ring electron is donated to the acid site, which makes the acidic nature of the α-hydrogen pronounced.

2) The basic OH group adjacent to the acid site mentioned above abstracts the α-hydrogen from the coordinated ethylbenzene on the acid site to give a relatively stable adsorbed species.

3) The water formed by the abstraction of α-hydrogen desorbs to give an anion vacancy which can activate oxygen.

4) Reversibly adsorbed surface oxygen is converted to O^- species on the site mentioned above, with the strength of such an active site from 17.2 to 26.5 in pKa value.

5) The reversibly adsorbed intermediate of ethylbenzene is activated and its β-hydrogen is abstracted by the O^- species to give styrene and basic OH, which regenerates the active site. This step determines the overall rate of this reaction on Na-SiAl catalysts.

REFERENCES

1 T. Tagawa, T. Hattori, and Y. Murakami, J. Catal., in press; chapter 4 of this thesis.

2 B.C. Gates, J.R. Katzer, and G.C.A. Schuit, "Chemistry of Catalytic Process." p. 325, McGraw Hill, New York, 1979.

3 W.M.H. Sachtler, N.H. De Boer, Proc. 3rd Int. conger. Catal. Amsterdam p. 252 (1965).

4 T. Dozono, D.W. Thomas, and H. Wise, JCS Faraday I 69, (1973) 620.

5 H.H. Voge, C.D. Wagner, and D.P. Stevenson, J. Catal. 2, (1963) 58.

6 C.R. Adams, and T.J. Jennings, J. Catal. 2, (1963) 63.

7 C.R. Adams, and T.J. Jennings, J. Catal. 3, (1964) 549.

8 R.K. Grasselli, and D.D. Suresh, J. Catal. 25, (1972) 273.

9 A.L. Dent, and R.J. Kokes, J. Am. Chem. Soc., 92,(1970) 6709 and 6718, and Z. Dolejsek, and J. Nováková, J. Catal. 37, (1975) 540.

10 W.R. Cares, and J.W. Hightower, J. Catal. 23, (1971) 193.

11 M.A. Gibson, and J.W. Hightower, J. Catal. 41, (1976) 420.

12 Y. Murakami, K. Iwayama, H. Uchida, T. Hattori and T. Tagawa, J. Catal., in press, Chapter 3.

13 J. Hanuza, B. Jeżowska-Trzebiatowska, and W. Oganowski, J. Mol. Catal., 4 (1978) 271.
14 J. Haber, and B. Grzybowska, J. Catal., 28 (1973) 489.
15 R.J. Rennard, and W.L. Kehl, J. Catal., 21 (1971) 282.
16 R.J. Rennard, R.A.Jr. Innes, and H.E. Swift, J. Catal., 30 (1973) 128.
17 K.M. Sancier, and P.R. Wentrecek, and H. Wise, J. Catal., 39 (1975) 141.
18 M. Akimoto, M. Akiyama, and E. Echigoya, Bull. Chem. Soc. Jap., 49 (1975) 141.
19 J.H. Lunsford, Catal. Rev. 8 (1973) 135.
20 G.W. Keulks, L.D. Krenzke, and T.M. Notermann, Adv. Catal., 27 (1978) 183.
21 W.N. Delgass, G.L. Haller, R. Kellerman, and J.H. Lunsford, "Spectroscopy in Heterogeneous Catalysis." p. 212, Academic Press, New York, 1979.
22 W.M.H. Sachtler, Catal. Rev., 4 (1969) 27.
23 N. Kanzaki, and I. Yasumori, Bull. Chem. Soc. Jap., 52 (1979) 1923, and the references therein.
24 E.G. Derouane, and V. Indovina, Chem. Phys. Lett., 14 (1972) 455.
25 W.B. Williamson, and J.H. Lunsford, Chem. Phys. Lett., 9 (1971) 33.
26 H. Arakawa, and H. Ueda, Nippon Kagaku Kaishi, 1979 (1979) 422, and D. Cordischi, V. Indovina, and M. Occhiuzzi, JCS Faraday Trans., I 74 (1978) 883.
27 J.C. Vedrine, G. Dalmai, C. Naccache, and B. Imerik, J. Chim. Phys., Physico Chim. Biol., 65 (1965) 2129.
28 K.M. Wang, and J.H. Lunsford, J. Phys. Cem., 74 (1970) 1712.
29 N. Wong, Y.B. Taarit, and J.H. Lunsford, J. Chem. Phys., 60 (1974) 2148.
30 R. Beringer, and J.G. Castle, Phys. Rev. 81 (1951) 82, and M. Tinkham, and M.W.P. Strandberg, Phys. Rev., 97 (1955) 951.
31 N. Kanzaki, and I. Yasumori, Bull. Chem. Soc. Jap., 51 (1978) 991, and the references therein.
32 Y. Murakami, and K. Hayashi, Kogyo Kagaku Zasshi, 72 (1969) 1038.
33 S. Meyerson, and P.N. Rylander, J. Am. Che, Soc., 79 (1957) 1058, P.N. Rylander, S. Meyerson, and H.M. Grubb, J. Am. Chem. Soc., 79 (1957) 842, and F.W. Mclatterty, "Mass Spectrometry of Organic Ions." p. 481, Academic Press, New York, 1963.
34 J.D. Danforth, Proc. 2nd. Int. Conger. Catal. Paris I, 1271 (1960), and B.D. Flockhart, and R.C. Pink, J. Catal., 4 (1965) 90.
35 H. Itoh, A. Miyamoto, and Y. Murakami, J. Catal., 64 (1980) 284.
36 A. Bielański, and J. Haber, J. Catal., 19 (1979) 1.
37 D.K. Bohme, and L.B. Young, J. Am. Chem. Soc., 92 (1970) 3301.
38 D.K. Bohme, and F.C. Fehsenfeld, Can. J. Chem., 47 (1969) 2717.
39 P. Neta, and R.H. Schuler, J. Phys. Chem., 79 (1975) 1.
40 S.L. Kaliaguine, B.N. Shelimov, and V.B. Kazansky, J. Catal., 55 (1978) 384.
41 K. Aika, and J.H. Lunsford, J. Phys. Chem., 81 (1977) 1393, and 82 (1978) 1794.

Chapter 6

EXTENTION OF THE REACTION MECHANISM TO VARIOUS SOLID ACID CATALYSTS AND ITS APPLICATION TO CATALYST DESIGN

SYNOPSIS

The generality of the reaction mechanism, which is presented on the Na-SiO_2·Al_2O_3 catalysts, has been confirmed in the oxidative dehydrogenation of ethylbenzene and cumene on various solid acid catalysts. The amount of adsorbed ethylbenzene is well correlated to the amount of effective acid sites with Ho between 1.5 and -5.6, while the turnover frequency is well correlated to the amount of effective base sites with pKa between 17.2 and 26.5. Thus, the effective acid and base sites can generally be considered to adsorb ethylbenzene and abstract β hydrogen of adsorbed ethylbenzene, respectively. The strong acid sites (-5.6 Ho) are suggested to be active for the cracking and total oxidation reactions. This reaction mechanism provides the plan for the catalyst design. The catalyst designed on the basis of the plan actually shows high activity and selectivity.

INTRODUCTION

In the previous chapters, SnO_2-P_2O_5 catalyst has been found to be the most active and selective catalyst for the oxidative dehydrogenation of ethylbenzene among various oxide catalysts, where the addition of phosphorus (the acidic component) enhanced the selectivity [1]. The details of the catalytic behavior of SnO_2-P_2O_5 catalyst have also suggested that the activity and selectivity of this reaction are controlled by the acid and base properties of the catalysts [2]. To confirm the role of the acid and base properties of the catalysts on the catalytic oxidation reactions, the effect of the acid and base sites has been studied in detail using a series of Na freated SiO_2-Al_2O_3 (Na-Si·Al) catalysts [3]. Fiedorow et. al. [5] and Alkhazov et. al. [6] have proposed that the role of the acid sites is to form carbonaceous deposit which is active in this reaction, however, we have reached a contradictory conclusion that the

acid-base sites with suitable strength ranges are the active sites [4]. The presented roles of above sites are as follows; and the following mechanism has been proposed on the basis of the revealed roles of the acid and base sites in a molecular aspect [4]: 1) Etylbenzene is coordinates to the acid site of Ho between 1.5 and -5.6 with electron withdrawing character, and its α-hydrogen is activated. 2) The α-hydrogen of ethylbenzene is abstracted by the base site adjacent to the acid site mentioned above to form an adsorbed intermediate. These steps to adsorb ethylbenzene take place reversibly. 3) Gas phase oxygen is activated on the base site of pKa between 17.2 and 26.5 to form the active oxygen species, O^-, and the β-hydrogen of the adsorbed intermediate of ethylbenzene is abstracted by the O^- species to form styrene. The active site is also regenerated in this step. In this mechanism, the step to abstract the β-hydrogen determines the overall rate of styrene formation.

Recently, the methods that form the basis of the scientific design of catalysts attract considerable attention [7,8]. Catalyst design can be regarded, in many ways, as a logical application of available information to the selection of catalyst for a given reaction, and the elucidation of reaction mechanism and its extension can play important roles in it. In order to design the effective catalysts for the oxidative dehydrogenation of ethylbenzene, the above mentioned mechanism which is proposed in the case of Na-Si·Al system should be proved to hold generally on other catalysts. Thus, it will provide the plans for the catalyst design.

In this study, ten types of solid acid catalysts, including SnO_2 and Sn-P, were examined in the oxidative dehydrogenation of ethylbenzene and cumene to prove the generality of the reaction mechanism and the catalytic behaviors were studied in detail to give the plans of the catalyst design for the oxidative dehydrogenation of ethylbenzene.

EXPERIMENTAL

Catalysts

SiO_2-Al_2O_3(L) (Nikki Chemical Co. N632(L)) (Si·Al(L)), SiO_2-MgO (Nikki Chemical Co. X661) (Si·Mg), Al_2O_3 (Sumitomo Activated Alumina KHD and KAT-6) and SiO_2 (Fuji-Davison Chemical LTD. Micro beads silica gel 5D) were sieved and calcined at 773 K for 2 h in air. The preparation of solid phosphoric acid, SnO_2, SnO_2-P_2O_5 (Sn-P) and Na-SiO_2·Al_2O_3 (Na-Si·Al) catalysts were described in the previous paper [3]. Li-SiO_2·Al_2O_3 (Li-Si·Al), K-SiO_2·Al_2O_3 (K-Si·Al), and Na-SiO_2·MgO (Na-Si·Mgl) were prepared by the ion exchange method in the same way as Na-SiO_2·Al_2O_3 [3]. For Al_2O_3-P_2O_5 (Al-P) and SiO_2-P_2O_5 (Si-P), a known amount of phosphoric acid was added to the hydroxide gel of Al and Si, dried, calcined at 500 °C for 2 h in air, and sieved. The hydroxide gels were prepared by either boiling tetraethylorthosilicate in H_2O + HCl or by adding $NH_4OH_{aq.}$ to the aqueous solution of $Al(NO_3)_3 \cdot 9H_2O$. Al_2O_3-B_2O_3 (Al-B) catalyst was prepared by impregnating Al_2O_3 (KAT-6) with an aqueous solution of H_3BO_3, drying and cal-

cinating at 793 K.

Procedure

The catalytic activity was measured by using a conventional continuous flow reactor at atmospheric pressure as described previously [3]. The standard reaction conditions were as follows; catalyst weight, 1.00 g; reaction temperature, 450 °C; total feed rate, 290 mmol/h; partial pressures, $P_{O_2}:P_{EB}:P_{H_2O} = 0.100 : 0.143 : 0.322$ (atm) with N_2 balance. Reaction conditions different from the standard one were described in the footnotes of figures and tables. The pulse reaction apparatus is shown in Fig. 1. A small amount of oxygen impurity in the carrier gas was removed by the silica gel trap at 77 K immediately before the sample inlet. A sample inlet was jacketed and purged with nitrogen to prevent the introduction of oxygen into the purified carrier gas. The flow of carrier gas was splitted into two at the outlet of the reactor: for the gas-analysis of gaseous products and for the liquid-analysis of liquid products. The chromatographic columns were the same as described in the previous paper [3]. Pulse I (EB(1 μl) only), Pulse II (EB 10 min after O_2(1 ml)) and Pulse III (EB and O_2 at the same time) were conducted onto the catalyst (0.20 g) at 723 K in the flow of oxygen free helium (100 ml/min).

Surface properties

The acidity and basicity of catalysts were determined by titrating with n-butyl amine and benzoic acid, respectively, using Hammet indicators as described previously. The surface ares of the catalysts were determined by the usual BET method.

ESR measurment of perylene radical on the surface

The catalyst (0.1 g) in an ESR sample tube was evacuated at 300 °C for 3 h, then the benzene solution of perylene was added into the tube through a rubber septum, and the tube was sealed. The measurment was carried out with JES-ME-ESR-1X after the sealed sample had been placed in the dark for 2 days. DPPH solution was used to calibrate the signal intensity.

RESULTS

Generality of the Role of Acid and Base Properties

The mechanism of this reaction has been proposed on Na ion exchanged SiAl catalysts. An adequate amount of Na promoted the catalytic activity for the formation of styrene and the effect have been correlated to the acid and base properties of the catalysts. In order to confirm the generality of this reaction mechanism, the effect of alkali ions to solid acid catalysts were studied on other series of catalysts. Li-Si·Al, K-Si·Al, and Na-Si·Mg catalysts were prepared in the same ion exchange method and tested by the pulse technique in the same way as reported previously [2]. As shown in

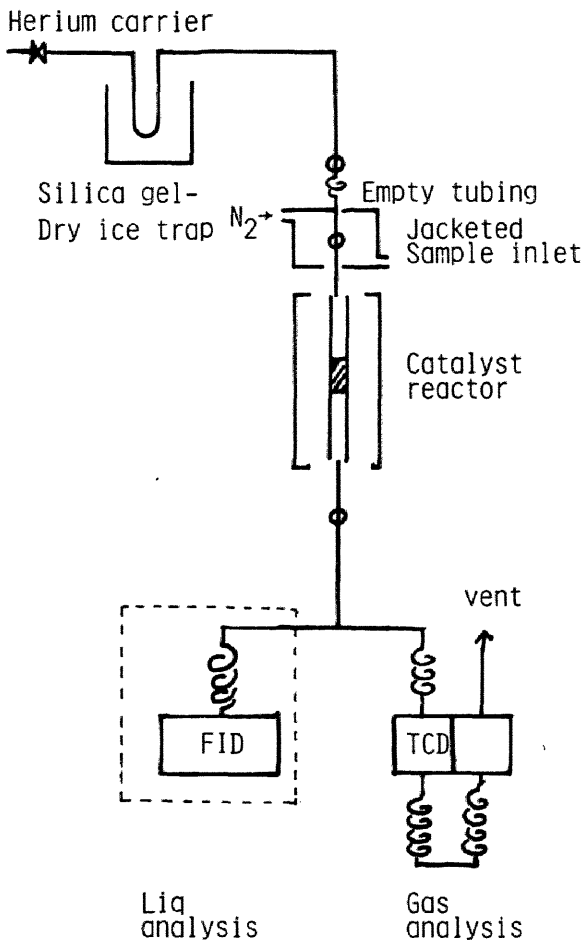

FIGURE 1 Pulse reaction apparatus.

Table 1, the promoting effect of alkali ions were observed on all alkali-Si·Al catalysts. The amount of formed styrene at 723 K increased in the following sequence; original < Li < K < Na. The promoting effect of Na was also observed on Na ion exchanged Si·Mg catalyst. The activity of Li exchanged SiAl catalysts and Na impregnated Al_2O_3 catalysts took the maximum at adequate contents of Li and Na as have been reported on Na exchanged Si·Al catalysts. All these results indicate that the promoting effects can be attributed to general acid and base properties of the catalysts but not to the limited effect of Na on SiAl catalyst, and that the reaction mechanism proposed previously holds in general on the solid acid and base catalysts.

Surface Properties

Typical solid acid catalysts, SnO_2, and SnO_2-P_2O_5 catalysts were used to examine further the generality of the reaction mechanism. Table 2 shows the surface properties of these catalysts. Considering the proposed reaction mechanism, the amount of effective acid ($1.5 > Ho > -5.6$), stronger acid ($-5.6 > Ho$) and effective base ($17.2 < pKa < 26.5$) were measured by the acid-base titrations. Only Si·Mg catalyst had no effective acid, but all of the other catalysts had the effective acid sites. In addition, Si·Al and Al-B catalysts had the stronger acid sites. The catalysts but Si·Mg and Solid-P catalysts possessed the base sites in the effective strength range ($17.2 < pKa < 26.5$). However, an unusual change in the color of the indicators was observed in the cases of SnO_2 and SnO_2-P_2O_5 catalysts, making it difficult to determine the basicity of the catalyst. The electron withdrawing property of the catalysts was measured by the reaction with perylene to form the perylene cation radicals using ESR spectroscopy.

Flow Reaction

The catalytic behavior of the catalysts contained in Table 2 were examined in the oxidative dehydrogenation of ethylbenzene and cumene by the continuous flow technique. As shown in Figs. 2 and 3, the catalysts showed relatively high selectivity, especially in the reaction of ethylbenzene. The order of activity was almost identical to each other in the reactions of cumene and ethylbenzene; Si-Al(H) ≈ Si-Al(L) ≈ Al-P > Al > Sn-P ≈ Al-B > Si-P > SnO_2 ≈ Si·Mg for ethylbenzene, and Al-P > Al ≈ Si·Al(L) ≈ Si·Al(H) > Al-B ≈ Sn-P ≈ Si-P > SnO_2 > Si·Mg for cumene.

In Fig. 4, the cracking activity of these catalysts were compared with the oxidative dehydrogenation activity, in the reaction of cumene. The rate of benzene formation in the absence of oxygen is plotted against the rate of α-methyl styrene formation in the presence of oxygen. The catalysts with the effective acid sites were active in the oxidative dehydrogenation, while only the catalysts with the stronger acid sites ($-5.6 > Ho$) were active in the cracking reaction. The poisoning of Si-Al catalyst with pyridine decreased only the cracking activity, but it did not change the activity for the oxidative dehydrogenation.

TABLE 1

Amount of Styrene Formed in the Pulse Reaction (μmol/g-cat)

Catalyst	I(EB)[a]	II (O_2 → EB)[b]	III(O_2 + EB)[c]
0.0-Si·Al	nil	nil	0.28
8.5Na-Si·Al	nil	nil	0.81
Li-Si·Al	nil	nil	0.31
K-Si·Al	nil	nil	0.73
0.0- Si·Mg	nil	nil	0.19
Na-Si·Mg	nil	nil	0.29

[a]I(EB): Ethylbenzene (1 μl) was pulsed, [b]II (O_2 → EB): O_2(2ml) was pulsed then ethylbenzene (1 μl) was pulseafter 10 minutes, [c]III(O_2 + EB): O_2(2 ml) and ethylbenzene (1 μl) were pulsed simultaneously.

TABLE 2

Surface Properties of Catalysts[a]

Catalyst	Amount of Acid[b] (μmol/g-cat) Ho: 1.5 ~	-5.6 ~	Amount of Base[c] (μmol/g-cat) pKa: 17.2 ~	26.5 ~	Surface Area (m^2/g-cat)	Amount of[d] Perylene Radical (μmol/g-cat)
Si·Al(L)	100	333	250	X	425	10.0
Si·Mg	X	X	X	X	55.8	0.04
Al_2O_3	213	X	88	X	361	0.82
Al-P (P/Al;1/10)	715	X	93	X	385	1.16
Si-P (P/Si;1/10)	406	c	12	X	246	0.01
Al-B (B/Al;1.5/10)	356	209	77	X	247	4.95
Solid-P	201	X	X	X	-	0.04
SnO_2	55	X	c	X	21.9	X
Sn-P(P/Sn;1/10)	117	X	c	X	29.8	0.17
SiO_2	X	X	X	X	210	X

[a]X; not observed, c; unusual change in color was observed.

[b]Estimated by titration using n-buthyl amine.

[c]Estimated by titration using benzoic acid.

[d]Estimated by ESR measurement of sample treated with perylene.

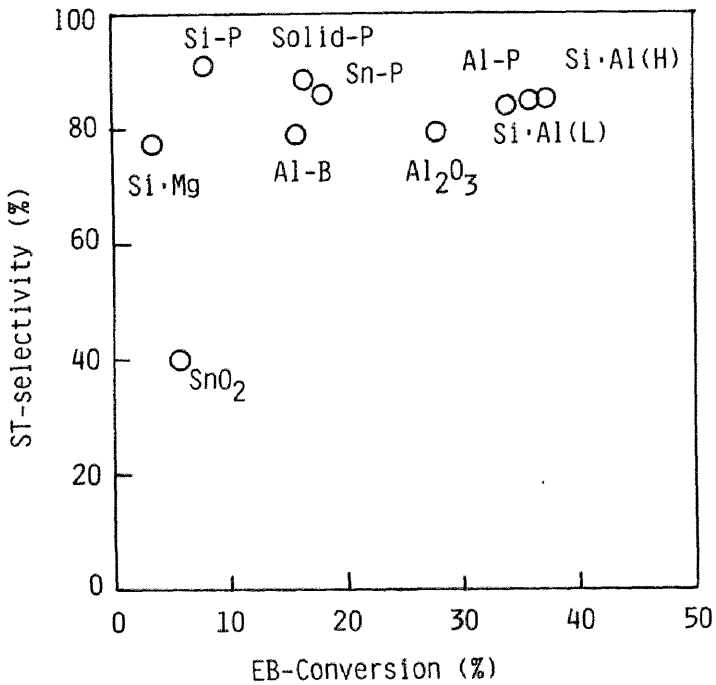

FIGURE 2 correlation between conversion and selectivity in the oxidative dehydrogenation of ethylbenzene. Catalyst weight; 1.00 g, Total feed rate; 290 mmol/h, Partial pressures; $P_{EB} : P_{O_2} : P_{H_2O} : P_{N_2}$ = 14.5 : 10.1 : 32.6 : 44.1 (kPa). Reaction temperature; 723 K.

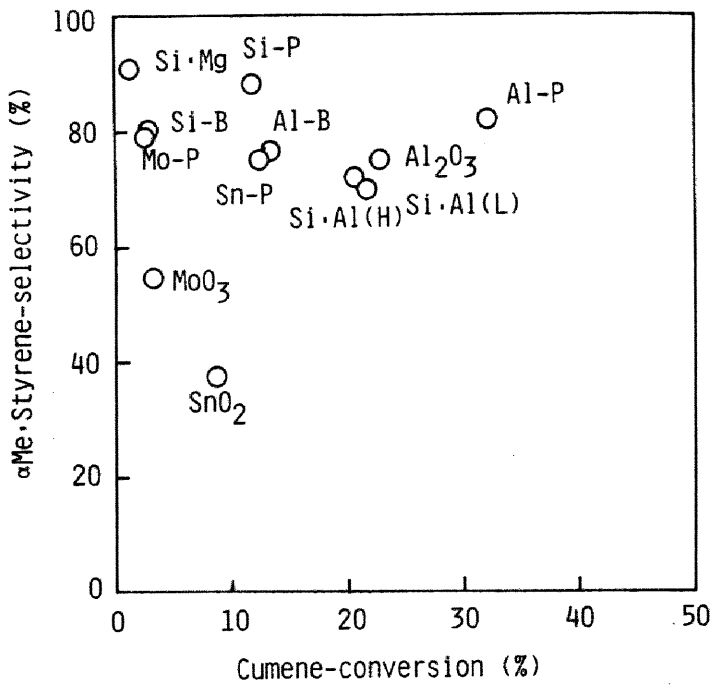

FIGURE 3 Correlation between conversion and selectivity in the oxidative dehydrogenation of cumene. Partial pressures; P_C : P_{O_2} : P_{H_2O} : P_{N_2} = 12.8 : 10.1 : 32.6 : 55.5 (kPa). For the other reaction conditions, see Fig. 2.

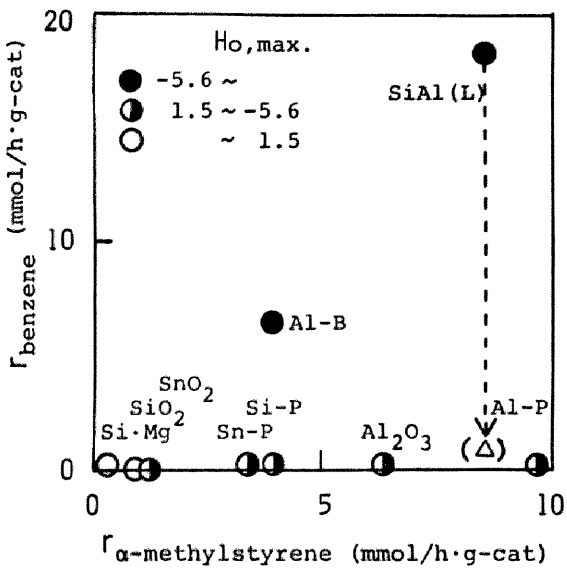

FIGURE 4 Correlation between oxidative dehydrogenation activity and cracking activity in the reaction of cumene. Partial pressures; P_C : P_{H_2O} = 12.8 : 32.6 (kPa), P_{O_2} was 10.1 kPa for the oxidative dehydrogenation reaction and was 0.00 kPa for the cracking reaction, with N_2 balance. For the other reaction conditions, see Fig. 2. Pyridine was added to the system (△).

In Fig. 5, the rate of styrene formation in the reaction of EB was plotted against the amount of effective acid sites. However, the correlation is not sufficient to explain the activity by only the acidic properties of the catalyst. The effect of the basic properties can be taken into account as well as the acidic properties.

Figure 6 shows the correlation between ST formation and combustion. The increase in the rate of styrene formation results in the increase in the rate of carbon oxides formation. The same correlation between oxidative dehydrogenation and total oxidation is observed in the reaction of comene.

Pulse Reaction

Further study was carried out using the pulse technique. The reactants were pulsed on the catalyst (0.2 g) in the following sequences: only ethylbenzene (1 μl) was pulsed (pulse I), oxygen (1 ml) was first pulsed (pulse II') and then ethylbenzene (1 μl) was pulsed 10 min later (pulse II), and oxygne (1 ml) and ethylbenzene (1 μl) was pulsed simultaneously (pulse III). Styrene, benzene, and carbon oxides were formed, and considerable amount of ethylbenzene was not recovered. Table 3 shows the results of styrene formation and Table 4 shows the results of combustion.

As shown in Table 3, SiO_2 showed no catalytic activity. Solid-P, Al_2O_3, Si-Al, Si·Mg, and Si-P formed styrene only in pulse III (ethylbenzene and oxygen were pulsed simultaneously), indicating that the oxygen species weakly adsorbed on the catalyst is active in this reaction. Al-P, Al-B, Sn-P, and SnO_2 formed styrene even in pulse I, indicating that the lattice oxygen or the strongly adsorbed oxygen species still has an activity. In the case of Sn-P and SnO_2 catalyst, the amount of styrene formed increased in the sequence of I < II < III, but the difference was not so large. In the cases of Al-P and Al-B, however, the amount of formed styrene in pulse III was much greater than that in pulse I or II, showing that the contribution of weakly adsorbed oxygen species were greater than that of strongly adsorbed one or lattice oxygen on these catalysts. In order to discuss the active oxygen species of these catalyst, further investigation is necessary.

As shown in Table 3, SiO_2, Al_2O_3, Si·Al, Si·Mg, Al-P, Al-B, SnO_2, and Sn-P formed carbon oxides in the oxygen pulse II' as well as in pulse III, Especially on Si·Al and SiO_2, the amount of carbon oxides formed in pulse II' was very close to that formed in pulse III. But no carbon oxides were formed on the catalysts but SnO_2 and Sn-P in the ethylbenzene pulse in pulse I and pulse II. These results indicate that carbon oxides are formed by the combustion of carbon species strongly adsorbed on the surface in the case of these catalysts. In the cases of SnO_2 and Sn-P catalysts, on the other hand, carbon oxides were formed without gaseous oxygen in pulses I and II. Furthermore, the amount of carbon oxides formed in the oxygen pulse II' is essentially equal to that formed in pulse III. These results indicate that the strongly adsorbed oxygen or the lattice oxygen plays a predominant role in the total oxidation of ethylbenzene.

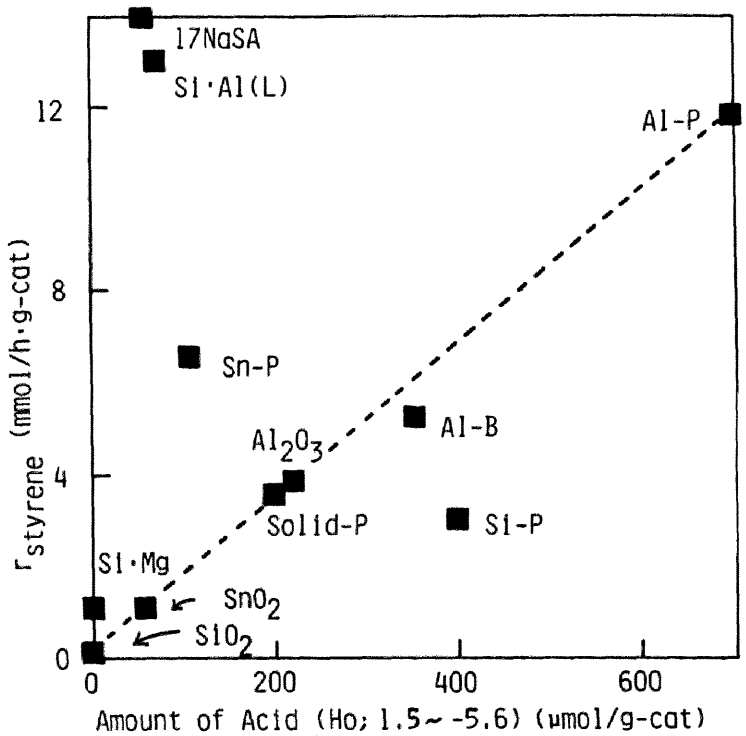

FIGURE 5 Correlation between the rate of styrene formation and amount of effective acid sites of Ho between 1.5 and -5.6, in the oxidative dehydrogenation of ethylbenzene. For the reaction conditions, see Fig. 2.

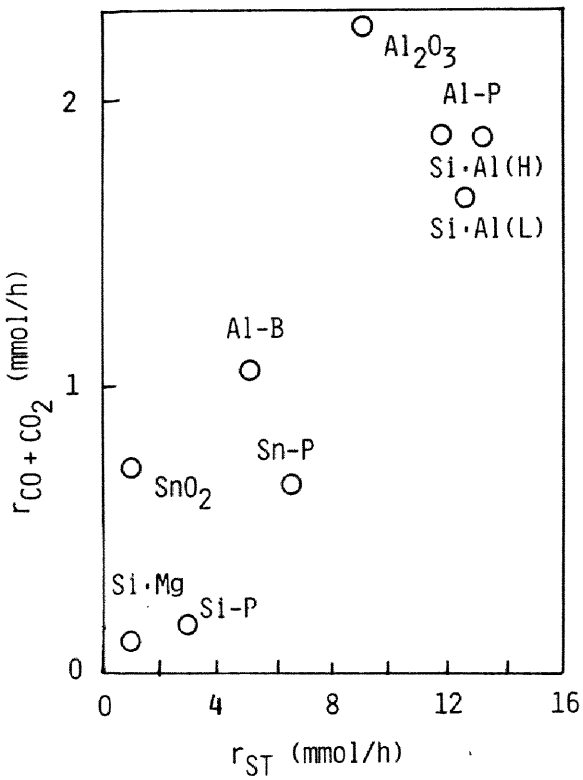

FIGURE 6 Correlation between the rate of styrene formation and total oxidation in the reaction of ethylbenzene. For the reaction conditions, see Fig. 2.

TABLE 3

Styrene formation by the pulse reaction (μmol/g)[a]

Catalyst	I(EB only)	II'(O_2)	II(EB)	III(O_2 + EB)	III - II
Al_2O_3	trace	nil	trace	0.40	0.40
Al-P	0.10	nil	0.08	1.12	1.12
Al-B	0.21	nil	0.14	0.38	0.24
Si·Al	trace	nil	trace	0.28	0.28
SiO_2	nil	nil	nil	nil	nil
Si·Mg	nil	nil	nil	0.05	0.05
Si-P	nil	nil	nil	trace	trace
Solid-P	trace	trace	nil	0.06	0.06
Sn-P	2.09	nil	3.54	3.67	0.13
SnO_2	1.10	nil	1.49	1.63	0.14

[a]Catalyst weight; 0.20 g, Reaction temperature; 718 K, Carrier gas; He 100 ml/min.

I(EB only): EB (1 μl) was pulsed.

II'(O_2) : O_2 (1 ml) was pulsed.

II (EB) : EB (1 μl) was pulsed after pulse II' with 5 minutes intervals.

III (O_2+EB): O_2 (1 ml) and EB (1 μl) was pulsed simultaneously.

TABLE 4

Total oxidation by the pulse reaction (μmol/g)[a]

Catalyst	I(EB only)	II' (O_2)	II(EB)	III (O_2 + EB)	III - II
Al_2O_3	nil	0.01	nil	0.16	0.15
Al-P	nil	0.02	nil	0.05	0.03
Al-B	nil	0.01	nil	0.11	0.10
Si·Al	nil	0.12	nil	0.13	0.01
SiO_2	nil	0.03	nil	0.05	0.02
Si·Mg	nil	nil	nil	0.09	0.09
Si-P	nil	nil	nil	nil	nil
Solid-P	nil	nil	nil	nil	nil
Sn-P	1.18	1.17	0.05	1.12	nil
SnO_2	1.28	2.08	1.00	2.11	0.03

[a]For the reaction conditions and the pulse sequence, see Table 3.

DISCUSSION

Reaction Mechanism

In the previous study on Sn-P(2) and Na-SiAl(4) catalysts, a considerable amount of ethylbenzene has not been recovered in the pulse reaction. Such an unrecovery has been correlated to the reversible absorption of ethylbenzene on the catalyst surface. The adsorption state has also been confirmed to be dissociated at the α-position from the isotope exchange study [4]. The correlation between the amount of reversible adsorbed ethylbenzene and the amount of acid sites ($1.5 > Ho > -5.6$) leads to the conclusion that the active site to adsorb ethylbenzene is the acid sites of Ho between 1.5 and -5.6 (effective acid sites). The turnover frequency, calculated from the rate of styrene formation and the amount of effective acid sites, was well correlated to the base site of pKa between 17.2 and 26.5. This leads to the conclusion that the abstraction of β-hydrogen form the adsorbed intermediate of ethylbenzene occurs on the base site of pKa between 17.2 and 26.5 (effective base sites). The role of effective base sites has also been determined to adsorb gaseous oxygen to from O^- species.

In this study, such an insufficient recovery of ethylbenzene was observed in the pulse reaction. As the flow rate of carrier gas was increased from 44.5 ml/min to 100 ml/min, the absolute value of the unrecovery was not the same as that reported in the previous study. The amount of adsorbed ethylbenzene is plotted against the amount of effective acid sites in Fig. 7. As the effective acid sites increase, the amount of adsorbed ethylbenzene increases, showing that the acid sites of Ho between 1.5 and -5.6 adsorb ethylbenzene, perhaps, in the dissociated state as in the proposed reaction mechanism mentioned above.

The turnover frequency of this reaction is calculated by assuming that the active site to adsorb ethylbenzene is the effective acid sites:

$$\text{turnover frequency} = \frac{\text{the rate of styrene formation in the flow reaction at 450 °C}}{\text{the amount of effective acid sites } (1.5 > Ho > -5.6)}$$

In Fig. 8, the calculated turnover frequency is plotted against the amount of effective base ($26.5 > pKa > 17.2$) together with the turnover frequency on Na-Si·Al catalysts reported in the previous paper [4]. The turnover frequency is well correlated to the amount of effective base sites, indicating that β-hydrogen is abstracted from the adsorbed ethylbenzene under the function of the effective base sites.

As shown in Table 3, the formation of styrene was observed in the case of pulse Ⅲ on almost all of the catalysts, showing that the weakly adsorbed oxygen on the catalyst surface is active in the abstraction of β-hydrogen of adsorbed ethylbenzene. This also agrees well with the conclusion obtained in the pulse reaction on Na-Si·Al catalysts [4]. The intrinsic effect of such weakly adsorbed oxygen can be represented by the difference in the styrene yield between pulse Ⅲ and pulse Ⅱ (Table 3 the last column). The effect decreases as follows; Al-P > Al_2O_3 > Si·Al ≒ Al-B > SnO_2 ≒ Sn-P > Solid-P ≒

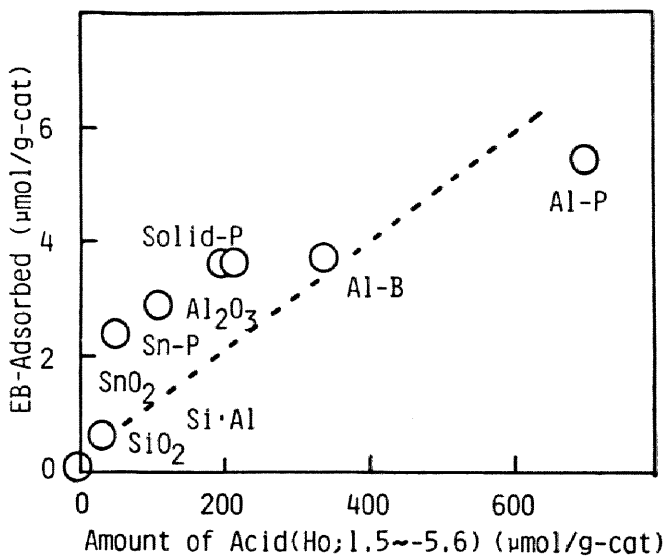

FIGURE 7 Correlation between the amount of the effective acid sites and that of ethylbenzene adsorbed by the pulse reaction. For the reaction conditions, see Table 3.

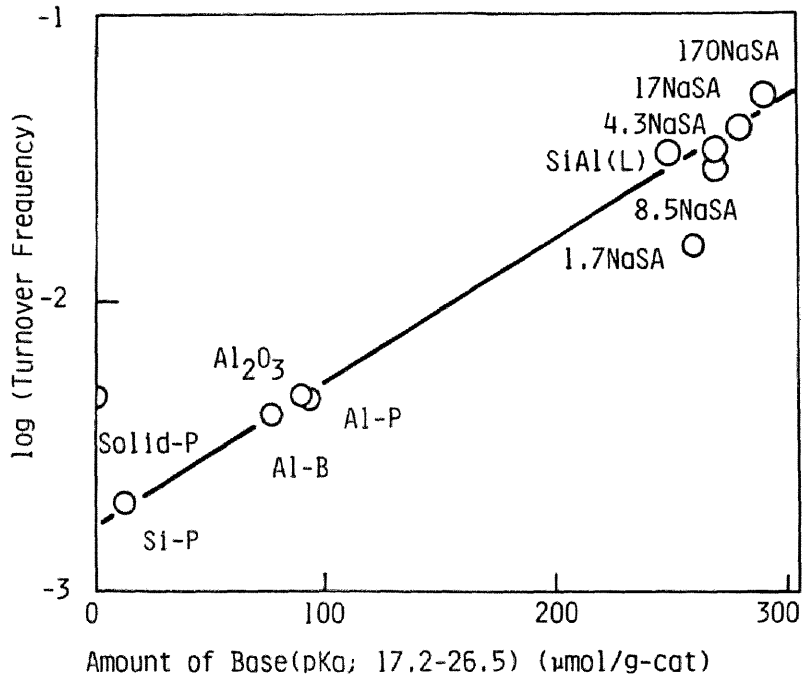

FIGURE 8 Correlation between the basicity and turnover frequency.

$$\text{Turnover Frequency} = \frac{\text{rate of styrene formation at 723 K}}{\text{amount of effective acid (Ho; 1.5 - -5.6)}} \quad (\text{sec}^{-1})$$

Si·Mg ≒ Si-P. This tendency almost agrees with the tendencies obtained by the continuous flow reaction, suggesting that the same reaction mechanism can hold both in the flow and pulse reactions.

Fiedorow [5] and Alkhazov [6] proposed that the active site of this reaction is the carbonaceous deposit formed on the acid sites, however, the direct correlation of the acid and base sites with this reaction discussed above leads to the conclusion that the effective acid and base sites are the active sites for the oxidative dehydrogenation of ethylbenzene.

All these discussions agree well with those in the Na-Si·Al systems. Consequently, the mechanism proposed previously [4] is not the limited model for Na and Si·Al system, but can hold generally for various catalysts.

Side Reactions

Carbon oxides are the predominant by-products in this reaction. On Sn-P catalyst, the selectivity of styrene was extrapolated to 100 % at zero contact time. This indicates that carbon oxides are formed by the subsequent oxidation of styrene once formed, though, on SnO_2 catalyst which is less selective, carbon oxides appear to be formed also by the oxidation of ethylbenzene [2].

In part II of these studies, it is suggested that the strong acid site ($-5.6 > H_o$) forms carbonaceous materials in the flow reaction and that carbon oxides are formed by the subsequent combustion of the carbonaceous materials thus formed [3].

As shown in Fig. 4, a strong acid site ($-5.6 > H_o$) is active in the formation of benzene which is a less predominant by-product. Only Si·Al and Al-B catalysts with the strong acid sites show the cracking activity, and the other catalysts without strong acid sites show no cracking activity. SiO_2 and Si·Mg catalysts which contain only weak acid sites ($1.5 < H_o$) are inactive for both cracking and oxidative dehydrogenation. It can be concluded from these results that the strong acid sites are active in the cracking reactions and that the effective acid sites are inactive in the benzene formation although they are active in the oxidative dehydrogenation. As shown in Fig. 4, the poisoning with pyridine reduced the catalytic activity on the cracking, but it did not change the activity in the oxidative dehydrogenation. Although considerable amounts of benzene were observed in the cracking of cumene on Si-Al(L) and Al-B (Fig. 3), in the steady state of the oxidative dehydrogenation of cumene the rate of benzene formation are reduced to 5.6 and 0.1 mmol/h·g-cat, respectively. This agrees well to the previously reported results that the strong sites become inactive in the steady state of the flow reaction because of the deposition of carbonaceous materials on them. The yields of carbon oxides in each of the pulses I, II, II', and III are summarized in Table 4. All the catalysts formed carbon oxides in the oxygen pulse of pulse II', except Si·Mg, Solid-P, and Si-P. This shows that the origin of carbon oxides are all or partly attributable to the carbon species deposited in pulse I on the catalyst surface. Carbon

oxides are formed also in pulse III on each catalyst, but the effect of the co-presence of ethylbenzene with oxygen, which can be evaluated from the difference between pulse II' and pulse III, are small on SiO_2, Solid-P, Si·Al, Al-P, SnO_2, Sn-P, and Si-P catalysts. Then the combustion reactions can be attributable to the oxidation of carbonaceous compounds deposited on the catalyst surface at lease on these catalysts. In the case of Sn containing catalysts, the combustion reaction occurs in the ethylbenzene pulse (pulse I), which makes it difficult to determine the origin of carbon oxides. It should be noted, however, that only a small amount of carbon oxides is formed in the ethylbenzene pulse of pulse II, on Sn-P catalyst. This suggests that, in the steady state condition, most of the carbon oxides are formed by the subsequent combustion of deposited carbon. The flow reaction on Sn-P catalyst [2] also suggested the same reaction paths. Good correlations were obtained between the rate of combustion and the rates of styrene formation and α-methylstyrene formation as shown in Figs, 5 and 6, respectively. Considering the above discussions, the amount of carbon oxides formed may depend on the amount of carbonaceous materials, and the amount of carbonaceous materials formed may depend on the amount of styrene or α-methylstyrene. These may result in the correlation shown in Fig. 6. It is well known that the carbonaceous materials are formed on the acid sites [5,9,10]. Moscou and Moné pointed out that this can occur on the strong acid site such as Ho about -8.2 [9]. The dependence of the rate of combustion on the coke concentration formed on zeolite catalysts has also been observed [11]. The subsequent combustion of coke formed on acid sites was observed in the oxidative dehydrogenation of ethylbenzene [5]. These discussions lead to the following conclusion that the combustion reactions occur by the oxidation of carbonaceous compound formed on the strong acid sites (around $-5.6 > Ho$) by the subsequent reaction of styrene on most of the solid acid catalysts. However further investigation is indispensable to clarify the details of the side reactions.

Brief Method for Estimation of Activity

In the design of catalysts for this reaction, it is important to estimate the acidity and basicity but it is difficult by titration in the case of colored samples using color indicators. Then a brief method to estimate the activity is needed. The nature of the active site is the electron withdrawing acid site with a suitable strength range and such active site can abstract the electron from the poly aromatics (i.e. perylene). The ESR spectra obtained by the reaction of perylene with catalyst is the same as those reported [12,13] and is identified as a perylene cation radical. The amount of the radical formed was nearly the same as reported [12,13,14,15]. In Fig. 9 the rate of styrene formation is plotted against the amount of perylene radical formed, together with the maximun acid strength of the catalysts. The activity is well related with the amount of perylene radical, except for Si·Al(L), Si·Al(H), and Al-B catalysts which possess stronger acid sites. Consequently, the activity of the catalyst without

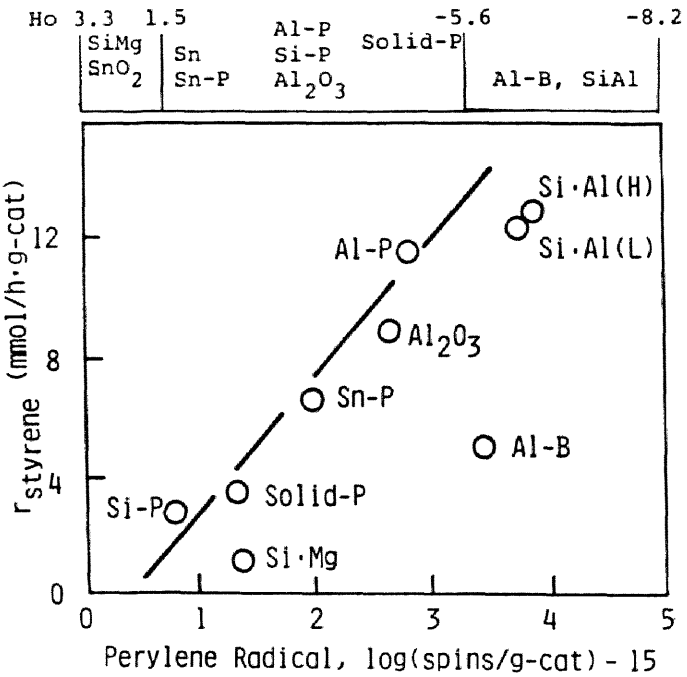

FIGURE 9 Correlation between the amount of perylene radical formed on the catalyst and the rate of styrene formation. For the reaction conditions, see Fig. 2.

stronger acid sites (-5.6 > Ho) can be predicted by the ability to form perylene cation radical.

Design of Catalyst for the Oxidative Dehydrogenation of Ethylbenzene

In order to design the catalyst, the active site to form desired products should be increased and the site for the side reactions should be decreased. The above mentioned reaction mechanism provides the following plans of the catalyst design for the oxidative dehydrogenation of ethylbenzene. The active sites to form styrene should be increased while the sites for cracking and total oxidation should be decreased. For the former, the acid sites of Ho between 1.5 and -5.6 as well as the base sites of pKa between 17.2 and 26.5 should be increased. For the latter, the strong acid sites (-5.6 > Ho) are undesirable. As shown in Table 1, the effective acid sites decrease in the sequence of Al-P > Si-P > Al-B > Al_2O_3 > Solid-P > Sn-P > Si·Al(L) > SnO_2. The effective base sites decrease in the sequence of Si·Al(L) > Al-P > Al_2O_3 > Al-B> Si-P ---. However Si·Al(L) and Al·B possess strong acid sites. Then, the above-mentioned plans for the catalyst design give the conclusion that Al-P catalyst will be the bast catalyst for the present reaction amoung the catalysts examined in this study. The Al-P catalyst, actually, shows the highest activity. The Si-Al catalysts show a high activity as the Al-P catalyst, but the selectivity of Al-P catalyst is higher than that of Si-Al catalysts as shown in Figs 2 and 3. Moreover, this catalyst can be predicted by the reaction of perylene with catalysts as shown in Fig. 9, too.

CONCLUSION

In order to design the catalysts, the active site to form the desired products should be increased while the site for the side reactions should be decreased. For this purpose, it is important to confirm the general reaction mechanism considering the active sites. The difference in the adsorption of ethylbenzene is explained by the difference in the effective acid sites (1.5 > Ho > -5.6) and the turnover frequency is correlated to the effective base sites (17.2 < pKa < 26.5), for various kinds of catalysts. The total oxidation is suggested to occur on the strong acid site (-5.6 > Ho) by the combustion of the coke deposited on the catalyst, which is formed by the subsequent reaction of styrene once formed. This reaction mechanism gives the plan of the catalyst design for the oxidative dehydrogenation of ethylbenzene. The catalyst which possesses a large amount of effective acid sites and effective base sites but not strong acid sites is Al-P catalyst, which actually shows high conversion and selectivity.

REFERENCES

1 Y. Murakami, K. Iwayama, H. Uchida, T. Hattori, and T. Tagawa, Appl. Catal., in press; Chapter 2 of this thesis.
2 Y. Murakami, K. Iwayama, H. Uchida, T. Hattori, and T. Tagawa, J. Catal., in press; Chapter 3 of this thesis.
3 T. Tagawa, T. Hattori, and Y. Murakami, J. Catal., in press; Chapter 4 of this thesis.
4 T. Tagawa, T. Hattori, and Y. Murakami, J. Catal., in press; Chapter 5 of this thesis.
5 R. Fiedorow, W. Przystajko, M. Sopa, and I.G. Dalla Lana, J. Catal., 68 (1981) 33.
6 T.G. Alkhazov and A.E. Lisovskii, Kinet. Katal., 17 (1976) 434.
7 D.L. Trimm, "Design of Industiral Catalysis," Elsevier Sci. Publ. Co. New York, (1980).
8 Y. Murakami, Shokubai, 21 (1979) 349, and 46th Annual Meeting of Japan Chemical Engineering Soc., p.564 (1981).
9 L. Moscou and R. Monē, J. Catal., 30 (1973) 417.
10 K. Mizuno, M. Ikeda, T. Imokawa, T. Take, and Y. Yoneda, Bull. Chem. Soc. Japan, 49 (1976) 1788.
11 T. Hano, F. Nakashio, and K. Kusunoki, J. Chem. Eng. Japan, 8 (1975) 127.
12 J.H. Raley and R.L. Hodgson, J. Catal., 4 (1965) 6.
13 W.K. Hall, J. Catal., 1 (1962) 53.
14 J.J. Rooney and R.C. Pink, J.C.S. Trans Faraday Soc., 58 (1962) 1632.
D.M. Brouer, J. Catal., 1 (1962) 372.

Chapter 7

SUPPORTED SnO_2 CATALYST FOR THE OXIDATIVE DEHYDROGENATION OF ETHYLBENZENE

SYNOPSIS

The design of the catalyst for the oxidative dehydrogenation of ethylbenzene has been performed by the plan that the suitable active sites for this reaction can be produced by combining SnO_2 with acidic supports. The designed SnO_2/SiO_2 catalyst shows excellent catalytic performances compared to the catalysts reported previously. The comparison of such acidic supports with the basic and amphoter supports is also studied and it shows the peculiar interaction of SnO_2 with SiO_2. The changes in the preparation method of SnO_2/Al_2O_3 are also studied.

INTRODUCTION

Oxidative dehydrogenation appears to be more attractive for the industrial production of styrene than the dehydrogenation process employed presently. In the oxidative dehydrogenation process, less steam is required and the reaction temperature is lower than the dehydrogenation process. Or, in other words, the oxidative dehydrogenation process can save energy.

In the previous chapter, SnO_2-P_2O_5 catalyst has been found to be effective in this reaction [1], and the bifunctional character has been assumed [2]: the basic component, SnO_2, contributes to activate oxygen while the acidic component, P_2O_5, contributes to activate ethylbenzene. Such contributions of the acid and base sites on this reaction have been confirmed using the solid acid catalysts [3,4], and it has been revealed that both acid and base sites are essential in this reaction.

In the design of industrial catalysts, the selection of suitable supports is an important step after the design of the active components because the supported catalysts have several advantages [5,6]. Trimm has classified the effect of supports into several functions, and one of the important roles of supports is to interact with the catalyst to improve specific activity or to minimize sintering [6]. Our previous

study on SnO_2-P_2O_5 catalysts has indicated that the chemical interaction of P_2O_5 with SnO_2 makes the acid and base sites suitable for this reaction [2]. This has brought about the plan to support SnO_2 onto the acidic oxides in order to design the suitable catalyst for this reaction. Since the bifunctional character mentioned above can be realized by supporting SnO_2 on acidic solid supports which can produce acidic sites by the chemical interaction with the basic component, SnO_2. Such interaction can also be altered by the preparation method of the supported catalysts.

In the present study, the effects of the variations in the preparation method on the catalytic properties of supported SnO_2/Al_2O_3 catalysts are investigated, and the performances of the use of acidic supports are compared with those of amphoter or basic supports.

EXPERIMENTAL

The reaction was carried out by the conventional flow technique. The experimental apparatus and procedure have been described elsewhere [1-3]. The reaction conditions were as follows; catalyst weight; 1.00 g dispersed in 4.00 g of fused alumina, total feed rate; 290 mmol/h, partial pressures; $P_{EB} : P_{O_2} : P_{H_2O} : P_{N_2} = 14.7 : 10.1 : 37.1 : 42.5$ (kPa). The supports employed in the present study were Al_2O_3 (Sumitomo Activated Alumina from Sumitomo Chem. Ind.; BET surface area, 274 $m^2 \cdot g^{-1}$), SiO_2 (Pore Dia Series S-90 A from Dokai Chem; 409 $m^2 \cdot g^{-1}$), $SiO_2 \cdot Al_2O_3$ (SiAl N632(H) from Nikki Chemicals Co. Ltd.; 320 $m^2 \cdot g^{-1}$), TiO_2 and MgO. TiO_2 was prepared by the hydrolysis of $TiCl_4$. $TiCl_4$ was slowly added to agitated water and boiled for 3 h, and the precipitates were filtered, washed dried at 393 K overnight and calcined at 773 K for 7.2 ks in a flow of air. BET surface area is 27.5 $m^2 \cdot g^{-1}$. MgO was prepared by the calcination of magnesium hydroxide at 773 K for 14.4 ks in the flow of air. The BET surface area of MgO is 106 $m^2 \cdot g^{-1}$. The support impregnated with $SnCl_2 \cdot 2H_2O$ from ethanol solution by the evaporation to dryness method, was washed repeatedly with 4N NH_4OH aqueous solution and then with water, dried at 383 K overnight, and then calcined at 773 K for 7.2 ks in a flow of air. Following preparation methods were applied to support SnO_2 on Al_2O_3. Al_2O_3 was impregnated with $SnCl_2 \cdot 2H_2O$ from ethanol solution by the evaporation to dryness method, dried at 383 K overnight and then calcined at 773 K for 7.2 ks in a flow of air, for Sn/Al(1); Sn/Al(1) was washed repeatedly with 4N NH_4OH aqueous solution and then washed with water, dried at 383 K overnight and then calcined at 773 K for 7.2 ks in a flow of air, for Sn/Al(2). Al_2O_3 was impregnated with $SnCl_2 \cdot 2H_2O$ from ethanol solution by the evaporation to dryness method, washed repeatedly with 4N NH_4OH aqueous solution and then with water, dried at 383 K overnight and then calcined, for Sn/Al(3). $SnCl_2 \cdot 2H_2O$ was dissolved into the 1N HCl solution of $Al(NO_3)_3 \cdot 9H_2O$ and the resulting solution was added into the 4N NH_4OH aqueous solution, washed with water after having left overnight, filtered, dried and calcined, for Sn-Al(4). Aqueous solution of $Al(C_3H_7O)_3$ and ethanol solution of $SnCl_2 \cdot 2H_2O$ were kneaded at the same time, dried and calcined, for Sn-Al(5). Al_2O_3(4) and

Al_2O_3(5), were prepared by the similar methods of Sn-Al(4) and Si-Al(5), respectively without adding the Sn-component. Sn/Al(6) was prepared from the HCl aqueous solution of $SnCl_2 \cdot 2H_2O$ using the same procedure as Sn/Al(1). SnO_2 calcined at 1273 K was added to the n-hexane solution of $(C_2H_5)_4SiO_4$, washed with water, dried and calcined, for Si/Sn.

RESULTS

The continuous flow reaction was conducted to compare the catalytic performances of supported SnO_2 catalysts prepared by various methods.

Effect of supporting method on the catalytic properties of Sn/Al catalysts

Al_2O_3, one of the typical supports, was selected in order to study the effect of the supporting method and SnO_2 content. Figure 1 shows the results on SnO_2, Sn/Al(3) and Al_2O_3. The Al_2O_3 supports alone produced styrene with relatively high selectivity. The origin of such activity and selectivity of alumina has already been reported elsewhere [3]. Conversion of ethylbenzene, yield of styrene and selectivity to styrene on Sn/Al(3) were essentially equal to those on Al_2O_3 alone, showing that the co-existence of SnO_2 has no effect on the catalytic properties. However, characteris-

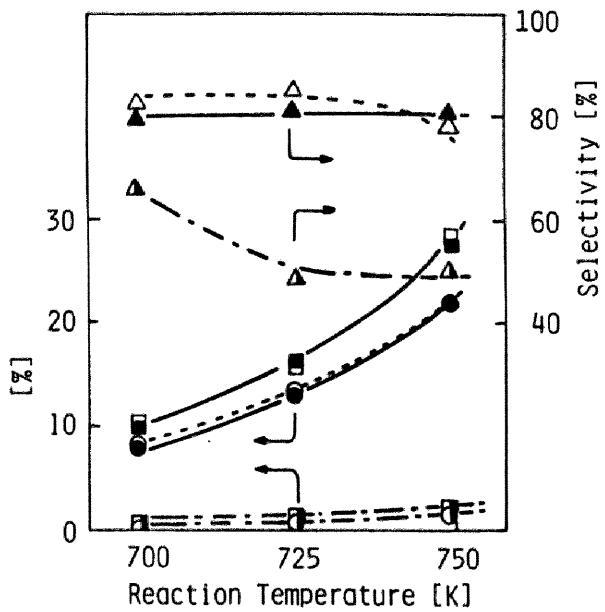

FIGURE 1 Catalytic properties of SnO_2 supported on Al_2O_3, Sn/Al(3), (●) compared to Al_2O_3 (○) and SnO_2 (◑). Styrene selectivity (△), Styrene yield (○), and Ethylbenzene conversion (□). Catalyst weight(W) = 1.00g, Total feed rate(F) = 290 mmol/h, and Partial pressures: $P_{EB} : P_{O_2} : P_{H_2O} : P_{H_2O} : P_{N_2}$ = 14.7 : 10.1 : 34.0 : 42.5, (kPa).

tics of SnO_2 (half-filled symbols in Fig. 1) with low selectivity and low conversion had disappeared. The effect of SnO_2 content on the catalytic properties of Sn/Al(1) and (6) was also studied. As shown in Fig. 2, the increase in the amount of SnO_2 in Sn/Al(1) prepared from ethanol solution content showed no effect on the catalytic properties, which resembles those of Al_2O_3 supports alone. This tendency has also been observed on Sn/Al(6) prepared from HCl aqueous solution. The effect of changes in the preparation method was also examined and shown in Fig. 3. The SnO_2 content of the catalysts was 4.8 mol% except for Sn/Al (6) with a 0.50 mol% of SnO_2. All the prepared Sn/Al catalysts [Sn/Al(1), (3) (4) (5) (6)] did not enhance the yields of styrene and CO compared to the case of Al_2O_3 supports alone. Co-precipitated Sn·Al(4) and co-kneaded Sn·Al(5) greatly lowered the yields of styrene and carbonoxides. Sn/Al (2) which was obtained by washing Sn·Al(1) with NH_4OH enhanced the yield of styrene to some extent with the yield of carbon oxides remaining constant. As the raw materials of Al_2O_3 in Sn-Al(4) and Sn-Al(5) are different from the other Sn/Al catalysts, their catalytic properties were compared with Al_2O_3(4) prepared from $Al(NO_3)_3$ and Al_2O_3(5) prepared from $Al(iPrO)_3$. As shown in Table 1, the catalytic properties of Al_2O_3(4) and Al_2O_3(5) are almost the same and resemble those of Al_2O_3 support shown in Fig 1 and 3. The addition of SnO_2 by the co-precipitation and co-kneading consid-

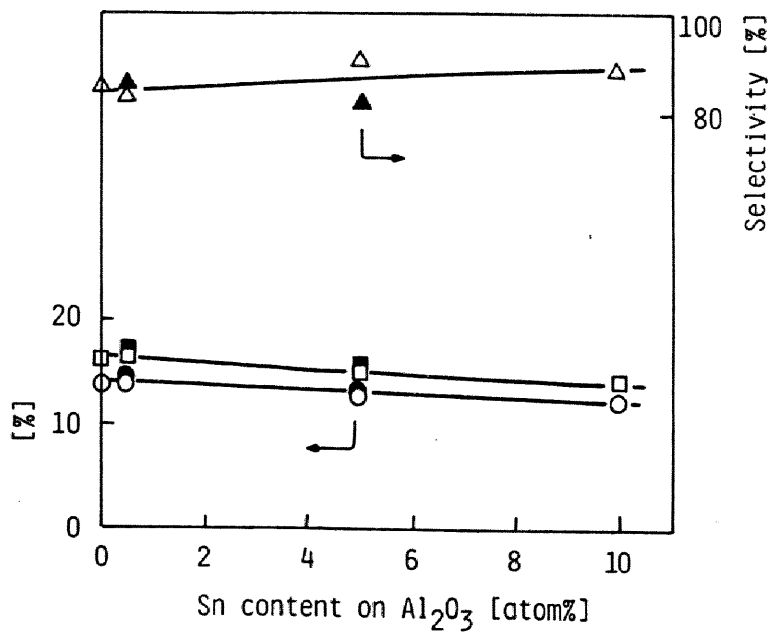

FIGURE 2 Effect of Sn content on the catalytic performances of Sn/Al(1), open symbols, and Sn/Al(2), filled symbols. For the reaction conditions and symbols, refer to Fig. 1.

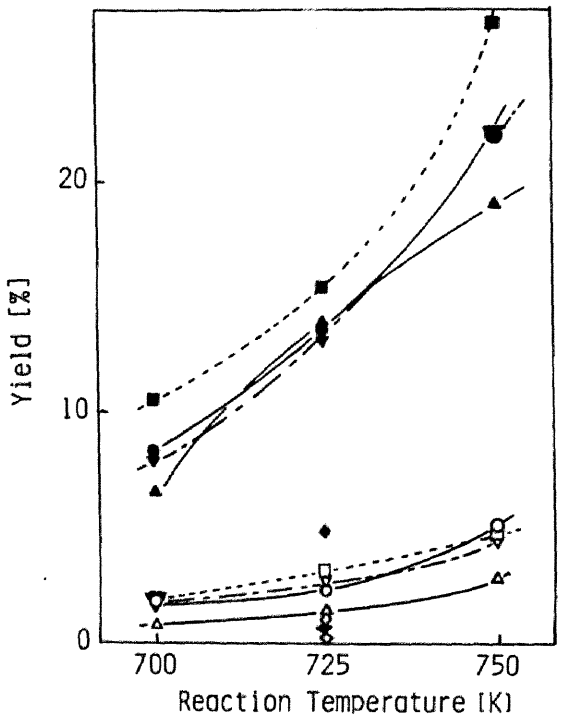

FIGURE 3Effect of the preparation methods of Sn/Al catalysts on the yield of carbon oxides (open symbols) and styrene (filled symbols). Al_2O_3 (○), Sn/Al(1) (△), Sn/Al(2) (□), Sn/Al(3) (▽), Sn-Al(4) (◇), and Sn-Al(5) (◇). For the reaction conditions, see Fig. 1.

TABLE 1

Catalytic behaviors of Sn-Al catalysts prepared by the co-precipitation and co-kneading method[a]

Catalyst	Surface Area (m^2/g)	Yield (%)				Selectivity (%)	Conversion (%)
		$CO+CO_2$	Benzene	Toluene	Styrene		
Al_2O_3(4)	253	3.3	nil	nil	11.2	77.0	14.5
Sn-Al(4)	240	1.3	trace	trace	6.4	79.1	8.1
Al_2O_3(5)	253	3.6	nil	trace	8.8	69.8	12.5
Sn-Al(5)	160	0.3	nil	nil	1.2	81.3	1.4

[a]Catalyst weight; 4.5 g, Total feed rate; 210 mmol/h, Partial pressures; $P_{EB} : P_{O_2} : P_{H_2O} : P_{N_2}$ = 20.3 : 20.3 : 31.3 : 29.4 (kPa).

erably lowered the conversion of ethylbenzene and the yields of carbonoxides and styrene while the selectivity to styrene increased a little.

Research of suitable supports

In the previous section, Al_2O_3 has been proved not to be suitable for the support of SnO_2 for this reaction. Thus, the research to find the suitable supports has been performed by using various types of supports. MgO has been selected as basic support, TiO_2 as Amphoters support, and SiO_2 and SiO_2-Al_2O_3 as acidic supports [6]. Figure 4 shows the results of MgO and Sn/Mg catalysts. MgO alone showed activity but the conversion of ethylbenzene and the selectivity to styrene were low. The conversion of ethylbenzene increased to some extent and the yield of styrene decreased to two thirds of that on MgO by supporting SnO_2, resulting to a significant decrease in the selectivity to styrene. Figure 5 shows the results of TiO_2 and Sn/Ti catalysts. TiO_2 showed activity and the dependence of the catalytic properties on the reaction temperature was almost the same as Al_2O_3 alone as shown in Fig. 1. However, the conversion, yield and selectivity are lower than those of Al_2O_3. The addition of SnO_2 did not change the catalytic properties of TiO_2. Figure 6 shows the results of $SiO_2 \cdot Al_2O_3$ and Sn/Si·Al catalysts. $SiO_2 \cdot Al_2O_3$ catalyst produced styrene selectively with relatively high conversion. The conversion of ethylbenzene and the yield of styrene decreased with the addition of SnO_2, however, the selectivity to styrene increased a little. Figure 7 shows the results of SiO_2 and Sn/Si catalysts. The activity of SiO_2 support was the lowest in all the supports investigated, and the selectivity was relatively low. Apparent changes in the catalytic properties were observed by supporting SnO_2. On the Sn/Si catalyst, the conversion of ethylbenzene and yield of styrene increased five times at 723 K as much as those on SiO_2 alone. The selectivity to styrene also increased above 90 % even at 748 K.

DISCUSSION

Figure 1 shows that SnO_2 supported on Al_2O_3, one of the typical supports, has no apparent effect on the catalytic properties and that the characteristics of SnO_2 catalyst disappeared. Such tendencies are also observed when the amount of SnO_2 was changed, showing that Al_2O_3 can support only a small amount of inactive SnO_2 or it cannot support SnO_2 at all. The enhancement of styrene yield by the NH_4OH aq. treatment shown in Fig. 3 suggests the former. These show that the amount of active sites to form styrene on the Al_2O_3 support does not change and that the active site on SnO_2 is deactivated, which can be regenerated by the NH_4OH treatment. As shown in Fig. 3, the change in the preparation method shows no effect on the above mentioned results. Moreover, as shown in Table 1, the Sn/Al(4) and (5) catalysts prepared by the co-precipitation method and co-kneading method show much lower activity than that on the Al_2O_3 alone prepared by the respective method. This shows that the increase in the interaction of SnO_2 with Al_2O_3 results in the decrease in the activity of both compo-

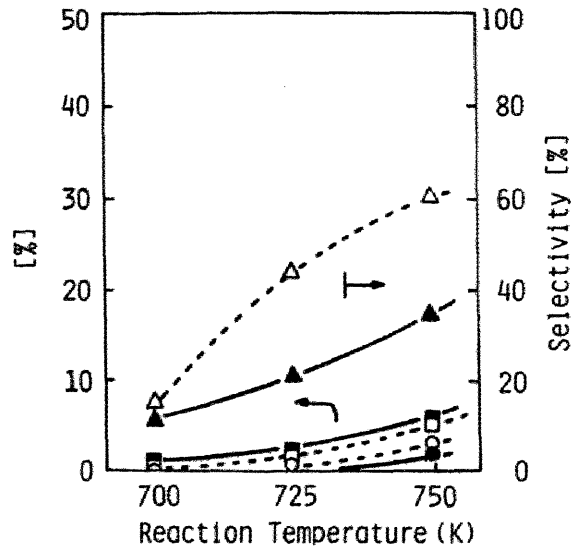

FIGURE 4 Comparison of the catalytic performances of MgO alone (open symbols) and SnO_2 supported on MgO, Sn/Mg (filled symbols). For the reaction conditions and symbols, see Fig. 1.

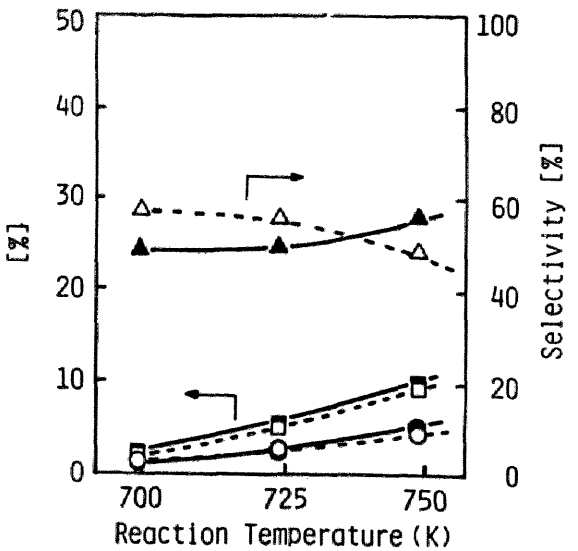

FIGURE 5 Comparison of the catalytic performances of TiO_2 alone (open symbols) and SnO_2 supported on TiO_2, Sn/Ti (filled symbols). For the reaction conditions and symbols, see Fig. 1.

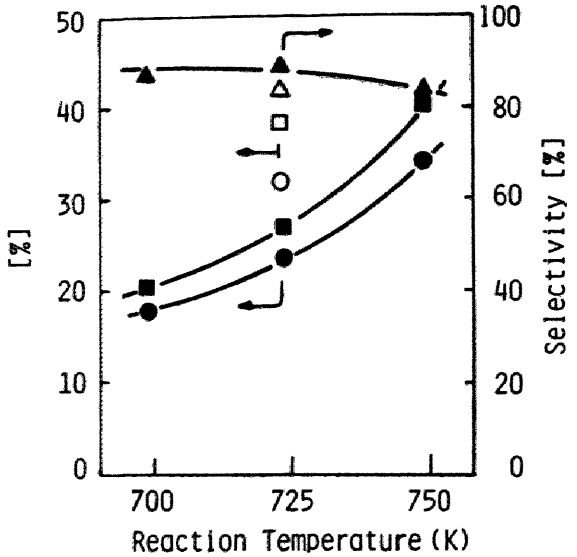

FIGURE 6 Comparison of the catalytic performances of SiO_2·Al_2O_3 alone (open symbols) and SnO_2 supported on SiO_2·Al_2O_3, Sn/Si·Al (filled symbols). For the reaction conditions and symbols, see Fig. 1.

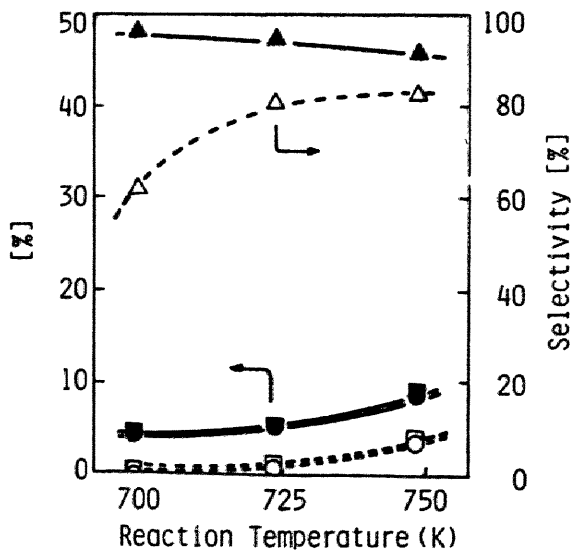

FIGURE 7Comparison of the catalytic performances of SiO_2 alone (open symbols) and SnO_2 supported on SiO_2, Sn/Si (filled symbols). For the reaction conditions and symbols, see Fig. 1.

nents. As a result, Al_2O_3 is not a suitable support of SnO_2 catalyst for the oxidative dehydrogenation of ethylbenzene.

The suitable supports of SnO_2 catalyst for this reaction are screened by several supports. Basic support (MgO), amphoteric supports (TiO_2 and Al_2O_3), and acidic supports (SiO_2 and $SiO_2 \cdot Al_2O_3$) were examined. The supports alone which produced styrene and the origin of the active site for this reaction has been discussed in the previous paper [3,4]. The results can be summarized as follows on the basis of the acidity of support.

(1) Supporting SnO_2 on basic oxide (MgO) reduced the yield and selectivity to styrene.

(2) Supporting SnO_2 on amphoter supports (Al_2O_3, and TiO_2) did not change the catalytic performance of amphoter supports.

(3) Supporting SnO_2 on strong acid support ($SiO_2 \cdot Al_2O_3$) reduced the conversion of ethylbenzene and the yield of styrene but increased the selectivity to styrene to some extent.

(4) Supporting SnO_2 on weak acid support (SiO_2) increased not only the conversion of ethylbenzene and the yield of styrene but also the selectivity to styrene, and SnO_2/SiO_2 catalyst is a good catalyst for the oxidative dehydrogenation of ethylbenzene.

Thus, supporting SnO_2 on acid supports can increase the selectivity to styrene compared to the case of SnO_2 or the support alone, while Si·Al support possesses considerable amounts of active sites for this reaction and such sites can be deactivated by the reaction with $SnCl_2$. The origin of such good results can be the special interaction of SnO_2 with the support, which may produce the effective acid and base sites as predicted form the results of Sn-P catalysts [2]. Such tendencies are observed in the case of supporting SiO_2 on SnO_2 support. As shown in Table 2, the catalytic performances of SiO_2/SnO_2 catalyst are compared with those of SnO_2 support alone. The yield

TABLE 2

Catalytic propertries of SiO_2 supported on SnO_2[a]

Catalyst[b]	Reaction temperature (K)	Yield (%)				Selectivity (%)	Conversion (%)
		$CO+CO_2$	Benzene	Toluene	Styrene		
SnO_2	723	3.3	nil	nil	2.8	45.7	6.1
	748	10.4	nil	trace	15.1	59.2	25.5
Si/Sn	723	2.0	nil	trace	25.3	91.8	27.6
	748	6.2	nil	0.5	30.3	81.9	37.0

[a]For the reaction conditions, refer to Table 1.

[b]SnO_2; calcined at 1273 K, Si/Sn; SiO_2 was supported on SnO_2 calcined at 1273 K using $(C_2H_5)_4SiO_4$.

of styrene on SiO_2/SnO_2 at 723 K is ten times as much as that on SnO_2 and the selectivity to styrene is also twice as much. Comparing them even at the same conversion range of 25 - 30 %, 748 K for SnO_2 and at 723 K for SiO_2/SnO_2, the yield of styrene and selectivity to styrene on SiO_2/SnO_2 are much higher than those of SnO_2, while the total oxidation decreases from 10.4 % on SnO_2 to 2.0 % on SiO_2/SnO_2 catalyst.

Above results also support that the active sites for the oxidative dehydrogenation of ethylbenzene can be produced by the peculiar interaction of SnO_2 with SiO_2. Such interactions of catalyst components and supports attract special interest for the design of catalysts and requires further investigation.

In the previous paper, SnO_2-P_2O_5 catalyst has also been reported to be a good catalyst for this reaction compared with the catalytic systems reported in the recent patents [7-18] and papers [19-22]. The catalytic performances of Sn/Si catalyst are then compared with those of Sn-P catalyst in high conversion regions. The performance of Sn/Si at high conversion levels is shown in Fig.8. The selectivity is about 90 % even at the conversion level of 60 %. The yield of styrene is as high as 55 %. On the other hand, Sn-P catalyst show about 90 % selectivity at the conversion level of 30 %

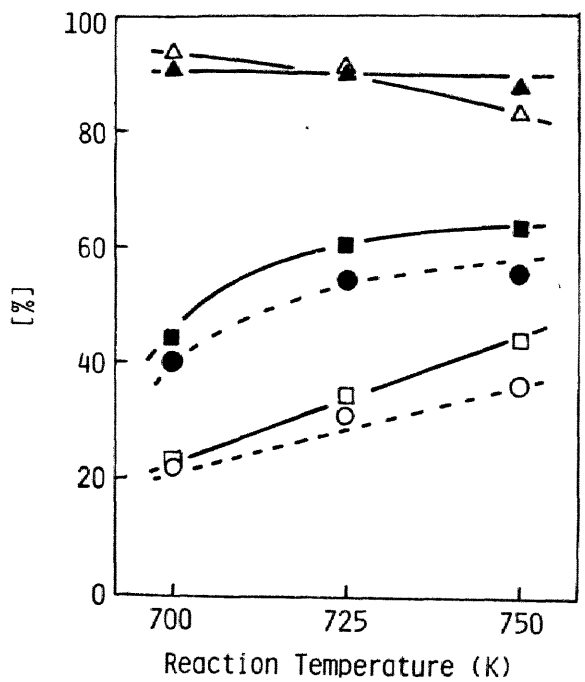

FIGURE 8 Catalytic performances of Sn-P(10/1) catalyst (open symbols) and Sn/Si catalyst (filled symbols) in the high conversion range. Catalyst weight(W); 4.5 g, Total Feed rate(F); 208 mmol/h, Partial pressures; $P_{EB} : P_{O_2} : P_{N_2} = 20.3 : 20.3 : 60.8$ (kPa). For the other symbols, refer to Fig. 1.

at the same reaction conditions of Sn/Si. Thus the conversion and the yield of styrene on Sn/Si are higher than those on Sn-P catalyst with similar selectivity as high as 90 %. This indicates that Sn/Si catalyst is superior, for the industrial production of styrene from ethylbenzene by the oxidative dehydrogenation, compared to Sn-P catalysts [1,2] and the other catalysts reported previously [7-23].

In summary, catalyst for the oxidative dehydrogenation of ethylbenzene is designed according to the plan of combining SnO_2 with acidic supports. The designed SnO_2/SiO_2 catalyst shows excellent catalytic properties compared to the other catalytic systems. The changes in the preparation method of Sn/Al catalyst show little effect on the catalytic properties. Comparing the acid supports with base and amphoter supports has suggested the peculiar interaction of SnO_2 with acid supports and SiO_2 support is particularly suitable for this reaction. For the interaction of SnO_2 with SiO_2 support, further investigation still proceeds.

REFERENCES

1 Y, Murakami, K. Iwayama, H. Uchida, T. Hattori, and T. Tagawa, Appl. Catal., in press; Chapter 2 of this thesis.

2 Y. Murakami, K. Iwayama, H. Uchida, T. Hattori, and T. Tagawa, J. Catal., in press; Chapter 3 of this thesis.

3 T. Tagawa, T. Hattori, and Y. Murakami, J. Catal., in press; Chapter 4 of this thesis.

4 T. Tagawa, T. Hattori, and Y. Murakami, J. Catal., in press; Chapter 5 of this thesis.

5 Y. Murakami, Shokubai, 21 (1979) 349; Chapter 1 of this thesis.

6 D.L. Trimm, Design of Industrial Catalysts, Elsevier, New York, 1980.

7 M. Imanari, and Y. Watanabe, Petrotech, 2 (1979) 332.

8 R.M. Benslay and A.L. Jones, U.S. Patent,3,652,698 (1970).

9 J.R. Ghublikian, British Patent, 1,176,916 (1970).

10 Dow Chemical Co., Japan Kokai, 74-12,790 (1974).

11 Nitto Chemical Industry Co. Ltd., Japan Kokai, 74-41,182 (1974).

12 Mitsubishi Chemical Industries Ltd., Japanese Patent, 75-30,061 (1975).

13 Y. Murakami, Japanese Patent, 77-29,299 (1977).

14 Nippon Kayaku Co. Ltd., Japanese Patent, 74-42,017 (1974).

15 Nippon Shokubai Kagaku kogyo Co. Ltd., Japanese Patent. 77-28,782 (1977).

16 K. Fujimoto, Y. Yamada, and T. Kunugi, Japan Kokai, 77-23,027 (1977).

17 Mitsubishi Petrichemical Co. Ltd., Japan Kokai, 78-44,525 (1978).

18 T. Imai, U.S. Patent, 4,180,690 (1979).

19 C. Conesa, A. Cortes, J. Marti, J.L. Seoane, and J. Soria, J. Catal., 58 (1979)34.

20 J. Hanuza, B. Jezowska-Trzebiatowska, and W. Oganowski, J. Mol. Catal., 4 (1978) 271.

21 C. Bagnasco, P. Ciambelli, S. Crescitelli, and G. Russo, React. Kinet. Catal.

Lett., 8 (1978) 293.

22 W. Oganowski, J. Hanuza, B. Jezowska-Trzebiatowska, and J. Wrzyszcz, J. Catal., 39 (1975) 161.

23 K. Fujimoto and T. Kunugi, Ind. Eng. Chem, Prod. Res. Dev., 20 (1981) 319.

Chapter 8

CATALYTIC BEHAVIORS OF SnO_2/SiO_2 CATALYSTS

SYNOPSIS

The effect of preparation method of supported SnO_2 on SiO_2 was investigated. 4.8 mol% SnO_2/SiO_2 catalyst, which was prepared by the impregnation from the ethyl alcohol solution of $SnCl_2$ and the treatment with NH_4OH aqueous solution,shows the highest conversion and the highest selectivity to styrene. The NH_4OH treatment is very important to prepare a good catalyst. The characterization of catalysts was carried out in relation to the NH_4OH treatment. The electron withdrawing ability and the state of SnO_2 on the support have been examined by ESR and XRD. Interactions of SnO_2 with various supports have been investigated by ESR and XRD. The active sites are considered to consist of the deficient Sn atom under the electron withdrawing effect of SiO_2 support. The effect of NH_4OH treatment is to remove residual chlorine ions. The residual chlorine ions reduces the interaction between SnO_2 and SiO_2 and produces inactive compound on the surface.

INTRODUCTION

In the design of industrial catalysts, the selection of promoter is one of the most important steps [1,2]. It has been found that the addition of P_2O_5 to SnO_2 remarkably increased yield and selectivity to styrene in the oxidative dehydrogenation of ethylbenzene [3]. In the recent studies about the mechanism on a series of Na-Si-Al catalysts, cooperative character of acid and base sites has been confirmed [4,5]; the acid sites of $1.5 > Ho > -5.6$ activate ethylbenzene and the base sites of $17.2 < pKa < 26.5$ activate oxygen to oxidize the activated ethylbenzene. This conclusion has been confirmed to be effective on various solid acid catalysts including SnO_2-P_2O_5 (Sn-P) catalyst [6]. A chemical interaction of SnO_2 with P_2O_5 has also been supposed to make the acid and base sites suitable for this reaction [7]. Another way to control catalytic properties in the design of industrial catalysts is supporting an active

components on supports. In general, supported catalysts have larger surface area than unsupported catalysts. This may resulted in higher activity. In the screening of the catalyst for the present reaction [3], the addition of acidic compound, P_2O_5, enhanced the activity and selectivity of SnO_2 catalyst, but the addition of basic compounds, LiO_2 and K_2O, resulted in the poor catalytic performance. This leads to a plan for the selection of the support for SnO_2, that is the supporting SnO_2 on acidic supports may increase the conversion and selectivity. According to this plan, SnO_2/SiO_2 catalyst have been designed and excellent catalytic performances have been obtained [8].

Interests are also attracted on the specific interactions of the catalyst component and support. Such interactions, electron transfer between SnO_2 and the support, may occur in the case of supported SnO_2 catalyst [8]. As Sn atom is one of the Mössbauer active elements, such interactions can be investigated by the Mössbauer spectroscopy. Many studies have been done on Fe containing catalysts using the Mössbauer spectroscopy [9,10,11,12]. However, only few studies have been reviewed on supported SnO_2 catalysts [11].

In this study, the preparation method of Sn/Si catalysts has been studied, and the nature of the active site has also been investigated using XRD and Mössbauer spectroscopy, comparing to unsupported SnO_2 catalysts. On the basis of these results, the effects of support and preparation method on the nature of active sites have been proposed.

EXPERIMENTAL

A silica gel used as the support was Pore Dia Series S-90 A from Dokai Chem. The surface area was 409 $m^2 \cdot g^{-1}$. Following preparation methods were employed to support SnO_2 on SiO_2. (1) SiO_2 was impregnated with $SnCl_2 \cdot 2H_2O$ from ethanol solution by the evaporation to dryness method, dried at 383 K overnight and then calcined at 773 K for 2 h in a flow of air, for Sn/Si(1). (2) Sn/Si(1) was washed repeatedly with 4N NH_4OH aqueous solution and then washed with water, dried and calcined, for Sn/Si(2). (3) SiO_2 was impregnated with $SnCl_2 \cdot 2H_2O$ from ethanol solution by the evaporation to dryness method, washed repeatedly with 4N NH_4OH aqueous solution and then washed with water, dried and calciend, for Sn/Si(3). (4) Sn/Si(3) was treated with 1N HCl aqueous solution by decantation, dried and calciend, for Sn/Si(4). (5) 0.48 g of Sn metal was dissolved into 50 ml of 2N HNO_3 aqueous solution. 8.5 g of silica gel was added into the solution, evaporated to dryness, dried and calciend, for Sn/Si(5). (6) Sn/Si(3) was treated with aqueous solution of acetic acid by the same method as shown in method (4), for Sn/Si(6). (7) Silica sol was used in the preparation method (1), for Sn/Si(7). (8) Silica sol was used in the preparation method (3), for Sn/Si(8). (9) Silica sol was used in the preparation method (5), for Sn/Si(9). (10) Sn/Si(3) was treated with 6N HNO_3 aqueous solution by the same method as shown in method (4), for Sn/Si(10). The

amount of SnO_2 supported was 4.8 mol% unless othersize noted. The supproted amount was indicated in the head of the catalyst name. For example, 4.8-Sn/Si(3) shows that 4.8 mol% of SnO_2 was supported on SiO_2 by the method (3). Unsupported SnO_2 was prepared by the method (1) and (3) for SnO_2(1) and SnO_2(3), respectviely. SnO_2 catalysts supported on MgO, TiO_2, Al_2O_3 were prepared by the method reported in the previous paper [8].

The catalytic performances were investigated by the conventional flow reactor. The experimental apparatus and procedure have been described elsewhere [3,7]. The reaction conditions were as follows unless otherwise noted: catalyst weight; 4.5 g, total feed rate; 210 mmol/h, partial pressures; $P_{EB} : P_{O_2} : P_{H_2O} : P_{N_2}$ = 20.3 : 20.3 : 31.3 : 29.4 (kPa), reaction temperature; 698 K, 723 K, and 748 K.

For the Mössbauer experiments, catalyst samples were pressed into thin wafers at 10^4 kg/cm^2 for 5 min. The Mössbauer spectra were recorded on a Shimazu MEG-W type Mössbauer spectrometer using $Ba^{119m}SnO_3$ source at 78 K. Pure Fe and stainless steal were used to calibrate the Doppler velocity and shift using ^{57}Co source.

XRD patterns and ESR spectra of perylene radical formed on the catalysts obtained as mentioned in the previous studies [7,6].

RESULTS

Effect of supporting method on the catalytic properties of Sn/Si catalysts

The continuous flow reaction was conducted to compare the catalytic performances of Sn/Si catalysts prepared by various methods. Figure 1 shows the conversion of ethylbenzene and selectivity to styrene on the Sn/Si catalysts at 698 K, 723 K and 748 K. SnO_2 impregnated from ethanol solution of $SnCl_2$, Sn/Si(1), showed relatively high selectivity but low conversion. The treatment of Sn/Si(1) with NH_4OH aqueous solution (referred as NH_4OH treatment), Sn/Si(2), resulted in increases of activity and selectivity. The NH_4OH treatment before calcination, Sn/Si(3), resulted in the highest conversion and the highest selectivity as high as 60 % and 90 %, respectively. The treatment of Sn/Si(3) with 1N HCl, Sn/Si(4), lowered the conversion and selectivity to almost the same values as Sn/Si(1). Sn/Si(5) catalyst impregnated by dissolving Sn metal in HNO_{3aq} showed almost the same values as Sn/Si(1). The treatment of Sn/Si-(3) with glacial acetic acid, Sn/Si(6), remarkably supressed the catalytic performances. Sn/Si(7) and (8) prepared by the same methods as Sn/Si(1) and (3), respectively, using silica sol showed similar performances which resembled to those of Sn/Si(2). The impregnation using Sn metal dissolved in 2N HNO_3, Sn/Si(9), resulted in low conversion with low selectivity. The effect of HNO_3 treatment, Sn/Si(10), was examined on 9.1 mol% SnO_2 supported on SiO_2. The results are shown in Table 1. The HNO_3 treatment reduced the conversion and the yield of styrene, but did not change the yield of carbon oxides. Thus, it reduced the selectivity, too. After all, the preparation method (3) gave the most active and selective catalyst.

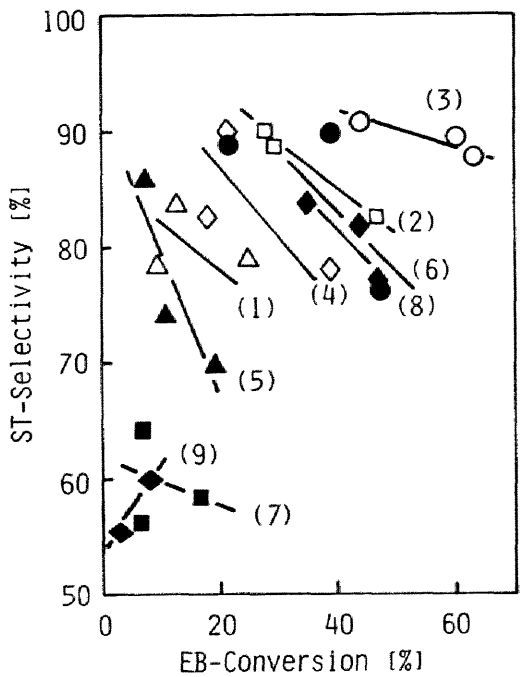

FIGURE 1 Effect of preparation method of Sn/Si catalysts on the conversion and selectivity. Catalyst weight; 4.5 g, Total feed rate; 210 mmol/h, Partial pressures; $P_{EB} = P_{O_2}$ = 20.3 kPa, P_{H_2O} = 31.3 kPa, P_{N_2} = 29.5 kPa, Reaction Temprature; 698 K, 723 K, and 748 K.

TABLE 1

Effect of Reaction Temperature on the Product Distribution of 4.8-Sn/Si(3), 9.1-Sn/Si(3) and 9.1-Sn/Si(10) Catalysts[a]

Catalyst	Reaction Temperature (K)	Conversion (%)		Yield (%)			Selectivity to Styrene (%)
		Ethylbenzene	Oxygen	Styrene	Carbon oxides	Benzene	
4.8-Sn/Si(3)	698	44.1	62.7	40.1	3.6	0.3	90.8
	723	60.6	92.7	54.3	5.2	1.0	89.6
	748	63.5	99.7	55.7	5.7	1.7	87.8
9.1-Sn/Si(3)	698	42.5	63.2	38.0	4.0	0.5	89.5
	723	54.5	86.4	46.6	5.6	2.2	85.7
	748	47.3	99.6	36.4	8.0	2.7	76.9
9.1-Sn/Si(10)	698	38.2	65.4	33.0	4.5	0.6	86.5
	723	46.3	78.9	38.7	5.8	1.6	83.8
	748	39.3	98.4	28.6	7.9	2.2	72.9

[a]For the reaction conditions, see Fig. 1.

Effect of calciantion temperature

The effect of calcination temperature was also studied on a series of 9.1-Sn/Si(3) catalysts. As shown in Fig. 2, The increase in the calcination temperature resulted in the decrease of conversion and the yields. The catalyst calcined at 1273 K showed a slight increase in the selectivity to styrene because of the considerable decreases in the yield of byproducts accompanied with the decrease of conversion.

Effect of SnO_2 content

The effect of SnO_2 content on the catalytic properties were studied in the cases of Sn/Si(3) catalysts. As shown in Fig. 3, the conversion of ethylbenzene and yield of styrene steeply increased with SnO_2 content below 4.8 mol% of SnO_2, and the yield of carbon oxides and benzene also increased a little. Above 4.8 mol% of SnO_2 , the conversion and the yield of styrene appeared to decrease a little with an increase in SnO_2 content. But it should be noted that at low conversion level, as shown in later, the catalytic activity of 9.1-Sn/Si(3) was higher than that of 4.8-Sn/Si(3). The selectivity on silica gel was significantly lower than those on SnO_2-containing catalyst in Fig. 2. The selectivity on 0.5-Sn/Si(3) was almost equal to those on 4.8- and 9.1-Sn/Si(3). However, the intrinsic selectivity of 0.5-Sn/Si(3) does not appear to be identical to those of the catalysts with high SnO_2 content, because the selectivity is sometimes a function of conversion. At the same conversion level, the selectivity of 0.5-Sn/Si(3) was lower than those of 4.8- and 9.1-Sn/Si(3).

Figure 4 shows Arrhenius plots of the rates of styrene formation on these catalysts. The conversions of ethylbenzene and oxygen were remained less than 11 % and 24 %, respectively, in these experiments. The activation energy on 0.5-Sn/Si(3) was essentially equal to that on silica gel support alone, though the rate of styrene formation was enhanced. The activation energy was significantly lowered by supporting SnO_2 with high concentration. The activation energy was 30 $\pm$ 5 kcal/mol on 4.8- and 9.1-Sn/Si(3) catalysts, while it was 50 $\pm$ 4 kcal/mol on 0.5-Sn/Si(3) and silica gel. This suggests that there is an essential difference between the catalysts with low SnO_2 content and high SnO_2 content. The relation between the selectivity and the contact time also shows big difference between them. Figures 5 and 6 show the effect of W/F at high ratio of oxygen to ethylbenzene. The high oxygen/ethylbenzene ratio would enhance the complete oxidation to carbon oxides and enlarge the difference in the selectivity. On 0.5-Sn/Si(3), as shown in Fig. 5, the conversion and the yield of styrene gradually increased with W/F. The yield of carbon oxides also gradually increased. The selectivity decreased, as a whole, with the increase of W/F, but the selectivity at W/F = 0, estimated by extrapolating the curve, was much lower than 100 %. This shows that a part of carbon oxides would be formed by the direct combustion of ethylbenzne. The results on 9.1-Sn/Si(3) are shown in Fig. 6. The conversion and the yield of styrene increased steeply with W/F below 0.01 h·g-cat/mmol. And then

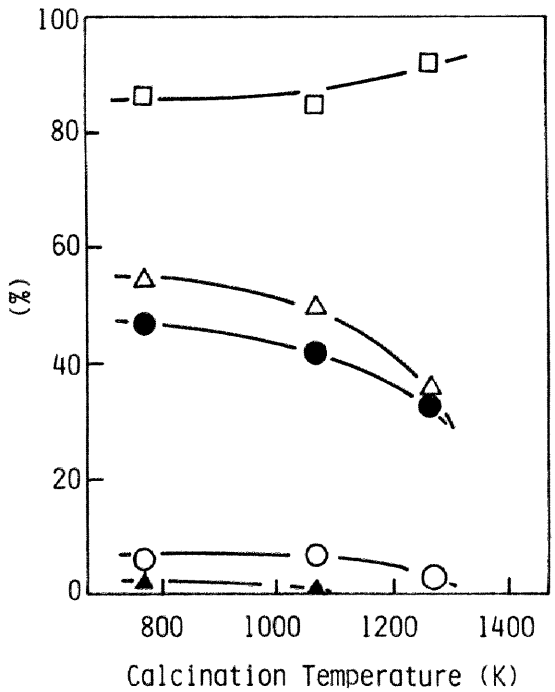

FIGURE 2 Effect of calcination temperature of 9.1-Sn/Si(3) on the conversion (△), selectivity (□), yield of styrene (●), benzene (▲), and carbon oxides (○). For the reaction conditions, see Fig. 1.

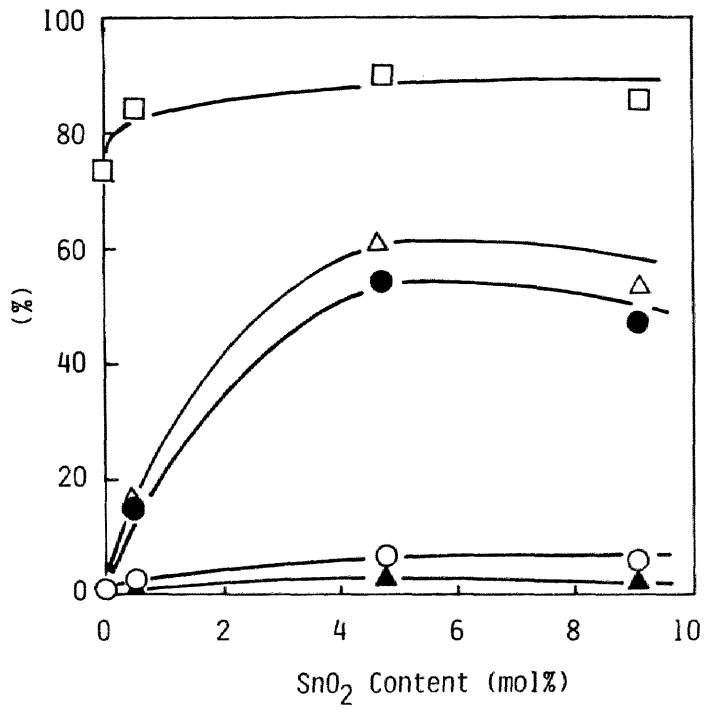

FIGURE 3 Effect of SnO_2 content of Sn/Si(3) on the catalytic performances. For the symbols and reaction conditions, see Fig. 2 and Fig. 1, respectively.

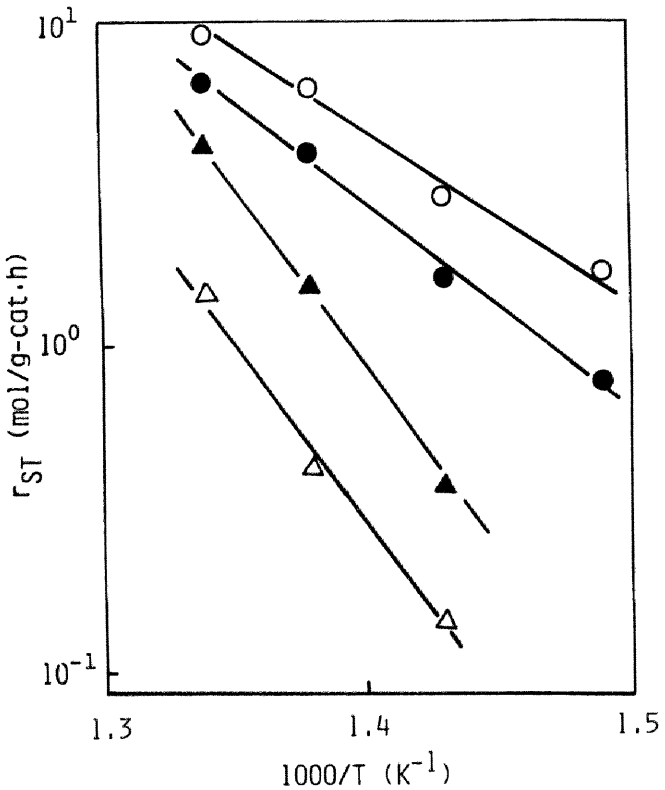

FIGURE 4 Arrhenius plot of SiO_2 support alone (△), 0.5-Sn/Si(3) (▲), 4.8-Sn/Si(3) (●), and 9.1-Sn/Si(3) (○). Total feed rate; 290 mmol/h, Partial pressures; $P_{EB} : P_{O_2} : P_{H_2O} : P_{N_2}$ = 14.6 : 10.1 : 34.0 : 42.6, Catalyst weight was changed to make the conversion below 10 %.

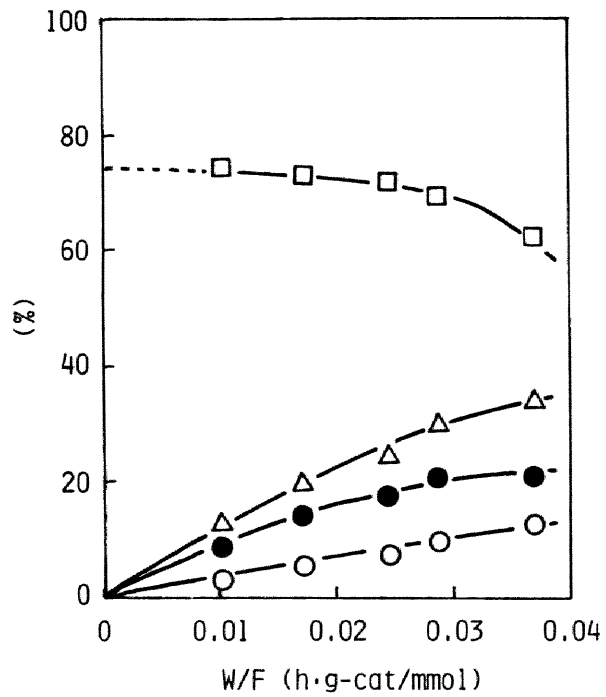

FIGURE 5 Effect of feed rate on 0.5-Sn/Si(3) catalyst. $P_{EB} : P_{O_2} : P_{N_2} = 5.1 : 20.3 : 75.9$ (kPa), Reaction temperature ; 723 K.
For the symbols, see Fig. 2.

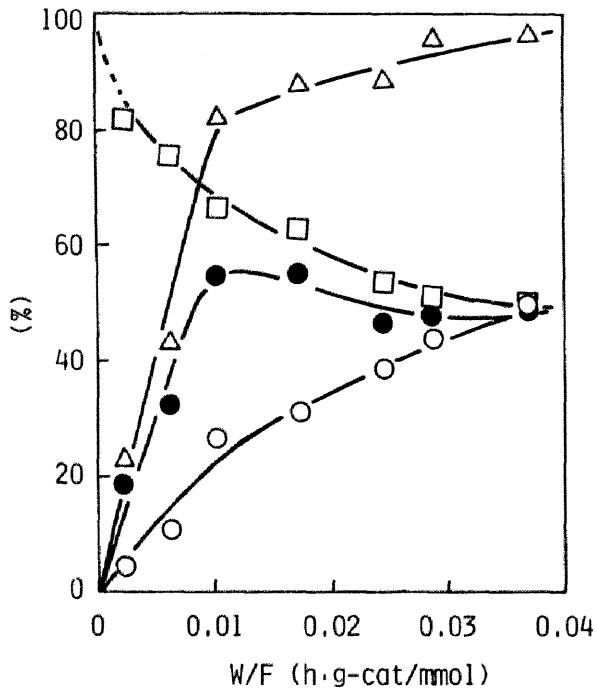

FIGURE 6 Effect of feed rate on 9.1-Sn/Si(3) catalyst. For the symbols and reaction conditions, see Figs. 2 and 5, respectively.

the conversion increased slowly, but the yield remained almost constant. On the other hand, the yield of carbon oxides increased almost steadily with W/F, resulting in the gradual decrease of the selectivity. The extrapolation of the selectivity curve to zero contact time indicates that the selectivity at W/F = 0 may be as high as 100 %, suggesting that the carbon oxides may be formed by the subsequent combustion of styrene once formed.

Effects of reaction conditions on the catalytic performances of 4.8-Sn/Si(3)

Effects of reaction conditions on the 4.8-Sn/Si(3) catalyst (most effective catalyst) were also studied by the continuous flow reaction. Reaction temperature were changed from 698 K to 748 K under the same reaction conditions shown in Fig. 1. The results are summarized in Table 1. The yields of styrene and carbon oxides increased with reaction temperature below 723 K. But it did not increase so much above it. This is due to the almost complete conversion of oxygen at high temperature. The conversion of oxygen was 93 % at 723 K and almost 100 % at 748 K. At 748 K, a little amount of benzene was formed, and this resulted in a little decrease of the selectivity at high temperature. Table 1 includes the results on 9.1-Sn/Si(3) for the comparison. The performance of 9.1-Sn/Si(3) was close to that of 4.8-Sn/Si(3) at 698 K, but the difference between them became large as the temperature increased. The conversion and the yield of styrene at 748 K were lower than those at 723 K. The lower conversion and yield at higher temperature were due to the complete conversion of oxygen resulted from the large yield of carbon oxides.

The oxigen partial pressure was raised from 20.3 Kpa to 40.6 kPa to examine the possibility of further increase in the yield of styrene. The results were shown in Fig. 7. As the partial pressure of oxygen increased the conversion increased up to 82 %. However, only the yield of carbon oxides increased, while the yield of styrene remained almost constant. As a result, the selectivity decreased with the increase of oxygen partial pressure. In the low conversion range, the partial pressure of ethylbenzene was lowered at 5.1 kPa. But low partial pressure of ethylbenzene also lead to low selectivity.

DISCUSSION

Comparison with the Other Catalysts

4.8-Sn/Si(3) was the best catalyst for the oxidative dehydrogenation of ethylbenzene among the catalysts examined in the present study. It gave the conversion of 60 %, the yield of 54.1 % and the selectivity of 90 % at 723 K with $P_{O_2} = P_{EB} = 20.3$ kPa and W/F = 0.0214 (g·h/mmol). In the previous chapters[3,7], Sn-P catalyst was reported to be an excellent catalyst for this reaction. But the conversion on Sn-P catalyst at the same condition was about 30 % with the selectivity of 90 % [7,8]. Sn-P catalyst calciend at 1273 K was most selective in the Sn-P catalysts [7]. With the increase

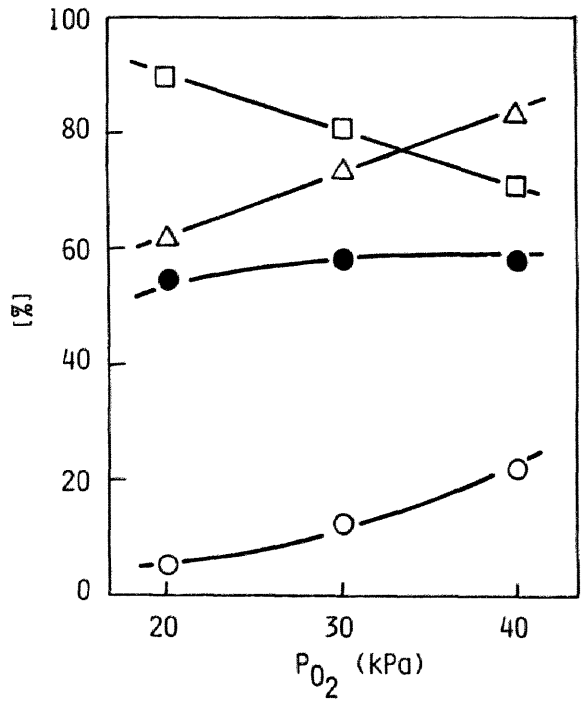

FIGURE 7 Effect of oxygen partial pressure on 4.8-Sn/Si(3). Catalyst weight; 4.5 g, Total feed rate; 208 mmol/h, Partial pressures; P_{EB} = 20.3 kPa, P_{H_2O} = 31.6 kPa, P_{O_2} = changed with N_2 balance. For the symbols, see Fig. 2.

in W/F, the conversion and the styrene-yield increased to 54.5 % and 43.5 %, respectively, but the selectivity decreased to 79.8 % [7]. The reaction rate on Sn-P catalyst was well expressed by the oxidation-reduction cycle of the catalyst surface [7].

$$EB + [O] \xrightarrow{k_1} ST + [\ ] \quad (1)$$

$$[\ ] + \frac{1}{2}O_2 \xrightarrow{k_2} [O] \quad (2)$$

This cycle is in good agreement with the detailed reaction mechanism proposed in the previous section [4,5,6]. In the mechanism, ethylbenzene is adsorbed on acid site and is dehydrogenated by oxygen activated by base sites to form styrene and water. The oxygen consumed are supplied from gas phase. The cycle (1) and (2) leads to the following equation:

$$1/r = 1/k_1P_{EB} + 1/k_2P_{O_2} \quad (3)$$

Figure 8 shows the reciprocal relations between rate and partial pressure. The rate constants k_1 and k_2 calculated from the plot of 1/r against $1/P_{EB}$ were 125 and 135, and those calculated from the plot of 1/r against $1/P_{O_2}$ were 133 and 123 (mmol/g-atm·h). The rate constants from both plots agreed very well with one another. The rate constants thus obtained on Sn/Si were about 20 % larger than those on Sn-P reported elsewhere [7]. But the difference of 20 % seems too small to explain the above-mentioned difference in the yield of styrene at high conversion range: 55 % on Sn/Si and 25.5 % on Sn-P. This larger yield at high conversion range is the most important charasteristics of Sn/Si catalyst for the industrial production of styrene from ethylbenzene by the oxidative dehydrogenation.

Many attractive catalytic systems appeared in a recent review article [13]. But Fe-Cr-K [14], Ce-P [15], and Bi-U-Al [16] systems required high reaction temperatures, above773 K. Zn-P-Si [17] and Zn-Si-Al [18] systems show selectivities lower than 80 %. On Cr-Ni-Al [19] and Pd-KBr-Al [20] catalysts, the partial pressures of oxygen should be limitted to lower values than the stoichiometric pressure, in other words, a high yield of styrene connot be expected. Although Pd-containing catalyst gave good results at lower temperature, HBr should be fed continuously during the reaction [21]. Thus, it is difficult to obtain styrene selectively with high conversion at low reaction temperatures on above catalysts. The catalysts which satisfy these requirements are Sn-P [3,7], Al-P [6], and Fe activated carbon [22]. The Sn/Si catalyst, developed in this study, is one of the catalysts which meets the above requirements and the performances were best one compared to the other catalytic systems.

Effect of Preparation Mehtods

The NH_4OH treatment enhanced the activity and the selectivity of Sn/Si catalysts, as shown in Fig. 1. Thus, the conversion and the selectivity on Sn/Si(3) and Sn/Si(8) were higher than Sn/Si(1) and Sn/Si(7), respectively. Such effect of NH_4OH treatment was observed also in the case of SnO_2/Al_2O_3 catalyst [8]. In the case of Sn-P

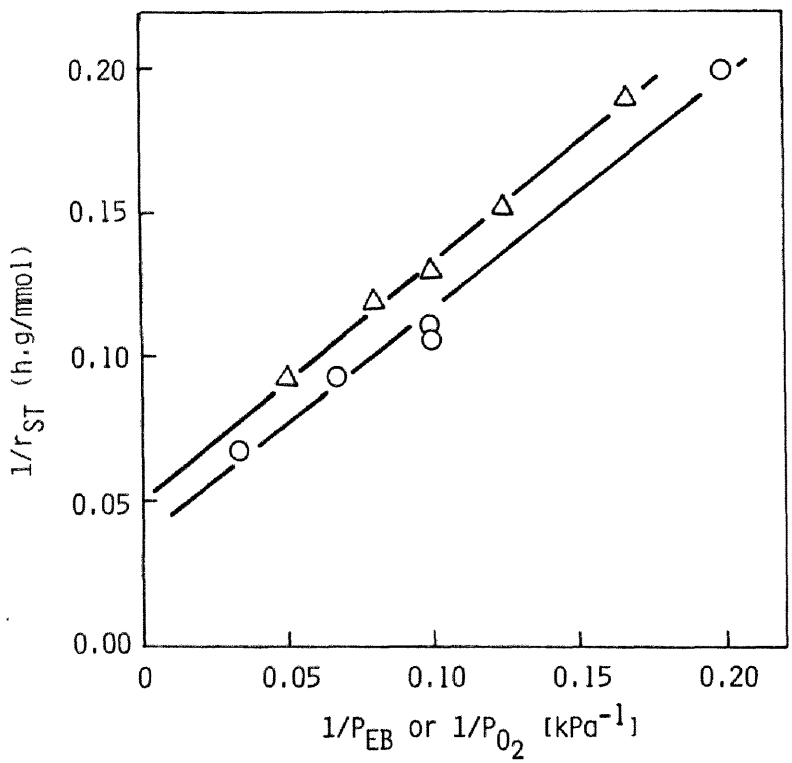

FIGURE 8 Reciprocal relations between rate and partial pressures. ○; P_{EB} was changed with P_{O_2} = 20.3 kPa, △; P_{O_2} was changed with P_{EB} = 15.2 kPa, P_{H_2O} = 23.5 kPa. Catalyst weight; 0.50 g, Total feed rate; 280 mmol/h, Reaction temperature; 723 K.

catalyst [7], the activity was enhanced by the HNO_3 treatment. The HNO_3 treatment removed the inactive phosphorous concentrated on the surface of the Sn-P catalyst.

The NH_4OH treatment of Sn/Si catalyst would remove some inactive species, maybe, chlorine ions remaining on the surface. This hypothesis was confirmed by the HCl treatment of Sn/Si(3) by which Sn/Si(4) was prepared. The conversion and selectivity of Sn/Si(4) were lower than Sn/Si(3), as shown in Fig. 1. The effect of NH_4OH treatment before calcination, Sn/Si(3), was larger than that after calcination Sn/Si(2). The calcination may promote solid reactions of chloride ions with catalyst, which may make chloride ions stable. Such an effect was observed in the treatment with the other acid, too. The active acetic acid treatment, Sn/Si(6), and the HNO_3 treatment, Sn/Si(10), also reduced the conversion and the selectivity, as shown in Fig. 1 and Table 1. Low conversion and selectivity of Sn/Si(5) and Sn/Si(9), which are prepared with nitric acid solution of Sn metal,may be caused by the effect of nitric acid.

In the oxidative dehydorgenation of ethylbenzene, acid sites of $1.5 > Ho > -5.6$ are required to adsorb and activate ethylbenzene. Such ability of catalysts can be estimated by the ability to form cation radicals of perylene. Figure 9 shows the relation between the amount of perylene radicals and the yield of styrene on Sn/Si (1), (3), (7), and (8). The amount of peryrene radicals on NH_4OH treated catalysts,Sn/Si(3) and Sn/Si(8), was larger than that on their precursor, Sn/Si(1) and Sn/Si(7). Thus, the formation of perylene radicals was enhanced by the NH_4OH treatment, by which yield of styrene also increased. This result suggests that the enhanced catalytic activity to form styrene by NH_4OH treatment is due to the enhanced ability to form perylene radicals, or, in others, due to the enhanced amount of acid sites.

The supported SnO_2 catalysts were examined by X-ray diffraction method to examine the structural effect of NH_4OH and HCl treatments. As shown in Fig. 10, the XRD patterns of Sn/Si(1), Sn/Si(3) and Sn/Si(4) showed broad lines which indetified as those of tin dioxides (ASTM card, 21-1250). The relative intensities of the lines of Sn/Si(1) and Sn/Si(4) were similar to that of SnO_2 crystal(Fig-10-a). In the case of Sn/Si(3), the relative intensity did not agree with SnO_2 crystal, as shown in Fig. 10-b. The intensity of [110] line was too small and that of [211] line was too large. The crystal size of SnO_2 on the support, calculated from the line broadening, was 5.1 nm in Sn/Si(1),6.8 nm in Sn/Si(3) and 13.6 nm in Sn/Si(4). These results suggest that chloride ion promotes crystalization of SnO_2, resulting in lower activity.

X-ray diffraction patterns of SnO_2, which was prepared by the same methods as Sn/Si catalyst was also measured. Fig. 10-c shows the diffraction patterns of SnO_2(3) prepared by the same method as Sn/Si(3). The diffraction patterns agreed very well with that of tin dioxide. In the case of SnO_2 (1), some compounds are formed on the outer surface of SnO_2 particles in the calcination step, (Fig. 10-d and e). Figure 10-d shows the diffraction patterns of SnO_2 (1) from which the surface deposite had been removed. The pattern agreed with that of tin dioxide. On the other hand, the

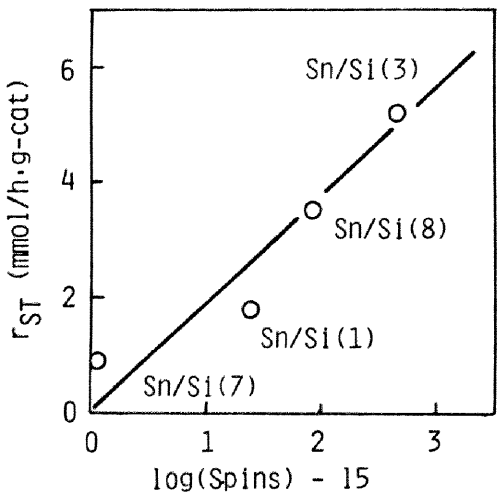

FIGURE 9 Correlation between the rate of styrene formation and amount of perylene radical formed on the catalysts. r_{ST} was obtained form the results shown in Fig. 1.

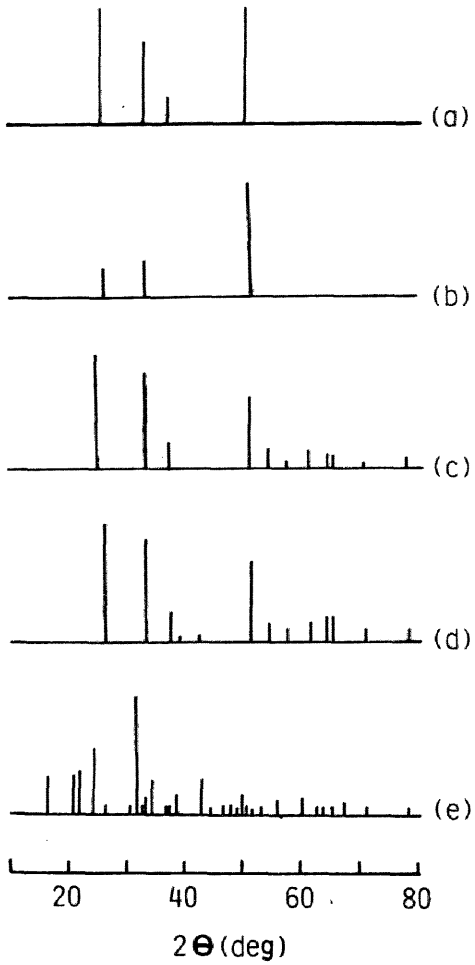

FIGURE 10 X-ray diffraction patterns of (a) 4.8-Sn/Si(1), (b) 4.8-Sn/Si(3), (c) SnO_2(3), (d) inner part of SnO_2(1), and (e) outer part of SnO_2(1). XRD patterns were obtained by Rigaku Denki diffractometer, Model Geigerflex with CuK radiation.

diffraction patterns of the deposited compound, shown in Fig. 10-e, was completely different from that of SnO_2, though it could not be identified. This results suggest that the residual chlorine may interact with Sn ion to form inactive compounds on the inner surface as well as on the outer surface in the calcination step. The same would be true in the case of the supported SnO_2 catalysts and it may be one of the reasons of lower activity of Sn/Si(1)and Sn/Si(4) than Sn/Si(3). In the case of Sn/Si(3), the NH_4OH treatment removed chlorine from the catalyst, which prevented from the formation of the inactive compounds on the surface. Although the effect of HNO_3 and acetic acid treatment was not investigated in detail, either or both of crystalization and formation of inactive species may reduce the catalytic activity.

Nature of the Active Sites

Two effects of addition of acid component to SnO_2 have been supposed in the previous study [7]. One is to reduce the size of SnO_2 crystal. Such effect was observed in the case of supporting SnO_2 on acid supports. For example, the particle sizes of 4.8-Sn/Si(3) calcined at 773 K is about 6.8 nm, as mentioned abive. Another effect is to form an active compund of tin and the additive [7]. The effect of SnO_2 content mentioned in the previous section shows that such chemical interaction has an effect on the activity and selectivity. Such nature of supported SnO_2 can be discussed with Mössbauer spectorscopy. The isomer shift is shown as follows [10]:

$$\text{Isomer Shift } (\delta) = \left(\frac{4\pi Ze^2R^2c}{5E}\right)\frac{\Delta R}{R}\left(\sum_A|\psi(0)|^2 - \sum_S|\psi(0)|^2\right)$$

where the third term represents the chemical contribution to δ, and $\sum_A|\psi(0)|^2$ and $\sum_S|\psi(0)|^2$ are the total electron densities at the nucleus of the absorber and source, respectively It is, therefore, possible to determine changes in oxidation state, or to know, an indication of the strength of bonding between the Mössbauer isotope and the surrounding atoms or ions [9]. Thus, the higher values of δ represents the higher electron densities and the lower values of δ represents the lower densities of electron at the Sn nucleus.

Figure 11 shows the correlation between the isomer shift (δ) and the electronegativity of supports per bond length (χ) in cases of supports screened in the previous chapter [8]. χ represents a electron withdrawing nature of the support calculated as follows [23]:

χ = electron negativity of support / bond length (M-O) of support oxides.

A clear correlation between the electron withdrawing ability and δ is observed. The basic support MgO may provide electron to Sn atom to increase the δ-value. Same effect is observed in the cases of TiO_2 and Al_2O_3, the amphoter supports. SiO_2, an acidic sopport, may withdraw electron from Sn atom which results in the remarkable decrease of δ-value. These results can be well correlated with the catalytic properties of these catalysts reported in the previous section [8]. A SnO_2/MgO catalyst was active

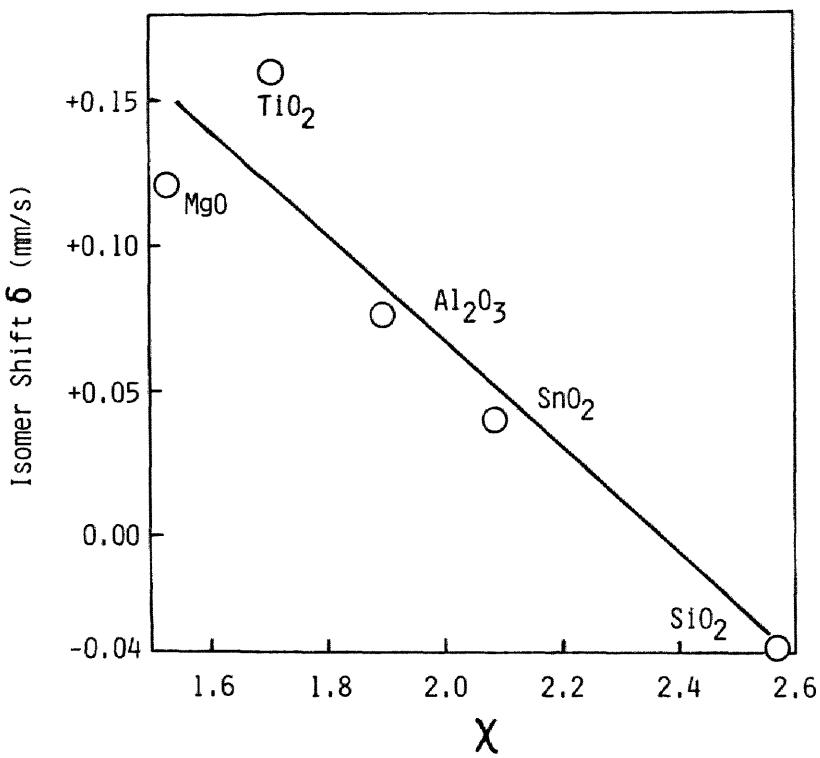

FIGURE 11 Correlation between the isomer shift (δ) and electron withdrawing nature of the support (χ).
χ = Electronegativity of support / bond length(M-O) of the support oxides.

in the total oxidation, but less active in the styrene formation. The catalytic properties of TiO_2 and Al_2O_3 were not changed by supporting SnO_2 on them. On the other hand, SnO_2/SiO_2 catalysts had high activity and selectivity. For the oxidative dehydrogenation of ethylbenzene, acid sites of Lewis type, or electron withdrawing sites are necessary to adsorb and activate ethylbezene [4,5,6]. Sn atoms which are electron-deficient under the effect of SiO_2 may play a role of electron withdrawing sites.

The NH_4OH treatment enhanced the formation of perylene radicals and the formation of styrene, as shown in Fig. 9. These results agree well with change of δ-value. δ-Value of Sn/Si catalyst shown in Fig. 12 was larger on Sn/Si(1) than on Sn/Si(3). Thus, the NH_4OH treatment resulted in large electron-deficiency of Sn atoms, which may enhance the formation of both perylene radical and styrene. The XRD pattern of Sn/Si(1) was similar to that of SnO_2 crystal, while that of Sn/Si(3) was different in the relative intensity of the lines from SnO_2 crystal. This result also indicates strong interactio of Sn atoms with SiO_2 in Sn/Si(3).

Figure 12 shows that the interaction became stronger as the SnO_2 content decreased, as generally expected. 0.5Sn/Si(3) had the smallest δ-value. However, as mentioned above, 0.5Sn/Si(3) is not so good catalyst. The activation energy of this catalyst, ca. 50 kcal/mol, was almost indentical to that of SiO_2 alone and less than those of high SnO_2 content, ca. 30 kcal/mol, as shown in Fig. 4. The selectivity at zero conversion on 0.5Sn/Si(3) was only 70 %, while that on 9.1Sn/Si(3) was almost 100 %, as shown in Figs. 5 and 6. Such poor performances of 0.5Sn/Si(3) inspite of small δ-value might be due to the lack of basicity. Both of acid and base sites are necessary for the present reaction [4,5,6]. The acid-base properties of SnO_2/SiO_2 catalysts in relation to the reaction mechanism will be a subject of further study.

CONCLUSION

4.8-Sn/Si catalyst which contained 4.8 mol % of SnO_2 and treated with NH_4OH before the calcination, shows a excellent catalytic performances compared to the catalytic systems described previously. The effect of preparation method on the state of supported SnO_2 and interactions between tin and support have been discussed on the basis of XRD, Mössbauer spectra, and ESR measurement of perylene radical fromation. The active site are considered to consist of Sn atoms which are electron deficient under the electron withdrawing effect of the support. The NH_4OH treatment removes chlorine contained in the reagent to prepare the catalyst, $SnCl_2$, and strengthens the interaction of SnO_2 with SiO_2 support. The calcination of catalyst in the presence of chlorine promotes the crystalization of SnO_2, which reduces the interaction. The NH_4OH treatment also preven from the deposition of inactive compounds on the surface by removing the residual chlorine ions.

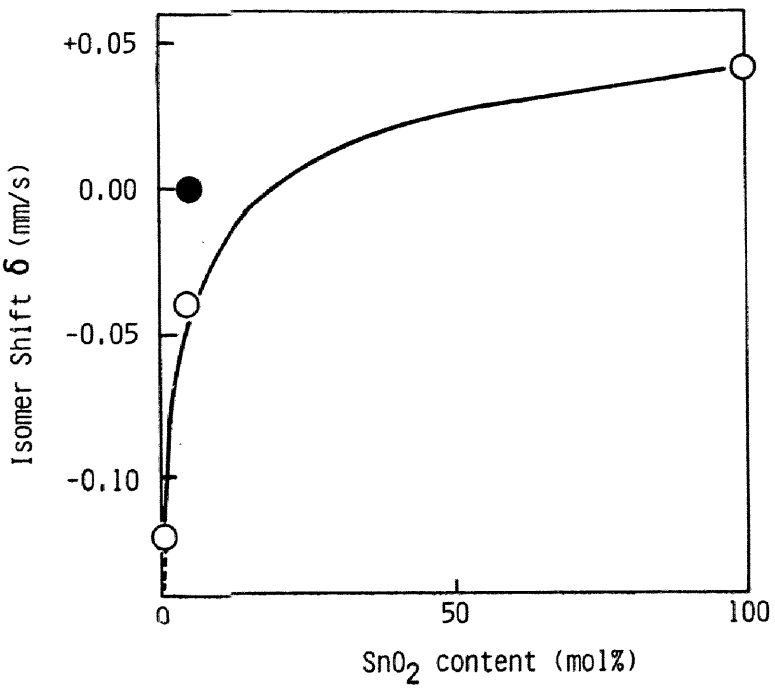

FIGURE 12 Correlation between the isomer shift (δ) and the SnO_2 content of Sn/Si(3) catalysts, for the open symbols, and of Sn/Si(1), for the filled symbols.

REFERENCES

1 Y. Murakami, Shokubai, 21 (1979) 349, and 46thannual Meeting of Japan Chemical Engineering Soc., p.564 (1981).
2 D.L.Trimm, "Design of Industrial Catalysis," Elsevier Sci. Publ. Co. New York, (1980).
3 Y. Murakami, K. Iwayama, H. Uchida, T. Hattori, and T. Tagawa, Appl. Catal., in press; chapter 2 of this thesis.
4 T. Tagawa, T. Hattori, and Y. Murakami, J. Catal., in press; Chapter 4 of this thesis.
5 T. Tagawa, T. Hattori, and Y. Murakami, J. Catal., in press; Chapter 5 of this thesis.
6 T. Tagawa, K. Iwayama, T. Hattori, and Y. Murakami, submitted; Chapter 6 of this thesis.
7 Y. Murakami, K. Iwayama, H. Uchida, T. Hattori, and T. Tagawa, J. Catal., in press; chapter 3 of this thesis.
8 T. Tagawa, S. Kataoka, T, Hattori, and Y. Murakami, submitted. ; chapter 9 of this thesis.
9 W. Jones, "Characterization of Catalysts," p.114, John Wiley and Sons. New York 1980.
10 W.N. Delgass, G.L. Haller, R. Kellerman, and J.H. Lunsford "Spectorscopy in Heterogeneous Catalysis" Chapter 5., Academic Press, New York,1979.
11 J.A. Dumesic, and H. Topose, "Mossbauer Spectroscopy, Applications to Heterogeneous Catalysis" Adv. Catal., 26 (1977) 121.
12 H.M. Gager and M.C. Hobson, Jr. Catal. Rev., 11 (1977) 121.
13 M.Imanari and W. Watanabe, Petrotech, 2 (1979) 339.
14 J.R. Ghublikian, British Patent, 1,176,916 (1970).
15 Dow Chemical Co., Japan Kokai 74-12,790 (1974).
16 Nippon Shokubai Kagaku Kogyo Co. Ltd., Japanese Patent, 77-28,782 (1977).
17 Nitto Chemical Industry Co Ltd., Japan Kokai, 74-41,182 (1974).
18 Nippon Kayaku Co. Ltd., Japanese Patent, 74-42,017 (1974).
19 Mitsubishi Chemical Industries Ltd., Japanese Patent, 75-30,061 (1975).
20 Mitsubishi Petrochemical Co. Ltd., Japan Kokai, 78-44,525 (1978).
21 K. Fujimoto and T. Kunugi, Ind. Eng. Chem. Prod. Res. Dev., 20 (1981) 319. and K. Fujimoto, J. Yamada, and T. Kunugi, Japan Kokai, 77-23,027 (1977).
22 R.M. Benslay and A.L. Jones, U.S. Patent, 3,652,698 (1970).
23 R.T. Sanderson "Inorganic Chemistry" Reinhold Publ Co. New York, 1967.

Chapter 9

APPLICATION OF VAPOR PHASE SUPPORTING (VPS) METHOD FOR PREPARING SnO_2/SiO_2 CATALYSTS

SYNOPSIS

Supported SnO_2/SiO_2 catalysts have been prepared by the reaction of surface hydroxyl groups of silica gel and gas phase tin chloride (VPS method). The catalytic properties have been examined by the reaction of 2-propanol to show the effect of VPS cycles on the amount and nature of the active sites.

INTRODUCTION

Several studies have been devoted to the reaction of metal chloride with the hydroxyl groups of the solid surface as a new modification method of solid surfaces.

$$m(SiOH) + EX_n \longrightarrow (SiO)_mEX_{n-m} + mHX \quad (1)$$

$$(SiO)_mEX_{n-m} + (n-m)H_2O \longrightarrow (SiO)_mE(OH)_{n-m} + (n-m)HX \quad (2)$$

Kol'tsov et al. showed that the repeated cycles of reactions (1) and (2) result in increasing the thickness of the oxide layers [1,2,3].

$$a(SiOEOH) \xrightarrow[2)\ H_2O]{1)\ EX_n} (SiOEO)_aE(OH)_{n-a} \quad (3)$$

Parfitt et. al. showed that the reaction of $TiCl_4$ with silica gel produces acid sites on the surface [4]. Such resulting materials can be used as a new type of supported metal oxide catalysts, however, only a few studies have been done regarding their application as a catalyst [5,6].

In this study, the above method referred to as VPS (vapor phase supporting) method was applied to prepare a new type of supported SnO_2/SiO_2 catalysts and the nature of the catalysts was also studied.

EXPERIMENTAL

Micro Beads Silica Gel Type 5D (Fuji Davison Chemical Co.) was used as the support. VPS-1 catalyst was prepared at 180 °C as follows; The support was calcined at 180 °C in the flow of dry N_2 for 2.5 h, then about 20 ml of $SnCl_4$ saturated in dry N_2 was fed onto the support for 19 h, and hydrolysis was performed by H_2O saturated in N_2 for 3 h after the purge of $SnCl_2$ by dry N_2 flow for 2 h. The resulting materials were calcined at 500 °C for 2 h in air. This VPS cycle was repeated from the initial calcination to the hydrolysis for two three, and five times for VPS-2, VPS-3, and VPS-5 catalysts, respectively. The content of Sn on the catalyst was determined by fluorescent X-ray analysis. The surface properties were examined by the reaction of 2-propanol conducted by conventional pulse technique at 330 °C in the flow of N_2 (70 ml/min).

RESULTS AND DISCUSSION

As shown in the first column of Table 1, about 4 - 5 wt% of additional SnO_2 was supported at every cycle till the third VPS cycle, and this increment decreased at the fifth cycle to about 2 wt%. The second and last columns of Table 1 show the changes in the surface area and pore volume. The surface area and pore volume of the catalyst appeared to decrease with increasing number of VPS cycles performed, as reported in the $TiCl_4/SiO_2$ system [7]. However, the pore volumn per unit weight of silica gel, shown in parentheses, was constant within the reasonable error. This result indicates that SnO_2 was supported occupying the silica gel surface to some extant while the pore structure of silica gel remained unchanged.

The catalytic properties of these VPS-catalysts were studied by the reaction of 2-propanol in the pulse reactor. 1 µl of 2-propanol was pulsed on 0.2 g of the catalyst calcined at 450 °C for 2 h in dried N_2 flow. One can correlate the dehydration activity of 2-propanol with acidity and dehydrogenation activity of

Table 1 Surface Properties of the VPS-SnO_2/SiO_2 Catalysts

Catalyst	SnO_2-content wt%	Surface area m^2/g	Pore volume ml/g
SiO_2 support	0.0	240	1.17
Sn/Si VPS-1	4.7[a] (4.9)[b]	213[a] (224)[b]	0.99[a] (1.04)[b]
VPS-2	8.9 (9.8)	191 (210)	0.95 (1.04)
VPS-3	12.5 (14.3)	191 (218)	0.99 (1.13)
VPS-5	14.5 (17.0)	184 (215)	0.97 (1.13)

[a]Based on g-catalyst; [b]Based on g-silica gel.

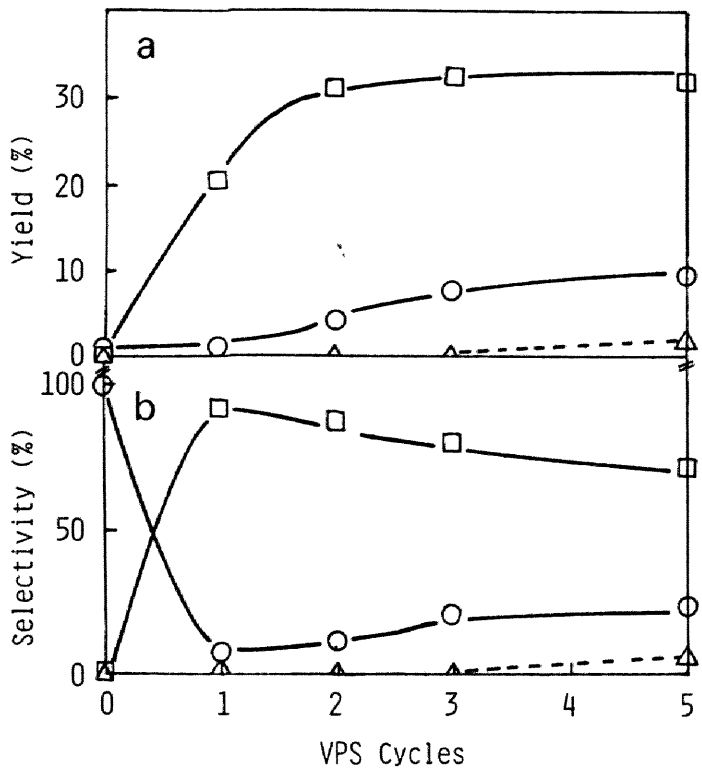

FIGURE 1 (a) Yield and (b) selectivity in the pulse reaction of 2-propanol on VPS-SnO_2/SiO_2 catalyst. ○; propylene, △; isopropyl ether, and □; acetone. 1 μl of 2-propanol was pulsed onto 0.2 g of the catalyst at 330 °C in the flow of 70 ml of dry N_2.

2-propanol with basicity [8,9]. As shown in Fig. 1-a, the yield of propylene, isopropyl ether, and acetone increase gradually with the VPS cycles, showing that the increase in SnO_2 content enhances the catalytic activity. The deydrogenation reaction was superior to the dehydration reaction in every case except in the absence of SnO_2 on SiO_2 support. Figure 1-b shows the change in the selectivities against the VPS-cycles. On silica gel, only a little propylene was formed but acetone and isopropyl ether could not be detected,indicating the exist of few acid sites. The selectivity to acetone (dehydrogenation) was at a maximum on VPS-1 catalyst and gradually decreased with the increase in the VPS cycles. The selectivity to propylene, on the other hand, was at a minimum on VPS-1 catalyst and increased gradually with the VPS cycles. The fifth VPS cycle did not increase SnO_2 content so much as the first to third VPS cycles. However, the fifth cycle changed the selectivity to propyl ether. Selectivity to propyl ether was very small on VPS-1,2, and 3 catalysts and increased appreciably on VPS-5 catalyst. Such changes in the selectivities with VPS cycles indicate that the nature of the active site specially the acid and base properties can be changed by repeating VPS cycles. Thus, the first VPS cycle drastically increased basicity, but further VPS cycles had large effect on acidity.

In summary, the number of VPS cycles performed can modify not only the amount but also the nature of the active sites, suggesting the usefullness of this mehtod for the preparation of a new type of catalyst.

REFERENCES

1 S.I. Kol'tsov and V.B. Aleskovskii, Zh. Prikl. Khim., 42 (1969) 1950, ibid., 40 (1967) 907.
2 S.I. Kol'tsov, ibid., 38 (1965) 1384.
3 R.R. Rachkovskii, S.I. Kol'tsov and V.B. Aleskovskii, Zh. Neorg. Khim., 15 (1970) 3158.
4 G.D. Parfitt, J. Ramsbotham and C.H. Rochester, J.C.S. Faraday Trans I, 68 (1972) 17.
5 S.I. Kol'tsov, V.M. Smirov, V.N. Postnov, A.M. Postonova, and V.B. Aleskovskii, Kinet. Catal., 21 (1980) 550.
6 V.A. Khalif, E.L. Aptekan, O.V. Krylov, and G.Öhlmann, Kinet. Catal., 18 (1977) 1055.
7 S.I. Kol'tsov, Zh.Prikl Khim., 43 (1970) 1956.
8 D.B. Dadyburjor, S.S. Jewur, and E. Ruckenstein, Catal. Rev., 19 (1979) 293.
9 M. Ai, J. Catal., 40 (1975) 327.

Chapter 10

OXIDATIVE DEHYDROGENATION OF ETHYLBENZENE ON VPS-SnO_2/SiO_2 CATALYSTS

SYNOPSIS

Supported SnO_2/SiO_2 catalysts have been prepared by the vapor phase supporting (VPS) method. The catalytic properties and surface characters of them have been compared to those of impregnated (IMP) SnO_2/SiO_2 catalysts. The TEM, XRD, EDR-IR, and UV data indicate that in the case of VPS method, SnO_2 deposits ununiformly on only a particular particle of SiO_2, remaining most of particle vacant, and that the SnO_2 aggregates up to 5 - 15 nm by repeating VPS cycles. On the other hand, SnO_2 particles of 1 - 2 nm are uniformly dispersed on the IMP catalysts. The acid-base properties determined by the acid-base titration and IR spectra of adsorbed base, and the redox properties, by TPR and pulse reduction experiments with ethylbenzene, can be explained on the basis of the above surface models. The catalytic properties have been examined by the continuous flow and pulse reaction on the oxidative dehydrogenation of ethylbenzene. The differences in the catalytic properties of each catalysts are discussed on the basis of the reaction mechanism and the surface models. IMP catalysts possess more active acid sites, while the active acid sites on the VPS catalysts show higher turnover frequency in the initiation of the reaction.

INTRODUCTION

The method of preparation is one of the keys to obtain a solid surface with high activity and selectivity and currently increasing in its importance in the view point of catalyst design. A new preparation method reffered as vapor phase supporting (VPS) method is one of the modification method of solid surface to support metal oxides onto the support. Several studies have been devoted to the reaction of chloride with the hydroxyl groups of the solid surface as a new modification method of soild surfaces.

Kol'tsov et. al. showed that the repeated cycles of following reactions (1) and (2) result in increasing the thickness of the oxide layers [1,2,3], as shown in scheme (3).

$$m(SiOH) + EX_n \longrightarrow (SiO)_m EX_{n-m} + mHX \quad (1)$$

$$(SiO)_m EX_{n-m} + (n-m)H_2O \longrightarrow (SiO)_m E(OH)_{n-m} + (n-m)HX \quad (2)$$

$$a(SiOEOH) \xrightarrow[2)\ H_2O]{1)\ EX_n} (SiOEO)_a E(OH)_{n-a} \quad (3)$$

Parfitt et. al. showed that the reaction of $TiCl_4$ with silica gel produces acid sites on the surface [4]. Thus obtained materials can be used as a new type of supported metal oxide catalysts, however, only a few studies have been done regarding their application as a catalyst [5,6]. In our recent studies on the application of VPS method to prepare supported metal oxide catalysts [7,8], it has been suggested that catalysts prepared by VPS method show different catalytic properties from those prepared by the typical impregnation (IMP) method. Especially, VPS-SnO_2/SiO_2 catalysts show remarkable change in the dehydration and dehydrogenation activity with the change of VPS cycles in the pulse reaction of isopropyl alcohol, suggesting the different nature in the acid-base properties on the surface [9]. This also attracts interest to apply the VPS catalysts in the oxidation reaction which is controlled by the acid-base properties of the catalyst.

In the previous study on the oxidative dehydrogenation of ethylbenzene, the screening of the catalyst has been preformed [10,11] and the reaction mechanism has also been clarified on a series of Na treated $SiO_2 \cdot Al_2O_3$ catalysts [12,13]. The design of the catalysts for this reaction has been conducted on the basis of the above mentioned results and reaction mechanism [14,15,16]. SnO_2-P_2O_5, SnO_2/SiO_2, and Al_2O_3-P_2O_5 catalysts have been designed and showed excellent performances, especially, SnO_2/SiO_2 catalyst showed the highest conversion and selectivity. Unusual interactions between SnO_2 and supprots are pointed out [15] and the formation of new acid and base sites is expected on SnO_2/SiO_2 catalyst considering the electron withdrawing effect of SiO_2 support [16]. In recent days, such interactions between supported metal oxides and the supports are increasing in importance [17].

In this study, VPS-SnO_2/SiO_2 catalysts are prepared by changing the number of the VPS cycles to compare with the IMP-SnO_2/SiO_2 catalysts with various SnO_2 content. The differences in the physical properties of these catalysts are studied to propose the surface model of SnO_2 on SiO_2. The differences in the catalytic properties are discussed on the basis of the supposed model and the reaction mechanism.

EXPERIMENTAL

Preparation of catalyst

Micro Beads Silica Gel Type 5D (Fuji Davison Chemical Co.) was used as the support. VPS-1 catalyst was prepared at 353 K as follows: The support was calcined in the flow

dry N_2 for 2.5 h, then about 20 ml of $SnCl_4$ saturated in dry N_2 was fed onto the support for 19 h, and hydrolysis was performed in the flow of steam (110 ml/min) for 3 h after the purge of $SnCl_4$ by dry N_2 flow for 2 h. The resulting materials were washed with 4N NH_4OH by decantation for five times to remove the residual Cl ions, washed with water to neutralize, and calcined at 773 K for 2 h in air. This VPS cycle, from the initial calcination to the hydroysis, was repeated for two, three, and five times and then washed with NH_4OH and water before the calcination for VPS-2, VPS-3, and VPS-5 catalysts, respectively. Impregnated (IMP) SnO_2/SiO_2 and unsupported SnO_2 catalysts were prepared by the previously mentioned method [15,16], that is the impregnation of $SnCl_2 \cdot 2H_2O$ from ethyl alcohol solution and the following NH_4OH treatment before calcination, which results in the best catalyst for the oxidative dehydrogenation of ethylbenzene. The content of SnO_2 on the catalysts were determined by the XRF measurement.

Catalytic activity

Catalytic performances of the catalysts were determined by continuous flow reaction and pulse reaction. The reaction apparatus and procedures were stated in the previous chapters together with the reaction conditions for the flow reaction [12] and the pulse reaction [14]. The amount of active oxygen was measured by reducing the preoxidized catalyst with repeating pulses of ethylbenzene in the oxygen free helium until any oxidation products could not be detected.

Surface characters

Previously reported procedures and apparatus were adopted to obtain the XRD patterns [11], maximum acid and base strength using the Hammet indicators [12,14], acidity distributions by titration method using n-butyl amine [12,14], and IR spectra of adsorbed base [18]. High temperature IR spectra of the catalysts were obtained at 603 K in the flow in dry helium (26.3 ml/min) using JASCO-EDR-IR Type EDR-31 [19]. The UV-VIS diffuse refrectance spectra were measured with JASCO-UVIDEC-505 equipped with diffuse refrectance attachiment model TIS-241 using SiO_2 as a reference. TEM microphotographs were registered on a H 700H Instrument. TPR profiles were obtained by heating 0.5 g of sample, which was precalcined at 773 K 2 h in the flow of $O_2 + N_2$ mixture (2 : 5) and cooled down to 173 K, in a flow if TPR gas (10 ml/min of 6.21 % of H_2 + 93.79 % of Ar mixture) with heating rate of 5 °/min.

RESULTS

Surface characters

State of SnO_2 on the support

Table 1 summarizes the content of SnO_2, size of SnO_2 particle, BET surface area, pore volume, UV λmax value and TEM-SAD data. The increase in VPS cycles resulted

Table 1
Physical Texture of SnO_2/SiO_2 Catalysts[a]

Catalyst	SnO_2 Content[b] (mol%)	(wt%)	BET Surface Area (m^2/g)		Pore Volume (ml/g)	SnO_2 Particle[c] Size (Å)	TEM SAD[d] SnO_2	UV λmax (nm)
SiO_2	0.0	0.0	248		1.17	-	-	-
VPS-1[e]	1.95	4.9	213[f]	(224)[g]	0.97[f] (1.04)[g]	-	-	257
VPS-2	3.91	9.8	191	(200)	0.95 (1.04)	-	-	265
VPS-3	5.70	14.3	191	(218)	0.99 (1.13)	56	-	267
VPS-5	6.47	16.9	184	(215)	0.97 (1.14)	83	SnO_2	269
IMP-2.4[h]	2.43	6.1	208	(220)		-	-	255
IMP-4.6	4.59	11.5	200	(223)		-	-	256
IMP-7.1	7.06	17.7	195	(220)		-	-	258
SnO_2			16.4			400	-	285

[a] -; not observed

[b] From XRF measurement.

[c] From XRD measurement.

[d] Selected Area Diffraction pattern was observed in the TEM measurement.

[e] Catalysts reffered as VPS- were prepared by the Vapor Phase Supporting (VPS) method.

[f] per gram catalyst.

[g] per gram SiO_2 support.

[h] Catalysts reffered as IMP- were prepared by the Impregnation method.

in the increase of SnO_2 content [7], as expected from Eq. (3). The SnO_2 content of the VPS catalysts is in the same range of SnO_2/SiO_2 catalyst which showed the highest conversion and selectivity [16]. BET surface area and pore volume per unit weight of catalyst were reduced by supporting SnO_2. But those values per unit weight of SiO_2, shown in parenceses, remained constant within the experimental error, suggesting that the physical texture of SiO_2 support was not changed so much by supporting SnO_2 by VPS and IMP methods.

In the X-ray diffraction (XRD) patterns, only a very broad line due to SiO_2 could be observed in the cases of VPS-1 and 2 catalysts. However, in the cases of VPS-3 and -5catalysts, broad and weak lines also were observed, and were identified as the diffraction lines of SnO_2. The average particle diameter, calculated from those lines by Scherrer's equation, was 5.6 nm for VPS-3 and 8.3 nm for VPS-5. In the cases of IMP catalysts, no diffraction lines due to SnO_2 could be observed, though IMP-7.1 catalyst containes more SnO_2 than VPS-5 catalysts. This result does not agree with that on SnO_2/SiO_2 catalyst in the previous Chapter, where the diffraction pattern due to SnO_2 was observed and the particle size from line broadening was about 6.0 nm. As the preparation method of catalyst is identical to one another, this difference may be due to the difference in the nature between SiO_2 supports. The effect of the nature of SiO_2 support on the catalytic performance of impregnated SnO_2/SiO_2 catalyst will be a subject of further study.

Figures 1 and 2 show transmission electron microscopic(TEM) photographs of SiO_2 (Fig. 1 - a), IMP catalysts (Fig. 1 - b, c, d) and VPS catalysts (Fig. 2). Dark spots in Figs. 1 - b, c, d, and Fig. 2 represent SnO_2 particles. Diffraction pattern of Fig. 2 - d by Selected Area Diffraction (SAD) method agreed with that of SnO_2. Figures 1 - b, c, d inticate that, in the case of IMP catalysts, SnO_2 particles with a diameter of about 1 nm for IMP-2.4 and of about 2 nm for IMP-4.6 and -7.1 are dispersed uniformly over the whole promary particles of SiO_2 support. In the case of VPS catalysts, on the other hand, SnO_2 particles depositted on only a part of primary particles of SiO_2, remaining most of SiO_2 paricles vacant, as shown in Fig. 2. In VPS-1, shown in Fig. 2 - a, several SnO_2 particles with a diameter of about 3 nm depositted on a primary particles, consisting a group. But most of SiO_2 particles remained vacant. In VPS-2 shown in Fig. 2 - b, the diameter of SnO_2 particles increased a little, resulting in the decrease of the number of SnO_2 particles in one group. But the number of group on the support was not changed so much. In VPS-3 and -5 shown in Figs. 2 - c and d, the diameter of SnO_2 increased up to 10 - 15 nm, and new groups, which were consisted of by small SnO_2 particels, were formed. But, most of the primary particles of SiO_2 still remained vacant.

Figure 3 shows high temperature infrared spectra of catalysts measured by EDR-IR [19]. In the case of SnO_2, a weak and broad band at 3600 - 2900 cm^{-1} was observed, and this band was attributed to H-bonded SnOH [20]. In SiO_2, a band of isolated SiOH at 3730 cm^{-1}

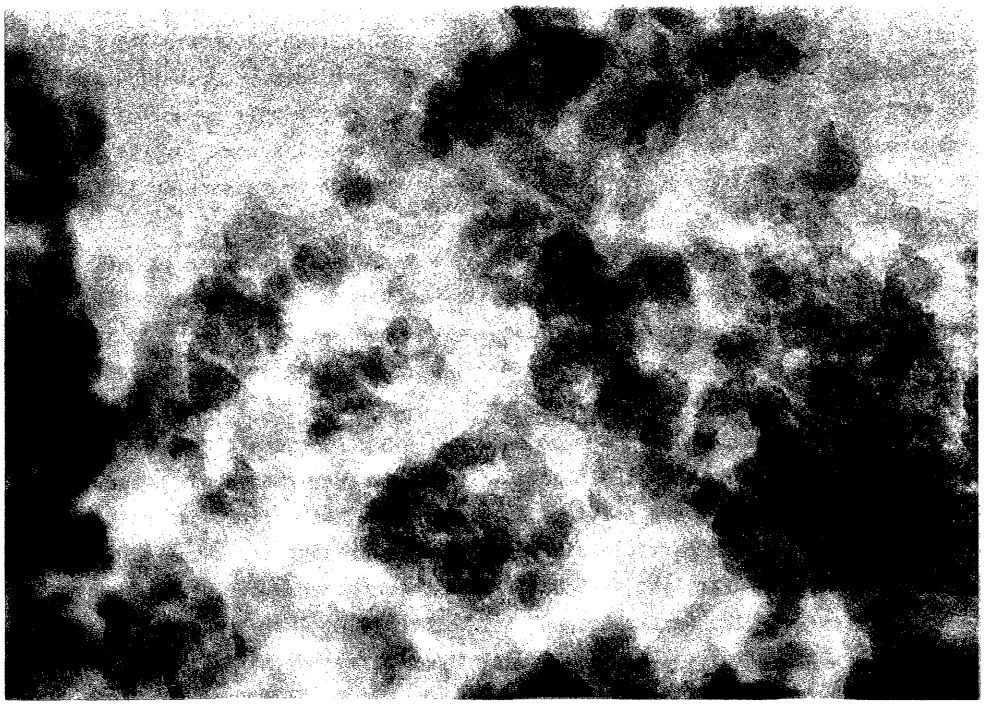

1-a

100 A

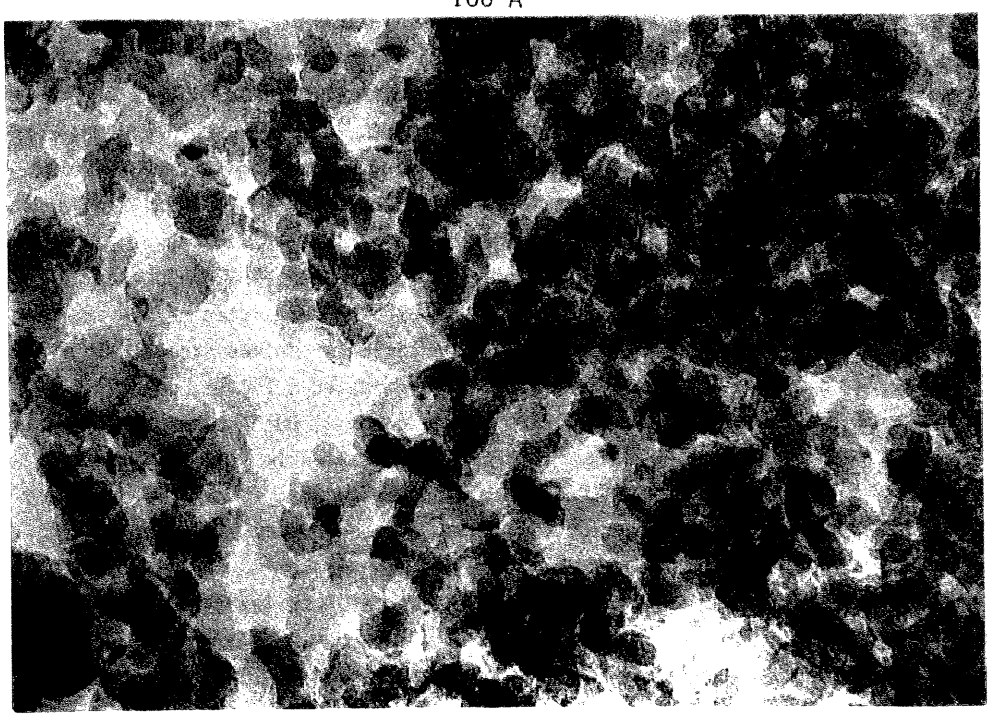

1-b

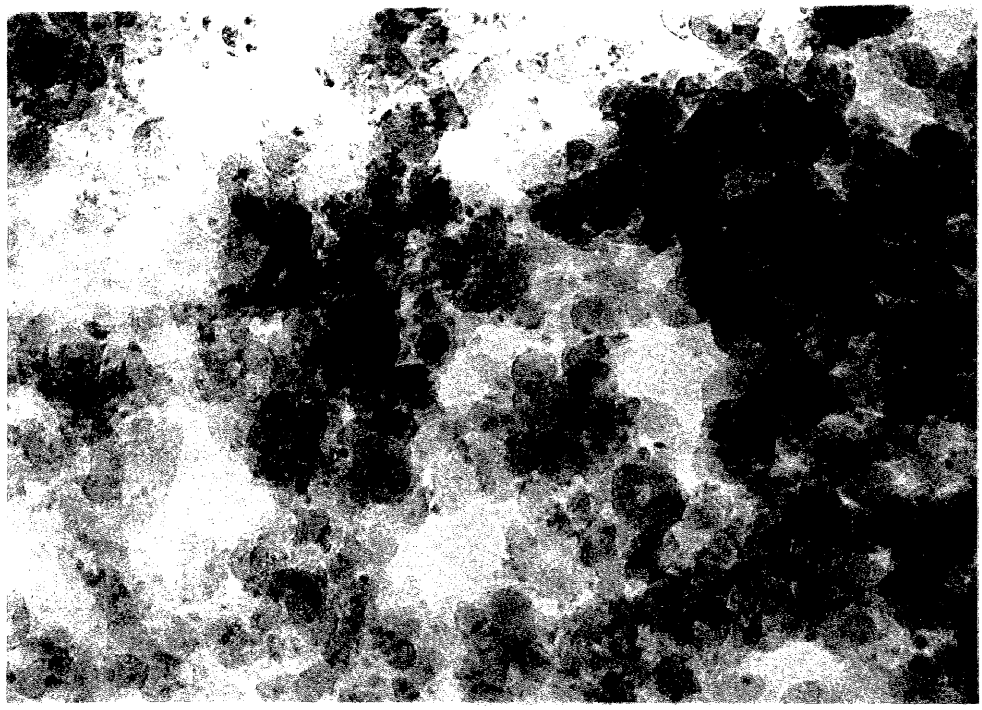

1-c

100 A

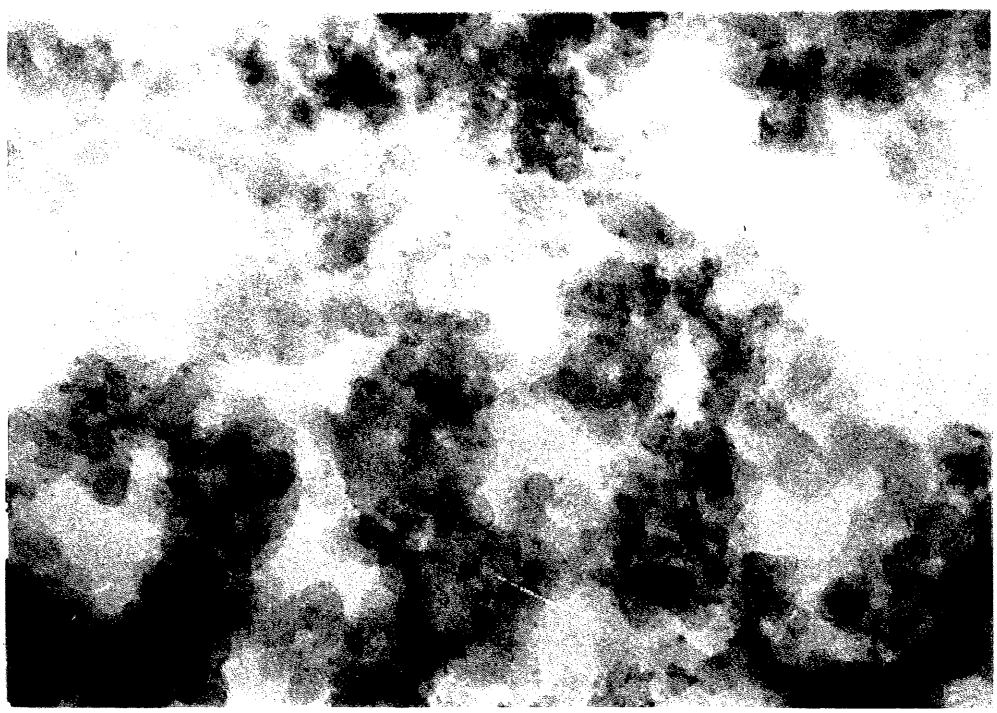

1-d

FIGURE 1 TEM Photographs of (a) SiO_2 Support, (b) IMP-2.4, (c) IMP-4.6, and (d) IMP-7.1

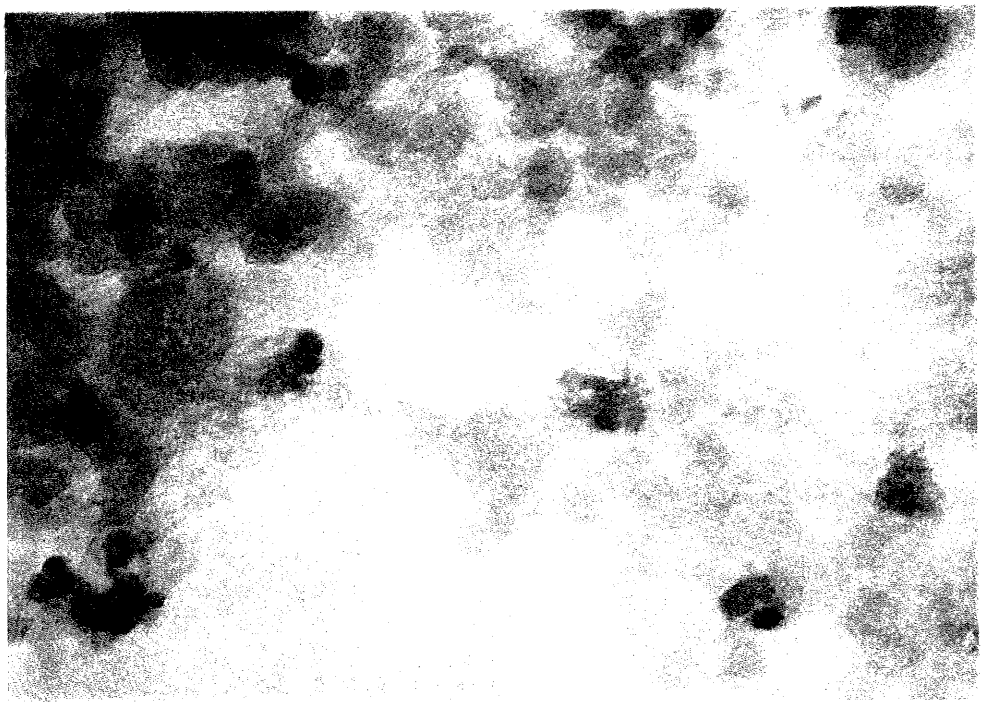

2-a

100 A

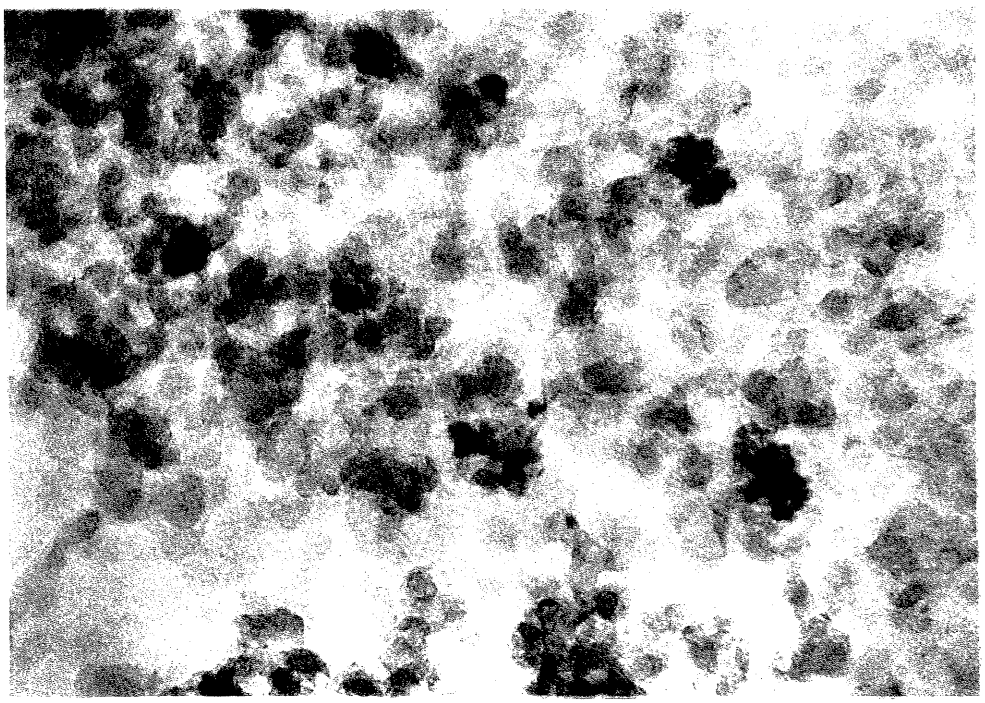

2-b

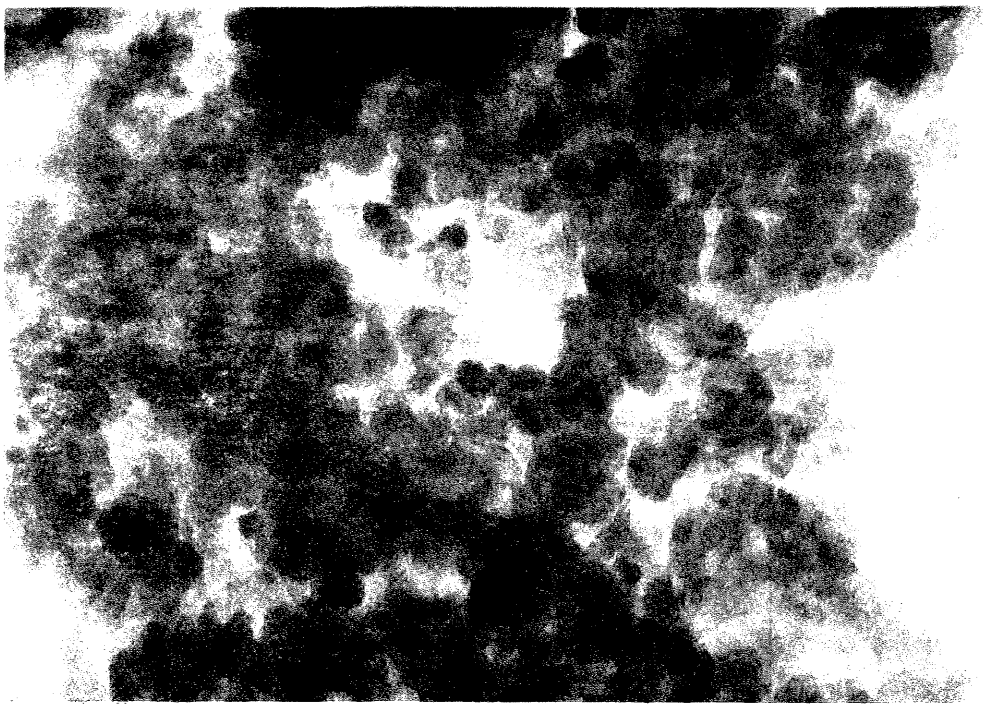

2-c

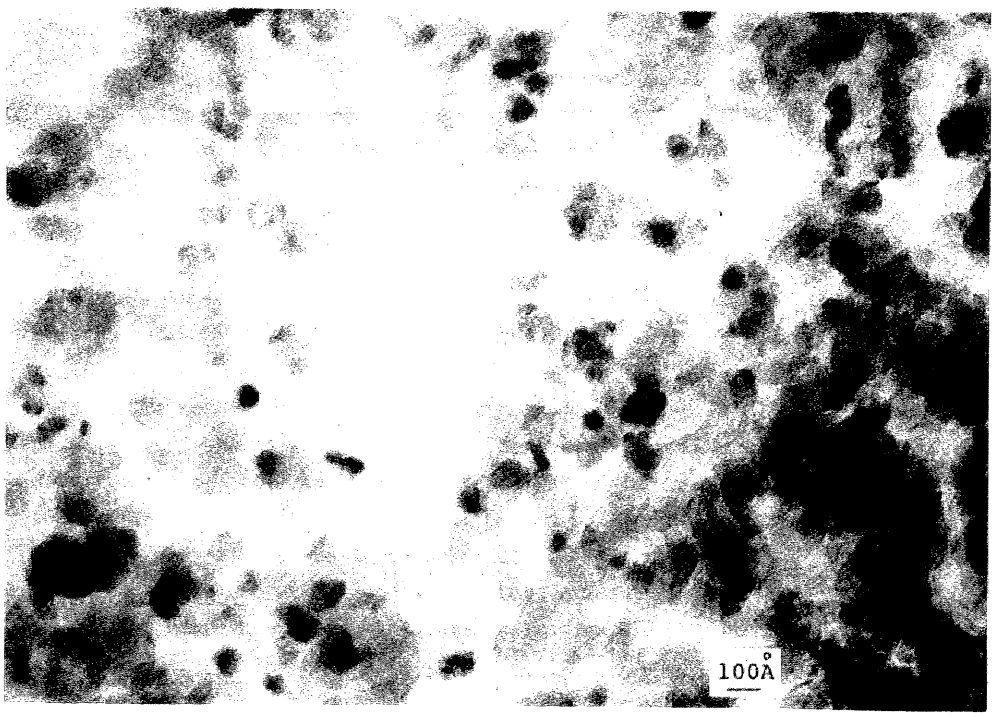

2-d

FIGURE 2 TEM Photographs of (a) VPS-1, (b) VPS-2, (c) VPS-3, and (d) VPS-5

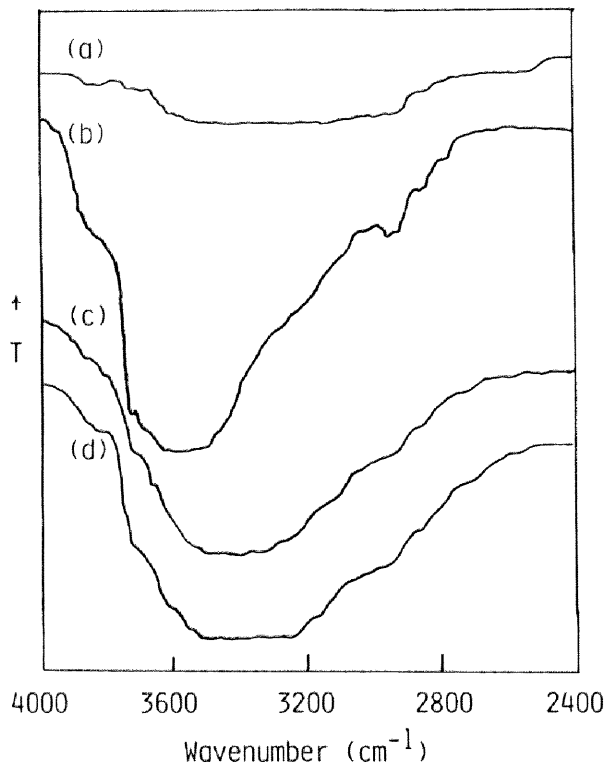

FIGURE 3 High temperature IR spectra of (a) unsupported SnO_2, (b) SiO_2 support, (c) VPS-5, and (d) IMP-7.1 measured at 605 K in the flow of dried helium.

and a broad band of H-bonded SiOH at 3600 cm^{-1} were observed. In the case of VPS and IMP catalysts, a weak band of isolated SiOH was observed, but a band of isolated SnOH at 3640 cm^{-1} was not detected. The H-bonded OH bands were observed between H-bonded SiOH and H-bonded SnOH band.The intensity of the band also was intermediate between both H-bonded SiOH and SnOH bands. These results suggested that the band between 3600 - 2800 cm^{-1} is an overlap of weaker H-bonded SiOH band and strong H-bonded SnOH band. The decrease in the intentsity of SiOH band agrees with that SiO_2 surface is covered by SnO_2, and the increases in the intensity and wavenumber of SnOH band might be due to the interaction of SnO_2 with SiO_2.

UV spectrum of SnO_2 was essentially the same as that reported by Sala and Trifro [21]. It had an absorption maximum at 285 nm with a broad tailing to 460 nm. Sala and Trifro ascribed the tailing at 350 - 460 nm to an intervalence charge transfer band. In the case of supported SnO_2catalysts, as shown in Table 1, the adsorption maximum was shifted to lower wavelength, especially in the case of IMP catalysts, suggesting an interaction with SiO_2. The intervalence charge transfer band could not be detected on the catalysts. The interaction with SiO_2 might reduce the electron transfer between Sn^{4+} and Sn^{3+}.

Figure 4 shows temperature programmed reduction (TPR) profiles of catalysts. The reduction of SnO_2 (curve a) started at 370 K (T_{init}), had a small maximum at 680 K and a small minimum at 770 K, and proceeded further at higher temperature. The amount of consumed hydrogen (H_2/Sn) was 0,12 below 770 K and 0.71 between 770 and 1100 K. T_{init} of VPS-1 (curve b) was higher than SnO_2 by 100 K and a broad reduction peak was observed between 670 and 820 K. The H_2/Sn ratio was 0.65. In the case of VPS-3 (curve c), T_{init} was almost the same as that of SnO_2, and two reduction maxima were observed at 870 K and 1020 K. H_2/Sn ratio was 0.71 and 0.35, respectively. The reduction profile of IMP-4.6 was quite similar to that of VPS-3, except that the reduction peak at higher temperature could not be observed.

Acid-base properties

Figure 5 shows IR spectra of adsorbed pyridine on SiO_2 and catalysts. On SiO_2 (spectrum a), only bands due to hydrogen bonded pyridine (HPy) were observed at 1447 cm^{-1} and 1597 cm^{-1}, but no bands due to pyridinum ion (BPy) and coordinated pyridine (LPy) could not be observed. On VPS-1 (spectrum b), LPY bands at 1453 cm^{-1} and 1613 cm^{-1} as well as HPy bands were observed. The intensity of LPy bands decreased on VPS-2 (spectrum c) and increased again on VPS-3 and -5 (spectra d and e). In the case of IMP-4.6 (spectrum f) strong bands of LPy as well as HPy bands were observed. No bands due to BPy was observed on these catalysts. After the evacuation at 473 K for 0.5 h, LPy bands remained on VPS-1 and IMP-4.6 and a weak LPy bands were observed on VPS-3 and -5. On the other hand, LPy bands disappeared on VPS-2 after the evacuation. HPy bands disappeared on all the catalysts.

IR spectra of adsorbed ammonia also were measured. The band due to ammonium ion on

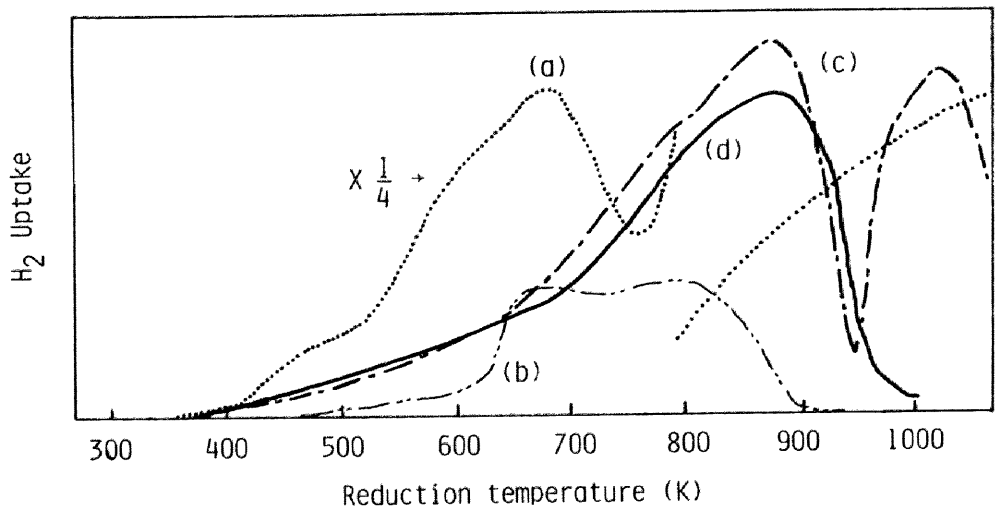

FIGURE 4 TPR profiles of SnO_2/SiO_2 catalysts. (a) SnO_2, (b) VPS-1, (c) VPS-3, (d) IMP-4.6.

Table 2

Acid and Base Properties and Reduction Properties of SnO_2/SiO_2 Catalyst[a]

Catalyst	Ho_{max} [b]					pKa_{max} [c]					Active oxygen (μeq)	
	+4.0	+3.3	+1.5	-3.0	-5.6	+9.8	+15.0	+17.2	+18.4	+26.5	(g-cat)	(g-SnO_2)
SiO_2	+	-	-	-	-	-	-	-	-	-	0.00[d]	0.00[e]
VPS-1	+	+	+	-	-	+	+	±	-	-	1.73	36.8
VPS-2	+	+	+	-	-	+	+	±	-	-	2.01	22.6
VPS-3	+	+	+	-	-	+	+	±	±	-	6.89	55.1
VPS-5	+	+	+	-	-	+	+	+	±	-	16.32	112.6
IMP-2.4	+	+	+	-	-	+	+	+	±	-	4.92	80.7
IMP-4.6	+	+	+	+	±	+	+	+	±	-	16.03	129.4
IMP-7.1	+	+	+	+	±	+	+	+	±	-	28.47	166.8
SnO_2	+	+	+	-	-	+	±	-	-	-	28.5	28.8

[a] +; observed, ±; observed but little, -; observed but little.

[b] Benzalacetophenone for -5.6, Dicinnamalacetone for -3.0, 4-Benzeneazodiphenyl amine for 1.5, p-Dimethylaminoazobenzene for 3.3, and 4-Benzeneazo-1-naphthylamine for 4.0.

[c] Phenolphthaleine for 9.8, 2,4-Dinitroaniline for 15.0, 4-Chloro-2-nitroaniline for 17.2, 4-Nitroaniline for 18.4, and 4-Chloroaniline for 26.5.

[d] active oxygen per g-catalyst.

[e] active oxygen per SnO_2.

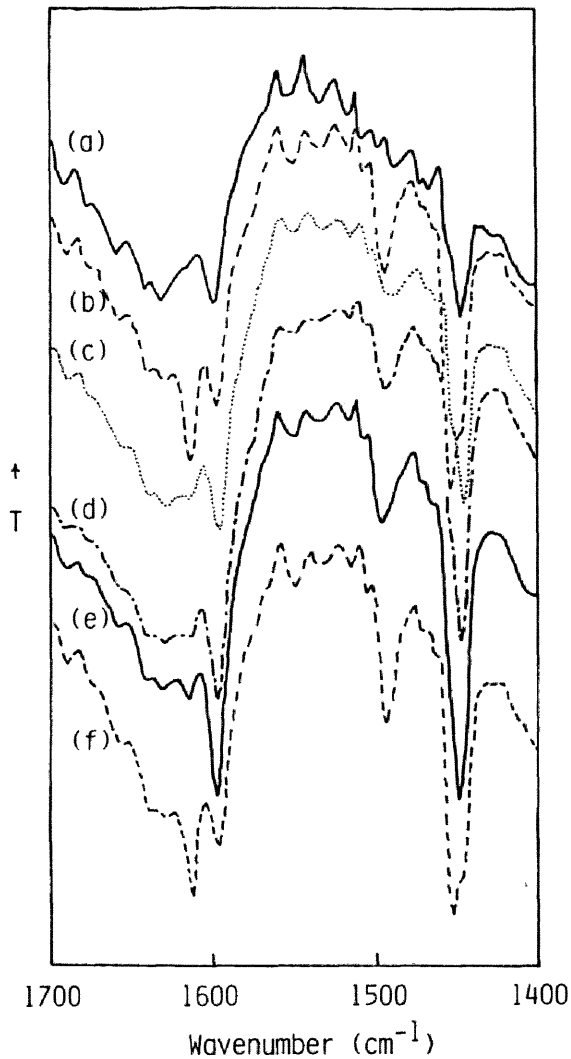

FIGURE 5 IR spectra of pyrinine adsorbed on (a) SiO_2, (b) VPS-1, (c) VPS-2, (d) VPS-3, (e) VPS-5, and (f) IMP-4.6. Samples were evacuated at 673 K for 1 h, pyridine vapor was adsorbed at room temperature for 0.5 h, evacuated at room temperature for 0.5 h, and then IR spectra were recorded.

B - acid sites could not be observed in accordance with the results of IR spectra of pyridine. The band due to ammonia coordinatively adsorbed on L-acid sites were observed only on VPS-1 and -5 and IMP-4.6 catalysts, but not on VPS-2 and -3 and SiO_2 support.

The maximum acid and base strength (Ho max and pKa max) of catalysts were shown in Table 2. SiO_2 had only very weak acid sites of $Ho > +3.3$, and SnO_2 had weak acid sites of $Ho > -3.0$. The maximum acid strength of VPS catalysts was identified to that of SnO_2, while IMP catalysts with high SnO_2 content had acid sites of $Ho < -3.0$ and, even, a small amount of strong acid sites of $Ho < -5.6$. Although SiO_2 and SnO_2 did not have strong base sites of $pKa > 17.2$, both VPS and IMP catalysts had such base sites.

It has been shown in the previous chapter, that acid sites of $1.5 > Ho > -5.6$ are necessary to adsorb and activate ethylbenzene in the oxidative dehydrogenation of ethylbenzene. Figure 6 shows the effect of VPS cycle on SnO_2 content on the amount of acid sites of $1.5 > Ho > -5.6$. It should be noted that acid sites of $Ho < -5.6$ were not present on VPS catalysts, and appeared to be few on IMP catalysts. Thus, the ordinate of Fig. 6 also represents the total amount of acid aites on the catalysts. The acidity of concern on both VPS and IMP catalysts was not changed so much after the oxidative dehydrogenation of ethylbenzene for 4 h followed by the calcination in a flow of oxygen at 773 K. The acidity of IMP catalysts, which were, as a whole, larger than the acidity of VPS catalysts, increased almostmonotonously with SnO_2 content. On the other hand, very interesting result was obtained on VPS catalysts. The acidity was the largest on VPS-1, took the minimum on VPS-2, and then increased again on VPS-3 and -5. This result suggests that the acid sites on VPS-1 is different in nature from VPS catalysts with high SnO_2 content.

The amount of effective base sites, $17.2 < pKa < 26.5$, could not be determined, because the color-change of indicators was very obscure on SnO_2 adn SnO_2 surpported on SnO_2.

Catalytic properties

Figure 7 shows the results of pulse reaction on VPS-5 and IMP-7.1 catalysts. In the case of VPS catalyst, the yield of styrene decreased by repeating pulses of ethylbenzene (pulse I), did not increase by oxygen pulse injected prior to ethylbenzene (pulse II) or by oxygen pulse injected simultaneously with ethylbenzene. Benzene was not formed in all experiments, and the yield of carbon oxides was not so large. In the oxygen pulse prior to ethylbenzene pulse, only carbon oxides were formed, but no styrene was detected. The result on VPS-3 was very close to that on VPS-5 shown in Fig, 7-a. The results on VPS-1 and -2 were qualitatively similar to that on VPS-5, though the yields of styrene and carbon oxides formed were smaller.

In the case of IMP-7.2 catalyst, the yield of styrene decreased by the repeated pulse of ethylbenzene (pulse I) in the same way as VPS-5. But it increased in pulse II after oxygen pulse or in pulse III with oxygen pulse injected simultaneously. This

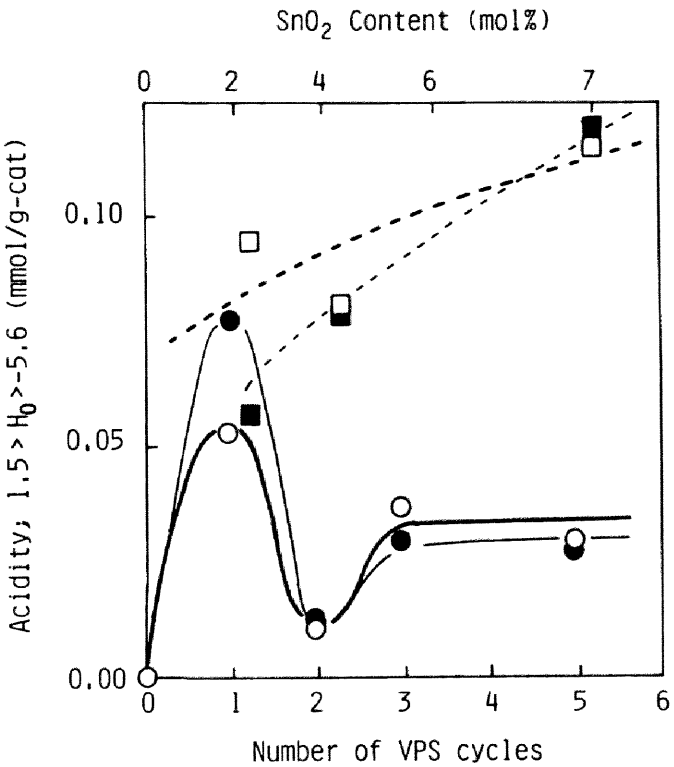

FIGURE 6 Effect of VPS cycles on the amount of acid sites of Ho between 1.5 and -5.6 on (○) VPS-catalysts and (□) IMP-catalysts of fresh state for open symbols and regenerated state of used catalysts for filled symbols.

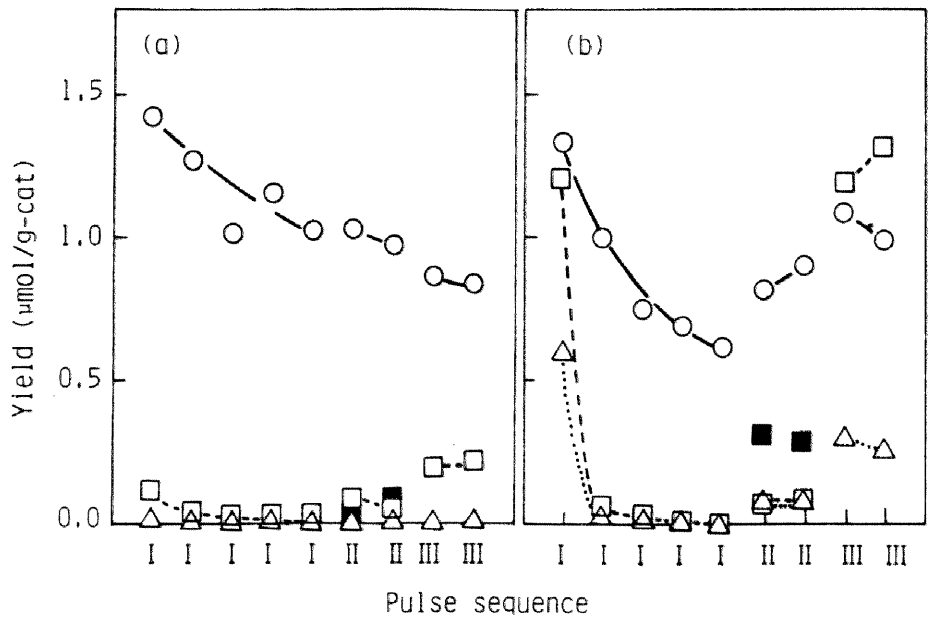

FIGURE 7 Product distribution in the pulse reaction on (a) VPS-5 and (b) IMP-7.1. Ethylbenzene (1 μl) was pulsed (pulse I), oxygen (1 ml) was pulsed (pulse II') and then ethylbenzene was pulsed (pulse II), and ethylbenzene and oxygen were pulsed simultaneously (pulse III) at 723 K. (○) Styrene, (□) carbon oxides, and (△) benzene were formed by each pulse. In pulse II' (oxygen pulse), only carbon oxides (filled square) were formed.

indicates that IMP-7.1 catalyst is more easily reoxidized than VPS catalysts. The result that the yield in pulse III was larger than that in pulse II suggests that adsorbed oxygen may be active species (12,13). Large amounts of by-products, benzene and carbon oxides, were formed in the first pulse of pulse I, but not so much were formed in the second pulse. In pulse III, large amounts of by-products were formed again. The result on IMP-4.6 was close to that on IMP-7.1, but that on IMP-2.4 was close to that on VPS-1 or 2.

As mentioned above, the yield of styrene and carbon oxides decreased by repeating ethylbenzene pulse (pulse I). This suggests that the amount of active oxygen decreases with increasing pulse number, and that the amount of active oxygen may be measured from the total yields of styrene and carbon oxides by repeating ethylbenzene pulse until any oxydation products could not be detected.

$$C_6H_5C_2H_5 + (O) \longrightarrow C_2H_5C_2H_3 + H_2O + (\ ) \quad (4)$$

$$C_6H_5C_2H_5 + 13(O) \longrightarrow 8CO + 5H_2O + 13(\ ) \quad (5)$$

$$C_6H_5C_2H_5 + 21(O) \longrightarrow 8CO_2 + 5H_2O + 21(\ ) \quad (6)$$

The amount of active oxygen thus obtained was summarized in Table 2.

Figure 8 shows the results of continuous flow reaction on VPS-3 and IMP-4.6. The selectivity on VPS-3 was as high as 90 % and that on IMP-4.6 was close to it. The selectivity on VPS-5 and IMP-7.1 was almost equal to that on VPS-3 and IMP-4.6, respectively, but the selectivity on catalysts with low SnO_2 content was significantly lower than the selectivity shown in Fig. 8. The rate of styrene formation on IMP-4.6 increased gradually with the time on stream and become constant. On the other hand, the rate on VPS-3 decreased gradually and become constant. The results on other VPS and IMP catalysts were similar to those on VPS-3 and IMP-4.6, respectively.

Reoxidation of used IMP-4.6 catalyst at 770 K in O_2/N_2 flow (1/10) for 2 h and in oxygen flow for 1 h resulted in essentially the same results as shown in Fig. 8 for fresh catalyst, i.e., the same initial activity and the same time course of an increase in activity. On the other hand, the activity of VPS-3 catalyst after the reoxidation was equal to the activity immediately before the reoxidation.

DISCUSSION

Schematic model of supported SnO_2 on SiO_2

The vapor phase supporting method was applied to prepare SnO_2 catalyst supported on SiO_2 for the oxidative dehydrogenation of ethylbenzene. In VPS method, $SnCl_4$ has been supposed to react with surface OH group to form surface chloride compound which is, in turn, hydrolized to form oxide layer, as shown by Eqs. (1) - (3). Repeating VPS cycles, Eqs. (1) and (2) has been supposed to result in the increase of the thickness of oxide layers. Actually, SnO_2 content increased with increasing VPS cycles, as shown in Table 1. However, the rate of the increase in SnO_2 content became small after the

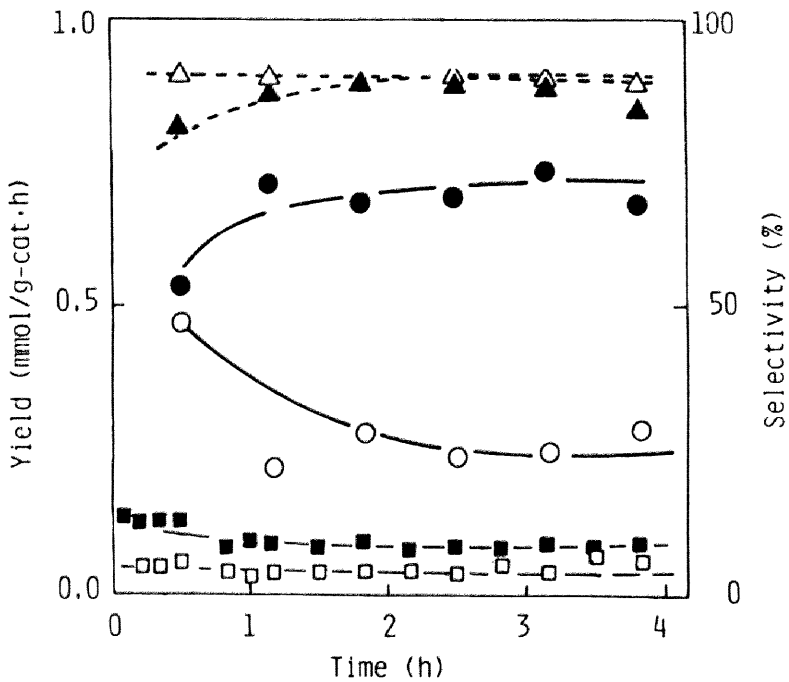

FIGURE 8 Time course of the oxidative dehydrogenation of ethylbenzene on VPS-3 (open symbols) and on IMP-4.6 (filled symbols). Rate of (○) styrene formation and (□) carbon oxides formation and (△) selectivity to styrene. Catalyst weight; 1.00 g, total feed rate; 300 mmol/h, partial pressures; $P_{EB} : P_{O_2} : P_{H_2O} : P_{N_2}$ = 0.051 : 0.247 : 0.404 : 0.298.

third cycle. The difference in SnO_2 content between VPS-3 and -5 is smaller than SnO_2 content in VPS-1. The concentration or the reactivity of surface OH group might decrease with increasing VPS cycles.

XRD patterns of VPS-3 and -5 were identified as SnO_2, and SAD patterns of VPS-5 also was identified as SnO_2. The particle size of supported SnO_2, calculated by the line broadening method of XRD line, was 5.6 nm on VPS-3 and 8.3 nm on VPS-5. These values agreed well with the average particle size calculated from TEM photographs. In the TEM photographs, the projected area of SnO_2 in VPS catalysts appears to be almost constant, though SnO_2 content increases with the increase in VPS cycles. This agrees that the thickness of oxide layer may increase with the increase in VPS cycles, as it has been expected. The average thickness was estimated from the projected area and SnO_2 content by assuming that the SnO_2 particels are semispherical. The average thickness thus estimated was about 1.4, 2.0, 4.0, and 5.0 nm for VPS-1, -2, -3, and -5 catalysts, respectively. On VPS-3 and -5, small particles were newly formed, which may introduce errors in the estimated thickness. The thickness in IMP catalysts, estimated in the same way, agreed well with the radious of SnO_2 particles observed in TEM photographs.

These discussions leads to the schematic model of supported SnO_2 shown in Fig. 9. The model will be useful to understand the difference in the catalytic properties between the catalysts.

In the previous chapter, it was shown from the isomer shift of Mössbauer spectra that SiO_2 withdraws electrons from SnO_2. The interaction with SiO_2 was observed in UV spectra shown in Table 1. The absorption maximum shifted to lower wavelength with the decrease of SnO_2 content, or with the decrease of SnO_2 particle diameter. The interaction was also observed in the reduction properties. The initiation temperature of reduction in TPR profile increased with decreasing SnO_2 content as shown in Fig. 4. The amount of active oxygen shown in Table 2 increased with increasing VPS cycles. The ratio of active oxygen to SnO_2 content was not constant, but it increased with VPS cycles. In the case of VPS-1, SnO_2 was supported as thin layers on SiO_2 and the interaction between SnO_2 and SiO_2 was significantly large. In VPS-2, SnO_2 was supported on SnO_2 layers of VPS-1. Further VPS cycles result in the depodition of SnO_2 on SnO_2 thus supported on SiO_2 to form SnO_2 crystals. The increase in the thickness of SnO_2 particle may reduce the average interaction of SnO_2 with SiO_2. In the case of IMP catalysts, SnO_2 was highly and uniformly dispersed. With increasing SnO_2 content, the the particle size increased only a little, but the number of SnO_2 particle increased significantly. This agrees well with almost constant absorption maximum in UV spectra shown in Table 1.

Acid and base sites

The acid properties of SnO_2/SiO_2 catalysts are examined by IR spectra of adsorbed pyridine shown in Fig. 5, by titration with n-butylamine shown in Fig. 6, and by color

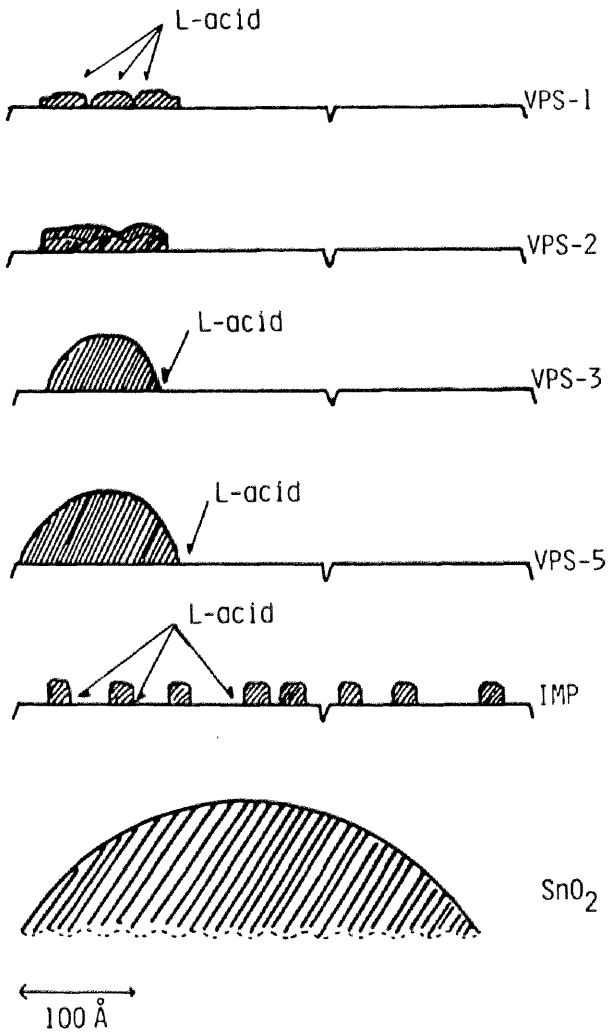

FIGURE 9 Schematic models of SnO_2 on the support.

change of the Hammet indicators shown in Table 2. These results indicate that new acid sites are generated by supporting SnO_2 on SiO_2, and verify the working hypothesis in the design of catalyst that supporing SnO_2 on SiO_2 would generate acid sites which is essential to the oxidaitve dehydrogeation of ethylbenzene [12,13,14].

The interaction of SnO_2 with SiO_2 was very strong in VPS-1. Mössbauer spectra of SnO_2/SiO_2 catalysts indicated that electron was withdrawn from SnO_2 by SiO_2 [16]. This suggests that Lewis acid site may be generated on SnO_2. In the case of VPS-2, SnO_2 was supported on SnO_2 layers of VPS-1, which may reduce the acidity.

As mentioned above, the relation between the acidity of $1.5 > Ho > -5.6$ wiht VPS cycles, shown in Fig. 6, suggests that acid sites on VPS-1 are different in the nature form those on VPS-3 and -5. In the cases of VPS-3 and -5, SnO_2 particles are too thick for the acid sites to be generated on SnO_2 particles under the effect of SiO_2. The acid sites may be around the interface of SnO_2 and SiO_2. According to Tanabe [22], Lewis acid sites are generated on Si atoms under the effect of SnO_2 in a mixture of SnO_2 and SiO_2. However, Mössbauer spectra, chapt. 8, indicated that electorn withdrawn from SnO_2 by SiO_2. This suggests that Lewis acid sites are generated on Sn atoms. Anyway, it is reasonable that another type of Lewis sites are generated around the interface between SnO_2 and SiO_2.

In IMP catalysts, Lewis acid sites may be formed on SnO_2 under the effect of SiO_2, because SnO_2 particles are so small. High dispersion of SnO_2 leads to large amount of acid sites as shown in Fig. 6.

In the reaction mechanism previously proposed, base sites abstract α- and β-hydrogen from ethylbezene adsorbed on acid sites to form styrene and water. But it was very difficult to examine the base-properties by titration method, because color change of the indicators was not clear on SnO_2/SiO_2 catalysts. Thus the reduction properties were examined by the TPR profile and the reduction with ethylbenzene. The amount of active oxygen per unit catalyst weight increased along with the increase of SnO_2 content, as shown in Table 2, and the amount per unit weight of SnO_2 shown in parenthesis also increased. In the case of VPS-1, the reducibility of SnO_2 was low. The initiation temperature of reduction in TPR was high, and the amount of active oxygen titrated with ethylbenzene was only 36.8 μeq/g-SnO_2. The low reducibility of VPS-1 may be caused by thin layers of SnO_2. VPS-3 and -5 catalysts with thick SnO_2 particles showed high reducibility. The initiation temperature in TPR was lower and the amount of active oxygen was larger than VPS-1. IMP catalysts also had larger amount of active oxygen and low initiation temperature. The large amount of active oxygen may be resulted in by the high dispersion of SnO_2 or, in other words, by the large surface area of SnO_2.

Schematic model and Catalytic performances

Figure 10 shows the effect of SnO_2 content on the activity and selectivity at initial stage (30 min) and at steady stage (230 min). As mentioned above, the yield

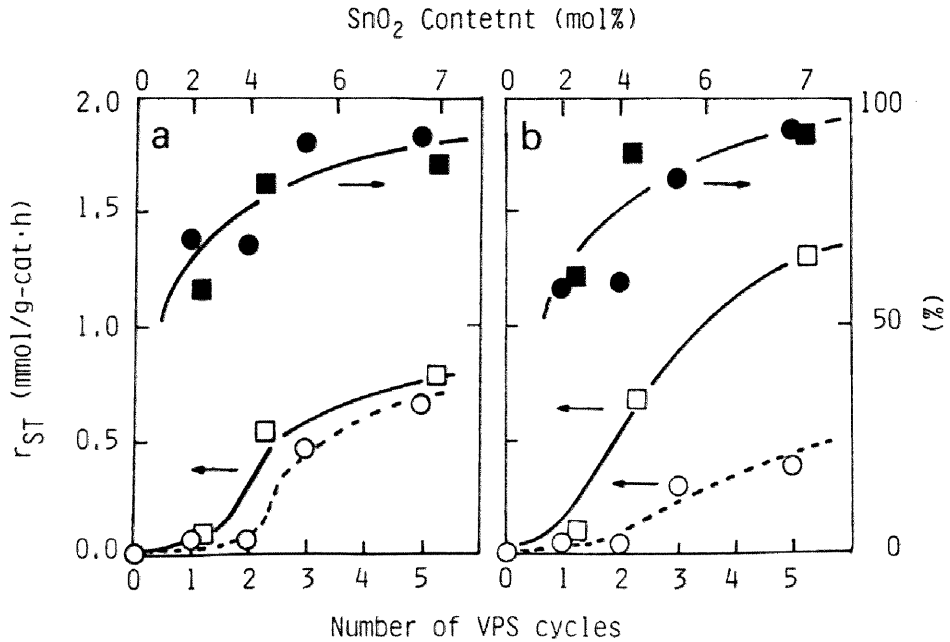

FIGURE 10 Effect of VPS cycles on the flow reaction after (a) 0.5 h and (b) 3.83 h, on (○) VPS- catalysts and (□) IMP- catalysts. Open symbols for the rate of styrene formation and filled synbols for the selectivity. For the reaction conditions, see Fig. 8.

of styrene on IMP catalysts increased with time on stream, but those on VPS catalysts decreased. At the initital stage, the activity on both catalysts was close to one another, but, at the steady state, the activity on IMP catalysts was higher than VPS catalysts. Both of the initial activity and the steady activity increased with SnO_2 content, and the increase in the activity was remarkable around 4 mol% of SnO_2. This result is in good agreement with the result in the pulse reaction shown in Fig. 11. The yield of styrene in the pulse reaction also increased with SnO_2 content, and it increased remarkably around 4 mol% of SnO_2.

The following reaction mechanism has been proposed for this reaction in the previous chapter. Ethylbenzene is dissociatively adsorbed on acid sites of $1.5 > Ho > -5.6$, and the catalytic activity per such acid site, turnover frequency, is determined by the base propertiy of catalysts. And it has been confirmed that this reaction mechanism can be applied to various solid acid catalysts, too. In the present case, the reaction mechanism appears to be applied. Figure 12 shows the effect of VPS cycles on SnO_2 content on the amount of reversibly adsorbed ethylbenzene which was calculated from the amount of unrecovered ethylbenzene in the pulse reaction. The effect is quite similar to that on the acidity of concern shown in Fig. 6, indicating that ethylbenzene is adsorbed on the acid sites of $1.5 > Ho > -5.6$. The activity of IMP catalysts increased with time on stream, but that of VPS catalysts decreased, as shown in Fig. 8. The reoxidation of used catalysts resulted in the same initial activity and the same time course of activity change in the case of IMP catalysts, but the activity of VPS catalysts was not recovered by the reoxidation. Thus, the activity change if IMP catalysts is reversible, that of VPS catalysts is irreversible. Figure 6 shows the acidity of concern of the fresh catalysts and the used - reoxidized catalysts. The acidity of both VPS and IMP catalysts was not changed by the use in flow reaction and the following reoxidation. As to the IMP catalysts, this result is in good agreement with that the initial activity was recovered by the reoxidation. However, in the case of VPS catalysts, the irreversible activity change should be explained by the other factor than the acidity, i.e., the change of the activity per an acid site. Figure 13 shows the turnover frequencies at 30 min and 230 min. As shown in the figure, the turnover frequency of VPS catalysts is high at the initial stage, but decreases with time. The activity change of IMP catalysts is the same as that observed on solid acid catalysts. At the initial stage, styrene once formed polymerizes to form coke, and it reduces the apparent yield of styrene. Coke thus formed blocks active sites for polymerization and suppresses the polymerization reaction, which increases the apparent yield of styrene. On the other hand, the activity change of VPS catalysts can not be explained either by the coke formation or by the decrease of active sites. Figure 14 shows the effect of SnO_2 content on the amount of active oxygen per an acid site of concern. The tendency is quite similar to that of the turnover frequency at the initial stage shown in Fig. 13. This indicate that lattice oxygen is responsible

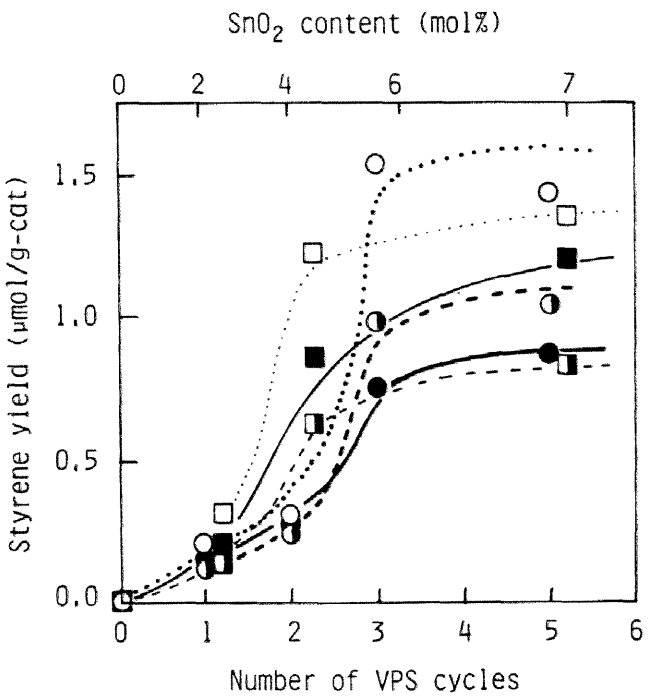

FIGURE 11 Effect of VPS cycles on the styrene formation in the pulse reaction on (○) VPS- and (□) IMP- catalysts. Pulse I (open symbols), pulse II (half filled symbols), and pulse III (filled symbols) were performed at 723 K onto 0.2 g of samples in the flow of oxygen free helium.

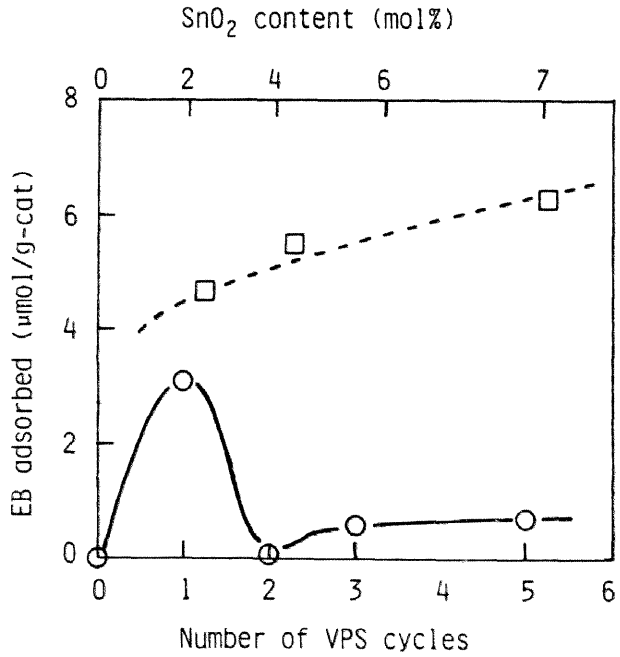

FIGURE 12 Effect of VPS cycles on the amount of ethylbenzene adsorbed on the catalysts estimated from the unrecoverly in the pulse reaction. (○) for the VPS-catalysts and (□) for the IMP-catalysts.

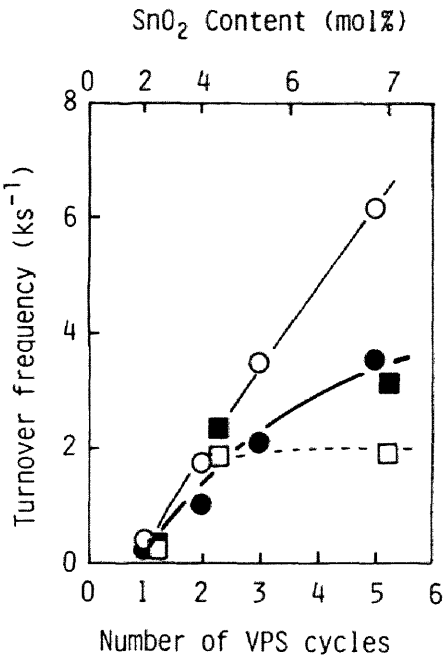

FIGURE 13 Effect of VPS cycles on the turnover frequency. For the symbols, see Fig. 6.

$$\text{Turnover frequency} = \frac{\text{Rate of styrene formation in the flow reaction at 723 K}}{\text{Amount of active acid sites of Ho between 1.5 and -5.6}}$$

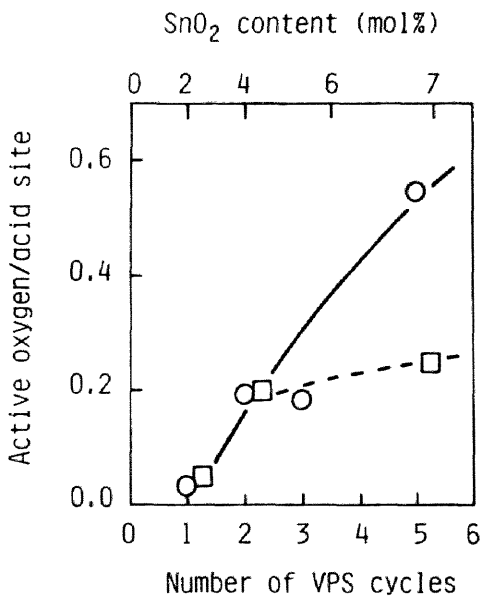

FIGURE 14 Effect of VPS cycles on the amount of active oxygen. For the symbols, see Fig. 6.

for the activity, at least, of VPS catalysts at the initial stage. In the pulse reaction, the yield of styrene decreased by repeating ethylbenzene pulses (pulse I), as shown in Fig. 7. This result indicates that the lattice oxygen is active for the reduction on both IMP and VPS catalysts and that the catalysts are easily by ethylbenzene. On VPS catalysts, the oxygen pulse injected prior to ethylbenzene pulse (pulse II') did not increase the yield of styrene so much. This indicates that the reoxidation of VPS catalyst is not so fast,which results in the gradual reduction of catalysts and the gradual decrease of catalytic activity with time on stream. On the other hand, the oxygen pulse significantly improved the yield of styrene on IMP catalysts, and oxygen injected simultaneously with ethylbenzene (pulse III) further improved the yield of styrene. These results indicate that the reoxidation of IMP catalysts is fast and that the weakly adsorbed oxygen with short life is acitve for the reaction on IMP catalysts. Thus, in the case of IMP catalysts, the oxidized state of catalyst remaines unchanged and, even if the catalyst was reduced, the weakly adsorbed oxygen, may be O^- [13], maintains the catalytic activity.

In summary, the VPS method gaines relatively large SnO_2 particles supported on SiO_2 surface, and the repeated VPS cycles increase the thickness of SnO_2 particles. VPS catalysts with high SnO_2 content show high catalytic activity per an active site, i.e., turnover frequency. However, the amount of active sites is so small that the overall activity is in the same range as that of IMP catalysts. And the VPS catalyst is easily reduced during the reaction, which results in the decrease of the catalytic activity with time on stream. If the amount of SnO_2 particles on SiO_2 surface can be increased and if the reoxidation can be promoted, further improved catalyst may be obtained.

REFERENCES

1 S.I. Kol'tsov and V.B. aleskovskii, Zh. Prikl. Khim., 42 (1969) 1950, and ibid., 40 (1967) 907.

2 S.I. Kol'tsov, ibid., 38 (1965) 1384.

3 R.R. Rachkovskii, S.I. Kol'tsov, and V.B. Aleskovskii, Zh. Zeorg. Khim., 15 (1970) 3158.

4 G.P. Oarfitt, J. Ramsbotham, and C.H. Rochester, J.C.S. Faraday Trans I, 68 (1972) 17.

5 S.I. Kol'tsov, V.M. Smirov, V.N. Postnov, A.M. Postonova, and V.B. Aleskovskii, Kinet. Catal., 21 (1981) 550.

6 V.A. Khalif, E.L. Aptekan, O.V. Krylov, and G. Ohlmann, Kinet Catal., 18 (1977) 1055.

7 T. Tagawa, S. Itoh, T. Hattori, and Y. Murakami, 48th annual meeting of catalysis society, Japan, 1W13 (1981), ibid., 46th,3Q03 (1980), and ibid., 44th,4L28 (1979).

8 K. Suzuki, T. Hattori, A. Miyamoto, and Y. Murakami, 48th annual meeting of catalysis society, Japan. 1V03 (1981).

9 T. Tagawa, S. Itoh, T. Hattori, and Y. Murakami, React. Kinet. Catal. Lett., submitted. Chapter 9.

10 Y. Murakami, K. Iwayama, H. Uchida, T. Hattori, and T.Tagawa, Appl. Catal., in press; Chapter 2 .

11 Y. Murakami, K.Iwayama, H. Uchida, T. Hattori, and T. Tagawa, J. Catal., in press; Chapter 3.

12 T.Tagawa, T. Hattori, and Y. Murakami, J. Catal., in press; Chapter 4.

13 T. Tagawa, T. Hattori, and Y. Murakami, J. Catal., in press; Chapter 5.

14 T. Tagawa, K. Iwayama, T. Hattori, and Y. Murakami, J. Catal., submitted; Chapter 6.

15 T. Tagawa, S. Kataoka, T. Hattori, and Y. Murakami, Appl. Catal. submitted; Chapter 7.

16 T. Tagawa, S. Kataoka, T. Hattori, and Y. Murakami, J. Catal. submitted; Chapter 8.

17 D.L. Trimm, "Design of Industrial Catalysis," Elsevier Sci. Publ. Co. New York, (1980).

18 H. Itoh, T. Hattori, and Y. Murakami, Appl. Catal., in press.

19 M. Niwa, T. Hattori, M. Takahishi, K. Shirai, M. Watanabe, and Y. Murakami, Anal. Chem., 51 (1979) 46, and T. Hattori, K. Shirai, M. Niwa, and Y. Murakami, ibid., 53 (1981) 1129.

20 E.W. Thornton and P.G. Harrison, J.C.S. Faraday 1, 71 (1975) 461.

21 F. Sala and F. Trifiro, J. Catal., 34 (1974) 68.

22 K. Tanabe, T. Sumiyoshi, K. Shibata, T. kiyoura, J. Kitagawa, Bull. Chem. Soc. Japan, 47 (1974) 1064, and M. Itoh, H. Hattori, and K. Tanabe, J. Catal., 35 (1974) 225.

Chapter 11

CONCLUSION

Summary of Each Chapters

As described in the foregoing chapters, fairly good results are obtained by conducting this study along with the program of the catalyst design which is stated in Chapter 1. A detailed mechanism for the present reaction is confirmed on the basis of the quantitative roles of the acid and base sites in a molecular aspect, which served to construct the plan of catalyst design. Fairly good catalysts are designed such as SnO_2-P_2O_5, Al_2O_3-P_2O_5, and SnO_2/SiO_2. The comparison of the designed catalysts with the reported catalysts are shown in Table 1, showing that the the target, value settled in Chapter1, is cleared by SnO_2/SiO_2 catalyst. The keys of each Chapters are summarized as follows.

A systematic screening of the catalysts are conducted under the working hypothesis to controll the oxidizing ability of SnO_2 by adding acid-base materials. An important information that the addition of acidic components enhances the catalytic performances has been obtained. SnO_2-P_2O_5 is selected as the best catalyst. (Chapter 2)

The optimum preparation method for SnO_2-P_2O_5 catalyst is confirmed. And the role of Sn and P are studied to conclude the addition of phosphorus results in the formation of new acid-base sites which may be the active sites. (Chapter 3)

Considering above hypothesis, the effect of the acid and base sites on the present reaction is studied using Na treated $SiO_2 \cdot Al_2O_3$ catalysts, the acid and base characters of which is controlled by the amount of Na loaded. Following quantitative correlations on the acidity and basicity are obtained. The adsorption of ethylbenzene is confirmed to be reversible and dissociated at the α-position on the acid site of Ho between 1.5 ann -5.6. While the activation of oxygen to form adsorbed oxygen species (may be O^-) occurs on the base site of pKa between 17.2 and 26.5. The formation of styrene occurs

Table 1

Catalysts for Oxidative Dehydrogenation of Ethylbenzene

Catalyst	Reaction Temperature (K)	Relative partial pressures			Results (%)		References
		Oxygen	Nitrogen	Steam	EB-conv.	ST-select	
SnO_2/SiO_2(3)	723	1.0	1.46	1.55	60.6	89.6	This study
SnO_2-P_2O_5(9/1)	723	1.0	4.87	3.13	38.4	84.6	This study
Al_2O_3-P_2O_5(9/1)	723	0.7	3.04	2.25	33.7	84.4	This study
Fe_2O_3-Cr_2O_3-K_2O	883	0.11	--	12.4	72	88(B/T=3/6)	1
Ce-P	824	1.16	--	13.7	77.5	91	2
Fe-Activ. Carbon	644	--	--	--	54.7	96.3	3
Zn-P-O-SiO_2	733	1.5	--	--	50	77	4
Cr_2O_3-NiO-Al_2O_3	723	0.42	--	0.6	40	95	5
ZnO-SiO_2·Al_2O_3	723	1.6	14.4	--	64	77	6
Bi-U-O-Al_2O_3	923	2.0	3.1	--	52.1	90.4	7
Pd-γ-Al_2O_3	563	1.0	3.5	10.0	46.0	98.5	8
Pd-KBr-α-Al_2O_3	558	0.43	1.7	2.8	42.9	97.6	9
Pd-KBr-γ-Al_2O_3	553	1.0	4.0	1.9 (with continuous flow of HBr)	29.0	98.0	10
Co-Cr-Al-Mg-Si	--	--	--	--	56.0	83.0	11

(CONTINUED)

Mn/Al	673	1.0	--	--	6.0	69.0	12
Co/Al	673	1.0	--	--	4.8	73.0	12
Ni/Al	673	1.0	--	--	4.6	71.0	12
Ni-W/Al(W/Ni=1/1.6)	733	1.0	--	0.0	30.0	70.0	13
$MgMoO_4$-MoO_3	773	2.0	--	--	26.0	60.0	14
MgO-MoO_3	773	2.0	--	--	48.0	82.0	14
Be-Si	--	--	--	--	41.6	90.0	15

[a]Calculated assuming $P_{ethylbenzene} = 1.00$.

[b]References; (1) J.R. Ghublikian, British Patent, 1,176,916 (1970). (2) Dow Chemical Co., Japan Kokai, 74-12,790 (1974). (3) R.M. Benslay and A.L. Jones, U.S. Patent, 3,652,698 (1970). (4) Nitto Chemical Industries Ltd., Japan Kokai, 74-41,182 (1974). (5) Mistubishi Chemical Industries Ltd., Japanese Patent, 75-30,061 (1975). (6) Nippon Kayaku Co. Ltd., Japanese Patent, 74-42,017 (1974). (7) Nippon Shokubai Kagaku Kogyo Co. Ltd., Japanese Patent, 77-28,782 (1977). (8) K. Fujimoto, J. Yamada, and T. Kunugi, Japan Kokai, 77-23,027 (1977). (9) Mitsubishi Petrochemical Co. Ltd., Japan Kokai, 78-44,525 (1978). (10) K. Fujimoto, and T. Kunugi, Ind. Eng. Chem. Prod. Res. Dev., 20 (1981) 319. (11) T. Imai, U.S. Patent, 4,180,690 (1979). (12) C. Bagnasco, P. Ciambelli, S. Crescitelli, and G. Russo, React. Kinet. Catal. Lett., 8 (1978) 293. (13) J.C. Conesa, B. Jezowska-Trzebiatowska, and W. Oganowski, J. Mol. Catal., 4 (1978) 271. (14) W. Oganowski, J. Hanuza, J. Wrzyszcz, and B. Jezowska-Trzebiatowska, Tezisy. Dokl. Resp. Konf. Okislitel'nomu Geterogennomu Katal., 3rd, 9 (1976) 4, Chem Abst., 89-147246. (15) D.B. Tagiev, A.B. Mamedov, Z.G. Zul'fganov and Kh. H. Minachev, Kinet Katal., 20 (1979) 541, Chem Abst. 91-039022.

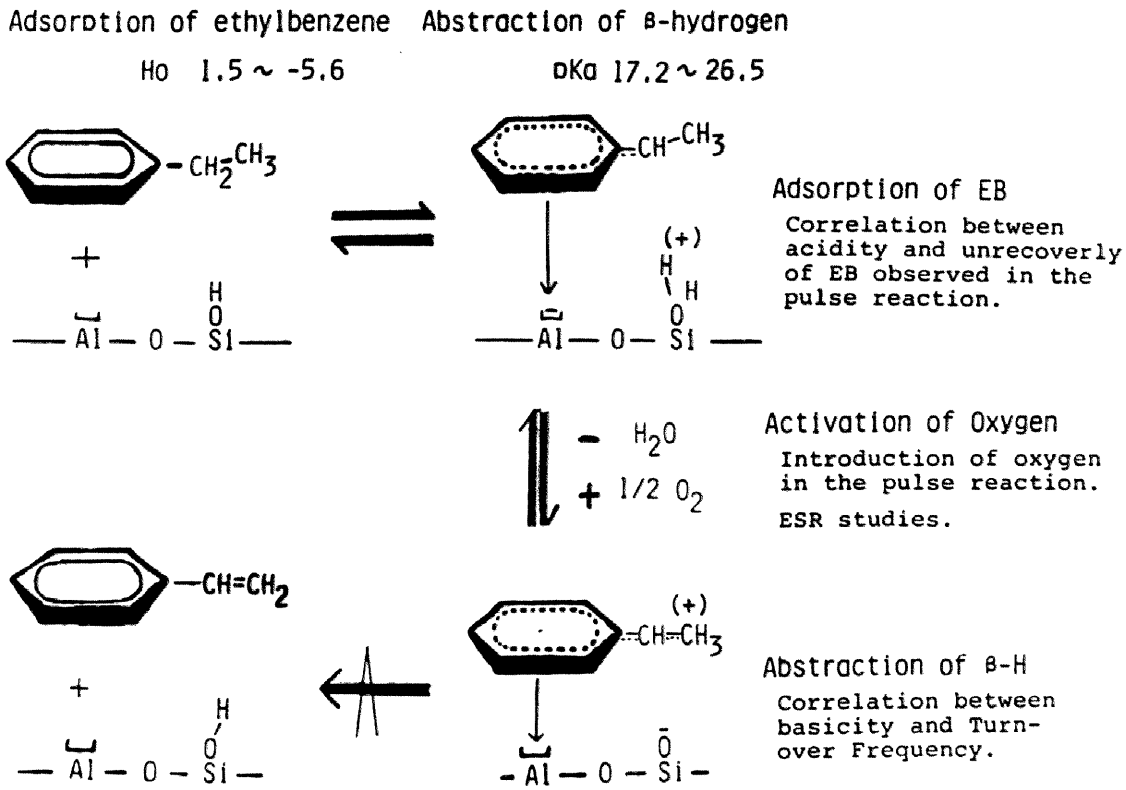

FIGURE 1 Reaction mechanism of oxidative dehydrogenation of Ethylbenzene

by the abstraction of β-hydrojen of the adsorbed ethylbenzene intermediate with the O^- species. These findings leads a detailed reaction mechanism in a molecular aspect and the resulted mechanism is shown in Fig. 1.

(Chapter 4 and 5)

The above reaction mechanism is extended to various solid acid catalysts including Si·Al, Si·Mg, Al_2O_3, SiO_2, Solid-P, SnO_2, Sn-P, Li-Si·Al, K-Si·Al, Na-Si·Mg, Al-P, Si-P and Al-B catalysts and the resulted mechanism leads to a plan to design catalyst for the oxidative dehydrogenation of ethylbenzene;

Increase the acid site of Ho between 1.5 and -5.6 as well as the base site of pKa between 17.2 and 26.5. (1)

Suppress the acid and base sites ranging in the stronger values. (2)

The designed catalyst is Al_2O_3-P_2O_5.

(Chapter 6)

The design of support for SnO_2 is also performed under the plan that instead of adding the acidic component to SnO_2, supporting SnO_2 on the acidic supports. New information is obtained that the catalytic properties depends on the acid and base properties of supports, using MgO as a base support, TiO_2 and Al_2O_3 as amphoter supports, SiO_2 and SiO_2·Al_2O_3 as acid supports. As a result, SnO_2/SiO_2 catalyst is designed.

(Chapter 7)

The optimum preparation method for SnO_2/SiO_2 is determined. The superiority of the designed SnO_2/SiO_2 catalyst to the other catalytic systems is also confirmed. The Mössbauer measurement is applied to investigate the electron transfer interactions between Sn atom and the supprot.

(Chapter 8)

A new preparation method of catalyst is developed. This is to support the metal chlorides onto the support surface through gas phase and convert them into oxide by the following hydration and calcination (Vapor Phase Supporting method = VPS method) This method is applied to the preparation of SnO_2/SiO_2 catalyst. Interesting knowledge that repeating the VPS cycles changes the acid and base properties of resulted catalyst.

(Chapter 9)

The VPS catalysts are compared to the impregnated (IMP) catalysts which are designed in Chapter 8 both from the view points of surface characters and catalytic activity. A model of SnO_2 on the SiO_2 support is proposed on each catakyst. The catalytic perfoemances of them are discussed on the basis of above model and the reaction mechanism determined in Chapter 4, 5, and 6.

(Chapter 10)

Brief Conclusions

As stated in the previous section, a numerous number of findings have been reported in this thesis. And they are supported by two principles as some times stated, that is;

(1) A new view point to understand oxidation reactions by the participation of the acid and base sites in a molecular aspect.

(2) A practical methodology to design the catalyst.

The elucidation of former probrem, as one part of chemistry of catalysis, directly serves the progress in the latter requirement through the feed back cycle shown in Capter 1 - Fig. 4. This is well confirmed in the case that the elucidation of reaction mechanism (Chapter 4 and 5) has directly served to construct the further working hypothesis to design the catalysts.

In a concrete sence, the fruits of this study could be classified into four; (1) reaction mechanism, (2) effect of support, (3) concrete plans of catalyst design, and (4) designed catalysts, and summarized as follows;

OXIDATIVE DEHYDROGENATION OF ETHYLBENZENE

Mechanism: New stand point; contribution of acid and base sites in molecular and quantitative aspect (Fig. 1 of this Chapter).

Adsorption of Ethylbenzne; (Chapter 4, 5)

reversible adsorption,
dissociated at α-position

ON

effective acid sites ($1.5 > Ho > -5.6$)

Activation of Oxygen; (Chapter 4, 5)

$O_{2gas} \rightleftharpoons O_{2ad} \longrightarrow O^-$

abstraction of β-hydrogen
(Turnover Frequency)

ON

effective base sites ($17.2 < pKa < 26.5$)

Side Reactions; (Chapter 3,4,5,6,8)

Ethylbenzene → Styrene → [Coke] → $CO + CO_2$

ON

strong acid sites ($Ho < -5.6$)

Effect of Support:

Specific interaction of SnO_2 with SiO_2 support to form new acid and base sites (Chapter 7,8,9,10)

New supporting method (VPS method) (Chapter 9, 10)

Concrete Plans of Catalyst Design: (Chapter 2,3,6,7,8)

enhance effective acid and base sites (evaluated by perylene radical formation)
avoid stronger acid and base sites.

adequate chemical treatment to remove the inactive materials

use of acidic supports instead of acidic additives for SnO_2

Designed Catalysts: Performances are compared in Table 1 of this Chapter.

Sn-P (10/1, HNO_3 treatment) (Chapter 2, 3)

Al-P (10/1) (Chapter 6)

Sn/Si (4.8 mol%, NH_4OH treatment) (Chapter 7, 8)

Considering the utility of combining the acid and base properties of catalysts with the oxidation reaction, as shown in Chapter 1, it is important that the reaction mechansim of the oxidative dehydrogenation of ethylbenzene is confirmed, under the principle that the acid and base sites controls the activity and selectivity of given partial oxidation reactions, with quantitative and molecular aspects. Thus, emphasis should be done that the reaction mechanism is the first trial on the completly new stand point that is quantitative and molecuar roles of the acid and base sites in the present reaction. Such reaction mechansims on the above new stand point can be applied to a wide spreaded field of catalytic reactions of aromatic hydrocarbons and partial or selective oxidation reactions of hydrocarbons. For example, this should be extended to the olefine oxidation. The oxidation of olefinic hydrocarbons also occupies a very important position in the chemical industries. For the mechansim of olefin oxidation, (1) irreversible adsorption of hydrocarbons in π-allyl state, (2) important participation of lattice oxygen, and (3) rate determining step in the dissociation of α-H, are usually pointed out. Moreover, this reaction does not proceed on a simple solid acid catalysts such as $SiO_2 \cdot Al_2O_3$. These are different from the case of ethylbenzene, therefore, the entirely same mechansim for ethylbenzene does not hold. Maybe, the difference in the state of π-electrons of olefins and aromatics determines the activated state of hydrocarbons. The ionization potentials of olefins, such as 938.8(kJ/mol) for C_3^1 and 926.2 for C_4^1, are much higher than that of ethylbenzne (845.2) and olefins are thusly difficult to be ionized. These show that the activation of olefinic compounds is insufficient on a simple acid sites, such as a pair of relatively strong acid site and relatively weak base site for ethylbenzene, and more strongly activated oxygen species such as O^{2-} or lattice oxygen with relatively weak acid site are required. Such differences in the stability of OH group resulted by the dissociation of α-hydrogen due to the degree of activation of original oxygen species determine the reversibility of adsorbed intermediate of hydrocarbons. Thus, the above mentioned reaction mechansim for ethylbenzene oxidation, based on the acid and base properties, still holds, even if it is not completely the same, in the case of olefinic compounds. At least, the principles of the above mechanism, that is the quantitative and molecular roles of the acid and base sites in the oxidation reaction, could be applied to the olefinic hydrocarbons.

The specific interactions of SnO_2 with the support, observed in this study, is also expected to play important roles in the progress of supported oxide catalysts together with the new preparation method developed in this study.

Another importance is exist on the proof of the utility of the methodology for the catalyst design. The sucessful catalyst design in this study expects the applicability of the program of catalyst design (see Chapter 1 - Fig. 3) to types of catalyst desing in every field.

The performances of all the designed catalysts meet the first target which was stated

in Capter 1, and the SnO_2/SiO_2 catalyst, especially, meets the further target. The details are shown in Table 1 in this Chapter. These meet, of course, the social requirement to save energy, even from the practical views. These also suggests the availability to realize the catalytic system which shows 100 % conversion with high selectivity. Such systems are desired form view point of process design because they make the separation of products from ethylbenzene easy.

LIST OF PUBLICATIONS

PLACES IN THIS THESIS

1 Screening of Catalysts for the Oxidative Dehydrogenation of Ethylbenzene — Chapter 2

Y. Murakami, K. Iwayama, H. Uchida, T. Hattori, and T. Tagawa
Applied Catalysis, in press.

2 Study of the Oxidative Dehydrogenation of Ethylbenzene
I. Catalytic Behavior of SnO_2-P_2O_5 — Chapter 3

Y. Murakami, K. Iwayama, H. Uchida, T. Hattori, and T. Tagawa
Journal of Catalysis, in press.

3 Study of the Oxidative Dehydrogenation of Ethylbenzene
II. Catalytic Activity and Acid and Base Properties of Na-$SiO_2 \cdot Al_2O_3$ — Chapter 4

T. Tagawa, T. Hattori, and Y. Murakami
Journal of Catalysis, in press.

4 Study of the Oxidative Dehydrogenation of Ethylbenzene
III. Mechanism for Styrene Formation — Chapter 5

T. Tagawa, T. Hattori, and Y. Murakami
Journal of Catalysis, in press

5 Study of the Oxidative Dehydrogenation of Ethylbenzene
IV. Extention of the Reaction Mechanism to Various Solid Acid Catalysts and Its Application to Catalyst Design — Chapter 6

T. Tagawa, K. Iwayama, T. Hattori, and Y. Murakami
Submitted.

6 Supported SnO_2 Catalysts for the Oxidative Dehydrogenation of Ethylbenzene — Chapter 7

T. Tagawa, S. Kataoka, T. Hattori, and Y. Murakami
Submitted.

7 Study of the Oxidative Dehydrogenation of Ethylbenzene V. Catalytic Behaviors of SnO_2/SiO_2 Catalysts — Chapter 8

T. Tagawa, S. Kataoka, T. Hattori, and Y. Murakami
Submitted.

8 Application of Vapor Phase Supporting (VPS) Method for Preparing SnO_2/SiO_2 Catalysts — Chapter 9

T. Tagawa, S. Kataoka, T. Hattori, and Y. Murakami
In press.

9 Oxidative Dehydrogenation of Ethylbenzene on VPS-SnO_2/SiO_2 Catalysts — Chapter 10

T. Tagawa, S, Itoh, T. Hattori, and Y. Murakami
Submitted.

OTHER PUBLICATIONS

1 Homogeneous Transfer Hydrogenation of Methyl Linoleate

K. Fukuzumi, T. Nishiguchi, T. Tagawa, and H. Imai
Yukagaku, 25 164 (1976).

2 Homogeneous Transfer Hydrogenation of Unsaturated Fatty Acid Esters

K. Fukuzumi, T. Nishiguchi, T. Tagawa, and H. Imai
Bull. Asahi Garasu-Industrial Technological Association, 28 309 (1976).

3 Studies on Homogeneous Transfer Hydrogenation of Unsaturated Fatty Acid Esters -- Discovery and Discussion of the Reaction system having 100% selectivity and No Trans Isomers Produced --

K. Fukuzumi, T. Nishiguchi, and T. Tagawa
Bull. Asahi Garasu-Industrial Technological Association, 31 351 (1977).

4 Transfer Hydrogenation and Transfer Hydrogenolysis
X. Selective Hydrogenation of Methyl Linoleate by Indoline and Isopropyl Alcohol

T. Nishiguchi, T. Tagawa, and K. Fukuzumi
J. Am. Oil. Chem. Soc., 54 144 (1977).

5 Transfer Hydrogenation and Transfer Hydrogenolysis
XII. Selective Hydrogenation of Fatty Acid Methyl Esters by Various Hydrogen Donors

T. Tagawa, T. Nishiguchi, and K. Fukuzumi
J. Am. Oil. Chem. Soc., 55 332 (1978).

6 Transfer Hydrogenation and Transfer Hydrogenolysis
XV. Homogeneous Selective Hydrogenation of Various Fatty Acid Methyl Esters by Organic Hydrogen Donors

T. Tagawa, T. Nishiguchi, and K. Fukuzumi
Yukagaku, 27 70 (1978).

7 Transfer Hydrogenation and Transfer Hydrogenolysis XVIII. Homogeneous Selective Hydrogenation of Fatty Acid Methyl Esters with Natural Products

T. Nishiguchi, T. Tagawa, and K. Fukuzumi
Yukagaku, 27 501 (1978).

8 Transfer Hydrogenation and Transfer Hydrogenolysis XIX. Heterogeneous Selective Reduction of Unsaturated Fatty Acid Methyl Esters by Hydrogen Transfer from Organic Compounds

T. Nishiguchi, T. Tagawa, and K. Fukuzumi
Yukagaku, 28 174 (1979).